BOUNDARY INTEGRAL EQUATIONS FOR THE COMPUTATIONAL MODELING OF THREE-DIMENSIONAL STEADY GROUNDWATER FLOW PROBLEMS

Raphic M. van der Weiden

TR diss
1649

4.273
317879
TR diss 1649

BOUNDARY INTEGRAL EQUATIONS FOR THE COMPUTATIONAL MODELING OF THREE-DIMENSIONAL STEADY GROUNDWATER FLOW PROBLEMS

PROEFSCHRIFT

ter verkrijging van de graad van doctor aan
de Technische Universiteit Delft, op gezag van
de Rector Magnificus, prof. dr. J.M. Dirken,
in het openbaar te verdedigen ten overstaan van
een commissie aangewezen door het College van Dekanen
op dinsdag 21 juni 1988 te 16.00 uur

door

RAPHAËL MARIA VAN DER WEIDEN

geboren te Amsterdam

elektrotechnisch ingenieur

BIBLIOTHEEK TECHNISCHE UNIVERSITEIT
Prometheusplein 1
2628 ZC
DELFT

TR diss
1649

Dit proefschrift is goedgekeurd door de promotoren
prof.dr.ir. A.T. de Hoop en prof.dr.ir. J.C. van Dam

The research reported in this thesis has been performed at the Delft University of Technology, Faculty of Civil Engineering, Water Management Group, Delft, the Netherlands, under the financial support of the Netherlands Technology Foundation (S.T.W.) and the Netherlands organization for scientific research (N.W.O.).

To Pimette

TABLE OF CONTENTS

(continued on next page)

CONTENTS

(continued on next page)

CONTENTS

(continued on next page)

CONTENTS

LIST OF SYMBOLS AND THEIR SI-UNITS

Throughout this thesis SI-units will be employed. The basic quantities, units and dimensions of the International System of Units (SI) are shown in Table 0.1. In Table 0.2 the SI-units and dimensions of the most important quantities that occur in this thesis are listed. Table 0.3 contains a list of conventions and frequently used symbols.

Table 0.1. Basic quantities, units and dimensions of the International System of Units (SI).

Basic quantity		Basic unit		Basic dimension
name	symbol	name	symbol	symbol
length	l	meter	m	L
mass	m	kilogram	kg	M
time	t	second	s	T
electric current	I	ampere	A	I
thermodynamic temperature	T	kelvin	K	Θ
amount of substance	n	mole	mol	N
luminous intensity	I	candela	cd	J

Table 0.2. SI-units and dimensions of the most important quantities occurring in this thesis.

Quantity		Unit		Dimension
name	symbol	name	symbol	symbol
volume density of fluid mass	ρ	kilogram/meter^3	kg/m^3	$L^{-3}M$
fluid velocity	v_i	meter/second	m/s	LT^{-1}
stress	τ_{ij}	pascal	Pa	$L^{-1}MT^{-2}$
volume density of body force	f_i	newton/meter^3	N/m^3	$L^{-2}MT^{-2}$
pressure	p	pascal	Pa	$L^{-1}MT^{-2}$
viscous stress	σ_{ij}	pascal	Pa	$L^{-1}MT^{-2}$
deformation rate	d_{ij}	*second*$^{-1}$	s^{-1}	T^{-1}
spin	w_{ij}	second^{-1}	s^{-1}	T^{-1}
viscosity	η_{ijpq}	pascal·second	Pa·s	$L^{-1}MT^{-1}$
bulk viscosity	ζ	pascal·second	Pa·s	$L^{-1}MT^{-1}$
dynamic viscosity	η	pascal·second	Pa·s	$L^{-1}MT^{-1}$
fluidity	Φ_{pqij}	(pascal·second)$^{-1}$	Pa^{-1}·s^{-1}	$LM^{-1}T$
kinetic energy	E_{kin}	joule	J	L^2MT^{-2}
work	W	joule	J	L^2MT^{-2}
time rate of work	$\dot{W}$	joule/second	J/s	L^2MT^{-3}
acceleration of free fall	g_i	meter/second^2	m/s^2	LT^{-2}
Mach number	Ma			
Strouhal number	Sr			
Reynolds number	Re			

(continued on next page)

Table 0.2. (continued)

Quantity		Unit		Dimension
name	symbol	name	symbol	symbol
Froude number	Fr			
volume of representative elementary domain D_ε	V_ε	$meter^3$	m^3	L^3
fluid fraction in D_ε	ϕ^f			
solid fraction in D_ε	ϕ^s			
tensorial resistivity of a fluid-saturated porous medium	R_{ij}	kilogram/($meter^3$·second)	$kg/(m^3 \cdot s)$	$L^{-3}MT^{-1}$
intrinsic resistivity	R'_{ij}	$meter^{-2}$	m^{-2}	L^{-2}
volume source density of volume injection rate	$\langle q \rangle$	$second^{-1}$	s^{-1}	T^{-1}
volume source density of external force (other than gravity)	$\langle f_i \rangle$	$newton/meter^3$	N/m^3	$L^{-2}MT^{-2}$
area of representative elementary surface Δ_ε	A_ε	$meter^2$	m^2	L^2
tensorial permeability (=inverse resistivity)	K_{ij}	$meter^3$·second/kilogram	$m^3 \cdot s/kg$	$L^3M^{-1}T$

Table 0.3. List of conventions and frequently used symbols.

∂_t	partial differentiation with respect to t (s^{-1})
∂_i	partial differentiation with respect to x_i (m^{-1})
δ_{ij}	symmetrical unit tensor of rank two (Kronecker tensor)
D_ε	representative elementary domain of a fluid-saturated porous medium
D_ε^f	subdomain of D_ε in which the fluid is present
D_ε^s	subdomain of D_ε in which the solid is present
$\langle\psi\rangle$	fluid average of a quantity ψ
$\langle\psi\rangle^f$	intrinsic fluid average of a quantity ψ
Σ_ε	interface(s) between fluid and solid phases in the interior of D_ε
Δ_ε	representative elementary surface of a fluid-saturated porous medium
$\delta(\underline{x}-\underline{x}')$	three-dimensional unit pulse (delta function) operative at $\underline{x}=\underline{x}'$
(α_{pq})	orthogonal transformation
$t^{(p)}$	p-th eigenvalue of (K_{ij})
Δ	determinant of (R_{ij})
π	pi (3.14159...)
$\lvert\underline{x}\rvert$	length of vector $\underline{x}$
$\sum$	summation
S_T	planar triangle
C_T	boundary curve of S_T

(continued on next page)

Table 0.3. (continued)

ε_{ijk}	completely antisymmetrical unit tensor of rank three (Levi-Civita tensor)
Π	product
sign(h)	+ 1 if h > 0 - 1 if h < 0

CHAPTER 1

INTRODUCTION

The subject of investigation of the present thesis is the application of the boundary-integral-equation method to the computational modeling of three-dimensional, steady groundwater flow problems.

Problems concerned with the flow of groundwater have a wide field of application. In the practice of groundwater hydrology, for example, they occur in the managing of subsurface water reservoirs employed for the supply of drinking water, and in the managing of irrigation systems for agriculture. Equally important are applications encountered in, for example, civil engineering practice, where the knowledge of the behavior and the characteristics of the flow of groundwater is needed in the design of all kinds of hydraulic structures like dams and drainage systems.

In any theoretical study concerning the flow of groundwater one's interest is to obtain insight in the average or so-called macroscopic behavior of the groundwater flow in the interior of some given porous substance. Solutions of groundwater flow problems (see, e.g., Muskat, 1946, Polubarinova-Kochina, 1962, Scheidegger, 1963, or Bear, 1972), are, in general, based on the fundamental laws of the flow of viscous fluids and on various, often rather intuitive, generalizations of an empirical law for one-dimensional flow discovered by Darcy in 1856 (Darcy, 1856) to deal with the permeability characteristics of some subsoil. Darcy's law expresses that the rate of flow through a bed of fine particles is

proportional to the pressure drop along it. Although with the aid of these generalizations many practical problems concerned with, e.g., groundwater flow in aquifers, seepage through and below dams, and the like, can successfully be solved, there is a need for a more profound theoretical justification of the various generalizations of Darcy's law, as well as for more explicit knowledge under which conditions these apply.

The first part of the present thesis is especially set up to serve this purpose. It provides a theoretical insight into Darcy's law and its generalizations. Envisaging the soil as a fluid-saturated porous medium, the underlying thought in the analysis is that the relevant macroscopic equations for the flow of groundwater can be obtained upon applying a suitable spatial averaging procedure to the well-established equations for common fluid flows, where the latter equations describe the fluid flow phenomena at the scale of the pores, i.e., the so-called microscopic scale. Once the relevant macroscopic equations for flow of groundwater have been derived in this manner, they serve to formulate steady groundwater flow problems as (mathematical) boundary-value problems for the relevant flow equations in porous media, i.e., a macroscopic continuity equation for incompressible fluid flow and Darcy's law.

The literature on solving boundary-value problems is very extensive. A review of the analytical techniques for solving these problems, especially concerning groundwater flow problems, can be found in, e.g., Polubarinova-Kochina (1963) and Bear (1972). In general, the applicability of analytical methods is limited to flow configurations of a simple shape and composition. In practice, however, we are often confronted with complex geometries with (partially) inhomogeneous and/or anisotropic media.

With the advent of high-speed, large-capacity digital computers, numerical techniques have started to play a role of increasing importance in groundwater flow calculations. The main advantage of these techniques is their general applicability: they are flexible as regards shape, size and physical composition of the different geometrical constituents that

together form the configuration that one wants to analyze. The main limitations are dictated by the speed and storage capacity of the computer system at one's disposal. The numerical techniques are based on a discretization of the equations governing the relevant groundwater flow phenomena. In this respect, discretized versions of the pertaining partial differential equations are used; in their simplest form they lead to finite-difference formulations. The application of this approach to the flow of groundwater, has been started in the 1960s (see, e.g., Remson, Appel and Webster, 1965). Later, also the finite-element method, which is more flexible as far as the geometry of the domain of computational interest is concerned, entered into the numerical solving of groundwater flow problems (see, e.g., Pinder and Gray, 1977). On the other hand, groundwater flow problems can also be formulated in terms of integral equations, the discretization of which leads again to a different type of numerical implementation.

In the present thesis, we have investigated a particular type of integral-equation technique, viz. the boundary-integral-equation method. The main attraction of this method as compared with the finite-difference and finite-element methods is that it achieves computational efficiency through a reduction in the problem's dimensionality. Especially in implementing three-dimensional problems, this advantage shows up. Moreover, the differential equations describing the groundwater flow in the interior of the relevant porous substance are in principle solved exactly; all approximations are made on the boundaries. Since, however, the boundary-integral-equation method can in practice only be handled for piecewise homogeneous subdomains in the flow configurations, it does not defeat the finite-difference and finite-element methods in all cases. In general, for groundwater flow problems concerned with flow in strongly inhomogeneous media, a finite-difference, finite-element, or a hybrid approach, may be a better choice.

In arriving at the boundary-integral-equation formulation for solving steady groundwater flow problems, the main tool is the use of suitable source-type integral representations for the flow field quantities

involved, i.e., the pressure and the flow velocity. The representations express the latter quantities in terms of related quantities on a closed surface bounding the flow configuration under consideration. The source-type integral representations, in their turn, follow from a suitable reciprocity theorem that interrelates, in a specific way, the field quantities of two admissible, but non-identical, states that can occur in one and the same bounded domain in space. This theorem can be regarded, both mathematically and physically, as one of the most fundamental theorems from which many properties of groundwater flow fields follow. In the reciprocity theorem one of the states is chosen as the actual one, the other is taken to be one of several "auxiliary states". Taking the latter to correspond to the presence of appropriate point sources, the desired source-type integral representations are obtained. The latter contain Green's type, singular kernel functions. Once these kernel functions are known, the different boundary-integral-equation-formulations follow upon taking, in the integral representations, the point of observation on the boundary surface of the domain for which the Green's functions have been determined. In practice, simple analytical expressions for the Green's kernels can be obtained for unbounded, homogeneous and reciprocal media only. As a consequence, the boundary-integral-equation method is, in practice, implemented for piecewise homogeneous flow configurations only. In order to solve the resulting boundary integral equations numerically, a suitable discretization scheme is developed. In the present thesis the boundary integral equations are applied to a number of simple, isotropic and anisotropic, test configurations, but the software developed for them is of general applicability. More details are given in the outline below.

Outline of the different chapters

In Chapter 2, the basic equations governing the theory of isothermal flow of viscous fluids is summarized. Envisaging the permeation of groundwater in a common (sub)soil as the flow of a fluid in a porous medium, these

equations describe the flow at the scale of the pores, i.e., the microscopic scale of the porous medium. It is shown that for common groundwater flows the conditions are satisfied under which the, in general, compressible fluid flow governed by a non-steady and non-linear equation of motion can be approximated by an incompressible one governed by a steady and linear equation of motion. These approximate equations adequately describe the flow inside the pores of the commonly encountered (sub)soils.

In Chapter 3, the latter pore-scale or microscopic equations serve to develop the macroscopic equations for the flow of groundwater. The latter describe the groundwater flow phenomena at a scale that complies with the one at which these flow processes are encountered in practice. To this aim the microscopic equations are averaged over a so-called representative elementary domain of the fluid-saturated porous medium under consideration. The expressions that arise after employing the volume-averaging operator all have a clear physical meaning and can, in a natural way, be identified with the quantities that one usually observes and measures in practice. It is shown that as far as the macroscopic equation of motion is concerned, an equation that essentially is Darcy's law is arrived at. In the literature on porous media flow, the idea of deriving macroscopic equations by applying a suitable averaging procedure to the well-established microscopic equations has been initiated by Slattery (1967) and Whitaker (1967 and 1969). Later, it has been exploited and extended by many others (see, e.g., Hassanizadeh and Gray, 1979a,b and 1980, and the references cited therein). Chapter 3 is concluded with formulating problems concerned with steady flow of groundwater as mathematical boundary-value problems.

In Chapter 4, boundary-integral-equation formulations for those steady groundwater flow problems that can mathematically be formulated as boundary-value problems are further developed. In the literature (see, e.g., Liggett and Liu, 1983), most boundary-integral-equation formulations for analyzing the steady flow of groundwater are based on the source-type integral representation for only one of the field

quantities that characterize the flow of groundwater, viz. the pressure. It is one of the purposes of Chapter 4 to give a general survey of the boundary-integral-equation formulations that follow from using both the source-type integral representation for the pressure and the source-type integral representation for the velocity.

In Chapter 5 an efficient and straightforward method is presented for solving numerically the relevant systems of boundary integral equations pertaining to the steady groundwater flow in piecewise homogeneous configurations. The technique amounts to the geometrical discretization into planar triangles of the boundary surfaces of the homogeneous subdomains involved, the approximation of the relevant flow quantities by piecewise linear interpolation functions, and, finally, the application of the method of collocation (point matching) at the nodal points of the discretized geometry. The procedure results into the replacement of the boundary integral equations and, hence, of the relevant flow problem, by a system of linear, algebraic equations. Particular emphasis is given to the analytic evaluation of all (matrix) coefficients occurring in the latter system.

In Chapter 6, numerical experiments are carried out in order to test the computer code developed. Simple test flows in homogeneous, isotropic and anisotropic, but reciprocal, media are considered. The results obtained look very promising for further applications.

CHAPTER 2

BASIC RELATIONS OF FLUID MECHANICS

In this chapter, the basic relations governing the theory of isothermal flow of viscous fluids are summarized. The equation of continuity, the equation of motion, the equation of deformation rate, and the constitutive relations for viscous fluids, together with (some of) their consequences, are discussed in Section 2.1. The boundary conditions at a surface of discontinuity in fluid properties are studied in Section 2.2. Section 2.3 deals with the exchange of mechanical energy that takes place in viscous fluid flow. Finally, in Section 2.4, we analyze the conditions under which a fluid flow can be regarded as incompressible, and discuss in some detail the conditions under which we may approximate the non-steady and non-linear equation of motion for a Newtonian fluid by a steady and linear one. In the remainder of Section 2.4, we discuss the important simplifications that can be made in case we are dealing with the permeation of groundwater inside the pores of common subsoils. The resultant equations are known as the equations for creeping motion; they play a fundamental role in Chapter 3, where they serve to develop the equations that describe, on a macroscopic scale, the permeation processes of groundwater in common subsoils.

2.1. BASIC EQUATIONS OF FLUID MECHANICS

A point in three-dimensional Euclidean space R^3 is referred to by its coordinates $\{x_1,x_2,x_3\}$ relative to a fixed, orthogonal, Cartesian reference frame with origin O and three mutually perpendicular base vectors $\{\underline{i}_1,\underline{i}_2,\underline{i}_3\}$ of unit length each. In the indicated order, the base vectors form a right-handed system. The subscript notation for vectors and tensors is employed; for repeated subscripts the summation convention applies. Occasionally, a direct notation will be used to denote a vectorial quantity; in particular, $\underline{x}=x_i\underline{i}_i$ will denote the position

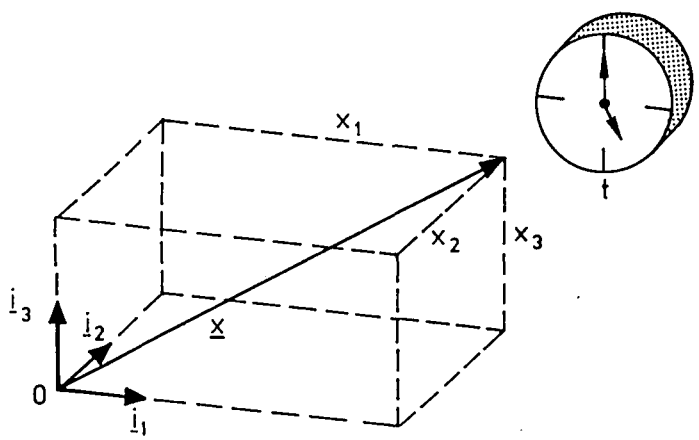

Fig. 2.1. Reference frame, Cartesian coordinates $\{x_1,x_2,x_3\}$, position vector $\underline{x}$ and time of observation t.

vector. The time of observation is denoted by t (see Figure 2.1). As system of units we use the International System of Units (SI). For the SI-units and the dimensions of the quantities occurring in the theory, we refer to the overview "List of symbols and their SI-units" that precedes Chapter 1.

For our summary of the basic equations of fluid mechanics we start with the local form of the equation of conservation of fluid mass in the absence of either mass production or mass annihilation (see, e.g., Malvern, 1969, p. 207, or Eringen, 1967, p. 85)

$$\partial_t \rho + \partial_i (\rho v_i) = 0, \tag{2.1.1}$$

where

∂_t = partial differentiation with respect to t,
ρ = volume density of fluid mass,
∂_i = partial differentiation with respect to x_i,
v_i = fluid velocity.

Equation (2.1.1) is known as the continuity equation of mass flow. Next, from the integral form of the equation of conservation of linear momentum and using (2.1.1) we obtain Cauchy's first law of motion (see, e.g., Malvern, 1969, p. 214, or Eringen, 1967, p. 103)

$$\partial_j \tau_{ij} + f_i = \rho(\partial_t v_i + v_j \partial_j v_i), \tag{2.1.2}$$

where

τ_{ij} = stress,
f_i = volume density of body force.

For nonpolar fluids (i.e., fluids in which neither body torques nor couple stresses are present, see, e.g., Aris, 1962, pp. 103-104, or

Malvern, 1969, pp. 217-220), and those are the ones that we consider here, the integral form of the equation of conservation of angular momentum, with the further use of both (2.1.1) and (2.1.2), leads to Cauchy's second law of motion (see, e.g., Malvern, 1969, p. 216, or Eringen, 1967, p. 103);

$$\tau_{ij} = \tau_{ji}, \tag{2.1.3}$$

i.e., the stress is a symmetrical tensor.

In fluid mechanics, the stress is usually written as the sum of a part that corresponds to an omnidirectional pressure and a viscous or dissipative part; the latter accounts for the internal friction in the fluid (see, e.g., Aris, 1962, p. 105, or Landau and Lifshitz, 1966, p. 47). We write

$$\tau_{ij} = - p\delta_{ij} + \sigma_{ij}, \tag{2.1.4}$$

where

p = scalar pressure,
σ_{ij} = viscous stress.

Here, δ_{ij} denotes the symmetrical unit tensor of rank two (Kronecker tensor), which is defined as $\delta_{ij}=0$ if $i\neq j$ and $\delta_{11}=\delta_{22}=\delta_{33}=1$. For a fluid at rest, the scalar pressure p can be identified with the pressure as introduced in classical thermodynamics. When the fluid is in motion, we retain, on the assumption of local thermodynamic equilibrium, this identification (see, e.g., Aris, 1962, p. 105, or Thurston, 1964, pp. 49-50). The internal friction in a fluid manifests itself only when adjacent fluid particles are in a relative motion. For this relative motion, the velocity gradients $\partial_i v_j$ are taken as a quantitative measure. Decomposition of $\partial_i v_j$ into its symmetric and antisymmetric parts leads to

$$\partial_i v_j = d_{ij} + w_{ij}, \tag{2.1.5}$$

with

$$d_{ij} = (1/2)(\partial_i v_j + \partial_j v_i) \tag{2.1.6}$$

and

$$w_{ij} = (1/2)(\partial_i v_j - \partial_j v_i), \tag{2.1.7}$$

where

d_{ij} = deformation rate,
w_{ij} = spin.

Since the spin corresponds to a local rigid-body rotation (see, e.g., Aris, 1962, p. 89), while the deformation rate provides a measure for the rate of change of the infinitesimal distance between two neighboring fluid particles, only the deformation rate plays a role in the processes that govern the internal friction.

The macroscopic viscous properties of a fluid are accounted for by a constitutive relation that relates the viscous stress to the deformation rate. If we assume the fluid to be time invariant and to react linearly, instantaneously and locally, we have (see, e.g., Aris, 1962, p. 111):

$$\sigma_{ij}(\underline{x},t) = \eta_{ijpq}(\underline{x})d_{pq}(\underline{x},t), \tag{2.1.8}$$

where

η_{ijpq} = viscosity.

Since both the viscous stress and the deformation rate are symmetrical tensors, η_{ijpq} satisfies the following symmetry relations:

$$\eta_{ijpq}(\underline{x}) = \eta_{ijqp}(\underline{x}) = \eta_{jiqp}(\underline{x}) = \eta_{jipq}(\underline{x}). \tag{2.1.9}$$

If, in addition, we assume the fluid to be isotropic, the properties of the fluid are, at each position, independent of the direction. For isotropic fluids the most general form of η_{ijpq} that complies with (2.1.9) is given by (see, e.g., Aris, 1962, p. 34, or Thurston, 1964, pp. 49-50, or Malvern, 1969, p. 298)

$$\eta_{ijpq}(\underline{x}) = a(\underline{x})\delta_{ij}\delta_{pq} + b(\underline{x})(\delta_{ip}\delta_{jq} + \delta_{iq}\delta_{jp}), \tag{2.1.10}$$

where a and b are arbitrary scalar quantities. Substituting (2.1.10) in (2.1.8) and taking into account the symmetry of d_{ij}, we arrive at

$$\sigma_{ij} = ad_{pp}\delta_{ij} + 2bd_{ij}. \tag{2.1.11}$$

Now, the standard form of (2.1.11) follows upon replacing a by $\zeta-(2/3)\eta$ and b by η, where (see, e.g., Aris, 1962, p. 34, or Truesdell and Toupin, 1960, p. 718, or Batchelor, 1983, p. 154)

ζ = bulk or expansion viscosity,
η = dynamic or shear viscosity.

Clearly, (2.1.11) then becomes

$$\sigma_{ij} = [\zeta - (2/3)\eta]d_{pp}\delta_{ij} + 2\eta d_{ij}, \tag{2.1.12}$$

and, hence, (2.1.4) is replaced by

$$\tau_{ij} = -p\delta_{ij} + [\zeta - (2/3)\eta]d_{pp}\delta_{ij} + 2\eta d_{ij}. \tag{2.1.13}$$

A fluid whose viscous properties are characterized by the constitutive equation (2.1.12) is usually denoted as a Newtonian one (see, e.g., Aris, 1962, pp. 110-111, or Malvern, 1969, p. 298). Upon writing the stress τ_{ij}

and the deformation rate d_{ij} each as the sum of an isotropic and a deviatoric part, i.e., writing

$$\tau_{ij} = (1/3)\tau_{pp}\delta_{ij} + \tau'_{ij} \tag{2.1.14}$$

and

$$d_{ij} = (1/3)d_{pp}\delta_{ij} + d'_{ij}, \tag{2.1.15}$$

where

τ'_{ij} = deviatoric stress,
d'_{ij} = deviatoric deformation rate,

we obtain from (2.1.13) the relations

$$(1/3)\tau_{pp} = - p + \zeta d_{pp} \tag{2.1.16}$$

and

$$\tau'_{ij} = 2\eta d'_{ij}. \tag{2.1.17}$$

Note that $\tau'_{ii}=0$ and $d'_{ii}=0$. The quantity $(1/3)\tau_{pp}$ is also known as the opposite of the mean (mechanical) pressure (see, e.g., Aris, 1962, p. 105, or Truesdell and Toupin, 1960, p. 545). From (2.1.16) it readily follows that for a vanishing bulk viscosity the mean pressure equals the thermodynamic pressure. Since in the majority of common fluid-flow situations the bulk viscosity proves to be relatively unimportant (see, e.g., Malvern, 1969, p. 301, or Batchelor, 1983, pp. 154-174, or Bird, Stewart and Lightfoot, 1960, p. 79), its influence is often neglected. Under this assumption (2.1.13) reduces to

$$\tau_{ij} = - [p + (2/3)\eta d_{pp}]\delta_{ij} + 2\eta d_{ij}. \tag{2.1.18}$$

Next, we substitute the constitutive equation (2.1.13) into Cauchy's first law of motion, use (2.1.6) and arrive at the following result:

$$- \partial_i p + \partial_i\{[\zeta - (2/3)\eta]\partial_p v_p\} + \partial_j[\eta(\partial_i v_j + \partial_j v_i)] + f_i$$

$$= \rho(\partial_t v_i + v_j \partial_j v_i). \qquad (2.1.19)$$

Equation (2.1.19) is denoted as the generalized Navier-Stokes equation. Now, assuming that the quantities ζ, η and f_i are known, it is clear that in order to determine the unknown quantities v_i, p and ρ, the Navier-Stokes equation (2.1.19) has to be supplemented by the equation of continuity (2.1.1) and by one other scalar equation. This additional equation is provided by the equation of state for the fluid under consideration and can be written as

$$\rho = \rho(p,T), \qquad (2.1.20)$$

where T denotes the temperature, which, in view of the assumed isothermal flow, has a constant value throughout the fluid.

To conclude this section, we sum up some special types of fluid flows and list some of their properties.

First of all, if the viscous stress σ_{ij} in (2.1.4) vanishes identically, the relevant fluid is denoted as an ideal one (see, e.g., Landau and Lifshitz, 1966, p. 4). In that case, we arrive from (2.1.2) and (2.1.4) at

$$- \partial_i p + f_i = \rho(\partial_t v_i + v_j \partial_j v_i), \qquad (2.1.21)$$

which is known as Euler's equation of motion (see, e.g., Landau and Lifshitz, 1966, p. 3). This equation is widely used for describing flow systems in which the viscous effects are relatively unimportant.

Secondly, we consider the case that a fluid is behaving as if it were incompressible. For this situation we have the internal constraint that

the volume density of fluid mass ρ is not affected by the motion of the fluid. Then, $\partial_t \rho + v_i \partial_i \rho = 0$, and the continuity equation reduces to (cf. (2.1.1)):

$$\partial_i v_i = 0. \tag{2.1.22}$$

The conditions under which a fluid flow can be regarded as an incompressible one, are discussed in some detail in Section 2.4. It is emphasized that if we assume that the fluid is behaving as if it were incompressible, the pressure p in (2.1.4) has to be considered as an independent variable since it is no longer thermodynamically defined (see, e.g., Aris, 1962, p. 105, or Malvern, 1969, pp. 295-298). Clearly, for an incompressible viscous fluid (2.1.22) leads to $d_{pp} = 0$, and the constitutive equation (2.1.12) reduces with the aid of (2.1.6) to

$$\sigma_{ij} = 2\eta d_{ij}, \tag{2.1.23}$$

while (2.1.13) is replaced by

$$\tau_{ij} = - p\delta_{ij} + 2\eta d_{ij}. \tag{2.1.24}$$

As a consequence, the generalized Navier-Stokes equation (2.1.19) reduces to

$$- \partial_i p + \partial_j[\eta(\partial_i v_j + \partial_j v_i)] + f_i = \rho(\partial_t v_i + v_j \partial_j v_i). \tag{2.1.25}$$

Note that (2.1.25) which, for an incompressible Newtonian fluid, constitutes the equation of motion, only has to be supplemented by the continuity equation (2.1.22) in order to determine the unknown quantities v_i and p (the quantities η, ρ and f_i are assumed to be known). Equation (2.1.25) will be studied in some more detail in Section 2.4.

2.2. BOUNDARY CONDITIONS

At those positions of a given flow configuration where the properties of the fluid show abrupt changes, (some of) the quantities that describe the motion of the fluid (such as the velocity and the stress) will, in general, change discontinuously, too. In particular, this situation arises when at the two sides of a surface two different fluids are present; the presence of such a surface of discontinuity, or interface, implies that the fluids are immiscible. On physical grounds we assume that the jumps in both the constitutive parameters and the field values will remain bounded; hence, across the discontinuity surface they can at most jump by finite amounts. At those locations the local form of the conservation equations (e.g., the continuity equation of mass flow, the equation of conservation of linear momentum and the equation of conservation of angular momentum), the kinematic equation (2.1.6), and all equations deduced from these, will in general cease to hold, since at least some of the derivatives occurring in these equations do not exist. As a consequence, they have to be supplemented by so-called boundary, or interface, conditions that interconnect, in a certain manner, (parts of) the relevant field values at either side of the surface of discontinuity under consideration.

In the present section, we derive the relevant interface conditions pertaining to the basic flow equations (2.1.1), (2.1.2) and (2.1.8). The standard manner to interrelate the solutions to these equations at either side of a surface of discontinuity in fluid properties is to replace, locally, the basic flow equations by another system of equations that for continuously varying fluid properties is equivalent to the system (2.1.1), (2.1.2) and (2.1.8), but that contains no spatial differentiations across the surface of discontinuity under consideration.

Let S denote the interface and assume that S has everywhere a unique tangent plane. Further, let ν_i denote the vector along the normal to S such that upon traversing S in the direction of ν_i, we pass from the domain D_2 to the domain D_1, D_1 and D_2 being located at either side of S (see Figure 2.2). Let $\underline{x}$ be the position vector of some point on S. Now,

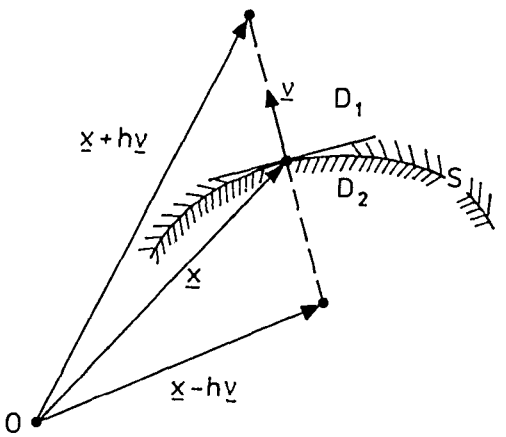

Fig. 2.2. Surface of discontinuity in fluid properties S.

to avoid the problem of differentiation along ν_i in (2.1.1), (2.1.2) and (2.1.8), we integrate these equations along a straight line joining a point with position vector $\underline{x} - h\underline{\nu}$ (with $h > 0$) located in D_2 to a point with position vector $\underline{x} + h\underline{\nu}$ located in D_1 (see Figure 2.2). Applying this procedure to Cauchy's first law of motion, we obtain (cf. (2.1.2))

$$\int_{s=-h}^{h} \partial_j \tau_{ij}(\underline{x}+s\underline{\nu},t)ds + \int_{s=-h}^{h} f_i(\underline{x}+s\underline{\nu},t)ds$$

$$- \int_{s=-h}^{h} \rho(\underline{x}+s\underline{\nu},t)[\partial_t + v_j(\underline{x}+s\underline{\nu},t)\partial_j]v_i(\underline{x}+s\underline{\nu},t)ds = 0. \qquad (2.2.1)$$

At this point, it should be noted that the operator $\partial_t + v_j\partial_j$ occurring in (2.2.1) produces the time rate of change that an observer registers when moving through the fluid with the velocity v_i. This rate of change is denoted as *the co-moving time derivative* and remains bounded at the interface between the two fluids. Furthermore, the spatial derivatives along the interface S remain continuous and bounded. To separate these from the derivatives along $\underline{\nu}$, we write

$$\partial_j = N_{js}\partial_s + T_{js}\partial_s, \qquad (2.2.2)$$

where

$$N_{js} = \nu_j\nu_s \qquad (2.2.3)$$

and

$$T_{js} = \delta_{js} - \nu_j\nu_s. \qquad (2.2.4)$$

Obviously, $N_{js}\partial_s$ is the part of ∂_j along $\underline{\nu}$ and $T_{js}\partial_s$ is the part of ∂_j perpendicular to $\underline{\nu}$, i.e., along S. All components of the integrands in (2.2.1) parallel to S remain bounded and hence, their contribution vanishes as $h \to 0$. The same applies to components of the integrands of the last two terms in (2.2.1) along $\underline{\nu}$. In view of these properties, upon letting h tend to zero in (2.2.1), we arrive at

$$\lim_{h\to 0} \int_{s=-h}^{h} \partial_j\tau_{ij}(\underline{x}+s\underline{\nu},t)ds = \lim_{h\to 0} \int_{s=-h}^{h} N_{js}\partial_s\tau_{ij}(\underline{x}+s\underline{\nu},t)ds$$

$$= \lim_{h\to 0} \nu_j[\tau_{ij}(\underline{x}+h\underline{\nu},t) - \tau_{ij}(\underline{x}-h\underline{\nu},t)] = 0, \qquad (2.2.5)$$

or

$$\nu_j[\tau_{ij}]_{1,2} = 0 \qquad \text{at } S, \tag{2.2.6}$$

where $[\tau_{ij}]_{1,2} = \tau_{ij}|_1 - \tau_{ij}|_2$, in which $|_\alpha$, with α=1,2, denotes the limiting value of the preceding quantity as S is approached via D_α. The interface condition (2.2.6) expresses the continuity of the traction $\tau_{ij}\nu_j$ across the interface S (see, e.g., Eringen, 1967, pp. 105-106, Landau and Lifshitz, 1966, pp. 50-51, or Truesdell and Toupin 1960, p. 546). Upon applying a similar procedure to the continuity equation in the following form (cf. (2.1.1)):

$$\partial_i v_i + (\partial_t \rho + v_i \partial_i \rho)/\rho = 0, \tag{2.2.7}$$

where, as far as the co-moving time derivative of the volume density of fluid mass is concerned the same condition as regards immiscibility is invoked as above, it follows that

$$\nu_i[v_i]_{1,2} = 0 \qquad \text{at } S, \tag{2.2.8}$$

i.e., the component of the fluid velocity that is normal to the interface is continuous across the interface (see, e.g., Eringen, 1967, pp. 105-106, or Landau and Lifshitz, 1966, p. 5). Upon rewriting the constitutive relation (2.1.8), in which we use (2.1.6), as

$$(1/2)(\partial_p v_q + \partial_q v_p) = \Phi_{pqij}\sigma_{ij}, \tag{2.2.9}$$

where Φ_{pqij} is the fluidity of the fluid, and employing the same procedure as above, we arrive at

$$\nu_p[v_q]_{1,2} + \nu_q[v_p]_{1,2} = 0 \qquad \text{at } S. \tag{2.2.10}$$

Contraction of this equation with ν_p leads to

$$[v_q]_{1,2} + \nu_p \nu_q [v_p]_{1,2} = 0 \qquad \text{at S.} \tag{2.2.11}$$

Combining (2.2.11) with (2.2.8), it follows that

$$[v_i]_{1,2} = 0 \qquad \text{at S,} \tag{2.2.12}$$

i.e., at a surface of discontinuity in matter separating two different viscous fluids, all components of the fluid velocity are to be continuous across this surface (see, e.g., Landau and Lifshitz, 1966, pp. 50-51). This boundary condition can also easily be understood physically: due to the presence of viscosity the fluid at one side of the interface drags the fluid at the other side along and vice versa. At a surface of discontinuity in matter separating two ideal fluids instead of two viscous ones, however, only the component of the fluid velocity normal to the interface is continuous across the interface (cf. (2.2.8)), and the continuity of the traction is replaced by the continuity of the pressure. Equation (2.2.6) is then replaced by (see, e.g., Landau and Lifshitz, 1966, pp. 50-51, or Truesdell and Toupin, 1960, p. 711)

$$[p]_{1,2} = 0 \qquad \text{at S.} \tag{2.2.13}$$

It is emphasized that in the above derivations of the interface conditions at S all interfacial effects, such as, e.g., surface tension, have been neglected. If one wants to deal with a surface of discontinuity with special properties, one usually accounts for the relevant effects by introducing so-called surface sources on the right-hand sides of the relevant boundary conditions. For a more detailed discussion on this subject we refer to Batchelor (1983, p. 60) and Slattery (1967), and to the references cited therein. Finally, we remark that if the procedure outlined above is applied to the local form of the equation of conservation of angular momentum no new interface conditions at S are obtained.

Finally, we analyze the boundary conditions at some special types of surfaces of discontinuity. First of all, at the boundary surface of a viscous fluid and a rigid and immovable body we have $v_i \to 0$ upon approaching the boundary surface of the body, i.e., the fluid adheres to the body (see, e.g., Landau and Lifshitz 1966, p. 50). On this type of boundary surface $\tau_{ij}\nu_j$ remains unspecified. For such a body in contact with an ideal fluid we have $\nu_i v_i \to 0$, and, hence, slip may occur parallel to the boundary surface, while instead of $\tau_{ij}\nu_j$ now p remains unspecified upon approaching the boundary surface. At a traction-free boundary surface of a viscous fluid we have $\tau_{ij}\nu_j \to 0$ upon approaching this boundary, while now v_i on the surface remains unspecified. For an ideal fluid in this latter case we have $p \to 0$, while, instead of v_i, now $\nu_i v_i$ remains unspecified upon approaching the traction-free surface (and the other components of v_i as well).

To conclude, a summary of the boundary conditions across a two-sided surface of discontinuity in material properties is given in Table 2.1. The explicit boundary conditions that have to be prescribed on boundaries of a specific type have been included as well.

Table 2.1. Boundary conditions for viscous and ideal fluids at a surface S of discontinuity in fluid properties.

type of boundary	viscous fluids	ideal fluids
interface between two fluids	v_i and $\tau_{ij}\nu_j$ continuous across S	$\nu_i v_i$ and p continuous across S
boundary surface of rigid and immovable body	$v_i \to 0$; $\tau_{ij}\nu_j$ remains unspecified on S	$\nu_i v_i \to 0$; p remains unspecified on S

(continued on next page)

Table 2.1. (continued)

traction-free boundary surface	$\tau_{ij}\nu_j \to 0$; v_i remains unspecified on S	$p \to 0$; $\nu_i v_i$ remains unspecified on S

2.3. ENERGY CONSIDERATIONS

In this section we consider the exchange of mechanical energy in a flowing fluid.

Consider a configuration where a fluid is present in some bounded domain D that moves along with the fluid. Let ∂D denote the closed boundary surface and let the unit vector along the normal to ∂D, pointing away from D, be denoted by ν_i (see Figure 2.3). As a first step to arrive

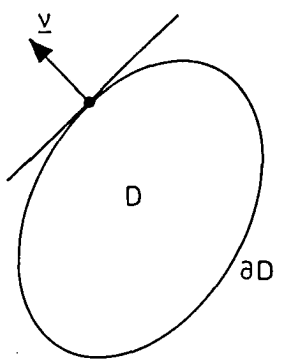

Fig. 2.3. Bounded domain D with closed boundary surface ∂D with unit vector ν_i along the normal to ∂D pointing away from D.

at the mechanical energy equation, we contract the equation of motion (2.1.2) with ν_i. This yields

$$v_i \partial_j \tau_{ij} + f_i v_i = \rho v_i (\partial_t v_i + v_j \partial_j v_i). \tag{2.3.1}$$

As a next step, we rewrite the first term on the left-hand side of (2.3.1) as

$$v_i \partial_j \tau_{ij} = \partial_j (v_i \tau_{ij}) - \tau_{ij} \partial_j v_i, \tag{2.3.2}$$

and the right-hand side as

$$\rho v_i (\partial_t v_i + v_j \partial_j v_i) = \partial_t [(1/2)\rho v_i v_i] + \partial_j [v_j (1/2)\rho v_i v_i]. \tag{2.3.3}$$

In (2.3.3) we have used the continuity equation (2.1.1). Subsequent integration of (2.3.1) over the domain D then leads with the aid of Gauss' theorem, (2.3.2), (2.3.3), and the identity

$$\int_D \partial_t [(1/2)\rho v_i v_i] dV + \int_{\partial D} (1/2)\rho v_j v_j v_i v_i dA$$

$$= d_t \int_D (1/2)\rho v_i v_i dV \tag{2.3.4}$$

to the result

$$\int_{\partial D} v_i \tau_{ij} \nu_j dA - \int_D \tau_{ij} \partial_j v_i dV + \int_D f_i v_i dV = d_t \int_D (1/2)\rho v_i v_i dV. \tag{2.3.5}$$

Now, since from (2.1.3) and (2.1.5) we further have

$$\tau_{ij} \partial_j v_i = \tau_{ij} d_{ij}, \tag{2.3.6}$$

(2.3.5) can be rewritten as

$$\dot{W}_{surface} + \dot{W}_{body} = d_t E_{kin} + \dot{W}_{def}, \tag{2.3.7}$$

in which the different terms can be interpreted as follows:

$$\dot{W}_{surface} = \int_{\partial D} v_i \tau_{ij} \nu_j dA \tag{2.3.8}$$

is the time rate at which the surface forces acting on ∂D deliver power to the fluid in D,

$$\dot{W}_{body} = \int_D f_i v_i dV \tag{2.3.9}$$

is the time rate at which work is done by the body forces acting on the fluid in D,

$$E_{kin} = \int_D (1/2)\rho v_i v_i dV \tag{2.3.10}$$

is the kinetic energy associated with the motion of the fluid in D, and

$$\dot{W}_{def} = \int_D \tau_{ij} d_{ij} dV \tag{2.3.11}$$

is the time rate at which work is done by the internal stresses in the fluid present in D. Equation (2.3.7) expresses the conservation of mechanical energy for the fluid during its motion, viz. the time rate at which work is done by the surface and the body forces acting on the fluid in D, is balanced by the sum of the rates of change of the kinetic energy of the fluid in D and the time rate at which work is done by the internal stresses of the fluid in D.

As regards the work done by the internal stresses, we note that some part of this work is, in general, reversibly stored, while the remaining part, which accounts for the different loss mechanisms in the fluid motion, is always irreversibly dissipated. In particular, working out the quantity $\tau_{ij} d_{ij}$ for a Newtonian fluid defined by (2.1.13) and using (2.1.4) and (2.1.15), it readily follows that

$$\tau_{ij} d_{ij} = - p d_{pp} + \zeta (d_{pp})^2 + 2\eta d'_{ij} d'_{ij}. \tag{2.3.12}$$

The first term on the right-hand side of (2.3.12) represents the volume density of the reversible rate of change of internal energy, while the sum of the last two terms represents the volume density of the time rate of dissipation of mechanical energy due to the viscosity of the fluid (see, e.g., Aris, 1962, p. 117, or Bird, Stewart and Lightfoot, 1960, p. 314, or Malvern, 1969, p. 300).

To conclude this section, we note that the mechanical energy quantity $\tau_{ij}d_{ij}$ often is referred to as the volume density of stress power (see, e.g., Eringen, 1967, p. 117).

2.4. MACH, STROUHAL, REYNOLDS AND FROUDE NUMBERS

In this section we examine the circumstances under which the flow of a Newtonian fluid can be regarded as incompressible. Furthermore, we discuss the conditions under which the non-linearity in the Navier-Stokes equations is sufficiently unimportant to be neglected, and the circumstances under which the non-steady flow of a Newtonian fluid can be approximated by a steady one. To conclude this section, we investigate for the case of subterranean flow of water, what simplified equations accurately describe the flow at the scale of the pores, i.e., in the interstices of the relevant subsoil. The latter equations will serve as a start, in the next chapter, for the analysis of groundwater flow.

In Section 2.1 we have listed the consequences of the important simplification that arises if a fluid flow behaves as if it were incompressible (see (2.1.22) and (2.1.25)). In this approximation, the variations in the volume density of fluid mass produced by the flow are sufficiently small to be negligible. Inspection of the continuity equation of mass flow (2.1.1) reveals that under these circumstances we must have (see, e.g., Batchelor, 1983, p. 167)

$$|(\partial_t \rho + v_i \partial_i \rho)/\rho| \ll |\partial_i v_i|. \tag{2.4.1}$$

From (2.1.20), the principle of local thermodynamic equilibrium, and the assumed isothermal flow, we further have

$$\partial_t \rho + v_i \partial_i \rho = (\partial_t p + v_i \partial_i p)/c_T^2, \tag{2.4.2}$$

where c_T denotes the isothermal speed of sound in the fluid. With the aid of (2.4.2), the condition (2.4.1) can be rewritten as (see, e.g., Batchelor, 1983, p. 167)

$$|(\partial_t p + v_i \partial_i p)/(\rho c_T^2)| << |\partial_i v_i|. \tag{2.4.3}$$

To elucidate the implications of (2.4.3), let us consider a given flow configuration and let l^*, v^*, Δp^*, ρ^* and c_T^* represent its characteristic linear dimension, characteristic fluid velocity, characteristic pressure difference, characteristic fluid-mass density and characteristic isothermal speed of sound, respectively. The non-steady fluid flow is further characterized by a characteristic frequency f^* that determines the rate at which the fluid quantities change in time. Then, the condition (2.4.3) under which a fluid flow may be regarded as incompressible leads to

$$Ma^2(1 + Sr)\Delta p^*/(\rho^* v^{*2}) << 1, \tag{2.4.4}$$

where

$$Ma = v^*/c_T^* \tag{2.4.5}$$

is known as the Mach number (see, e.g., Landau and Lifshitz, 1966, p. 171, or Batchelor, 1983, p. 168), and

$$Sr = l^* f^*/v^* \tag{2.4.6}$$

is known as the Strouhal number (see, e.g., Landau and Lifshitz, 1966, p. 63, or Batchelor, 1983, p. 216). To estimate the order of magnitude of Δp^* in (2.4.4), we now consider the Navier-Stokes equation (2.1.19) in some more detail. First of all, we note that in the course of our applications of (2.1.19) the only body force to be present is assumed to be the one due to gravity. Hence, we write

$$f_i = \rho g_i, \tag{2.4.7}$$

in which g_i denotes the local acceleration of free fall. In analyzing (2.1.19), we start with gaining some insight in the orders of magnitude of the convective inertia forces and the viscous forces. The former is given by $\rho^* v^{*2} / l^*$ and the latter by $\eta^* v^* / l^{*2}$, in which η^* represents the characteristic dynamic viscosity, and where it should be noted that in this last estimation it is assumed that the order of magnitudes of the bulk viscosity ζ and the dynamic viscosity η are the same, although the effects of the former viscosity can be neglected in most fluid flow situations met in practice (see Section 2.1). Now, the ratio of the orders of magnitude of the two forces [(convective inertia forces)/(viscous forces)], designated as Re, is given by

$$Re = \rho^* v^* l^* / \eta^* \tag{2.4.8}$$

and is known as Reynolds number (see, e.g., Landau and Lifshitz, 1966, p. 62, or Batchelor, 1983, p. 214). For a fluid flow at small Reynolds number, the convective inertia forces are at each point in the fluid negligible with respect to the viscous forces; the flow is only controlled by the pressure forces, the viscous forces, the forces due to gravity and the local inertia forces, and as a consequence, the characteristic pressure difference Δp^* is of the order of magnitude of $(\eta^* v^* / l^* + \rho^* g^* l^* + \rho^* f^* v^* l^*)$, where g^* represents the characteristic local acceleration of free fall. Hence, with the aid of (2.4.6) and (2.4.8), the condition (2.4.4) for incompressible fluid flow at low Reynolds numbers becomes (cf., e.g., Tritton, 1977, p. 59)

$$Ma^2 (1 + Sr)(1/Re + 1/Fr^2 + Sr) << 1, \tag{2.4.9}$$

where

$$Fr = v^* / (l^* g^*)^{1/2} \tag{2.4.10}$$

is known as the Froude number (see, e.g., Landau and Lifshitz, 1966, p. 63). Thus, under the circumstances that Re << 1, the fluid is behaving as if it were incompressible whenever the condition (2.4.9) is satisfied.

In addition to the above, we determine the conditions under which the non-steady flow of the fluid at small Reynolds numbers can be approximated by a steady one. To this end, we compare in (2.1.19) the local inertia force term with the viscous force term; the ratio of these two [(local inertia forces)/(viscous forces)] is (cf. (2.4.6) and (2.4.8))

$$\rho^* f^* l^{*2} / \eta^* = \mathrm{Re} \cdot \mathrm{Sr}. \qquad (2.4.11)$$

Hence, for small Reynolds numbers a non-steady Newtonian-fluid flow can be approximated by a steady one whenever the additional condition $\mathrm{Re} \cdot \mathrm{Sr} << 1$ is satisfied. Finally, it should be noted that, in general, only for periodic fluid flows the Strouhal number is taken to have a value different from unity. For a non-periodic flow we take $f^* = v^*/l^*$, which entails that Sr = 1; as a consequence, a non-periodic flow of a Newtonian fluid at small Reynolds number is only controlled by the pressure forces, the viscous forces and forces due to gravity.

As already remarked in the introduction to this section, we need in Chapter 3 the equations that accurately describe the flow of groundwater in the interstices of common subsoils, the soil being envisaged as a water-saturated porous medium. Hence, at this stage in our analysis, we may gain some insight into the possible approximations of the general basic equations that govern the flow inside the pores of water-saturated soils. First of all, we note that in the case of subterranean water flow it seems to be fair that, due to the large heat capacity of the water-solid composite, all flow processes involved can be considered as isothermal processes. Now, for permeation of water in common subsoils, a typical value of the volume density of fluid mass is given by $\rho^* \approx 1.0 \times 10^3$ kg/m^3, a typical value of the viscosity by $\eta^* \approx 1.5 \times 10^{-3}$ Pa·s, and a representative value of the characteristic

linear dimension of the pores in the porous system by $l^* \approx 1.0\times10^{-5}$ m. Then, for a characteristic fluid velocity of $v^* \approx 1.0\times10^{-3}$ m/s, which in common groundwater flow situations is considered as rather high, a Reynolds number of $Re \approx 6.7\times10^{-3}$ results. Hence, in all applications to groundwater flow we have $Re << 1$. Furthermore, on the assumption that the groundwater flow under consideration is non-periodic, we have (cf. (2.4.6)) $Sr = 1$, and hence, as outlined above, the fluid flow in the pores is controlled by the pressure forces, the viscous forces, and the forces due to gravity only. Now, in order to determine whether or not the fluid flow inside the pores can be approximated by an incompressible one, we are left with the task of estimating Ma^2, Ma^2/Re, and $(Ma/Fr)^2$ (cf. (2.4.9)). For the configurations at hand, a characteristic value of the isothermal speed of sound is $c_T \approx 1.4\times10^3$ m/s, and a typical value of the local acceleration of free fall is $g^* \approx 10$ m/s^2. Utilizing (2.4.5), (2.4.8), and (2.4.10), we then find $Ma^2 \approx 5.1\times10^{-13}$, $Ma^2/Re \approx 7.7\times10^{-11}$, and $(Ma/Fr)^2 \approx 5.1\times10^{-11}$, respectively. Clearly, with these values, and $Sr = 1$, the condition (2.4.9) under which a Newtonian-fluid flow behaves as if it were incompressible is found to be not a very restrictive one.

In summary, the flow phenomena inside the pores of common, water-saturated, subsoils, are, first of all, governed by the continuity equation as given in (2.1.22). Secondly, we have Cauchy's first law of motion in the absence of the inertia forces and identification of the body forces with the force due to gravity, i.e., (cf. (2.1.2) and (2.4.7))

$$\partial_j \tau_{ij} + \rho g_i = 0, \tag{2.4.12}$$

which is known as the equation for creeping motion (see, e.g., Tritton, 1977, p. 82). Finally, (2.1.22) and (2.4.12) have to be supplemented by (2.1.4), the constitutive equation (2.1.23), and the equation of deformation rate (2.1.6). These equations will play a fundamental role in the next chapter, where they serve as the point of departure for

developing the theory of permeation processes of groundwater in common subsoils, such as aquifers, dams, etc.

CHAPTER 3

BASIC MACROSCOPIC RELATIONS FOR FLOW OF GROUNDWATER

In this chapter, we develop the basic relations, on a macroscopically averaged scale, for the flow of a single-phase fluid in a porous medium. In particular, we discuss the macroscopic relations for the flow of groundwater, where the soil is envisaged as a water-saturated porous substance.

In principle, once the equations that govern the flow phenomena inside the pores of a porous medium are known and once the geometry of all interstices in the porous material is determined, the flow problem can, on this scale, be solved. However, due to the fact that measurements inside the pores can, in general, not be easily performed, and the fact that the detailed geometries of the interstices cannot properly be described for the majority of porous media that one observes in practice, this procedure will usually amount to an unfeasible task. Fortunately, in most practical civil-engineering groundwater flow problems, one's interest is not to gain a detailed insight into the behavior of fluid-flow phenomena on the scale of the pore sizes (the so-called microscopic scale), but merely to analyze fluid/solid systems on the gross, or average scale (the so-called macroscopic scale). For example, the design of civil-engineering structures calls for the determination of the macroscopic flow pattern of the groundwater in formations like aquifers, dams, etc., where the average or macroscopic quantities are associated with the ones that one usually observes and measures in a practical field situation.

Solutions of groundwater flow problems are generally based on various, often rather intuitive, generalizations of the one-dimensional empirical law formulated by Darcy in 1856 (Darcy, 1856). Examples of this partly heuristic and empirical approach to the modeling of three-dimensional fluid flows in homogeneous and inhomogeneous anisotropic subsoils can be found in Muskat (1946, pp. 127-136), Morse and Feshbach (1953, p. 172), Polubarinova-Kochina (1962, pp. 343-345), Scheidegger (1963, pp. 76-79), Bear (1972, pp. 119-125), and Batchelor (1983, pp. 223-234). Although with the aid of these generalizations many practical problems concerned with, e.g., groundwater flow in aquifers, seepage from dams, etc., can successfully be solved, there is a need for a more profound theoretical justification of the various generalized Darcy's laws, as well as for explicit knowledge under which conditions they apply.

The literature on the many theoretical aspects of the behavior of multi-component systems, such as fluid/solid systems, on a macroscopic scale is very extensive. Apart from the partly phenomenological and heuristic approaches referred to above, one distinguishes between the so-called direct and indirect approaches. In the direct approach, the multi-component system is treated directly at the relevant macroscopic level and hence, in terms of continuum physics, the multi-component system is envisaged as a system of overlapping continua. The relevant conservation equations are postulated directly at the macroscopic level and are intuitive extensions of the basic equations that hold for a single-phase continuum. The constitutive equations are then developed at this macroscopic level as well, often in a manner similar to the one used in the theory of mixtures (see, e.g., Bowen, 1976). For example, Bowen (1984, pp. 63-119), employes this method for formulating various mathematical models of porous media. The resultant equations are, however, in most cases too general for practical use. In the indirect approach, one starts from the well-established conservation equations at the microscopic level pertaining to each constituent separately, sometimes supplemented by the relevant constitutive equations at this

level. Then, upon applying to these equations some mathematical averaging procedure, one arrives at equations that hold on a higher level, viz. the macroscopic one. As a first example of this indirect approach we mention the so-called two-space method of homogenization used in statistical physics, where one uses a spatial averaging procedure in addition to a rather complicated asymptotic analysis. This method reveals which effects at the microscopic level play a role at the macroscopic level. Keller (1980) has employed this method to assert Darcy's law, while Burridge and Keller (1981) and later Auriault, Borne and Chambon (1985) have used it to treat various aspects of poroelasticity. A different type of indirect approach is furnished by the spatial averaging procedure. Here, the equations at the microscopic scale are averaged over a so-called representative elementary domain of the relevant multi-component composite. This kind of averaging was initiated by Slattery (1967) and by Whitaker (1967 and 1969) and was employed to arrive at macroscopic equations for the flow of single-phase fluids in porous solids. The method has later been used and extended by many others in order to develop "rigorous" theories for more complicated flow phenomena in porous systems, for example, systems containing multi-phase fluids together with multi-phase solids (see, e.g., Dybbs and Schweitzer, 1973, Gray and O'Neill, 1976, or De la Cruz and Spanos, 1983). In particular, we mention the work by Hassanizadeh and Gray (1979a,b, and 1980), who adopted the spatial averaging method to derive general macroscopic conservation laws for multi-phase systems. They postulate a general set of admissible constitutive relations at the macroscopic scale and then apply a special method from thermodynamics (the method of Coleman and Noll (1963)) to reduce this general set to proper ones that do not violate the second law of classical thermodynamics. However, the constitutive equations thus obtained are often, even after applying, for example, an extensive linearization procedure, too general for use in practice. This is partly due to the fact that the method does not exploit often important additional information from some of the fluid and/or solid properties at the microscopic level. For example, in the case of flow of a single-phase

fluid in some porous material, one can often determine the viscosity of the fluid rather easily. Furthermore, due to the large heat capacity of, for example, the fluid-solid composites one observes in common water-saturated subsoils, one may consider, in a first approximation, the flow processes to proceed under isothermal conditions and, in addition to this, one may often approximate the interstitial fluid flow by an incompressible one.

To conclude this brief overview of some of the numerous theories of the modeling of multi-phase systems at a macroscopic scale, it should be noted that recently, by using consistently a particular procedure of *volume averaging only*, a *macroscopic theory for acoustic wave phenomena* in porous solids has been developed (De la Cruz and Spanos, 1985, and De Vries and De Hoop, 1988).

Finally, for a more detailed overview of the various attempts to develop correct and adequate macroscopic descriptions for multi-component composites we refer to Hassanizadeh and Gray (1979a,b, and 1980), and Bachmat and Bear (1987, pp. 5-20), as well as to the references cited therein.

In the present analysis, the basic equations, on a macroscopic scale, for the creeping, incompressible flow of a Newtonian fluid in a porous solid are developed upon utilizing an indirect method which to some extent is similar to the one introduced by Slattery (1967) and Whitaker (1969), i.e., we average the "microscopic" conservation and constitutive equations over a representative elementary domain of the fluid-solid composite; the solid matrix material being envisaged as rigid and immovable. The choice in favor of this kind of averaging procedure is based on the fact that the expressions that arise after applying the volume averaging operator all have, in general, a clear physical meaning, and can be identified in a natural way with the quantities one usually observes and measures in practice. An additional advantage of the volume averaging method applied here is that all mathematical procedures involved are straightforward.

Section 3.1 deals with the relevant averaging definitions and provides the necessary tools for Section 3.2 in which they are applied to the linearized equations for quasi-steady, incompressible, viscous fluid flow. It is shown that, as far as the macroscopic equation of motion for the permeation of groundwater is concerned, we end up with an equation that essentially is Darcy's law. In Subsection 3.2.1 we incorporate in the macroscopic equations for subterranean waterflow the action of external sources that comply with the structure of these equations. In Subsection 3.2.2 it is shown how the quantity that one observes in a practical pressure-gauge measurement in groundwater flow is related to the volume-averaged pressure introduced in the section preceding it. The boundary conditions that are compatible with the relevant macroscopic groundwater flow equations and that apply at a surface of discontinuity in material properties are discussed in Section 3.3. Finally, in Section 3.4, the uniqueness of the solution of those groundwater flow problems that can mathematically be formulated as boundary-value problems is investigated upon utilizing energy considerations.

3.1. AVERAGING CONSIDERATIONS

The basic assumption underlying our analysis is that the macroscopic, large-scale, properties of a fluid-filled porous medium and a corresponding description of the flow phenomena involved can be arrived at by the spatial averaging of the relevant pore-scale quantities and equations over a so-called representative elementary domain of the porous medium under consideration.

Although the concept of a representative elementary domain of a multi-phase system is well established in the literature on flow in porous media (see, e.g., Whitaker, 1969, Bear, 1972, pp. 19-22, Hassanizadeh and Gray, 1979a, or Baveye and Sposito, 1984), we first summarize for completeness in some detail its essential features. To this end, it is helpful to consider the following hypothetical experiment applied to some fluid-saturated porous material. At a fixed time, we average a local, pore-scale, fluid quantity over a spatial domain whose characteristic linear dimension, to be denoted by d, varies from very small to very large (e.g., we integrate the relevant local quantity over a sphere whose radius varies from less than the size of the diameter of the pores up to several thousands of times of the latter value). In the beginning, rapid fluctuations in the averaged fluid quantity may occur; clearly, these can be ascribed to the fact that relatively large portions of the fluid phase and/or the solid phase of the porous medium become gradually included in the averaging domain and therefore strongly affect the averaged quantity. Let the representative length scale over which these rapid variations occur be denoted by $L_<$. Then, $L_<$ represents the so-called microscopic characteristic length scale of the porous medium under consideration. An increase of the characteristic linear dimension d of the averaging domain will smooth out these rapid fluctuations and the averaged fluid quantity will, within some interval, be independent of d.

A further increase of d may lead again to variations in the averaged fluid quantity. These ones are due to the large-scale (gross) inhomogeneities of the porous medium and occur at the so-called macroscopic scale of the relevant porous medium. Now, in order to arrive at a meaningful averaged quantity and so at a meaningful averaging procedure, the averaged quantity should be insensitive to small changes of d. Clearly, this does not happen if d is either so small that it is of the order of the diameter of the interstices, or so large that the macroscopic inhomogeneities affect the averaging procedure. Hence, the reasonings outlined above lead to the following criterion for d:

$$L_< \ll d \ll L_>, \tag{3.1.1}$$

where $L_>$ represents the characteristic scale of the macroscopic inhomogeneities. At this stage it should be noted that for those fluid-filled porous media for which (3.1.1) does not apply (e.g., if $L_>$ cannot be identified), the "representative elementary domain concept" fails, and instead of the domain averaging procedure one has to resort to other techniques. For those cases where (3.1.1) does apply, the representative elementary domain for the pertaining quantity can be introduced.

Recently, Bachmat and Bear (1987, pp. 5-20) have presented, upon utilizing a statistical procedure, quantitative upper and lower limits of d. In an actual multi-phase system these upper and lower limits can serve to select an appropriate value for d and hence for the volume of the representative elementary domain (see, e.g., Van der Grinten, 1987).

In what follows, it is assumed that a common representative elementary domain can be determined for all relevant microscopic quantities to be averaged. This representative elementary domain will be denoted as D_ε; it is taken to be time- and shift-invariant, and its position is specified by the position vector $\underline{x}$ of its "center", for which we take its barycenter, given by (see Figure 3.1)

$$\underline{x} = V_\varepsilon^{-1} \int_{\underline{x}' \in D_\varepsilon(\underline{x})} \underline{x}' dV, \tag{3.1.2}$$

where

$$V_\varepsilon = \int_{\underline{x}' \in D_\varepsilon(\underline{x})} dV = \int_{\underline{\xi} \in D_\varepsilon(\underline{0})} dV \tag{3.1.3}$$

is the volume of $D_\varepsilon = D_\varepsilon(\underline{x})$, and where the shift invariance of D_ε implies that if $\underline{x}' \in D_\varepsilon(\underline{x})$ with $\underline{x}' = \underline{x} + \underline{\xi}$, then $\underline{\xi} \in D_\varepsilon(\underline{0})$. All averages over D_ε of

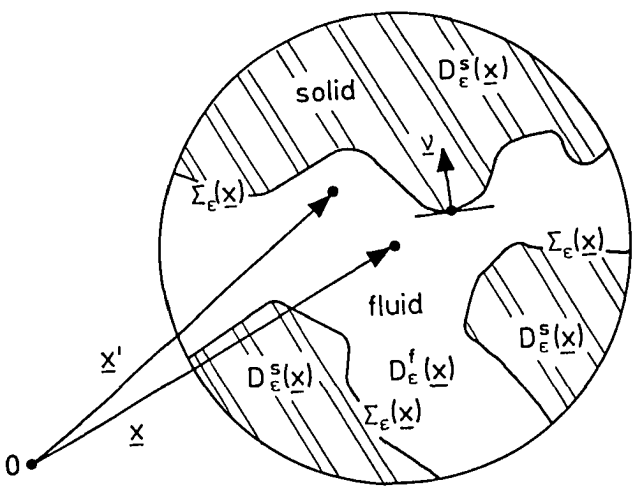

Fig. 3.1. The position vector $\underline{x}'$ of the fluid and solid particles in the subdomains D_ε^f and D_ε^s inside the (schematic) representative elementary domain D_ε with position vector $\underline{x}$. The solid matrix material is assumed to be rigid and immovable.

the pore-scale quantities are assigned to the position of the barycenter of D_ε, and are subsequently identified with the corresponding quantities on the macroscopic scale. By following this procedure, we use in fact the so-called continuum hypothesis (of statistical physics): appropriate averages over D_ε of microscopic quantities lead to the associated macroscopic quantities, where the latter are assumed to vary piecewise continuously with position. By this spatial averaging process, the actual fluid-filled porous medium is replaced by a model continuum.

In our applications we assume the solid phase of the fluid-saturated porous material to be rigid and immovable, and to be noninteracting with the fluid filling the void space, while the interstices of the porous system are assumed to be interconnected.

In the two-component composite of the fluid-saturated porous medium, $D_\varepsilon = D_\varepsilon(\underline{x})$ is the union of the subdomain $D_\varepsilon^f(\underline{x})$ in which the fluid is present and the subdomain $D_\varepsilon^s(\underline{x})$ in which the solid is present (see Figure 3.1). The volumes of $D_\varepsilon^f(\underline{x})$, and $D_\varepsilon^s(\underline{x})$ are denoted by $V_\varepsilon^f(\underline{x})$, where

$$V_\varepsilon^f(\underline{x}) = \int_{\underline{x}' \in D_\varepsilon^f(\underline{x})} dV, \tag{3.1.4}$$

and $V_\varepsilon^s(\underline{x})$, where

$$V_\varepsilon^s(\underline{x}) = \int_{\underline{x}' \in D_\varepsilon^s(\underline{x})} dV, \tag{3.1.5}$$

respectively. The volume fractions occupied by the fluid in D_ε is denoted by

$$\phi^f(\underline{x}) = V_\varepsilon^f(\underline{x})/V_\varepsilon; \tag{3.1.6}$$

it is also known as the volumetric porosity of the medium. The volume fraction ϕ^s occupied by the solid in D_ε is denoted by

$$\phi^s(\underline{x}) = V_\varepsilon^s(\underline{x})/V_\varepsilon. \tag{3.1.7}$$

Since $V_\varepsilon = V_\varepsilon^f(\underline{x}) + V_\varepsilon^s(\underline{x})$, it readily follows that for all $\underline{x}$ throughout the domain of application we have (cf. (3.1.3) - (3.1.7))

$$\phi^f(\underline{x}) + \phi^s(\underline{x}) = 1 \quad \text{and} \quad 0 \leq \phi^f(\underline{x}) \leq 1, \quad 0 \leq \phi^f(\underline{x}) \leq 1. \tag{3.1.8}$$

For any quantity ψ associated with the fluid phase in D_ε (ψ may be a scalar, or a Cartesian component of a vector, or a tensor of arbitrary rank) we now define its corresponding "fluid average", designated as $\langle\psi\rangle$, and its corresponding "intrinsic fluid average", to be denoted by $\langle\psi\rangle^f$, as

$$\langle\psi\rangle(\underline{x},t) = V_\varepsilon^{-1} \int_{\underline{x}' \in D_\varepsilon^f(\underline{x})} \psi(\underline{x}',t)dV \tag{3.1.9}$$

and

$$\langle\psi\rangle^f(\underline{x},t) = [V_\varepsilon^f(\underline{x})]^{-1} \int_{\underline{x}' \in D_\varepsilon^f(\underline{x})} \psi(\underline{x}',t)dV, \tag{3.1.10}$$

respectively. From (3.1.6) and (3.1.9) - (3.1.10) the interrelation between $\langle\psi\rangle$ and $\langle\psi\rangle^f$ follows as

$$\langle\psi\rangle(\underline{x},t) = \phi^f(\underline{x})\langle\psi\rangle^f(\underline{x},t). \tag{3.1.11}$$

In the volume averaging of the pore-scale equations to be carried out in Section 3.2, a mathematical relation is needed which links the averages of the spatial derivatives of microscopic quantities to the spatial derivatives of their averages, i.e., to the spatial derivatives of the macroscopic quantities. In the literature on the subject the relevant relation is known as the "Slattery-Whitaker averaging theorem", formulated independently by Slattery and by Whitaker in 1967. For ψ the relevant interrelation between $\partial_i\langle\psi\rangle$ and $\langle\partial_i\psi\rangle$ amounts to (see, e.g., Slattery, 1967, p. 1067, or Whitaker, 1969, p. 20)

$$\partial_i \langle\psi\rangle(\underline{x},t) = \langle\partial'_i\psi\rangle(\underline{x},t) - V_\varepsilon^{-1} \int_{\underline{x}'\in\Sigma_\varepsilon(\underline{x})} \nu_i(\underline{x}')\psi(\underline{x}',t)dA, \qquad (3.1.12)$$

where ∂'_i denotes partial differentiation with respect to x'_i, Σ_ε represents the interface(s) between the fluid phase and solid phase as far as they are present in the interior of D_ε, and ν_i denotes the unit vector along the normal to Σ_ε pointing away from D_ε^f (see Figure 3.1). The proof of this theorem as given by Slattery (1967, p. 1067) and Whitaker (1969, pp. 18-20) has been obtained by applying several, rather tedious and inconvenient, manipulations with the general Reynolds transport theorem (Truesdell and Toupin, 1960, p. 347). Later, Gray and Lee (1977) have presented a different proof of (3.1.12) based, to some extent, on the theory of generalized functions. In Appendix A, an alternative, less verbose, proof of (3.1.12) is presented that is based on Gauss' theorem.

To conclude this section, we observe that upon substituting $\psi = 1$ in (3.1.12), we are led to (cf. (3.1.6))

$$\partial_i \phi^f(\underline{x}) = - V_\varepsilon^{-1} \int_{\underline{x}'\in\Sigma_\varepsilon(\underline{x})} \nu_i(\underline{x}')dA. \qquad (3.1.13)$$

The averaging operators (3.1.9) and (3.1.10), and the property (3.1.12) are used in the next section.

3.2. VOLUME AVERAGING OF THE PORE-SCALE EQUATIONS

In this section it is shown how the equations governing the flow of groundwater on a macroscopic scale arise from the volume averaging over the representative elementary domain D_ε of the pore-scale equations for creeping flow.

As argued in Section 2.4, the isothermal flow in the interstices of a water-saturated soil can, for most cases met in practice, be accurately described by the equations for quasi-steady, incompressible, viscous fluid flow. The relevant equations are recapitulated below (cf. (2.1.22), (2.4.12), (2.1.4), (2.1.23), and (2.1.6)):

$$\partial_i v_i = 0, \tag{3.2.1}$$

$$\partial_j \tau_{ij} + \rho g_i = 0, \tag{3.2.2}$$

$$\tau_{ij} = - p\delta_{ij} + \sigma_{ij}, \tag{3.2.3}$$

where

$$\sigma_{ij} = 2\eta d_{ij} \tag{3.2.4}$$

and

$$d_{ij} = (1/2)(\partial_i v_j + \partial_j v_i). \tag{3.2.5}$$

We start the averaging procedure by applying the volume averaging operator as defined in (3.1.9) to (3.2.1) - (3.2.5). In view of the assumption that ρ and g_i in (3.2.2) and η in (3.2.4) can be taken to be constant over D_ε^f, and observing the property (3.1.12), we then obtain

$$\partial_i \langle v_i \rangle = - V_\varepsilon^{-1} \int_{\underline{x}' \in \Sigma_\varepsilon(\underline{x})} \nu_i v_i \, dA, \tag{3.2.6}$$

$$\partial_j \langle \tau_{ij} \rangle + \phi^f \rho g_i = - V_\varepsilon^{-1} \int_{\underline{x}' \in \Sigma_\varepsilon(\underline{x})} \nu_j \tau_{ij} \, dA, \tag{3.2.7}$$

$$\langle \tau_{ij} \rangle = - \langle p \rangle \delta_{ij} + \langle \sigma_{ij} \rangle, \tag{3.2.8}$$

$$\langle \sigma_{ij} \rangle = 2\eta \langle d_{ij} \rangle, \tag{3.2.9}$$

and

$$\langle d_{ij} \rangle = (1/2)(\partial_i \langle v_j \rangle + \partial_j \langle v_i \rangle) + V_\varepsilon^{-1} \int_{\underline{x}' \in \Sigma_\varepsilon(\underline{x})} (1/2)(\nu_i v_j + \nu_j v_i) \, dA, \tag{3.2.10}$$

where the second term on the left-hand side of (3.2.7) has been obtained with the aid of (3.1.4) and (3.1.6). In interpreting the different surface integrals over the fluid/solid interface(s) Σ_ε in (3.2.6), (3.2.7) and (3.2.10), we first recall that the solid matrix of the porous system was assumed to be rigid and immovable. Then, with the aid of the boundary conditions listed in Table 2.1, we have upon approaching Σ_ε from D_ε^f (see Figure 3.1)

$$v_i = 0 \qquad \text{at } \Sigma_\varepsilon, \tag{3.2.11}$$

and, as an immediate consequence, the surface integrals over Σ_ε in the right-hand sides of (3.2.6) and (3.2.10) vanish identically. Hence, (3.2.6) and (3.2.10) reduce to

$$\partial_i \langle v_i \rangle = 0, \tag{3.2.12}$$

and

$$\langle d_{ij} \rangle = (1/2)(\partial_i \langle v_j \rangle + \partial_j \langle v_i \rangle), \tag{3.2.13}$$

respectively. This leaves us with the task of interpreting the remaining integral at the right-hand side of (3.2.7). At this stage in our analysis, it should be emphasized that the averaged equations (3.2.6) - (3.2.10) and (3.2.12) - (3.2.13) are exact within the approximations that have already been made. However, without a further relationship between the remaining surface integral in (3.2.7) and some averaged, macroscopic, field quantity, the equations are not yet fully on the macroscopic scale. Clearly, the relevant integral represents the volume density of the total force that the fluid via the fluid/solid interface(s) Σ_ε exerts on the rigid solid material. To get some idea of what the fluid/solid interaction integral amounts to, we apply the volume averaging procedure to the simpler pore-scale equation for hydrostatic equilibrium.

For a fluid in hydrostatic equilibrium, (3.2.2) reduces to

$$- \partial_i p + \rho g_i = 0, \tag{3.2.14}$$

from which we have

$$p = \rho g_i x_i + p_o, \tag{3.2.15}$$

where p_o is an arbitrary constant pressure. Upon applying the volume averaging operator (3.1.9) to (3.2.14) we arrive with the aid of (3.1.12) and (3.1.6) at

$$- \partial_i \langle p \rangle + \phi^f \rho g_i - V_\varepsilon^{-1} \int_{\underline{x}' \in \Sigma_\varepsilon(\underline{x})} p \nu_i dA = 0. \tag{3.2.16}$$

To obtain a macroscopic value for the surface integral in (3.2.16), which represents the volume density of force that the fluid, in equilibrium, exerts on the rigid solid material in D_ε^s, we further apply the intrinsic

volume averaging operator as defined in (3.1.10) to (3.2.15). The result can be written as

$$\langle p\rangle^f(\underline{x}) = \rho g_i x_i + \rho g_i\left(\langle x_i'\rangle^f(\underline{x}) - x_i\right) + p_o, \tag{3.2.17}$$

in which $(\langle x_i'\rangle^f(\underline{x}) - x_i)$ represents the vectorial distance between the position vector of the barycenter of the subdomain D_ε^f of D_ε and the position vector of the barycenter of D_ε itself (cf. (3.1.2)). However, the difference between these two position vectors is of the order of magnitude of the microscopic length scale $L_<$ of the porous medium under consideration; on the scale d the term averages out (this condition is inherent to the assumption that the volume averages introduced are, within certain limits, insensitive to the choice of d). Upon differentiating both sides of (3.2.17) with respect to x_i, we then have (cf. (3.1.1))

$$\partial_i\langle p\rangle^f = \rho g_i\left[1 + \text{Order}(L_</L_>)\right] \approx \rho g_i. \tag{3.2.18}$$

Now, upon utilizing (3.2.18) in (3.2.16) it is with the further aid of (3.1.11) easily verified that the following expression for the surface integral in (3.2.16) results:

$$V_\varepsilon^{-1}\int_{\underline{x}'\in\Sigma_\varepsilon(\underline{x})} p\nu_i dA = -\langle p\rangle^f\partial_i\phi^f. \tag{3.2.19}$$

The macroscopic picture associated with (3.2.19) can be elucidated as follows. Due to the fact that the solid phase in D_ε is, in general, not completely surrounded by the fluid phase (see Figure 3.1) the volume density of force which the fluid, under hydrostatic conditions, exerts on the solid material in D_ε differs from $-\phi^S\rho g_i$ and is, as (3.2.19) shows, balanced by the product of the intrinsically averaged hydrostatic fluid pressure and the gradient of the volumetric porosity. Finally, upon identifying $\langle p\rangle^f$ with the macroscopic pressure that one usually observes

and measures in practice (see Subsection 3.2.2), (3.2.18) constitutes the equation for hydrostatic equilibrium at the macroscopic scale.

Now, let us return to the analysis of the fluid/solid interaction integral in (3.2.7). Since rigidity and immovability of the porous material have been preassumed, it is obvious that its hydrodynamic part (its hydrostatic part led to (3.2.19)) can be seen as the volume density of resultant resistance or drag force that the fluid in D_ε^f experiences when it permeates through the interconnected interstices of the porous substance. In general, these resistance or drag forces depend on the statistical properties of the interface Σ_ε and on the physical properties of the fluid under consideration. For instance, the latter forces vanish if there is either no fluid motion, or no viscosity, or no solid phase at all. In principle, we could via methods of statistical physics arrive at the macroscopic value of these forces. This, however, is beyond the scope of the present analysis. On the other hand, it is well known that an isolated, rigid and immovable, spherical solid particle of radius r, immersed in an unbounded, uniform, steady fluid flow at a small Reynolds number, whose velocity at a large distance from the particle is v_i^∞, experiences a hydrodynamic surface force F_i^h given by (see, e.g., Landau and Lifshitz, 1966, p. 66, or Batchelor, 1983, pp. 230-235)

$$F_i^h = 6\pi\eta r v_i^\infty, \tag{3.2.20}$$

which is known as Stokes' formula and which constitutes a linear relationship between F_i^h and v_i^∞. Now, Brenner (1963) has shown that for an object of arbitrary shape, the direction of the hydrodynamic surface force is not necessarily the same as the one of the "velocity at a large distance" and has derived the following linear relationship between F_i^h and v_i^∞:

$$F_i^h = \eta a_{ij} v_j^\infty, \tag{3.2.21}$$

where a_{ij} is a symmetric and positive definite tensor that only reflects the intrinsic properties of the solid particle, viz. its geometrical shape and dimensions. Now, upon identifying v_i^{∞} with the averaged velocity $\langle v_i \rangle$, it seems fair to assume that on the macroscopic scale the net part of the hydrodynamic surface force in (3.2.7) (produced by the fluid motion) is also linearly related to $\langle v_i \rangle$ and is a fraction of the value that would hold for the isolated solid particles considered above. Accordingly, with the further aid of the results obtained from the hydrostatic case we now postulate the following linear expression for the relevant interaction integral on the right-hand side of (3.2.7):

$$V_\varepsilon^{-1} \int_{\underline{x}' \in \Sigma_\varepsilon(\underline{x})} \nu_j \tau_{ij} dA = - \phi^f R_{ij} \langle v_j \rangle + \langle p \rangle^f \partial_i \phi^f . \qquad (3.2.22)$$

Equation (3.2.22) constitutes, within the realm of a linear theory, the most general relationship that exists between the fluid/solid interaction integral and the averaged macroscopic field quantities. In (3.2.22), R_{ij} is denoted as the tensorial resistivity of the fluid-filled porous medium and incorporates the topological properties of the rigid solid material in D_ε^s as well as the viscous properties of the fluid. By analogy with a_{ij} in (3.2.21), we assume R_{ij} to be symmetric and positive definite. The inclusion of the factor ϕ^f in the flow resistance term in (3.2.22) accounts for the fact that in the absence of a fluid phase the concept of a flow resistance is no longer meaningful. Relations similar to (3.2.22), but based on other arguments, have also been formulated by, for example, Lehner (1979) and Hassanizadeh and Gray (1980). In the work of Hassanizadeh and Gray (1980), the right-hand side of (3.2.22) only arises after a strong reduction of their general set of macroscopic constitutive equations, viz. after applying a linearization procedure, neglecting inertia and thermal effects, etc. Lehner (1979) ends up with (3.2.22) as an immediate result of a reciprocity relation that involves the volume averaged stress and the volume averaged fluid velocity. However, in deriving this reciprocity theorem by averaging an approximated form of

the mechanical energy balance for fluid flow at the pore-scale, he directly links the volume average of the product of two microscopic fluid quantities to the product of the volume average of each of the two quantities, without proving that such relationship applies. The reciprocity theorem arrived at shows that, in fact, the symmetry of R_{ij} has been preassumed in the onset of the procedure.

A straightforward dimensional analysis shows that we can write

$$R_{ij} = \eta R'_{ij}, \tag{3.2.23}$$

where R'_{ij} is the so-called *intrinsic resistivity of the porous medium*. The inverse of R'_{ij} can be identified with the tensorial (intrinsic) permeability that one is accustomed to use in practical groundwater flow problems. Henceforth, we shall use R_{ij} as the fundamental constitutive parameter that is representative of the resistance that the flow encounters.

Returning to (3.2.7), with (3.2.22) now substituted in it, and using (3.1.11) and (3.2.8), we are led to the following equation of motion:

$$- \phi^f \partial_i \langle p \rangle^f + \partial_j \langle \sigma_{ij} \rangle - \phi^f R_{ij} \langle v_j \rangle = - \phi^f \rho g_i, \tag{3.2.24}$$

which has to be supplemented by (3.2.9), (3.2.13), and (3.2.12). The macroscopic picture associated with these equations is that the fluid and the solid phases are fully mixed and simultaneously present in some domain in space, while their interaction is incorporated in the coefficient R_{ij}. Henceforth, the averaged quantities occurring in the latter equations are identified with the associated macroscopic quantities and the relevant equations are considered as the macroscopic equations for fluid flow in porous media, applicable under the conditions and assumptions outlined above. Upon examining (3.2.24), one can now say that the macroscopic behavior of the fluid (water) flow in a porous substance is controlled by the macroscopic pressure forces, the macroscopic viscous stress forces, the resistance forces due to the

presence of the matrix material, and by the earth's gravity. It should further be noticed that in the absence of fluid motion, (3.2.24) directly reduces to the macroscopic equation for hydrostatic equilibrium as given in (3.2.18).

With a view to the application to common groundwater flow problems, we examine in (3.2.24) in some more detail the relative importance of the macroscopic viscous stress term $\partial_j \langle \sigma_{ij} \rangle$ as compared with the macroscopic resistance term $\phi^f R_{ij} \langle v_j \rangle$. To this end, we use scaling arguments similar to the ones discussed in Section 2.4. Let $L_>$ (cf. (3.1.1)) denote the characteristic linear dimension of the groundwater flow problem under consideration and let a typical value of L be 10^2 m. Then, if in (3.2.23), as we suggested earlier, R'_{ij} is of the same order of magnitude as the inverse of the usual permeability of subsoils, which for isotropic soils varies from $\approx 10^{-15}$ m^2 for peat to $\approx 10^{-10}$ m^2 for coarse sands, it readily follows that the ratio of the orders of magnitude of macroscopic viscous stress and the macroscopic resistivity (i.e., the (second term)/(third term) in (3.2.24)) will be in the range of $\approx 10^{-19}$ to $\approx 10^{-14}$. Clearly, in common groundwater flow problems one can therefore neglect the influence of the macroscopic viscous stress forces with respect to the macroscopic resistance forces, and accordingly approximate (3.2.24) by

$$- \phi^f \partial_i \langle p \rangle^f - \phi^f R_{ij} \langle v_j \rangle = - \phi^f \rho g_i , \tag{3.2.25}$$

which is equivalent to

$$- \partial_i \langle p \rangle^f - R_{ij} \langle v_j \rangle = - \rho g_i . \tag{3.2.26}$$

Equation (3.2.26) is essentially Darcy's law. It expresses that in common groundwater flows, for example, seepage through dams and aquifers, etc., the flow phenomena involved are predominantly governed by the pressure forces, the resistivity of the porous mass, and the forces due to the earth's gravity.

With reference to (3.2.24), we remark that the term $\partial_j \langle \sigma_{ij} \rangle$ is often denoted as the Brinkman correction term, after Brinkman (1947) who rather heuristically proposed this extra term in Darcy's law in order to deal with some special situations. In particular, he added this term to develop boundary conditions different from the ones that comply with (3.2.12) and (3.2.26) (see Section 3.3) for problems of fluid flow through common porous substances with low permeability and adjoining media with a very high permeability, i.e., a very low solid particle density. Scaling arguments similar to the ones discussed above to justify the neglect of the macroscopic viscous forces in (3.2.24), have also been used by Slattery (1969). Lehner (1979) confirms, upon using different arguments, the relative unimportance of the Brinkman correction term in (3.2.24) for most situations met in practice.

Finally, we note that Darcy's formula only has to be supplemented by the macroscopic continuity equation as given in (3.2.12) to complete the set of equations in the flow-field quantities $\langle p \rangle^f$ and $\langle v_i \rangle$ (ϕ^f, ρ, g_i, and R_{ij}, and/or η and R'_{ij}, are assumed to be known).

3.2.1. INTRODUCTION OF MACROSCOPIC SOURCES

In many problems concerned with fluid flow in porous media we encounter the presence of sources, for instance sources that either inject into or abstract fluid from the fluid-solid composite. In view of this, we discuss in present subsection the introduction of macroscopic sources in the macroscopic fluid flow equations.

Since the detailed physical behavior of the sources is either irrelevant to or beyond the scope of the present analysis, it suffices here to incorporate the action of the sources in a manner that is compatible with the structure of the basic equations discussed in the previous section. Consider a fluid-saturated porous medium present in some bounded domain D and let the macroscopic sources be located in some

bounded subdomain D_{SRC} of D. The closed boundary surface of D_{SRC} is denoted by ∂D_{SRC} and the unit vector along the normal to ∂D_{SRC} pointing away from D_{SRC} by ν_i. The part of ∂D_{SRC} that is occupied by the fluid phase is denoted by ∂D^f_{SRC}, and the part of ∂D_{SRC} that is occupied by the solid phase by ∂D^s_{SRC} (see Figure 3.2). The two types of sources that are

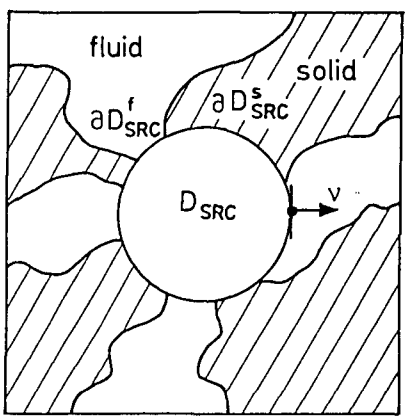

Fig. 3.2. The bounded source domain D_{SRC} interior to the closed boundary surface $\partial D_{SRC} = \partial D^f_{SRC} \cup \partial D^s_{SRC}$ (schematically).

compatible with the structure of the macroscopic equations (3.2.12) and (3.2.24), and hence (3.2.25), are those that either inject (or abstract) a certain net volume across ∂D^f_{SRC} or exert a certain net force across ∂D^f_{SRC}.

First, let us consider the presence of a volume injection source in D_{SRC}, and let Q represent the net time rate of outward flow across ∂D^f_{SRC} produced by this source, i.e.,

$$Q = \int_{\underline{x}' \in \partial D^f_{SRC}} \nu_i v_i dA, \tag{3.2.27}$$

where Q is positive for volume injection and negative for volume abstraction. To arrive at the local form of (3.2.27), we extrapolate this equation to the level of the representative elementary domain D_ε, centered at the position $\underline{x}$. Accordingly, we have

$$\langle q \rangle = V_\varepsilon^{-1} \int_{\underline{x}' \in S^f_\varepsilon(\underline{x})} \nu_i v_i dA, \tag{3.2.28}$$

where $\langle q \rangle$ is the local equivalent time rate of volume source density of volume injection (abstraction) and S^f_ε denotes the part of ∂D_ε that is occupied by the fluid phase. Accordingly, the macroscopic continuity equation (3.2.12) is to be extended to

$$\partial_i \langle v_i \rangle = \langle q \rangle. \tag{3.2.29}$$

Secondly, we consider a force source to be present in D_{SRC}. Let F_i denote the net surface force transmitted by this source across ∂D^f_{SRC} onto the surrounding fluid, i.e.,

$$F_i = \int_{\underline{x}' \in \partial D^f_{SRC}} \nu_j \tau_{ij} dA. \tag{3.2.30}$$

To arrive at the local form of (3.2.30), we extrapolate this equation to the level of the representative elementary domain as well. Accordingly, we have

$$\langle f_i \rangle = V_\varepsilon^{-1} \int_{\underline{x}' \in S^f_\varepsilon(\underline{x})} \nu_j \tau_{ij} dA, \tag{3.2.31}$$

where $\langle f_i \rangle$ is the equivalent volume source density of force. Accordingly, Equation (3.2.24) is to be extended to

$$- \phi^f \partial_i \langle p \rangle^f + \partial_j \langle \sigma_{ij} \rangle - \phi^f R_{ij} \langle v_j \rangle = - \phi^f \rho g_i - \langle f_i \rangle. \qquad (3.2.32)$$

Now, upon applying to (3.2.32) similar arguments as that have led us from (3.2.24) to Darcy's law (3.2.26), it readily follows that (cf. (3.1.11)):

$$- \partial_i \langle p \rangle^f - R_{ij} \langle v_j \rangle = - \rho g_i - \langle f_i \rangle^f. \qquad (3.2.33)$$

Note that in a source-free domain D, i.e., a domain throughout which both $\langle q \rangle = 0$ and $\langle f_i \rangle = 0$, (3.2.29), (3.2.32), and (3.2.33) reduce to (3.2.12), (3.2.24), and (3.2.26), respectively. In the theory of groundwater flow a source abstracting water from the subsoil is often referred to as a "sink"; further, in most practical situations $\langle f_i \rangle = 0$. For reasons of symmetry in the equations, however, the latter source term has been retained which will prove to be helpful in the course of our further analysis in Chapter 4.

At this point it is remarked that, through the action of external sources, we can introduce a time dependence in the flow problem, i.e., $\langle q \rangle$ and $\langle f_i \rangle$ can be functions of both space and time. This time dependence induces a corresponding time dependence in $\langle p \rangle^f$ and $\langle v_i \rangle$.

Equations (3.2.29) and (3.2.33) will serve as the basic field equations for groundwater flow and in order to fully specify a groundwater flow problem they only have to be supplemented by appropriate boundary conditions. The latter conditions are discussed in Section 3.3.

3.2.2. PRACTICAL PRESSURE-GAUGE MEASUREMENT IN GROUNDWATER FLOW

In this subsection it is argued that the quantity that one observes in a practical measurement of the (macroscopic) pressure in a water-saturated subsoil corresponds to the intrinsic fluid averaged pressure $\langle p \rangle^f$ that has been introduced in Section 3.2.

In a practical pressure-gauge measurement in groundwater flow, the pressure-gauge probe (also known as a piezometer) usually consists of a tube injected into the subsoil up to the depth where one wants to measure the local macroscopic pressure. The endface of a pressure-gauge probe, inserted into the subsoil, is schematically shown in Figure 3.3. Now, let us assume that the cross-sectional surface of the probe coincides with a representative elementary surface Δ_ε, located around the position $\underline{x}$. The

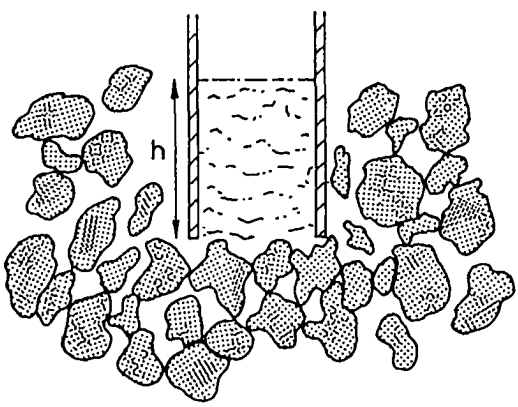

Fig. 3.3. Schematic detail of the endface of a pressure-gauge probe injected in the water-saturated subsoil.

part of Δ_ε that is occupied by the fluid is referred to as Δ_ε^f; the part of Δ_ε that is occupied by the solid as Δ_ε^s. Hence,

$$\Delta_\varepsilon = \Delta_\varepsilon^f \cup \Delta_\varepsilon^s. \tag{3.2.34}$$

The areas of Δ_ε, Δ_ε^f and Δ_ε^s are denoted as A_ε, A_ε^f and A_ε^s, respectively. The probe is considered to be an ideal one: it does not influence the

fluid flow in the subsoil and all capillary effects that might occur inside the tube are neglected.

Let us consider a situation where the groundwater has reached a level h above the endface of the probe, at which level it is at rest (see Figure 3.3). Then, the pressure P at the endface of the probe will be related to the height h by

$$P = \rho g h, \tag{3.2.35}$$

where g is the constant scalar acceleration of free fall at the earth's surface, or near to it, and where we have used the fact that in groundwater flow the vectorial acceleration of free fall is directed along $-\underline{i}_3$ (see Figure 2.1). Note that P in (3.2.35) is to be taken zero at the height h in the tube. Now, the force F acting on the water just beneath the endface of the probe is given by

$$F = PA_{\epsilon}^{f}. \tag{3.2.36}$$

Since, however, the groundwater in the probe is assumed to be at rest, F also equals

$$F = \int_{\underline{x}' \in \Delta_{\epsilon}^{f}(\underline{x})} p(\underline{x}')\,dA. \tag{3.2.37}$$

Then, on the assumption that (for arguments that support this assumption for predominantly capillary flow we refer to Whitaker (1969), and Bear and Bachmat (1983)),

$$[A_{\epsilon}^{f}(\underline{x})]^{-1} \int_{\underline{x}' \in \Delta_{\epsilon}^{f}(\underline{x})} p(\underline{x}')\,dA$$

$$\approx [V_{\epsilon}^{f}(\underline{x})]^{-1} \int_{\underline{x}' \in D_{\epsilon}^{f}(\underline{x})} p(\underline{x}')\,dV = \langle p \rangle^{f}(\underline{x}), \tag{3.2.38}$$

we arrive from (3.2.36) and (3.2.37) at the following interrelation between P and $\langle p \rangle^f$:

$$P = \langle p \rangle^f . \tag{3.2.39}$$

For the water level h that is measured in a practical pressure-gauge measurement, we then obtain from (3.2.35) and (3.2.39)

$$h = (\rho g)^{-1} \langle p \rangle^f . \tag{3.2.40}$$

Equation (3.2.40) directly relates h to the intrinsically fluid-averaged, macroscopic, pressure $\langle p \rangle^f$.

3.3. MACROSCOPIC BOUNDARY CONDITIONS

In fluid-saturated porous media configurations, one often encounters regions where (some of) the constitutive parameters (the volumetric porosity, the resistance of the fluid-saturated porous medium, and/or the volume density of fluid mass) experience rapid changes within a distance of the order of the characteristic linear dimension of the relevant representative elementary domain. From a macroscopic point of view the relevant constitutive parameters suffer jump discontinuities and in view of the macroscopic theory developed sofar, it seems natural to treat these regions macroscopically as surfaces of discontinuity in material properties. For any type of these surfaces (interfaces) we assume that the fluids at either side of it neither mix nor move away from it.

Since across a discontinuity surface (interface) the constitutive parameters show abrupt changes, also (some of) the dependent field quantities will, in general, show a discontinuous behavior, where, similar to the case of a single-phase continuum (see Section 2.2), on physical grounds only jumps by finite amounts are admissible. Now, due to these jump discontinuities that arise in (some of) the field quantities, the latter quantities are no longer continuously differentiable throughout a domain that contains (part of) a discontinuity surface and hence the partial differential equations that govern the relevant fluid-flow phenomena cease to hold in the immediate vicinity of these surfaces. Therefore, the latter equations have to be supplemented by a certain set of boundary conditions that interrelate the flow-field quantities at either side of the surface of discontinuity.

For groundwater flow, the basic equations are (3.2.29) and (3.2.33). Now, to interconnect the solutions to (3.2.29) and (3.2.33) at either side of a surface of discontinuity in medium (fluid and/or solid) properties, we apply the same method as outlined in Section 2.2 : we

locally replace the flow equations (3.2.29) and (3.2.33) by another system that contains no spatial differentiations across the relevant discontinuity surface, but that for continuously varying medium properties is equivalent to the system (3.2.29) and (3.2.33). Let S denote a smooth surface of discontinuity that intersects a bounded domain D, containing a fluid-saturated porous medium; S divides D into the subdomains D_1 and D_2, respectively. The unit vector ν_i along the normal to S is pointing into D_1. Now, let $\underline{x}$ be the position vector of some point on S. Then, to circumvent the problem of the differentiation along ν_i in (3.2.29) and (3.2.33), we integrate these equations along a straight line joining a point with position vector $\underline{x} - h\underline{\nu}$ (with $h > 0$) located in D_2 to a point with position vector $\underline{x} + h\underline{\nu}$ located in D_1 (see Figure 3.4).

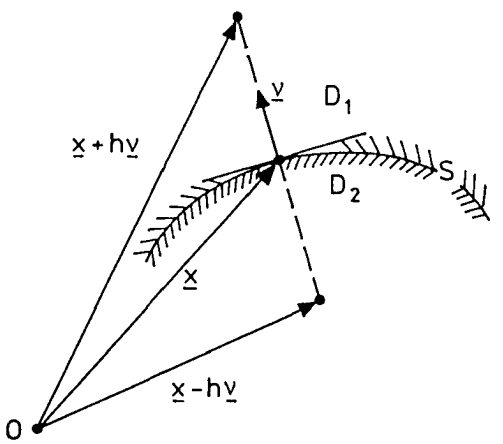

Fig. 3.4. Configuration employed for the derivation of the boundary conditions at the interface S.

Applying this procedure to (3.2.33), we obtain

$$- \int_{s=-h}^{h} \partial_i \langle p \rangle^f (\underline{x}+s\underline{\nu}) ds - \int_{s=-h}^{h} R_{ij}(\underline{x}+s\underline{\nu}) \langle v_j \rangle (\underline{x}+s\underline{\nu}) ds$$

$$+ \int_{s=-h}^{h} \rho(\underline{x}+s\underline{\nu}) g_i ds + \int_{s=-h}^{h} \langle f_i \rangle^f (\underline{x}+s\underline{\nu}) ds = 0. \qquad (3.3.1)$$

As a next step, we use (2.2.2) in (3.3.1) and take into account that all components of the integrands in (3.3.1) parallel to S remain bounded; hence, their contribution vanishes as $h \downarrow 0$. The same remarks apply to the components along $\underline{\nu}$ of the integrands of the last three terms in the left-hand side of (3.3.1). As a consequence, if h tends to zero in (3.3.1), we are led to (cf. (3.3.1) and (2.2.2))

$$\lim_{h \downarrow 0} \int_{s=-h}^{h} \partial_i \langle p \rangle^f (\underline{x}+s\underline{\nu}) ds = \lim_{h \downarrow 0} \int_{s=-h}^{h} N_{is} \partial_s \langle p \rangle^f (\underline{x}+s\underline{\nu}) ds$$

$$= \lim_{h \downarrow 0} \nu_i [\langle p \rangle^f (\underline{x}+h\underline{\nu}) - \langle p \rangle^f (\underline{x}-h\underline{\nu})] = 0, \qquad (3.3.2)$$

or

$$[\langle p \rangle^f]_{1,2} = 0 \qquad \text{at S,} \qquad (3.3.3)$$

where N_{is} is defined in (2.2.3). Equation (3.3.3) expresses that the intrinsically fluid-averaged, i.e., the macroscopic, pressure is to be continuous across a surface of discontinuity in material properties. In deriving (3.3.3) we have assumed that no surface sources are concentrated on S. Upon applying a similar procedure to the continuity equation as given in (3.2.29), it is easily verified that in the absence of any sources acting on S we arrive at

$$\nu_i [\langle v_i \rangle]_{1,2} = 0 \qquad \text{at S;} \qquad (3.3.4)$$

the component of the fluid-averaged, i.e., the macroscopic, fluid velocity that is normal to the interface is to be continuous across the interface.

Finally, we mention the explicit boundary conditions that have to be prescribed on boundaries of a specific type. First of all, for an immovable and fluid-impenetrable body immersed in a fluid-saturated porous substance, we have $n_i\langle v_i\rangle \to 0$ upon approaching the body's boundary surface via the interior of the porous medium. For this situation, $\langle p\rangle^f$ remains unspecified on the relevant boundary. In groundwater flow, this boundary condition applies for instance at an impervious base of some water-saturated subterranean formation. Secondly, we mention the occurrence of pressure-free surfaces, for which we have $\langle p\rangle^f \to 0$ upon approaching them. On this type of surface, $n_i\langle v_i\rangle$ remains unspecified.

In groundwater flow we are also often confronted with the situation where the location of a part of an interface is unknown beforehand, but must be determined from other considerations in the groundwater flow problem. As an example, we first mention the flow of groundwater in a dam, where the position of the water/air interface in the porous medium has to determined. Now, the boundary conditions at such an interface are: $\langle p\rangle^f \to p_{atm}$ and $n_i\langle v_i\rangle \to 0$, in which p_{atm} represents the atmospheric pressure. Secondly, we mention the problem of the determination of the position of fresh-water/salt-water interfaces occurring, for example, in subsoils located in the vicinity of seas. Here, the position of the interfaces follows from the requirement that both boundary conditions (3.3.3) and (3.3.4) are simultaneously satisfied.

Henceforth, for reasons of convenience in the subsequent chapters, we denote the quantities $\langle p\rangle^f$, $\langle v_i\rangle$, $\langle q\rangle$, and $\langle f_i\rangle^f$, as p, v_i, q, and f_i, respectively. In addition to this we shall denote v_i as the velocity instead of the (averaged) flow velocity. Adopting this nomenclature in (3.2.29), (3.2.33), and in (3.3.3) and (3.3.4), we are led to

$$\partial_i v_i = q, \tag{3.3.5}$$

$$\partial_i p + R_{ij} v_j = \rho g_i + f_i, \tag{3.3.6}$$

and

$$[p]_{1,2} = 0 \qquad \text{at } S, \tag{3.3.7}$$

$$\nu_i [v_i]_{1,2} = 0 \qquad \text{at } S, \tag{3.3.8}$$

respectively. In our applications, (3.3.5) - (3.3.8) are referred to as the basic (macroscopic) relations for flow of groundwater.

3.4. UNIQUENESS THEOREM FOR GROUNDWATER FLOW, BASED ON ENERGY CONSIDERATIONS

The purpose of the present section is to investigate the uniqueness of the solution of those groundwater flow problems that can mathematically be formulated as boundary-value problems.

Quite a number of groundwater flow problems can mathematically be formulated as boundary-value problems. In problems of this kind, we have to construct, in a certain bounded domain D that is either a bounded subdomain of the actual flow configuration or contains the entire actual flow configuration, solutions to the basic groundwater flow equations (3.3.5) - (3.3.6), that satisfy certain additional conditions at the boundary surface ∂D of D. As such we mention the flow of groundwater in bounded subterranean formations like confined aquifers. From a physical point of view, a unique flow field exists in these flow configurations, and hence, the question arises what boundary conditions do represent the physical situation such that uniqueness results. In this respect, it is known from the theory of partial differential equations that three types of admissible, local, boundary conditions deserve attention. They may apply to different parts of ∂D and therefore, we assume ∂D to be the union of three parts (see Figure 3.5):

$$\partial D = \partial D_1 \cup \partial D_2 \cup \partial D_3, \tag{3.4.1}$$

where at least one of the parts is not the null set. Consider again the basic equations for flow of groundwater (cf. (3.3.5) and (3.3.6))

$$\partial_i v_i = q \qquad \text{when } \underline{x} \in D, \tag{3.4.2}$$

and

$$\partial_i p + R_{ij} v_j = \rho g_i + f_i \quad \text{when } \underline{x} \in D. \tag{3.4.3}$$

For the first boundary-value problem (Dirichlet problem) we have

$$p = \psi_1 \quad \text{when } \underline{x} \in \partial D_1; \tag{3.4.4}$$

for the second boundary-value problem (Neumann problem)

$$\nu_i v_i = \psi_2 \quad \text{when } \underline{x} \in \partial D_2, \tag{3.4.5}$$

and for the third boundary-value problem (Robin problem)

$$-\alpha \nu_i v_i + \beta p = \psi_3 \quad \text{when } \underline{x} \in \partial D_3. \tag{3.4.6}$$

Here, ψ_1, ψ_2, and ψ_3 denote prescribed surface source distributions on ∂D (see Figure 3.5), while the known quantities α and β incorporate the relevant physical properties of the boundary surface ∂D_3 (see, e.g., Aziz and Settari, 1983, p. 73). The boundary condition on ∂D_3 is passive: α and β have positive values and, hence, an excess pressure in D leads to an outward normal flow across ∂D_3. To complete the boundary-value problem posed by (3.4.2) - (3.4.6) we note that upon integrating (3.4.2) over D and applying Gauss' theorem, the following compatibility relation results:

$$\int_{\underline{x} \in \partial D} \nu_i v_i dA = \int_{\underline{x} \in D} q \, dV, \tag{3.4.7}$$

in which ν_i denotes the unit vector along the normal to ∂D pointing away from D and where the contributions from the (possible) interfaces present in D have cancelled in view of the continuity condition (3.3.8).

Before we shall prove that the relations (3.4.2) - (3.4.7) uniquely determine the flow field $\{p, v_i\}$ in D, we give some physical explanation of the different conditions (3.4.4) - (3.4.6). First of all, the boundary condition (3.4.4) applies whenever the porous flow domain D is adjacent

to a (porous) fluid continuum body of relatively large size. Then, any fluid flow between the fluid continuum body and D will not appreciably alter the (known) pressure distribution in the relevant continuum body and hence (3.4.4) can be used on the boundary surface of D. In groundwater flow, this situation occurs, for example, at the interface between a saturated subsoil and a water reservoir of sufficiently large size (e.g., a relatively large lake). A special case of (3.4.4) occurs if $p = p_o$ in which p_o is a given constant on ∂D_1. In this case, ∂D_1 is an equipressure surface.

The boundary condition (3.4.5) applies whenever we want to specify

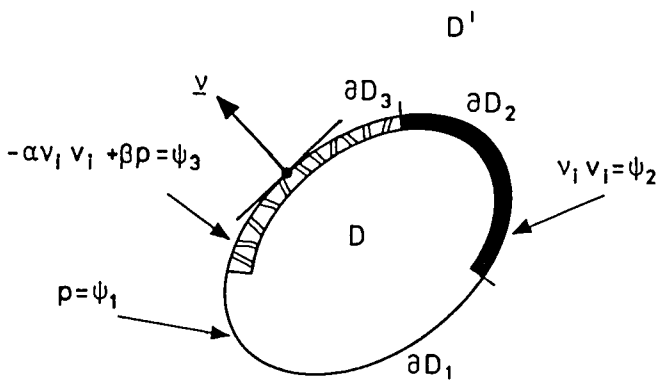

Fig. 3.5. Domain D with closed boundary surface $\partial D = \partial D_1 \cup \partial D_2 \cup \partial D_3$, for which the uniqueness theorem is derived.

the normal outflow (inflow) across the boundary surface of a porous flow domain into (from) some adjacent aquifer or reservoir. A special case of (3.4.5) is the occurrence of an impermeable surface bounding (part of)

the porous flow domain D, for which we have $\psi_2 = 0$ everywhere on the relevant surface.

Finally, the more general type of boundary condition (3.4.6) applies whenever the normal flow across (part of) the boundary surface of a porous-medium domain D is related to the pressure difference across that surface. In porous-media flow this occurs if the relevant porous flow domain is separated from an adjacent fluid continuum or another porous flow domain by some relatively thin semipermeable layer. For example, in practical groundwater flow configurations, (part of) the relevant subsoil may be separated from the open air by a relatively thin semipervious clay layer. Upon approaching such an interface via the subsoil we then have (cf. (3.4.6)) $-(\alpha/\beta)v_i v_i + p = p_{atm}$ on the relevant surface, where the quantity α/β, with $\alpha/\beta > 0$, expresses the resistivity of the thin layer, and p_{atm} is the atmospheric pressure at the level of the interface. It is observed that upon comparing (3.4.6) with (3.4.4) and (3.4.5), one can say that $\alpha = 0$ and $\beta = 1$ on ∂D_1 (with $\psi_3 = \psi_1$), while $\alpha = 1$ and $\beta = 0$ on ∂D_2 (with $\psi_3 = -\psi_2$).

Returning to the uniqueness proof itself, we shall presuppose the existence of at least one solution to the groundwater flow problem posed by (3.4.2) - (3.4.7). Obviously, this assumption, too, needs a mathematical proof; this, however, is beyond the scope of the present monograph. Let $\{p^{(1)}, v_i^{(1)}\}$ and $\{p^{(2)}, v_i^{(2)}\}$ be two non-identical solutions of the boundary-value problem posed by (3.4.2) - (3.4.7). Then, the flow field defined by

$$\{p, v_i\} = \{p^{(1)} - p^{(2)}, v_i^{(1)} - v_i^{(2)}\}, \tag{3.4.8}$$

will satisfy (3.4.2) - (3.4.7) in which the right-hand sides are replaced by zero, i.e.,

$$\partial_i v_i = 0 \qquad \text{when } \underline{x} \in D, \tag{3.4.9}$$

$$\partial_i p + R_{ij} v_j = 0 \qquad \text{when } \underline{x} \in D, \tag{3.4.10}$$

$$p = 0 \qquad \text{when } \underline{x} \in \partial D_1, \tag{3.4.11}$$

$$\nu_i v_i = 0 \qquad \text{when } \underline{x} \in \partial D_2, \tag{3.4.12}$$

$$-\alpha \nu_i v_i + \beta p = 0 \qquad \text{when } \underline{x} \in \partial D_3, \tag{3.4.13}$$

and

$$\int_{\underline{x} \in \partial D} \nu_i v_i dA = 0. \tag{3.4.14}$$

Now, upon successively multiplying (3.4.9) by p, (3.4.10) by v_i, combining the results, integrating the result over the domain D, and applying Gauss' theorem, we arrive at

$$\int_{\underline{x} \in \partial D} p \nu_i v_i dA + \int_{\underline{x} \in D} v_i R_{ij} v_j dV = 0, \tag{3.4.15}$$

where the contributions from the (possible) interfaces in the interior of D have cancelled in view of the continuity conditions (3.3.7) and (3.3.8). Obviously, the part in the left-hand side of (3.4.15) over ∂D_1 vanishes in view of (3.4.11); similarly, the part over ∂D_2 vanishes in view of (3.4.12). On ∂D_3 we use (3.4.13) and end up with either

$$\int_{\underline{x} \in \partial D_3} (\alpha/\beta)(\nu_i v_i)^2 dA + \int_{\underline{x} \in D} v_i R_{ij} v_j dV = 0, \tag{3.4.16}$$

or

$$\int_{\underline{x} \in \partial D_3} (\beta/\alpha)(p)^2 dA + \int_{\underline{x} \in D} v_i R_{ij} v_j dV = 0. \tag{3.4.17}$$

Now, R_{ij} is positive definite as a result of the dissipativity of the viscous fluid flow (cf. Section 3.2). Consequently, the last term on the left-hand sides of (3.4.16) and (3.4.17) is positive for any

non-identically vanishing v_i. Further, since $\alpha/\beta > 0$ and $\beta/\alpha > 0$, the first term on the left-hand sides of (3.4.16) and (3.4.17) is positive, too, for any non-identically vanishing $\nu_i v_i$ or p on ∂D_3. Hence, a contradiction in both (3.4.16) and (3.4.17) arises, unless $\nu_i v_i$ and p are identically zero *on* ∂D_3 and v_i is identically zero in D. Reusing (3.4.10), it then follows that $\partial_i p = 0$ *in* D and, hence, p is constant throughout D. However, in view of (3.4.17) this constant must be zero on ∂D_3, and, hence, p = 0 throughout D. Consequently, the assumption that the problem posed by (3.4.2) - (3.4.7) admits more than one single solution has been contradicted: the difference of the two solutions $\{p^{(1)}, v_i^{(1)}\}$ and $\{p^{(2)}, v_i^{(2)}\}$ proves to be identically the null solution throughout D. Hence, at most a single solution results, provided that at least one solution to (3.4.2) - (3.4.7) exists.

If the part ∂D_3 of ∂D is the null set and ∂D_1 is not present either, (3.4.16) leads to $v_i = 0$ throughout D, which in view of (3.4.10) entails p is constant throughout D. Since ∂D_1 is absent, this constant now remains unspecified, and hence, upon taking into account (3.4.8), the relevant boundary-value problem admits a single solution up to an arbitrary additive constant.

CHAPTER 4

GENERAL CONSIDERATIONS ON THE BOUNDARY-INTEGRAL-EQUATION FORMULATION OF STEADY GROUNDWATER FLOW PROBLEMS

This chapter deals with the general aspects of the boundary-integral-equation formulation of problems concerned with the steady flow of groundwater.

The integral-equation method has proved its usefulness in a wide variety of engineering problems. We mention the fields of electrocardiography (see, e.g., Barr et al., 1966), gravimetry (see, e.g., De Jong, 1981), quasi-magnetostatics (see, e.g., Lindholm, 1980, Van Herk, 1981, and De Hoop, 1982), electromagnetic scattering and diffraction (see, e.g., De Hoop, 1977), elastostatics (see, e.g., Cruse, 1969, and Rizzo and Shippy, 1977), scattering and diffraction of acoustic and elastic waves (see, e.g., Tan, 1975a,b, and Herman, 1981a,b, 1982), and flow in porous media (see, e.g., Liggett and Liu, 1983, and Van der Weiden and De Hoop, 1988). Evidently, this list is far from exhaustive, and for recent developments the reader is referred to the proceedings of the conferences on integral-equation methods and the references cited therein. In particular, as far as the boundary-integral-equation method applied in solid and fluid mechanics is concerned, we refer to Cruse (1988).

The main advantage of the integral-equation method lies in its flexibility as regards shape, size and physical composition of the different geometrical constituents that together form the configurations that can be analyzed with it. Also, its implementation on a computer

offers no extreme difficulties and the main limitations are put by the speed and the storage capacity of the computer system at one's disposal.

The first step in the integral-equation method consists of acquiring appropriate integral representations for the field quantities involved. These representations follow, in their turn, from a suitable reciprocity theorem that interrelates, in a specific manner, the field quantities associated with two possible, but different, physical states that can occur in one and the same domain in space. The reciprocity theorem needed in our analysis is derived from the basic equations of groundwater flow given in Section 4.1; it can be regarded as a basic theorem, both mathematically and physically, from which many properties of groundwater flow fields follow. For example, in Section 4.2 it is used to reinvestigate the uniqueness of the solution of those groundwater flow problems that can mathematically be formulated as boundary-value problems. In Section 4.3, the reciprocity theorem for groundwater flow serves as a point of departure in the derivation of the integral representations for the two field quantities that characterize the flow state of groundwater, viz. the pressure and the velocity. In this derivation, one of the two states occurring in the reciprocity theorem is identified with the actual flow state, while the remaining one is identified with an auxiliary (Green's) flow state generated by, successively, a point injection source and a point force source. The source-type integral representations that result from this procedure express the relevant flow quantities in the interior of some bounded domain in space in terms of related quantities at the boundary surface of this domain.

In the literature on boundary-integral-equation formulations for groundwater flow problems, most formulations are based on the source-type integral representation for the pressure only (see, e.g., Liggett and Liu, 1983, p. 22). A survey of the several types of boundary-integral-equation formulations that follow from employing the source representations for both the pressure and the velocity is given in Section 4.4. In Section 4.5, the solution to the auxiliary point-source

excitation states, i.e., the Green's functions, occurring in the integral representations are determined explicitly for the case of a homogeneous and reciprocal medium of infinite extent. Further, suitable scalar and vector potentials are introduced in the above representations; they are employed to arrive at a standard form of the source-type integral representations for the pressure and the velocity and apply to an arbitrary, bounded, domain in a fluid-saturated, homogeneous and reciprocal porous medium.

4.1. RECIPROCITY THEOREM FOR GROUNDWATER FLOW

Starting from the basic equations for the steady flow of groundwater, viz. the continuity equation and Darcy's law, we derive in the present section a reciprocity theorem in the two field quantities, pressure and velocity, that characterize the flow of groundwater. The reciprocity theorem applies to two admissible, but non-identical groundwater flow states that can occur in one and the same bounded domain in some fluid-saturated porous medium. It serves as a point of departure for the derivation of the source-type integral representations for the velocity and the pressure. The latter will play a vital role in arriving at the boundary-integral-equation formulation of a groundwater flow problem.

We consider a bounded domain D in three-dimensional space R^3, in which two non-identical groundwater flow states can occur. The closed boundary surface of D is denoted by ∂D and the complement of $D \cup \partial D$ in R^3 by D'. The unit vector along the normal to ∂D, pointing away from D, is denoted by ν_i. The two flow states in D are marked as States A and B, respectively (see Figure 4.1). The quantities associated with each of the two States A and B are denoted by their corresponding symbol to which the superscripts A and B, respectively, are attached.

State A is characterized by the flow field $\{p^A, v_i^A\}$, the external source distributions $\{q^A, f_i^A\}$ and the constitutive parameters $\{\rho^A, R_{ij}^A\}$. The basic groundwater flow equations pertaining to this state are given by (cf. (3.3.5))

$$\partial_i v_i^A = q^A, \tag{4.1.1}$$

and (cf. (3.3.6))

$$\partial_i p^A + R_{ij}^A v_j^A = \rho^A g_i + f_i^A. \tag{4.1.2}$$

Similarly, State B is characterized by the flow field $\{p^B, v_i^B\}$, the external source distributions $\{q^B, f_i^B\}$ and the constitutive parameters

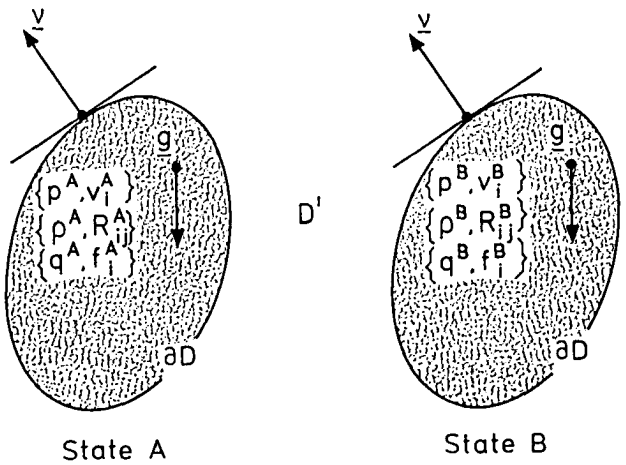

Fig. 4.1. Bounded domain D with closed boundary surface ∂D and two non-identical groundwater flow states (States A and B) to which the reciprocity theorem applies.

$\{\rho^B, R_{ij}^B\}$. The basic groundwater flow equations pertaining to this state are (cf. (4.1.1) and (4.1.2))

$$\partial_i v_i^B = q^B, \tag{4.1.3}$$

and

$$\partial_i p^B + R_{ij}^B v_j^B = \rho^B g_i + f_i^B. \tag{4.1.4}$$

To arrive at the reciprocity theorem, we consider the following fundamental interaction quantity between the two states:

$$\partial_i(p^A v_i^B - p^B v_i^A) = v_i^B \partial_i p^A + p^A \partial_i v_i^B - v_i^A \partial_i p^B - p^B \partial_i v_i^A. \qquad (4.1.5)$$

Upon multiplying (4.1.1) by p^B, (4.1.2) by v_i^B, (4.1.3) by p^A and (4.1.4) by v_i^A, and using the resulting relations in (4.1.5), we are led to

$$\partial_i(p^A v_i^B - p^B v_i^A) = (R_{ij}^B - R_{ji}^A) v_i^A v_j^B + (\rho^A v_i^B - \rho^B v_i^A) g_i + f_i^A v_i^B - f_i^B v_i^A - q^A p^B + q^B p^A. \qquad (4.1.6)$$

Equation (4.1.6) is the local (or differential) form of the reciprocity theorem for groundwater flow. The corresponding global (or integral) form of the reciprocity theorem is obtained by the integration of (4.1.6) over the bounded domain D, followed by the use of Gauss' theorem. This yields

$$\int_{\underline{x} \in \partial D} (p^A v_i^B - p^B v_i^A) \nu_i \, dA = \int_{\underline{x} \in D} (R_{ij}^B - R_{ji}^A) v_i^A v_j^B \, dV + \int_{\underline{x} \in D} [(\rho^A v_i^B - \rho^B v_i^A) g_i + f_i^A v_i^B - f_i^B v_i^A - q^A p^B + q^B p^A)] dV, \qquad (4.1.7)$$

where the left-hand side of (4.1.6) has been assumed to be continuously differentiable. Note that on account of the boundary conditions at a surface of discontinuity in matter, viz. the continuity of the pressure and the continuity of the normal component of the velocity, in State A as well as in State B, we can extend the validity of (4.1.7) to regions in which the field quantities, together with their first-order derivatives, are only piecewise continuous.

As regards the local and global forms of the reciprocity theorem, it should be noted that the first term on the right-hand sides of (4.1.6) and (4.1.7) is characteristic for the difference in resistivity of the media present in the States A and B, while the remaining part represents

the interaction between the sources and the accompanying fluid-flow states. Further, we observe that the first terms on the right-hand sides of (4.1.6) and (4.1.7) vanish in case the media in the two states are chosen such that

$$R^A_{ij} = R^B_{ji} \tag{4.1.8}$$

for all $\underline{x} \in D$. Under this condition, the interaction between the two states is only related to the external influences acting on the flow in the two states. If (4.1.8) holds, the medium in State B is denoted as the medium *adjoint* to the one in State A, and vice versa. In particular, (4.1.8) can hold for one and the same medium; the relevant medium is then denoted as self-adjoint or reciprocal. For a reciprocal medium, R_{ij} must therefore be a symmetrical tensor everywhere in D. A special case of the latter arises for isotropic media, for which we have

$$R_{ij} = R\delta_{ij}, \tag{4.1.9}$$

in which R is the scalar resistance. Obviously, an isotropic medium is always reciprocal.

The reciprocity theorem as given in (4.1.6) or (4.1.7), can, both physically and mathematically, be regarded as one of the most fundamental theorems of applied groundwater flow theory. Physically, it describes the interaction between two groundwater flow states, a feature that is characteristic for any type of measurement situation. In the latter, one state can be identified as the one to be probed, the other as the one that is probing (i.e., the one that is handled by the observer who carries out the measurement). Mathematically, the global form of the reciprocity theorem will serve to construct the source-type integral representations for both the pressure and the velocity, which, in their turn, are employed to arrive at the desired boundary-integral-equation formulation of a groundwater flow problem. This procedure is discussed in the Sections 4.3 and 4.4. Furthermore, as we shall see in the next

section, the reciprocity theorem as given in (4.1.7) enables us to reinvestigate the uniqueness of those groundwater flow problems that can mathematically be formulated as boundary-value problems (cf. Section 3.4).

4.2. UNIQUENESS THEOREM FOR GROUNDWATER FLOW, BASED ON RECIPROCITY

In the present section we investigate again the uniqueness of the solution of those groundwater flow problems that can mathematically be formulated as boundary-value problems. In distinction to the uniqueness theorem derived in the Section 3.4, the one to be presented here is based on the reciprocity theorem developed in Section 4.1.

Similar to Section 3.4, we start from the boundary-value problem posed by the relations (3.4.2) - (3.4.7) that applies to a bounded domain D that is either a bounded subdomain of the actual flow configuration or contains the entire actual flow configuration. The boundary surface of D is denoted by ∂D; it is the union of three parts: ∂D_1, ∂D_2, and ∂D_1, respectively, where at least one of them is not the null set (cf. (3.4.1)). The unit vector ν_i along the normal to ∂D is pointing away from D. For convenience, the relevant boundary-value problem is recapitulated below and schematically visualized in Figure 4.2. We have

$$\partial_i v_i = q \qquad \text{when } \underline{x} \in D, \tag{4.2.1}$$

$$\partial_i p + R_{ij} v_j = \rho g_i + f_i \qquad \text{when } \underline{x} \in D, \tag{4.2.2}$$

$$p = \psi_1 \qquad \text{when } \underline{x} \in \partial D_1 \quad \text{(Dirichlet problem)}, \tag{4.2.3}$$

$$\nu_i v_i = \psi_2 \qquad \text{when } \underline{x} \in \partial D_2 \quad \text{(Neumann problem)}, \tag{4.2.4}$$

$$-\alpha \nu_i v_i + \beta p = \psi_3 \qquad \text{when } \underline{x} \in \partial D_3 \quad \text{(Robin problem)}, \tag{4.2.5}$$

and

$$\int_{\underline{x}\in\partial D} v_i v_i dA = \int_{\underline{x}\in D} q \, dV \quad \text{(compatibility relation)}, \tag{4.2.6}$$

where ψ_1, ψ_2, and ψ_3, are the prescribed surface source distributions on ∂D. For a physical explanation of the different boundary conditions (4.2.3) - (4.4.5) we refer to Section 3.4. Further, as in Section 3.4, we shall presuppose the existence of at least one solution of the problem posed by (4.2.1) - (4.2.6).

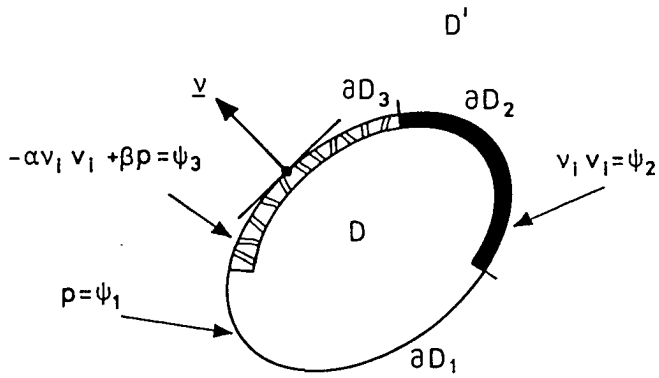

Fig. 4.2. Domain D with closed boundary surface $\partial D = \partial D_1 \cup \partial D_2 \cup \partial D_3$, for which the uniqueness theorem is derived.

From (4.2.1) - (4.2.2) it is apparent that the reciprocity theorem of Section 4.1 applies to the domain D. Let now $\{p^{(1)}, v_i^{(1)}\}$ and $\{p^{(2)}, v_i^{(2)}\}$ be two non-identical solutions of the boundary-value problem (4.2.1) - (4.2.6). Then, it readily follows that the flow field defined as State A through

$$\{p^A, v_i^A\} = \{p^{(1)} - p^{(2)}, v_i^{(1)} - v_i^{(2)}\}, \tag{4.2.7}$$

will satisfy (4.2.1) - (4.2.6) in which the right-hand sides are replaced by zero, i.e.,

$$\partial_i v_i^A = 0 \qquad \text{when } \underline{x} \in D, \tag{4.2.8}$$

$$\partial_i p^A + R_{ij}^A v_j^A = 0 \qquad \text{when } \underline{x} \in D, \tag{4.2.9}$$

$$p^A = 0 \qquad \text{when } \underline{x} \in \partial D_1, \tag{4.2.10}$$

$$\nu_i v_i^A = 0 \qquad \text{when } \underline{x} \in \partial D_2, \tag{4.2.11}$$

$$-\alpha \nu_i v_i^A + \beta p^A = 0 \qquad \text{when } \underline{x} \in \partial D_3, \tag{4.2.12}$$

and

$$\int_{\underline{x} \in \partial D} \nu_i v_i^A dA = 0. \tag{4.2.13}$$

As a next step, we identify State B through the following relations:

$$\partial_i v_i^B = q^B \qquad \text{when } \underline{x} \in D, \tag{4.2.14}$$

$$\partial_i p^B + R_{ij}^B v_j^B = \rho^B g_i + f_i^B \qquad \text{when } \underline{x} \in D, \tag{4.2.15}$$

$$p^B = 0 \qquad \text{when } \underline{x} \in \partial D_1, \tag{4.2.16}$$

$$\nu_i v_i^B = 0 \qquad \text{when } \underline{x} \in \partial D_2, \tag{4.2.17}$$

and

$$-\alpha \nu_i v_i^B + \beta p^B = 0 \qquad \text{when } \underline{x} \in \partial D_3. \tag{4.2.18}$$

Note that (4.2.14) entails a compatibility relation of the type (4.2.6). If, in addition to the above considerations, we choose the medium in

State B to be the adjoint of the one in State A, it follows from (4.1.7) that

$$0 = \int_{\underline{x}\in D} \rho^B g_i v_i^A dV + \int_{\underline{x}\in D} (f_i^B v_i^A - q^B p^A) dV. \qquad (4.2.19)$$

This equation must hold irrespective of the sofar arbitrary values of q^B and f_i^B. In (4.2.19) we now choose f_i^B to be equal to $-\rho^B g_i - c_1 v_i^A$ and q^B to be equal to $c_2 p^A$, in which c_1 and c_2 denote arbitrary but positive constants. Then, the resulting right-hand side only vanishes if both p^A and v_i^A vanish identically throughout D. In view of (4.2.7), this implies that $\{p^{(1)}, v_i^{(1)}\} = \{p^{(2)}, v_i^{(2)}\}$ throughout D. Consequently, the boundary-value problem posed by the basic groundwater flow equations (4.2.1) - (4.2.2), together with the boundary conditions (4.2.3) - (4.2.5) and the compatibility relation (4.2.6), has a single solution at most, provided, of course, that at least one solution of (4.2.1) - (4.2.6) exists.

If neither ∂D_1 nor ∂D_3 is present, only ∂D_2 remains and (4.2.14) and (4.2.17) are contradictory, which implies that State B does not exist. In that case we take $q^B = 0$ throughout D, and (4.2.19) is replaced by

$$0 = \int_{\underline{x}\in D} \rho^B g_i v_i^A dV + \int_{\underline{x}\in D} f_i^B v_i^A dV. \qquad (4.2.20)$$

Again, this equation must hold irrespective of the sofar arbitrary value of f_i^B. Now, choosing in (4.2.20) f_i^B to be equal to $-\rho^B g_i - c_1 v_i^A$, in which c_1 denotes an arbitrary non-zero constant, the resulting right-hand side only vanishes if v_i^A vanishes identically throughout D. In view of (4.2.9), p^A then has a constant value throughout D. The latter constant remains unspecified, and as a result of this, the relevant boundary-value problem admits a single solution up to an arbitrary additive constant (cf. (4.2.7)).

Finally, it is emphasized that the uniqueness theorem presented in the current section puts less restrictions on the values of R_{ij}, α and β than the one proved in Section 3.4.

4.3. SOURCE-TYPE INTEGRAL REPRESENTATIONS FOR THE GROUNDWATER FLOW FIELD

In the present section it is outlined how the reciprocity theorem for the flow of groundwater in its global form (4.1.7) leads to source-type integral representations for the two flow quantities that characterize the flow state of groundwater, viz. the pressure and velocity.

State A is chosen as the actual flow field for which the integral representations are to be obtained; it satisfies the basic groundwater flow equations (4.2.1) and (4.2.2) throughout the bounded subdomains of D where the constitutive coefficients change continuously with position, and the supplementing boundary conditions (3.3.7) and (3.3.8) at the interfaces. The closed boundary surface of D is denoted by ∂D, the domain exterior to ∂D by D', and the unit vector along the normal to ∂D,

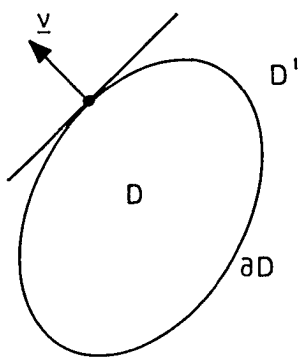

Fig. 4.3. Configuration to which the source-type integral representations for the pressure field and the velocity field apply.

pointing away from D, by n_i (see Figure 4.3). Accordingly, we write

$$\{p^A, v_i^A\} = \{p, v_i\}, \tag{4.3.1}$$

$$\{q^A, f_i^A\} = \{q, f_i\}, \tag{4.3.2}$$

and

$$\{\rho^A, R_{ij}^A\} = \{\rho, R_{ij}\}. \tag{4.3.3}$$

Next, the flow state B in (4.1.7) is chosen such that (4.1.7) leads to the values of $\{p, v_i\}$ at any point in space. Inspection of the right-hand side of (4.1.7) reveals that this is accomplished by making appropriate choices with respect to the external source distributions $\{q^B, f_i^B\}$ present in D: if a representation for the pressure field is wanted, we choose q^B to be a point source of volume injection and take f_i^B to be equal to a source distribution that compensates the gravity term $-\rho^B g_i$, while if a representation for the velocity field is wanted, we take q^B to be equal to zero and f_i^B to be equal to a point source of force in addition to the compensating distribution $-\rho^B g_i$.

Accordingly, we first take

$$\{q^B, f_i^B\} = \{a\delta(\underline{x} - \underline{x}'), -\rho^B g_i\}, \tag{4.3.4}$$

where a denotes an arbitrary constant and $\delta(\underline{x} - \underline{x}')$ is the three-dimensional spatial unit pulse (delta function) operative at the point $\underline{x} = \underline{x}'$, where $\underline{x}'$ may be located anywhere in space. As a next step, we take the medium in State B the adjoint of the one in the actual configuration and denote the flow field generated by the source distributions as given in (4.3.4) as

$$\{p^B, v_i^B\} = \{p^{Gq}, v_i^{Gq}\}(\underline{x},\underline{x}'). \tag{4.3.5}$$

For the choice (4.3.5), State B is denoted as an injection-source Green's state. The basic flow equations pertaining to such a Green's state readily follow from (4.1.3) and (4.1.4) as

$$\partial_i v_i^{Gq} = a\delta(\underline{x} - \underline{x}'), \tag{4.3.6}$$

and

$$\partial_i p^{Gq} + R_{ji} v_j^{Gq} = 0, \tag{4.3.7}$$

while this Green's state, too, satisfies the interface conditions (3.3.7) and (3.3.8). No explicit boundary conditions on ∂D are imposed on the Green's state (4.3.6) - (4.3.7). Now, upon using (4.3.1) - (4.3.5) in (4.1.7) and employing the integral property of the delta function, i.e.,

$$\int_{\underline{x}\in D} p(\underline{x})\delta(\underline{x} - \underline{x}')dV = \chi_D(\underline{x}')p(\underline{x}'), \tag{4.3.8}$$

where

$$\chi_D(\underline{x}') = \{1, 1/2, 0\} \quad \text{when } \underline{x}' \in \{D, \partial D, D'\}, \tag{4.3.9}$$

is the characteristic function of the domain D, (4.1.7) leads to

$$\int_{\underline{x}\in\partial D} (pv_i^{Gq} - p^{Gq}v_i)\nu_i dA - \int_{\underline{x}\in D} [(\rho g_i + f_i)v_i^{Gq} - qp^{Gq}]dV$$

$$= a\chi_D(\underline{x}')p(\underline{x}'). \tag{4.3.10}$$

In (4.3.10), the results for $\underline{x}' \in D$ and $\underline{x}' \in D'$ are clear, while from a detailed analysis it follows that the result for $\underline{x}' \in \partial D$ holds at points where ∂D has a unique tangent plane. For the latter case, the aforementioned analysis further reveals that the surface integral occurring in (4.3.10) has to be interpreted a Cauchy principal value,

i.e., the relevant integral is, when necessary, calculated by a limiting procedure that excludes a singularity of the integrand in a symmetrical manner. In Appendix B the derivation of (4.3.10) is presented in more analytical detail in case the relevant medium in D is homogeneous. There, it also shows up that for both $\underline{x}' \in \partial D$ and $\underline{x}' \in D$, the volume integral in (4.3.10) is to be understood as a convergent improper integral. Finally, from (4.3.10) an integral relation for the pressure itself follows by taking into account that both p^{Gq} and v_i^{Gq} are linearly related to the constant a (cf. (4.3.6) - (4.3.7)). Expressing this dependence by introducing the quantities $\{G^q, \Gamma_i^q\}$ as

$$\{p^{Gq}, v_i^{Gq}\}(\underline{x},\underline{x}') = a\{G^q, -\Gamma_i^q\}(\underline{x}',\underline{x}), \tag{4.3.11}$$

where G^q and Γ_i^q are denoted as the injection-source scalar and vector Green's functions, respectively, and recalling that (4.3.10) has to hold for arbitrary values of a, we end up with

$$-\int_{\underline{x}\in\partial D} [G^q(\underline{x}',\underline{x})v_i(\underline{x}) + \Gamma_i^q(\underline{x}',\underline{x})p(\underline{x})]\nu_i(\underline{x})dA + p^{ext}(\underline{x}')$$

$$= \chi_D(\underline{x}')p(\underline{x}'), \tag{4.3.12}$$

in which p^{ext} is the pressure due to the volume source distributions present in D and is given by

$$p^{ext}(\underline{x}') = \int_{\underline{x}\in D} \{G^q(\underline{x}',\underline{x})q(\underline{x}) + \Gamma_i^q(\underline{x}',\underline{x})[\rho(\underline{x})g_i + f_i(\underline{x})]\}dV. \tag{4.3.13}$$

Equation (4.3.12) is the desired source-type integral relation for the pressure field. Note, that if $\underline{x}' \in D$, (4.3.12) constitutes an integral representation.

Comparing, in (4.3.12), the structure of the surface integral with the one of the volume integral, we conclude that $-\nu_i v_i$ can be regarded as the density of equivalent surface injection rate, while $-\nu_i p$ can be

regarded as the density of equivalent surface force. Hence, when $\underline{x}' \in D$, (4.3.12) expresses the value of the pressure in the point $\underline{x} = \underline{x}'$ as the sum of the contributions from the volume sources present in D and the equivalent surface sources present on ∂D.

Secondly, to arrive at the integral representation for the velocity field, we take in (4.1.7) the external source distributions pertaining to State B as

$$\{q^B, f_i^B\} = \{0, b_i \delta(\underline{x} - \underline{x}') - \rho^B g_i\}, \tag{4.3.14}$$

where b_i denotes an arbitrary constant vector. As before, the medium in State B is taken to be the adjoint of the one in the actual configuration in D. The flow field generated by the source distributions as given in (4.3.14) is now denoted as

$$\{p^B, v_i^B\} = \{p^{Gf}, v_i^{Gf}\}(\underline{x},\underline{x}'). \tag{4.3.15}$$

For the choice (4.3.15), State B is denoted as a force-source Green's state. As regards the basic flow equations pertaining to such a state, these result from (4.1.3) and (4.1.4) as

$$\partial_i v_i^{Gf} = 0, \tag{4.3.16}$$

and

$$\partial_i p^{Gf} + R_{ji} v_j^{Gf} = b_i \delta(\underline{x} - \underline{x}'). \tag{4.3.17}$$

This Green's state, too, is taken to satisfy the interface conditions (3.3.7) and (3.3.8), while no explicit boundary conditions on ∂D are imposed on (4.3.16) - (4.3.17). As a next step, we use (4.3.14) - (4.3.15) in (4.1.7), employ (4.3.8), in which we replace p by $b_i v_i$, and arrive at

$$\int_{\underline{x}\in\partial D} (pv_i^{Gf} - p^{Gf}v_i)\nu_i dA - \int_{\underline{x}\in D} [(\rho g_i + f_i)v_i^{Gf} - qp^{Gf}]dV$$

$$= - b_i\chi_D(\underline{x}')v_i(\underline{x}'). \qquad (4.3.18)$$

As regards the result in (4.3.18) the same remarks apply as have been made with regard to (4.3.12); for a more detailed analytical analysis pertaining to (4.3.18) for the case of a homogeneous medium, we refer to Appendix B. Finally, from (4.3.18) the desired integral relation for the velocity field itself is obtained by expressing the linear dependence of p^{Gf} and v_i^{Gf} on b_i (cf. (4.3.16) and (4.3.17)) as

$$\{v_i^{Gf}, p^{Gf}\}(\underline{x},\underline{x}') = b_j\{G_{ji}^f, -\Gamma_j^f\}(\underline{x}',\underline{x}), \qquad (4.3.19)$$

where the quantities G_{ij}^f and Γ_i^f are denoted as the force-source tensor Green's function of rank two and the force-source vector Green's function, respectively. Now, using (4.3.19) in (4.3.18)) and recalling that (4.3.18) has to hold for arbitrary values of b_i, we end up with

$$- \int_{\underline{x}\in\partial D} [\Gamma_i^f(\underline{x}',\underline{x})v_j(\underline{x}) + G_{ij}^f(\underline{x}',\underline{x})p(\underline{x})]\nu_j(\underline{x})dA + v_i^{ext}(\underline{x}')$$

$$= \chi_D(\underline{x}')v_i(\underline{x}'), \qquad (4.3.20)$$

in which v_i^{ext} is the velocity due to the volume source distributions present in D and is given by

$$v_i^{ext}(\underline{x}') = \int_{\underline{x}\in D} \{\Gamma_i^f(\underline{x}',\underline{x})q(\underline{x}) + G_{ij}^f(\underline{x}',\underline{x})[\rho(\underline{x})g_j + f_j(\underline{x})]\}dV. \qquad (4.3.21)$$

Equation (4.3.20) is the desired source-type integral relation for the velocity field. If $\underline{x}'\in D$, (4.3.20) constitutes an integral representation for the velocity field. It expresses the value of the velocity at the

point $\underline{x} = \underline{x}'$ as the sum of the contributions from the volume sources present in D and the equivalent surface sources present on ∂D.

At this stage in the analysis, it is emphasized that the construction of the different Green's tensor functions is, in general, complicated for inhomogeneous media, but is rather straightforward for homogeneous media. In Section 4.5, the Green's functions G^q, Γ_i^q, G_{ij}^f and Γ_i^f will be calculated explicitly for a homogeneous and reciprocal medium of infinite extent.

4.4. BOUNDARY-INTEGRAL-EQUATION FORMULATIONS OF GROUNDWATER FLOW PROBLEMS

In this section we present several types of boundary-integral-equation formulations that apply to problems of the steady flow of groundwater. These integral-equation formulations enable us to determine, in principle, the flow fields in given configurations if on their boundary surfaces appropriate boundary values are prescribed.

In R^3 we consider a bounded domain D with closed boundary surface ∂D. The domain exterior to ∂D is denoted by D' and the unit vector along the normal to ∂D, pointing away from D, by ν_i (see Figure 4.2). D is assumed to be occupied by a given fluid-saturated porous medium. As regards the boundary conditions that hold on the outer boundary surface, we refer to the Sections 3.4 and 4.2, where we have seen that a flow field in D is

Table 4.1. Summary of the boundary conditions together with the unknown field quantities on the different parts of the closed boundary surface ∂D bounding the domain D.

part of ∂D	prescribed quantity	unknown quantity
∂D_1	$p = \psi_1$	$\nu_i v_i$
∂D_2	$\nu_i v_i = \psi_2$	p
∂D_3	$-\alpha \nu_i v_i + \beta p = \psi_3$	p or $\nu_i v_i$

The boundary surface ∂D consists of three parts: ∂D_1, ∂D_2, and ∂D_3, that together form ∂D; at least one of them is not the null set.

uniquely determined if on ∂D either the pressure, or the normal component of the velocity, or a linear combination of these quantities is prescribed (see Figure 4.2). The boundary conditions, with their accompanying unknown field quantities on ∂D, are summarized in Table 4.1, where we have adopted the nomenclature that has been introduced in Section 3.4 (cf. (3.4.4) - (3.4.6)). It is noted that in a practical configuration not all three parts of ∂D need be present; however, at least one of them is not the null set.

In view of the considerations made in the previous section, it is apparent that the two integral relations (4.3.12) and (4.3.20) both apply. As regards the Green's (scalar, vector, and tensor) functions that occur in them, these are considered as known functions; they are determined explicitly in Section 4.5 for an unbounded, homogeneous and reciprocal medium.

To formulate the boundary-integral-equation method, we first employ the integral relation (4.3.12). By taking in it the point of observation on ∂D, we are led to

$$-\int_{\underline{x}\in\partial D}[G^q(\underline{x}',\underline{x})v_i(\underline{x}) + \Gamma_i^q(\underline{x}',\underline{x})p(\underline{x})]\nu_i(\underline{x})dA + p^{ext}(\underline{x}')$$

$$= (1/2)p(\underline{x}') \qquad \text{where } \underline{x}'\in\partial D. \qquad (4.4.1)$$

As a next step, we decompose the surface integral into its contributions over ∂D_1, ∂D_2 and ∂D_3, respectively, take successively $\underline{x}'\in\partial D_1$, $\underline{x}'\in\partial D_2$ and $\underline{x}'\in\partial D_3$, and rearrange the resulting equations such that all unknown quantities appear on the left-hand sides and all known quantities on the right-hand sides. In this way, we obtain

$$-\int_{\underline{x}\in\partial D_1} G^q\nu_i v_i dA - \int_{\underline{x}\in\partial D_2}\Gamma_i^q\nu_i p dA - \int_{\underline{x}\in\partial D_3}[(\beta/\alpha)G^q + \nu_i\Gamma_i^q]pdA$$

$$= (1/2)\psi_1(\underline{x}') + \int_{\underline{x}\in\partial D_1}\Gamma_i^q\nu_i\psi_1 dA + \int_{\underline{x}\in\partial D_2} G^q\psi_2 dA - \int_{\underline{x}\in\partial D_3} G^q(\psi_3/\alpha)dA$$

$$- p^{ext}(\underline{x}') \qquad \text{where } \underline{x}' \in \partial D_1, \quad (4.4.2)$$

$$- \int_{\underline{x} \in \partial D_1} G^q \nu_i v_i dA - (1/2)p(\underline{x}') - \int_{\underline{x} \in \partial D_2} \Gamma_i^q \nu_i p dA$$

$$- \int_{\underline{x} \in \partial D_3} [(\beta/\alpha)G^q + \nu_i \Gamma_i^q] p dA$$

$$= \int_{\underline{x} \in \partial D_1} \Gamma_i^q \nu_i \psi_1 dA + \int_{\underline{x} \in \partial D_2} G^q \psi_2 dA - \int_{\underline{x} \in \partial D_3} G^q (\psi_3/\alpha) dA - p^{ext}(\underline{x}')$$

$$\text{where } \underline{x}' \in \partial D_2, \quad (4.4.3)$$

and

$$- \int_{\underline{x} \in \partial D_1} G^q \nu_i v_i dA - \int_{\underline{x} \in \partial D_2} \Gamma_i^q \nu_i p dA - (1/2)p(\underline{x}')$$

$$- \int_{\underline{x} \in \partial D_3} [(\beta/\alpha)G^q + \nu_i \Gamma_i^q] p dA$$

$$= \int_{\underline{x} \in \partial D_1} \Gamma_i^q \nu_i \psi_1 dA + \int_{\underline{x} \in \partial D_2} G^q \psi_2 dA - \int_{\underline{x} \in \partial D_3} G^q (\psi_3/\alpha) dA - p^{ext}(\underline{x}')$$

$$\text{where } \underline{x}' \in \partial D_3. \quad (4.4.4)$$

Equations (4.4.2), (4.4.3) and (4.4.4) constitute a system of three simultaneous boundary integral equations, from which, in principle, the unknown field distributions $\nu_i v_i$ on ∂D_1, p on ∂D_2, and p on ∂D_3 can be determined (cf. Table 4.1). If in an equation of this system the unknown quantity, i.e., p or $\nu_i v_i$, only occurs under the integral sign, the relevant equation is an integral equation of the first kind in that quantity, while if the unknown quantity also occurs outside the integral sign, the relevant integral equation is an integral equation of the second kind. Hence, the above system of boundary integral equations is, as far as the unknown field distributions p on ∂D_2 and p on ∂D_3 are concerned, a system of the second kind, while as far as the unknown field

distribution $\nu_i v_i$ on ∂D_1 is concerned, it is of the first kind. On the whole, in accordance with common usage, the system is denoted as a system of the mixed kind. At this point it should be noted that, since on ∂D_3 the Robin condition (3.4.6) applies, p could be eliminated at each point on ∂D_3 in (4.4.2) - (4.4.4) by means of (3.4.6). Clearly, (4.4.4) would then amount to a boundary integral equation of the second kind in $\nu_i v_i$.

The integral relation (4.3.20) for the velocity field leads to a system of boundary integral equations as well from which, in principle, the unknown field distributions of p and $\nu_i v_i$ on ∂D can be determined. To this end, we apply (4.3.20) to the configuration shown in Figure 4.2, take the point of observation on ∂D, and arrive at

$$- \int_{\underline{x}\in\partial D} [\Gamma_i^f(\underline{x}',\underline{x})v_j(\underline{x}) + G_{ij}^f(\underline{x}',\underline{x})p(\underline{x})]\nu_j(\underline{x})dA + v_i^{ext}(\underline{x}')$$

$$= (1/2)v_i(\underline{x}') \qquad \text{where } \underline{x}'\in\partial D. \qquad (4.4.5)$$

As a next step, we multiply (4.4.5) on both sides by $\nu_i(\underline{x}')$, and decompose the surface integral into its contributions over ∂D_1, ∂D_2 and ∂D_3, respectively. Then, upon taking successively $\underline{x}'\in\partial D_1$, $\underline{x}'\in\partial D_2$ and $\underline{x}'\in\partial D_3$, and rearranging the resulting equations such that all unknown quantities appear on the left-hand sides and all known quantities on the right-hand sides, we arrive at

$$- (1/2)\nu_i(\underline{x}')v_i(\underline{x}') - \nu_i(\underline{x}')\int_{\underline{x}\in\partial D_1} \Gamma_i^f\nu_j v_j dA - \nu_i(\underline{x}')\int_{\underline{x}\in\partial D_2} G_{ij}^f\nu_j pdA$$

$$- \nu_i(\underline{x}')\int_{\underline{x}\in\partial D_3} [(\beta/\alpha)\Gamma_i^f + G_{ij}^f\nu_j]pdA$$

$$= \nu_i(\underline{x}')\int_{\underline{x}\in\partial D_1} G_{ij}^f\nu_j\psi_1 dA + \nu_i(\underline{x}')\int_{\underline{x}\in\partial D_2} \Gamma_i^f\psi_2 dA$$

$$- \nu_i(\underline{x}')\int_{\underline{x}\in\partial D_3} \Gamma_i^f(\psi_3/\alpha)dA - \nu_i(\underline{x}')v_i^{ext}(\underline{x}') \quad \text{where } \underline{x}'\in\partial D_1, \qquad (4.4.6)$$

$$- \nu_i(\underline{x}') \int_{\underline{x} \in \partial D_1} \Gamma_i^f \nu_j v_j dA - \nu_i(\underline{x}') \int_{\underline{x} \in \partial D_2} G_{ij}^f \nu_j p dA$$

$$- \nu_i(\underline{x}') \int_{\underline{x} \in \partial D_3} [(\beta/\alpha)\Gamma_i^f + G_{ij}^f \nu_j] p dA$$

$$= (1/2)\psi_2(\underline{x}') + \nu_i(\underline{x}') \int_{\underline{x} \in \partial D_1} G_{ij}^f \nu_j \psi_1 dA + \nu_i(\underline{x}') \int_{\underline{x} \in \partial D_2} \Gamma_i^f \psi_2 dA$$

$$- \nu_i(\underline{x}') \int_{\underline{x} \in \partial D_3} \Gamma_i^f (\psi_3/\alpha) dA - \nu_i(\underline{x}') v_i^{ext}(\underline{x}') \quad \text{where } \underline{x}' \in \partial D_2, \qquad (4.4.7)$$

and

$$- \nu_i(\underline{x}') \int_{\underline{x} \in \partial D_1} \Gamma_i^f \nu_j v_j dA - \nu_i(\underline{x}') \int_{\underline{x} \in \partial D_2} G_{ij}^f \nu_j p dA - (\beta/2\alpha) p(\underline{x}')$$

$$- \nu_i(\underline{x}') \int_{\underline{x} \in \partial D_3} [(\beta/\alpha)\Gamma_i^f + G_{ij}^f \nu_j] p dA$$

$$= - (1/2\alpha)\psi_3(\underline{x}') + \nu_i(\underline{x}') \int_{\underline{x} \in \partial D_1} G_{ij}^f \nu_j \psi_1 dA + \nu_i(\underline{x}') \int_{\underline{x} \in \partial D_2} \Gamma_i^f \psi_2 dA$$

$$- \nu_i(\underline{x}') \int_{\underline{x} \in \partial D_3} \Gamma_i^f (\psi_3/\alpha) dA - \nu_i(\underline{x}') v_i^{ext}(\underline{x}') \quad \text{where } \underline{x}' \in \partial D_3. \qquad (4.4.8)$$

Equations (4.4.6), (4.4.7) and (4.4.8) constitute again a system of simultaneous boundary integral equations that is of the mixed kind. As far as the unknown field distributions $\nu_i v_i$ on ∂D_1 and p on ∂D_3 are concerned (cf. Table 4.1), it is of the second kind, while as far as the unknown distributions p on ∂D_2 is concerned, it is of the first kind. At this point it is noted again that at each point on ∂D_3 in (4.4.6), (4.4.7) and (4.4.8), p could, with the aid of the Robin condition (3.4.6), be rewritten in terms of $\nu_i v_i$ and ψ_3. Equation (4.4.8) would then amount to an integral equation of the second kind in $\nu_i v_i$.

It is clear that in arriving at a boundary-integral-equation formulation suitable for determining the unknown field distributions on ∂D, we can either use the system of equations (4.4.2) - (4.4.4), or the system (4.4.6) - (4.4.8), or a proper combination of these two systems. When solving (systems of) integral equations with the aid of iterative methods, preference is usually given to equations of the second kind, the latter having better convergence properties than (systems of) integral equations of the first kind. As an example, we write down a system that is consistently of the second kind; it consists of (4.4.6), (4.4.3) and (4.4.4), i.e.,

$$
\begin{aligned}
&- (1/2)\nu_i(\underline{x}')v_i(\underline{x}') - \nu_i(\underline{x}')\int_{\underline{x}\in\partial D_1} \Gamma_i^f \nu_j v_j dA - \nu_i(\underline{x}')\int_{\underline{x}\in\partial D_2} G_{ij}^f \nu_j p dA \\
&- \nu_i(\underline{x}')\int_{\underline{x}\in\partial D_3} [(\beta/\alpha)\Gamma_i^f + G_{ij}^f \nu_j] p dA \\
&= \nu_i(\underline{x}')\int_{\underline{x}\in\partial D_1} G_{ij}^f \nu_j \psi_1 dA + \nu_i(\underline{x}')\int_{\underline{x}\in\partial D_2} \Gamma_i^f \psi_2 dA \\
&- \nu_i(\underline{x}')\int_{\underline{x}\in\partial D_3} \Gamma_i^f (\psi_3/\alpha) dA - \nu_i(\underline{x}')v_i^{ext}(\underline{x}') \quad \text{where } \underline{x}'\in\partial D_1, \qquad (4.4.9)
\end{aligned}
$$

$$
\begin{aligned}
&- \int_{\underline{x}\in\partial D_1} G^q \nu_i v_i dA - (1/2)p(\underline{x}') - \int_{\underline{x}\in\partial D_2} \Gamma_i^q \nu_i p dA \\
&- \int_{\underline{x}\in\partial D_3} [(\beta/\alpha)G^q + \nu_i \Gamma_i^q] p dA \\
&= \int_{\underline{x}\in\partial D_1} \Gamma_i^q \nu_i \psi_1 dA + \int_{\underline{x}\in\partial D_2} G^q \psi_2 dA - \int_{\underline{x}\in\partial D_3} G^q (\psi_3/\alpha) dA - p^{ext}(\underline{x}') \\
&\qquad \text{where } \underline{x}'\in\partial D_2, \qquad (4.4.10)
\end{aligned}
$$

and

$$- \int_{\underline{x}\in\partial D_1} G^q \nu_i v_i dA - \int_{\underline{x}\in\partial D_2} \Gamma_i^q \nu_i p dA - (1/2)p(\underline{x}')$$

$$- \int_{\underline{x}\in\partial D_3} [(\beta/\alpha)G^q + \nu_i \Gamma_i^q] p dA$$

$$= \int_{\underline{x}\in\partial D_1} \Gamma_i^q \nu_i \psi_1 dA + \int_{\underline{x}\in\partial D_2} G^q \psi_2 dA - \int_{\underline{x}\in\partial D_3} G^q(\psi_3/\alpha) dA - p^{ext}(\underline{x}')$$

where $\underline{x}'\in\partial D_3$. (4.4.11)

For reference, we have listed the properties of each of the integral equations that arise from (4.4.1) and (4.4.5) in Table 4.2.

Table 4.2. Properties of the integral equations resulting from the integral relations (4.4.1) and (4.4.5).

part of ∂D	representation for the field quantity	unknown field quantity	resulting integral equation
∂D_1	p	$\nu_i v_i$	1st kind in $\nu_i v_i$
∂D_2	p	p	2nd kind in p
∂D_3	p	p	2nd kind in p
∂D_3	p	$\nu_i v_i$	1st kind in $\nu_i v_i$
∂D_1	$\nu_i v_i$	$\nu_i v_i$	2nd kind in $\nu_i v_i$
∂D_2	$\nu_i v_i$	p	1st kind in p
∂D_3	$\nu_i v_i$	p	1st kind in p
∂D_3	$\nu_i v_i$	$\nu_i v_i$	2nd kind in $\nu_i v_i$

At this point in the analysis it is recalled that the construction of the different Green's functions is, in general, for inhomogeneous media an unfeasible task. For a homogeneous and reciprocal media, however, they

can be obtained in a straightforward manner (cf. Section 4.5). In view of this, the use of the boundary-integral-equation method is, in practice, restricted to piecewise homogeneous domains. In configurations of this kind, the integral relations (4.3.12) and (4.3.20) are applied to each homogeneous subdomain out of which the relevant flow configuration is assumed to be composed. Let D denote the domain that is occupied by the given piecewise homogeneous flow configuration and assume D to be the union of N homogeneous subdomains $\{D_n;\ n=1,\ldots,N\}$ (see Figure 4.4). Let, further, ∂D_n be the boundary surface of D_n. We now apply either

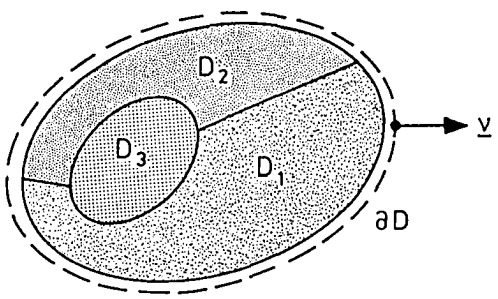

Fig. 4.4. Example of configuration with piecewise homogeneous subdomains. $D = D_1 \cup D_2 \cup D_3$ and ∂D is the outer boundary surface of D.

(4.3.12) or (4.3.20) to each homogeneous subdomain D_n. In this, the Green's functions pertaining to each of the subdomains are taken to be the ones that apply to the "infinite medium" with the adjoint properties of the actual homogeneous medium. Then, by taking in either (4.3.12) or (4.3.20) the *point of observation on* ∂D_n *for each* $n=1,\ldots N$, *either*

(4.3.12) or (4.3.20) leads to a number of boundary integral equations. At the interfaces between adjacent subdomains, the continuity requirements for the pressure and the normal component of the velocity are used to introduce these quantities as (unique) unknowns in the integral equations. In addition, at the outer boundary ∂D of D, the non-prescribed field quantities (see Table 4.1) occur as unknowns in the boundary integral equations.

Obviously, since for each subdomain we can either start from the source-type integral relation for the pressure, i.e., (4.3.12), or from the one for the velocity, i.e., (4.3.20), there is a freedom in choice of the boundary integral equations to be employed in the actual formulation. Since for nearly all configurations met in practice, all the above boundary integral equations have to be solved with the aid of numerical techniques, it is, at the present stage, rather difficult to make a proper selection which integral equations are to be used. A full discussion of the numerical aspects of solving the boundary integral equations is postponed to Chapter 5, while in Chapter 6 the results of some numerical experiments carried out on test configurations are reported.

Finally, it is noted that once the unknown field distributions p and/or $\nu_i v_i$ on ∂D, and on the possible interfaces in the interior of D, have been determined, the values of the flow field $\{p, v_i\}$ at any point in D straightforwardly follow upon reusing the integral representations (4.3.12) and (4.3.20).

4.5. CALCULATION OF THE GREEN'S SOLUTIONS PERTAINING TO A HOMOGENEOUS AND RECIPROCAL MEDIUM OF INFINITE EXTENT

In the present section the Green's states pertaining to the flow fields generated by a point source of volume injection and a point source of volume force, present in a homogeneous and reciprocal medium of infinite extent, are determined. In Subsection 4.5.1, we also introduce for this case the injection-rate scalar and force vector potentials and rewrite the two source-type integral relations developed in Section 4.3 in terms of these pore-flow potentials. Their explicit forms in case the reciprocal medium is isotropic are presented as well.

To evaluate the injection-source Green's flow state pertaining to a homogeneous and reciprocal medium of infinite extent we first multiply (4.3.7) on both sides by the, symmetric and positive definite, inverse K_{ij} of R_{ij}. We then have

$$K_{ij}\partial_j p^{Gq} + v_i^{Gq} = 0. \tag{4.5.1}$$

Now, upon applying to both sides of (4.5.1) the operator ∂_i and using (4.3.6), it follows that

$$K_{ij}\partial_i\partial_j p^{Gq} = -a\delta(\underline{x} - \underline{x}'). \tag{4.5.2}$$

To determine the solution of (4.5.2) we subject $x_i - x_i'$ to an orthogonal transformation such that the first term on the left-hand side is transformed on to its principal axes. Let

$$y_p = \alpha_{pq}(x_q - x_q') \tag{4.5.3}$$

be the relevant transformation, then the columns of the matrix (α_{pq}) are the normalized right eigenvectors of (K_{ij}) corresponding to the p-th eigenvalue $t^{(p)}$ of (K_{ij}). We then have

$$K_{ij}\partial_i\partial_j {}^pG^q = t^{(p)}\partial_{y_p}\partial_{y_p} {}^pG^q, \tag{4.5.4}$$

where ∂_{y_p} denotes differentiation with respect to y_p. Since (α_{pq}) is orthogonal, we have $\det(\alpha_{pq}) = 1$ and, hence

$$\delta(\underline{x} - \underline{x}') = \delta(\underline{y}). \tag{4.5.5}$$

Next, we introduce the variables z_p through

$$z_p = \left(t^{(p)}\right)^{-1/2} y_p, \tag{4.5.6}$$

then

$$t^{(p)}\partial_{y_p}\partial_{y_p} {}^pG^q = \partial_{z_p}\partial_{z_p} {}^pG^q, \tag{4.5.7}$$

and

$$\delta(\underline{y}) = \left[t^{(1)}t^{(2)}t^{(3)}\right]^{-1/2}\delta(\underline{z}) = \Delta^{1/2}\delta(z), \tag{4.5.8}$$

where

$$\Delta = \det(R_{ij}). \tag{4.5.9}$$

With the aid of (4.5.3) - (4.5.8), (4.5.2) transforms into

$$\partial_{z_p}\partial_{z_p} {}^pG^q = -a\Delta^{1/2}\delta(\underline{z}). \tag{4.5.10}$$

Equation (4.5.10) is nothing but Poisson's equation for a point source with strength $a\Delta^{1/2}$ (see, e.g., Kellogg, 1954, p. 156) and its solution that is regular at infinity, i.e., vanishes as $|\underline{z}| \to \infty$, uniformly in all directions, is given by

$$p^{Gq} = aG, \tag{4.5.11}$$

where G is given by

$$G = \Delta^{1/2}/(4\pi|\underline{z}|). \tag{4.5.12}$$

However, p^{Gq} is needed in terms of the original coordinates. Now, using (4.5.6) and (4.5.3), we obtain

$$|\underline{z}| = [\alpha_{pi}\alpha_{pj}(t^{(p)})^{-1}(x_i - x_i')(x_j - x_j')]^{1/2}. \tag{4.5.13}$$

Now, $R_{pi}K_{ij}\alpha_{qj} = R_{pi}t^{(q)}\alpha_{qi}$, or, since $R_{pi}K_{ij} = \delta_{pj}$, $\alpha_{qp} = R_{pi}t^{(q)}\alpha_{qi}$ for any q. With this we have

$$\alpha_{pi}\alpha_{pj}(t^{(p)})^{-1} = \alpha_{pi}R_{jr}\alpha_{pr} = R_{jr}\delta_{ir} = R_{ji} = R_{ij}. \tag{4.5.14}$$

Using (4.5.14) in (4.5.13), the following expression for p^{Gq} in the $\{x_1,x_2,x_3\}$ coordinate system is obtained (cf. (4.5.12) and (4.5.11))

$$p^{Gq} = aG(\underline{x} - \underline{x}'), \tag{4.5.15}$$

in which G is given by

$$G(\underline{x} - \underline{x}') = \Delta^{1/2}/(4\pi D), \tag{4.5.16}$$

and D by

$$D = [R_{ij}(x_i - x_i')(x_j - x_j')]^{1/2}. \tag{4.5.17}$$

The quantity D can be considered as the geodetical distance from $\underline{x}'$ to $\underline{x}$ with the resistivity as the metric tensor. From (4.5.1) it further follows that

$$v_i^{Gq} = - aK_{ij}\partial_j G(\underline{x} - \underline{x}'). \tag{4.5.18}$$

Comparing (4.3.11) with p^{Gq} and v_i^{Gq} as given in (4.5.15) and (4.5.18), respectively, it follows that the injection-source Green's tensor functions (of ranks zero and one, respectively) pertaining to a homogeneous and reciprocal medium of infinite extent are given by

$$G^q = G(\underline{x} - \underline{x}'), \tag{4.5.19}$$

and

$$\Gamma_i^q = K_{ij}\partial_j G(\underline{x} - \underline{x}'). \tag{4.5.20}$$

To arrive at the force-source Green's flow state pertaining to a homogeneous medium of infinite extent, we apply K_{ij} to both sides of (4.3.17) and obtain

$$K_{ij}\partial_j p^{Gf} + v_i^{Gf} = K_{ij}b_j\delta(\underline{x} - \underline{x}'). \tag{4.5.21}$$

Next, we apply the operator ∂_i to both sides of this equation. Taking (4.3.16) into account, it then follows that

$$K_{ij}\partial_i\partial_j p^{Gf} = \partial_i K_{ij}b_j\delta(\underline{x} - \underline{x}'). \tag{4.5.22}$$

In view of the fact that (cf. (4.5.15), (4.5.2) and (4.5.8))

$$K_{ij}\partial_i\partial_j G(\underline{x} - \underline{x}') = - \delta(\underline{x} - \underline{x}'), \tag{4.5.23}$$

p^{Gf} can be expressed in terms of G through

$$p^{Gf} = - K_{ij} b_j \partial_i G(\underline{x} - \underline{x}'). \tag{4.5.24}$$

Finally, from (4.5.21) and (4.5.24) the expression for v_i^{Gf} follows as

$$v_i^{Gf} = K_{iq} b_j K_{pj} \partial_q \partial_p G(\underline{x} - \underline{x}') + K_{ij} b_j \delta(\underline{x} - \underline{x}'). \tag{4.5.25}$$

Comparing (4.3.19) with p^{Gf} in (4.5.24) and v_i^{Gf} in (4.5.25), it follows that the force-source Green's functions (of ranks two and one, respectively) pertaining to a homogeneous and reciprocal medium of infinite extent are given by

$$G_{ij}^f = K_{jp} K_{qi} \partial_p \partial_q G(\underline{x} - \underline{x}') + K_{ji} \delta(\underline{x} - \underline{x}'), \tag{4.5.26}$$

and

$$\Gamma_i^f = K_{ji} \partial_j G(\underline{x} - \underline{x}'). \tag{4.5.27}$$

To complete the analysis on the Green's functions we observe that G only depends on $\underline{x}$ and $\underline{x}'$ through the term $R_{ij}(x_i - x_i')(x_j - x_j')$ (cf. (4.5.17)). Hence, the Green's functions G^q, Γ_i^q, G_{ij}^f, and Γ_i^f can also be written as (cf. (4.5.19), (4.5.20), (4.5.26) and (4.5.27))

$$G^q = G(\underline{x}' - \underline{x}), \tag{4.5.28}$$

$$\Gamma_i^q = - K_{ij} \partial'_j G(\underline{x}' - \underline{x}), \tag{4.5.29}$$

$$G_{ij}^f = K_{jp} K_{qi} \partial'_p \partial'_q G(\underline{x}' - \underline{x}) + K_{ji} \delta(\underline{x}' - \underline{x}), \tag{4.5.30}$$

and

$$\Gamma_i^f = - K_{ji} \partial'_j G(\underline{x}' - \underline{x}), \tag{4.5.31}$$

respectively, where ∂_i' denotes spatial differentiation with respect to the coordinate x_i'.

4.5.1. THE PORE-FLOW SCALAR AND VECTOR POTENTIALS

To account for the special structure of the Green's functions evaluated above, we introduce in this subsection the so-called pore-flow scalar and vector potentials that are associated with the pore-flow from distributed sources in an unbounded, homogeneous, reciprocal medium.

Consider the source-type integral representations (4.3.12) and (4.3.20) and apply them to a bounded domain D with boundary surface ∂D present in a homogeneous and reciprocal medium. Obviously, the Green's functions G^q, Γ_i^q, G_{ij}^f, and Γ_i^f, as given in (4.5.28), (4.5.29), (4.5.30) and (4.5.31), respectively, apply to (4.3.12) and (4.3.20). It should be noted that for the expressions of the Green's functions we have chosen the ones in which the spatial differentiations are carried out with respect to the observation-point coordinates $\underline{x}'$. We now introduce the following quantities:

$$\{A^D,\ F_i^D\}(\underline{x}') = \int_{\underline{x}\in D} G(\underline{x}' - \underline{x})\ \{q,\ \rho g_i + f_i\}(\underline{x})dV, \tag{4.5.32}$$

In (4.5.30), A^D is denoted as the pore-flow scalar potential associated with the distribution of volume injection present in D and F_i^D is denoted as the pore-flow vector potential associated with the distribution of the volume force present in D. Similarly, we introduce the quantities $A^{\partial D}$ and $F_i^{\partial D}$ defined as

$$\{A^{\partial D},\ F_i^{\partial D}\}(\underline{x}') = -\int_{\underline{x}\in\partial D} G(\underline{x}' - \underline{x})\ \{v_i v_i,\ v_i p\}(\underline{x})dA, \tag{4.5.33}$$

as the pore-flow scalar and vector potentials associated with the distribution of equivalent surface source densities of injection rate and force, respectively, present on ∂D. Now, with the aid of (4.5.28) - (4.5.31), (4.5.32) and (4.5.33), the source-type integral relations (4.3.12) and (4.3.20) can be written as

$$A - K_{ij}\partial'_j F_i = \chi_D(\underline{x}')p(\underline{x}') \tag{4.5.34}$$

and

$$- K_{ji}\partial'_j A + K_{jp}K_{qi}\partial'_p\partial'_q F_j = \chi_D(\underline{x}')\{v_i(\underline{x}') - K_{ji}[\rho g_j + f_j(\underline{x}')]\}, \tag{4.5.35}$$

respectively, in which A is given by

$$A = A^{\partial D} + A^D, \tag{4.5.36}$$

and F_i by

$$F_i = F_i^{\partial D} + F_i^D. \tag{4.5.37}$$

Equations (4.5.34) - (4.5.37) serve as the standard source-type integral representations for the groundwater flow field in a bounded subdomain of a homogeneous and reciprocal, fluid-saturated porous medium.

With the aid of (4.1.9), it is easily verified that for a homogeneous and isotropic medium the standard source-type representations (4.5.34) and (4.5.35) are given by

$$A - R^{-1}\partial'_i F_i = \chi_D(\underline{x}')p(\underline{x}') \tag{4.5.38}$$

and

$$- R^{-1}\partial'_i A + R^{-2}\partial'_i\partial'_j F_j = \chi_D(\underline{x}')\{v_i(\underline{x}') - R^{-1}[\rho g_i + f_i(\underline{x}')]\}, \tag{4.5.39}$$

respectively, to which (4.5.32), (4.5.33), (4.5.36) and (4.5.37) apply, with $G(\underline{x}' - \underline{x})$ now given by

$$G(\underline{x}' - \underline{x}) = R/4\pi|\underline{x}' - \underline{x}|. \qquad (4.5.40)$$

CHAPTER 5

NUMERICAL ASPECTS IN SOLVING THE BOUNDARY INTEGRAL EQUATIONS FOR GROUNDWATER FLOW IN PIECEWISE HOMOGENEOUS CONFIGURATIONS

Except for the very few configurations where analytical techniques are applicable, all boundary integral equations discussed in the previous chapter have to be solved with the aid of numerical techniques. In the present chapter an efficient and straightforward method to solve the systems of integral equations that apply to groundwater flow configurations with piecewise homogeneous media is discussed. Like in most numerical methods for solving integral equations, the relevant equations are replaced by a system of linear, algebraic equations. To obtain representative numerical results for practical situations, all steps involved must be implemented on a high-speed, large-capacity, digital computer.

For the ease of discussing the numerical aspects in solving the boundary integral equations, they are assumed to apply to a flow configuration in a domain that is occupied by a single homogeneous and reciprocal medium. The extension to configurations composed out of a finite number of homogeneous subdomains is discussed later on.

In Section 5.1 we discuss the geometrical discretization of the boundary surface of the domain of computation. In this process, the planar triangle is employed as the fundamental surface element. In Subsection 5.1.1, we introduce the barycentric coordinates of the position of observation in the triangle. These serve, in Subsection 5.1.2, to construct a local interpolation function that varies linearly with position in the interior and on the boundary of each triangle. In

Section 5.2 this linear interpolation function is used to represent locally, i.e., on each planar triangle, both the known and the unknown surface distributions of the pressure and the normal component of the velocity. In this manner, the continuity of these two flow quantities across the common edges of adjacent triangles is automatically satisfied. The structure of the global field representations follows straightforwardly from the local representations; they are presented in Section 5.3. In Subsection 5.4.1, the triangulation scheme and the global field representations are substituted in the source-type integral relations developed in Section 4.4 for the pressure and the velocity fields. Once a particular choice as regards which boundary integral equations to use has been made, we employ the method of collocation (or point matching) in the relevant discretized system of boundary integral equations in order to arrive at the square system of linear, algebraic equations that will replace it. The choice of the sequence of collocation points is discussed in Subsection 5.4.2. After applying the collocation scheme of Subsection 5.4.2, we are led to the final approximate versions of the selected system of boundary integral equations. To conclude Section 5.4, we show in Subsection 5.4.3 how to evaluate analytically the (singular) surface integrals over the planar triangles that occur in the discretized versions of the integral equations. Finally, in Section 5.5, the problem is addressed of how to incorporate in the resulting system of linear, algebraic equations the (discretized) version of the compatibility relation that pertains to the basic equations for the steady flow of groundwater.

5.1. THE DISCRETIZATION OF THE GEOMETRY

In the present section, we discuss the first steps towards the discretization of any of the systems of boundary integral equations developed in Section 4.4. We start with the geometrical discretization of the surface bounding the domain of computation. For this process, the planar triangle (simplex in R^2) is used as the elementary surface element. We then introduce on each triangle a local reference frame and employ this to construct a local, linear interpolation function. This interpolation function will be utilized to represent, on each triangle, the pertaining flow field distributions.

Let D denote the computational domain, i.e., the domain occupied by the homogeneous flow configuration of interest, and let ∂D be its closed boundary surface. We first subdivide or approximate ∂D by a finite number of elementary surface elements, the maximum diameter of which is so small that expressions of a simple nature, in fact linear expansions, suffice to represent the variations of the pertaining flow field quantities over it. Considerations in algebraic topology (see, e.g., Naber, 1980, p. 49) learn that the simplex (the point in R^0, the line segment in R^1, the triangle in R^2, and the tetrahedron in R^3) is the most fundamental shape. For these reasons (and some others as well), we discretize ∂D into planar, triangular surface elements. Let $\{S_T(N);\ N=1,\ldots,NT\}$ be the collection of planar triangles that together (approximately) span ∂D; we then have

$$\partial D \approx \bigcup_{N=1}^{NT} S_T(N), \tag{5.1.1}$$

NT being the total number of triangles. Obviously, for polyhedral domains the subdivision (5.1.1) can be made exact. The oriented boundary curve of each planar triangle $S_T(N)$ is denoted by $C_T(N)$. We take the orientation

such that the direction of circulation along $C_T(N)$ and the unit vector along the outward normal to $S_T(N)$ form a right-handed system. As regards the error introduced by approximating the, in general, curved surface ∂D, it is fortunately so that in the geometrical modeling of commonly encountered groundwater flow configurations (confined aquifers, and the like), it often suffices to model the possible interfaces and the outer boundary surface of the relevant flow configuration by a relatively small number of relatively large flat surfaces. Hence, the actual surfaces met in practice are usually well represented by utilizing planar triangles. Henceforth, in our analysis we only consider computational domains that are interiors of polyhedral surfaces (e.g., brick-like domains) for which the subdivision (5.1.1) can be made exact.

The subdivision (5.1.1) is arranged in such a manner that the triangles all have vertices and edges in common. In practice, the representation of ∂D by NT planar, triangular elements is obtained by choosing a finite number NP points on ∂D and connecting the latter points by straight line segments such that a network (grid) of NT triangles results. Since in (5.1.1) it is assumed that the triangles all have vertices and edges in common, we restrict in this procedure every point chosen on ∂D to be vertex of all triangles meeting at that point. Then, for a closed surface, we have a unique relationship between the number of surface or nodal points NP and the number of triangles NT, viz.

$$NT = 2NP - 4. \tag{5.1.2}$$

Hence, for a closed surface subdivided into a large number of planar triangles, the number of triangles is about twice as large as the number of nodal points.

In the subsequent analysis we need several geometrical quantities associated with the triangles. For each triangle S_T these are, first of all, the position vectors of its vertices with respect to the common background Cartesian reference frame (see Figure 2.1) and, secondly, its oriented edges. In their turn, these quantities enable us to determine

other necessary geometrical quantities pertaining to each triangle, such as, for example, its vectorial area, its scalar area, its unit vector along the normal. To this end, we first introduce a local numbering of the vertices of S_T. In this numbering, the vertices carry the labels $\{1,2,3\}$ and are denoted by $\{P_1,P_2,P_3\}$. From algebraic topology it follows that each simplex (apart from the point in R^0) can have two orientations. Since the computations can only be carried out for a particular orientation, we have to select one; the one that is chosen here is indicated in Figure 5.1a. It is such that the orientations of the edges P_1P_2, P_2P_3 and P_3P_1, induce a direction of circulation along C_T that forms a right-handed system with the unit vector along the normal to the (discretized) boundary surface ∂D, this normal pointing away from the domain D (see Figure 4.3). In view of later considerations, we further denote the edges of each triangle S_T by the labels $\{1,2,3\}$ according to the rule that each edge carries the label of the vertex opposite to it. These edges are referred to as $\{C_T(1),C_T(2),C_T(3)\}$ (see Figure 5.1a). Let $\{x_p(1),x_p(2),x_p(3)\}$ denote the position vectors with respect to the origin of the chosen background reference frame shown in Figure 2.1 of the vertices $\{P_1,P_2,P_3\}$ of S_T, then the vectorial edges $\{a_p(1),a_p(2),a_p(3)\}$ follow as (see Figure 5.1b)

$$a_p(I) = x_p(K) - x_p(J) : P_JP_K \quad \text{with } \{I,J,K\}=\text{cycl}\{1,2,3\}, \tag{5.1.3}$$

being the vectorial edge oriented from P_J to P_K, and "cycl" being short for "cyclic permutation of" (note, that I, J and K are different from each other). For example, if I=1 in (5.1.3), we have J=2 and K=3, while if I=2, we have J=3 and K=1. The lengths $\{a(1),a(2),a(3)\}$ of the respective edges $\{C_T(1),C_T(2),C_T(3)\}$ of S_T follow as (cf. (5.1.3))

$$a(I) = [a_p(I)a_p(I)]^{1/2} \qquad \text{with } I\in\{1,2,3\}. \tag{5.1.4}$$

The vectorial area of S_T, to be denoted by A_i, forms with the edges $\{C_T(1),C_T(2),C_T(3)\}$, in the indicated order, a right-handed system and

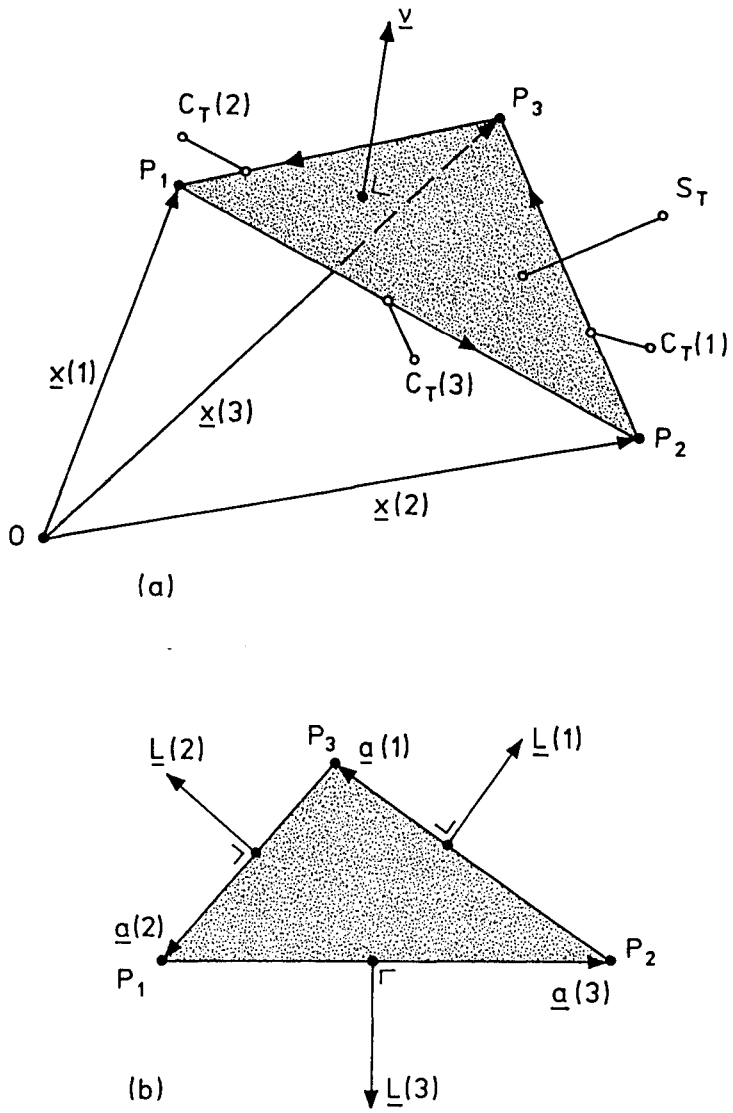

Fig. 5.1. Nomenclature of the (geometrical) quantities associated with the triangle S_T: (a) spatial view of S_T, (b) perpendicular view on S_T.

can be expressed in terms of the vectorial edges through (cf. (5.1.3))

$$A_i = (1/2)\varepsilon_{ijk}[x_j(I) - x_j(K)][x_k(J) - x_k(I)]$$

$$= (1/2)\varepsilon_{ijk}a_j(J)a_k(K) \qquad \text{with } \{I,J,K\}=\text{cycl}\{1,2,3\}, \qquad (5.1.5)$$

or in the symmetrical form

$$A_i = (1/2)\varepsilon_{ijk}[x_j(1)_k(2) + x_j(2)x_k(3) + x_j(3)x_k(1)], \qquad (5.1.6)$$

where ε_{ijk} is the completely antisymmetric unit tensor of rank three (Levi-Civita tensor):

$$\varepsilon_{ijk} = \begin{cases} +1 \text{ if } \{i,j,k\} \text{ is an even permutation of } \{1,2,3\}, \\ -1 \text{ if } \{i,j,k\} \text{ is an odd permutation of } \{1,2,3\}, \\ 0 \text{ if not all subscripts are different.} \end{cases} \qquad (5.1.7)$$

Now, the unit vector ν_i along the normal to S_T follows from

$$\nu_i = A_i/A, \qquad (5.1.8)$$

where A denotes the scalar area of S_T which is given by (cf. (5.1.5) or (5.1.6))

$$A = [A_iA_i]^{1/2}. \qquad (5.1.9)$$

Note that ν_i has a constant value on S_T. In our subsequent analysis we further need the vectors $\{L_p(1),L_p(2),L_p(3)\}$ that are oriented along the outward normals to the respective edges $\{C_T(1),C_T(2),C_T(3)\}$ in the plane of $S_T(n)$, each of them having a magnitude that equals the length of the relevant edge. We have (see Figure 5.1b).

$$L_i(I) = \varepsilon_{ijk}a_j(I)\nu_k \qquad \text{with } I\in\{1,2,3\}. \qquad (5.1.10)$$

With the aid of (5.1.10) and (5.1.3) it readily follows that

$$\sum_{I=1}^{3} L_i(I) = 0, \tag{5.1.11}$$

and

$$L_p(I)a_p(I) = 0, \qquad L_p(I)a_p(J) = -2A,$$

$$L_p(I)a_p(K) = +2A, \qquad \text{with } \{I,J,K\}=\text{cycl}\{1,2,3\}. \tag{5.1.12}$$

The above geometrical quantities together with some of their properties will be used in the next (sub)sections.

5.1.1. THE BARYCENTRIC COORDINATES

To arrive at the desired local representations of the flow field quantities in the interior and on the boundary of each planar triangle, it is advantageous to employ the so-called barycentric coordinates of the position of observation in the triangle.

Let S_T be the triangle under consideration to which the geometrical quantities introduced in Section 5.1 apply and let $\{\lambda(1),\lambda(2),\lambda(3)\}$ denote the barycentric coordinates pertaining to S_T. Then, the position of observation x_p in the interior and on the boundary of S_T can be specified by the barycentric coordinates through the relation (see, e.g., McConnell, 1957, pp. 52-54)

$$x_p = \sum_{I=1}^{3} \lambda(I)x_p(I), \text{ where } 0\leq\lambda(I)\leq 1 \text{ with } \sum_{I=1}^{3} \lambda(I) = 1 \text{ for } \underline{x}\in S_T, \tag{5.1.13}$$

where $\{x_p(1),x_p(2),x_p(3)\}$ are the position vectors of the respective vertices $\{P_1,P_2,P_3\}$ of S_T. Equation (5.1.13) yields the value of x_p for

given values of $\{\lambda(1),\lambda(2),\lambda(3)\}$. However, we would also like to have an expression that yields the values of $\{\lambda(1),\lambda(2),\lambda(3)\}$ for a given value of $x_p \in S_T$. This problem can be addressed as follows.

Select one of the vertices of S_T as the preferred one and eliminate the barycentric coordinate that has the value one at that vertex. As an example, we take in (5.1.13) P_1 to be the preferred vertex, and accordingly eliminate $\lambda(1)$. This yields (cf. (5.1.13))

$$x_p - x_p(1) = \sum_{I=2}^{3} \lambda(I)[x_p(I) - x_p(1)]. \tag{5.1.14}$$

Next, with the aid of (5.1.12) and (5.1.3), it is easily verified that (cf. (5.1.14))

$$[x_p(I) - x_p(1)]L_p(J) = -2A\delta(I,J) \text{ with } I\in\{2,3\} \text{ and } J\in\{2,3\}, \tag{5.1.15}$$

where $\delta(I,J)$ is the "two-subscript" Kronecker symbol

$$\delta(I,J) = \begin{cases} 1 \text{ if } I = J, \\ 0 \text{ if } I \neq J. \end{cases} \tag{5.1.16}$$

Equation (5.1.15) implies that at the vertex P_1 the vectors $\{x_p(2) - x_p(1), x_p(3) - x_p(1)\}$ and the vectors $\{-L_p(2)/2A, -L_p(3)/2A\}$ form a reciprocal system. Furthermore, upon applying (5.1.15) to (5.1.14), we conclude that

$$[x_p - x_p(1)]L_p(J) = -2A\lambda(J) \qquad \text{with } J\in\{2,3\}. \tag{5.1.17}$$

Adding the results for J=2 and J=3, and using the fact that (cf. (5.1.11))

$$L_p(1) = -L_p(2) - L_p(3), \tag{5.1.18}$$

we obtain

$$[x_p - x_p(1)]L_p(1) = 2A[\lambda(2) + \lambda(3)] = -2A\lambda(1). \qquad (5.1.19)$$

Using in (5.1.14) the expressions for $\lambda(2)$ and $\lambda(3)$ that result from (5.1.17), and the one for $\lambda(1)$ that results from (5.1.19), it readily follows that

$$x_p - x_p(1) = -(2A)^{-1}\sum_{I=1}^{3}\{[x_q - x_q(1)]L_q(I)\}x_p(I). \qquad (5.1.20)$$

Results similar to (5.1.20) hold when $x_p(1)$ is replaced by $x_p(2)$ and $x_p(3)$, respectively. Upon adding the relevant results, we end up with the symmetrical expression

$$x_p - b_p = -(2A)^{-1}\sum_{I=1}^{3}[(x_q - b_q)L_q(I)]x_p(I), \qquad (5.1.21)$$

in which

$$b_p = (1/3)[x_p(1) + x_p(2) + x_p(3)] \qquad (5.1.22)$$

is the position vector of the barycenter of S_T. Upon comparing the structure of (5.1.21) with the one of (5.1.13), we conclude that

$$\lambda(I) = 1/3 - (2A)^{-1}(x_q - b_q)L_q(I) \qquad \text{with } I\in\{1,2,3\}. \qquad (5.1.23)$$

Equation (5.1.23) yields the values of the barycentric coordinates of the position of observation in S_T whose position vector is x_q, which was the expression that we were after.

5.1.2. *THE LINEAR, SCALAR, LOCAL INTERPOLATION FUNCTION*

Inspection of (5.1.23) and (5.1.13) reveals that the barycentric coordinates perform, in the interior and on the boundary C_T of S_T, a

linear interpolation between the values of the expanded function (i.e., x_p in (5.1.13)) at the vertices of S_T. We further observe that this interpolation function takes on the value one at one of the vertices and the value zero at the remaining vertices. When stressing this aspect of the barycentric coordinates, we shall write $\phi(I,\underline{x})$ instead of $\lambda(I)$, i.e., (5.1.23) is rewritten as

$$\phi(I,\underline{x}) = 1/3 - (2A)^{-1}(x_q - b_q)L_q(I) \qquad \text{with } I\in\{1,2,3\}, \qquad (5.1.24)$$

with the property

$$\phi(I,\underline{x}(J)) = \delta(I,J) \qquad \text{with } I\in\{1,2,3\} \text{ and } J\in\{1,2,3\}, \qquad (5.1.25)$$

that is easily verified with the aid of (5.1.22), (5.1.10), (5.1.8), and (5.1.9), respectively. In our computations we also need the spatial derivatives of $\phi(I,\underline{x})$. Upon differentiating both sides of (5.1.24) with respect to x_i, it follows that

$$\partial_i\phi(I,\underline{x}) = -(2A)^{-1}L_i(I) \qquad \text{with } I\in\{1,2,3\}. \qquad (5.1.26)$$

In Section 5.2, the function $\phi(I,\underline{x})$ and some of its properties will be used to represent locally, i.e., on each planar triangle S_T, both the pressure and the normal component of the velocity.

5.2. THE LOCAL FIELD REPRESENTATIONS

In this section we discuss the structure of the local representations of the groundwater field quantities at an elementary surface element (i.e., a planar triangle) of the discretized surfaces.

The easiest, but at the same time coarsest, way to approximate the field distributions is to represent them by a constant value over S_T. The value of this constant can then be attributed to the value of the relevant quantity at some point of S_T, e.g., its barycenter. The next, more advanced, manner to represent the field quantities locally, is to employ interpolation formulas that vary linearly with position in the interior and on the boundary of each triangle. In our analysis, we have chosen this last approach, i.e., both the pressure and the normal component of the velocity are expanded in functions that vary linearly between the values of these quantities attributed to the vertices of the triangle. The reasons for using this type of local expansion function are discussed in Section 5.3.

In view of the results of Subsection 5.1.2, it is clear that the linear, scalar, local interpolation function $\phi(I,\underline{x})$ defined by (5.1.24) can serve directly to arrive at the desired local expansions for the flow field quantities. For the distribution of the pressure on S_T we have

$$p(\underline{x}) = \sum_{I=1}^{3} p(I)\phi(I,\underline{x}) \qquad \text{with } \underline{x}\in S_T. \tag{5.2.1}$$

In view of the property (5.1.25), $p(I)$ is the value of $p(\underline{x})$ at $x_q = x_q(I)$, approaching this vertex via the interior of S_T. Similarly, for the local expansion of the normal component of the velocity on S_T we write

$$\nu_i(\underline{x})v_i(\underline{x}) = \sum_{I=1}^{3} \nu_i(I)v_i(I)\phi(I,\underline{x}) \quad \text{with } \underline{x}\in S_T, \tag{5.2.2}$$

where $\nu_i(I)v_i(I)$ is the value of $\nu_i(\underline{x})v_i(\underline{x})$ at $x_q=x_q(I)$, approaching this vertex via the interior of S_T. Note that since $\nu_i(\underline{x})$ has a constant value for all $\underline{x}\in S_T$, $\nu_i(I)$ has the same (constant) value (5.1.8) for all $I\in\{1,2,3\}$.

The local field representations (5.2.1) and (5.2.2) will serve to construct the global field representations over the discretized boundary surface ∂D; this will be discussed in the next section.

5.3. THE GLOBAL FIELD REPRESENTATIONS

In this section we discuss the structure of the global representations of the flow field quantities over the discretized boundary surface of the homogeneous domain under consideration. They result upon using the local representations of Section 5.2 on each planar, triangular surface element of the discretized surface and putting these expansions properly together. We also summarize the major computational advantages of the representations of the flow field quantities employed here, as compared to other, simpler, representations.

The global field representations of the flow field quantities for all $\underline{x}\in\partial D$, where $\partial D = \sum_{N=1}^{NT} S_T(N)$, are written as (cf. (5.2.1) and (5.2.2))

$$p(\underline{x}) = \sum_{N=1}^{NT} \sum_{I=1}^{3} p(N,I)\phi(N,I,\underline{x}) \tag{5.3.1}$$

and

$$v_i(\underline{x})v_i(\underline{x}) = \sum_{N=1}^{NT} \sum_{I=1}^{3} v_i(N,I)v_i(N,I)\phi(N,I,\underline{x}), \tag{5.3.2}$$

where $\phi(N,I,\underline{x})$ is given by (cf. (5.1.24))

$$\phi(N,I,\underline{x}) = 1/3 - [2A(N)]^{-1}[x_q - b_q(N)]L_q(N,I), \tag{5.3.3}$$

in which $A(N)$ is the scalar area of $S_T(N)$, $b_q(N)$ the position vector of the barycenter of $S_T(N)$ and $\{L_q(N,1),L_q(N,2),L_q(N,3)\}$ are the vectors normal to the respective edges $\{C_T(N,1),C_T(N,2),C_T(N,3)\}$ in the plane of $S_T(N)$ (cf. (5.1.10)). In these quantities we have incorporated the ordinal number N to indicate that they belong to the triangle $S_T(N)$.

The representations (5.3.1) and (5.3.2) will be employed in the discretization of any of the boundary integral equations discussed in

Section 4.4 both for the known and unknown surface distributions. In this manner, both (5.3.1) and (5.3.2) provide us with 3•NT vertex expansion coefficients. Not all of these are, however, also global expansion coefficients. In this respect a distinction must be made between nodal points that are located on the flat parts of the discretized geometry and at which a unique unit normal is defined, and nodal points that are located on edges or in corners of the discretized geometry where the unit normal is not uniquely defined. At the nodal points of the first category (the so-called simple nodes), p and $v_i v_i$ are continuous and hence the values of p(N,I) and $v_i(N,I)v_i(N,I)$ at the vertices that meet at that nodal point are equal. This condition could be enforced after setting up the system of linear algebraic equations that results from applying the method of collocation (cf. Section 5.4). However, enforcing that condition before setting up the system of equations leads to a much more efficient handling of the computer's storage capacity. Hence, we shall introduce the relevant vertex values as single global knowns and unknowns and correspondingly let the support of their global expansion functions be the union of the triangles to a vertex of which the considerations apply. The corresponding variables will be denoted as nodal variables. At those nodal points that do not have a uniquely defined unit normal (the so-called multiple nodes) we retain (5.3.1) and (5.3.2) as they stand; the relevant variables will be denoted as vertex variables and they will be used as the global ones. Hence, the number of global expansion coefficients NG is smaller than or equal to 2×(3•NT) and greater than 2×NP = 2×[(NT+4)/2] (cf. (5.1.1) and (5.1.2)). As we have stipulated in Section 5.1, however, the surface(s) that have to be subdivided into planar triangles, usually involve relatively large flat parts (brick-like geometries) and the number of multiple nodes (at which the unit normals are not uniquely defined) is, in general, relatively small.

Apart form the discussion on the nodal points at which the unit normals are not uniquely defined, we have in fact in the considerations made above already highlighted implicitly some of the major advantages of our piecewise linear interpolation scheme as compared to the piecewise

constant one as suggested by, e.g., Jawson and Symm (1977, p. 233). In the latter, the field quantities are, on each surface element, approximated by a constant, whose value is attributed to the field value at a particular point (e.g., the barycenter) of the relevant surface element. These values are subsequently taken as the expansion coefficients. Doing this for a domain with a closed boundary surface that has been subdivided into NT planar triangles, we end up with NT unknowns. If, like in our situations, the relevant boundary surface is composed out of a relatively small number of relatively large flat parts, we have to compare this number of unknowns with the somewhat more than (NT+4)/2 ones resulting from the piecewise linear interpolation scheme. Hence, whenever in the discretization of a boundary integral equation a relatively large number of triangles is needed and a piecewise linear interpolation scheme is used instead of a piecewise constant one, the final number of unknowns will be reduced by a factor of about two. In addition to this, it is evident that in a piecewise constant approximation more surface elements are, in general, needed to follow the field variations over the elements, than in a piecewise linear one. The piecewise constant interpolation scheme also leads to (unphysical) discontinuities in the field values across the common edges of adjacent triangles, whereas in the linear interpolation scheme continuity is automatically guaranteed (except, of course, for the values of the pressure and the normal component of the velocity at those locations where these quantities do jump indeed).

These considerations have motivated us to use the linear field representations (5.3.1) and (5.3.2) in the discretization of any of the boundary integral equations of Section 4.4.

5.4. THE METHOD OF COLLOCATION

As outlined in the introduction to this chapter, our aim is to replace any of the systems of boundary integral equations developed in Section 4.4 to forms amenable to numerical solution. To this end, we employ, in addition to the discretization procedure discussed in the previous sections, the method of collocation (also denoted as the method of point matching) (see, e.g., Kantorovich and Krylov, 1964, pp. 97-110). This method can be seen as a special case of the method of moments (see, e.g., Harrington, 1968, pp. 5-21).

The discretized forms of the boundary integral relations for both the pressure and the velocity that result after applying the triangulation scheme of Section 5.1 and using the global field representations of Section 5.3, are presented in Subsection 5.4.1. In Subsection 5.4.2, the choice of the sequence of collocation points is discussed. In this subsection it is further outlined how the square system of linear, algebraic equations is obtained. The latter replaces (approximately) the system of boundary integral equations under consideration. In Subsection 5.4.3, we outline how the (singular) integrals over planar triangles that arise from the discretization procedure and the collocation method are evaluated analytically. These integrals occur as coefficients in the square system of linear, algebraic equations.

5.4.1. THE DISCRETIZED BOUNDARY INTEGRAL RELATIONS

In this subsection we present the discretized forms of the boundary integral relations for both the pressure field and the velocity field that result after applying the triangulation scheme of Section 5.1 and

after insertion of the global field representations (5.3.1) and (5.3.2). We further list the (singular) integrals over planar triangles that occur in the two discretized integral relations.

Inserting the global field representations (5.3.1) and (5.3.2) in (4.4.1) and (4.4.5) (after multiplying both sides by the unit normal vector at $\underline{x}'$) and taking into account (5.1.1), we end up with the approximate equations

$$- \sum_{N=1}^{NT} \sum_{I=1}^{3} [\nu_i(N,I)v_i(N,I)IG^q(N,I,\underline{x}') + p(N,I)I\Gamma^q(N,I,\underline{x}')]$$

$$+ p^{ext}(\underline{x}') \approx (1/2)p(\underline{x}') \quad \text{when } \underline{x}' \in \partial D, \tag{5.4.1}$$

and

$$\nu_i(\underline{x}')\{- \sum_{N=1}^{NT} \sum_{I=1}^{3} [\nu_j(N,I)v_j(N,I)I\Gamma_i^f(N,I,\underline{x}') + p(N,I)IG_i^f(N,I,\underline{x}')]$$

$$+ v_i^{ext}(\underline{x}')\} \approx (1/2)\nu_i(\underline{x}')v_i(\underline{x}') \quad \text{when } \underline{x}' \in \partial D, \tag{5.4.2}$$

in which

$$IG^q(N,I,\underline{x}') = \int_{\underline{x} \in S_T(N)} \phi(N,I,\underline{x})G^q(\underline{x}',\underline{x})dA, \tag{5.4.3}$$

$$I\Gamma^q(N,I,\underline{x}') = \int_{\underline{x} \in S_T(N)} \phi(N,I,\underline{x})\Gamma_i^q(\underline{x}',\underline{x})\nu_i(N)dA, \tag{5.4.4}$$

$$I\Gamma_i^f(N,I,\underline{x}') = \int_{\underline{x} \in S_T(N)} \phi(N,I,\underline{x})\Gamma_i^f(\underline{x}',\underline{x})dA, \tag{5.4.5}$$

$$IG_i^f(N,I,\underline{x}') = \int_{\underline{x} \in S_T(N)} \phi(N,I,\underline{x})G_{ij}^f(\underline{x}',\underline{x})\nu_j(N)dA, \tag{5.4.6}$$

with $\phi(N,I,\underline{x})$ defined by (5.3.3), and where ν_i has the constant value $\nu_i(N)$ for all $\underline{x} \in S_T(N)$. In (5.4.3) - (5.4.6) the Green's functions G^q, Γ_i^q,

Γ_i^f and G_{ij}^f are known (cf. (4.5.19), (4.5.20), (4.5.27) and (4.5.26)). It is emphasized that all integrals in (5.4.3) - (5.4.6) can be evaluated analytically; this will be discussed in Subsection 5.4.3 and Appendix C. In Subsection 5.4.3, it is also outlined how to deal with the (known) source functions p^{ext} and v_i^{ext} occurring in (5.4.1) and (5.4.2), respectively.

5.4.2. THE SEQUENCE OF COLLOCATION POINTS

In the present subsection the choice of the sequence of collocation points on the triangulated boundary surface ∂D is discussed.

In applying the collocation method to (5.4.1), (5.4.2), or some suitable combination of these (cf. Section 4.4), one has to take care that the indicated (approximate) equality only holds at points of the discretized boundary surface where the unit normal is uniquely defined. In our collocation scheme we shall strictly adhere to this condition.

In view of this, in choosing the sequence of collocation points, we must distinguish between simple nodal points, i.e., nodal points having a unique unit normal, and multiple ones, i.e., nodal points at which planar triangles with different (constant) unit normal vectors meet. At a simple nodal point, (5.4.1), (5.4.2), or some suitable combination of them (cf. Section 4.4), are straightforwardly used. At a multiple node, (5.4.1), (5.4.2), or some suitable combination of them are used at the vertices that meet at that node (each with its own unit normal). In Figure 5.2 we have schematically visualized the choice of collocation points for the different situations.

After applying the above collocation scheme and carrying out the appropriate rearrangements we end up with a square system of linear, algebraic equations for the unknown (vertex and nodal) expansion

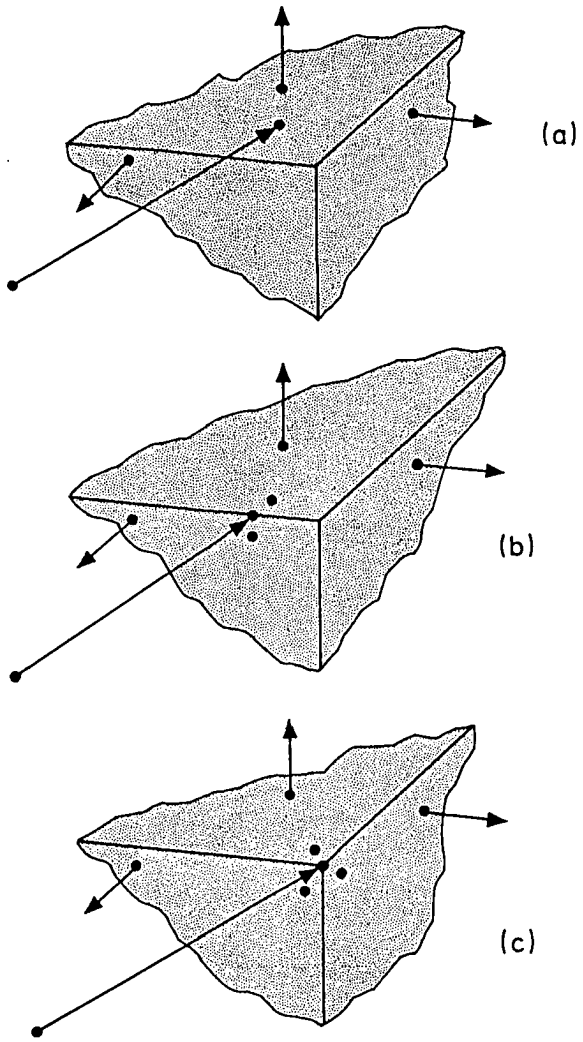

Fig. 5.2. The sequence of collocation points in different situations: (a) simple node; unique unit normal, (b) multiple node on edge; two unit normals, and (c) multiple node in corner; three unit normals.

coefficients that can be written as

$$\sum_{j=1}^{NG} a_{i,j} b_j = c_i \qquad \text{for } i\in\{1,\ldots,NG\}, \tag{5.4.7}$$

where NG denotes the total number of global unknown (vertex and nodal) expansion coefficients on ∂D (cf. Section 5.3). In (5.4.7), the known coefficients $\{a_{i,j};\ i\in\{1,\ldots,NG\}$ and $j\in\{1,\ldots,NG\}\}$ result from the (analytic) evaluation of $IG^q(N,I,\underline{x}')$ and $I\Gamma^q(N,I,\underline{x}')$, and/or $I\Gamma_i^f(N,I,\underline{x}')$ and $IG_i^f(N,I,\underline{x}')$ for the pertaining values of N and I. The coefficients $\{c_i;\ i\in\{1,\ldots,NG\}\}$ contain the contributions from the prescribed surface distributions and the known source terms p^{ext} and/or v_i^{ext} (cf. (5.4.1) and (5.4.2)).

The global representation scheme discussed in Section 5.3, together with the collocation procedure outlined above, has been tested for a mathematical test flow, viz., a uniform flow with linearly varying pressure and constant flow velocity in a homogeneous, cube-like domain. Obviously, in this case also at the multiple nodes there must exist a unique pressure. This is confirmed by the numerical experiment that shows equal values of all pressures at the vertices that meet at the common nodal points located on the edges and in the corners of the triangulated boundary of the computational domain. This and other numerical experiments are discussed in detail in Chapter 6.

5.4.3. ANALYTIC EVALUATION OF THE SURFACE INTEGRALS OCCURRING IN THE DISCRETIZED BOUNDARY INTEGRAL EQUATIONS

In this subsection it is outlined how the integrals IG^q, $I\Gamma^q$, $I\Gamma_i^f$ and IG_i^f (cf. (5.4.3) - (5.4.6)) can be evaluated analytically. They are in fact the potentials due to certain single-, double-, and triple-layer distributions on a triangular disk in an anisotropic medium.

In the literature, surface potentials for constant surface densities on polygonal disks have been treated analytically by, e.g., Birtles, Mayo and Bennett (1973), Rao et al. (1979), Waldvogel (1979), and Herman (1981, pp. 171-176). Analytic expressions for surface potentials with linearly varying surface densities on polygonal disks are given by, e.g., Van Herk (1980, pp. 157-166) and Wilton et al. (1984). All these authors consider only surface potentials due to single- and double-layer distributions in isotropic media. We shall derive analytic expressions for all integrals (5.4.3) - (5.4.6) both for isotropic and anisotropic media.

The main tool to evaluate the above integrals is to rewrite their integrands in such a form that Stokes' theorem can be employed. Subsequent use of this theorem replaces the surface integrals by line integrals along the boundary curve of the disk. Each boundary curve of the triangular disk is the union of three straight line segments and it can easily be shown that the resulting line integrals along these straight line segments can be expressed in terms of elementary functions. Obviously, this method is not restricted to planar triangles, but can be applied to any polygonal surface element as well.

For the isotropic case the method indicated above can be employed straightforwardly. For the anisotropic case, however, we first apply to the relevant integrals an orthogonal transformation, followed by a stretching procedure of the (transformed) coordinates. In this manner, the "anisotropic" integrals will acquire an "isotropic" structure, and hence, we can reuse the techniques applicable to the latter.

As an intermediate step in transforming the surface integrals to forms amenable to the application of Stokes' theorem, we come across a particular integral that cannot be handled in this manner. Since the relevant integral also has a geometrical interpretation (viz., the solid angle at which the relevant triangle is observed from the point of observation), a closed-form expression can be obtained from the theory of spherical trigonometry. On the other hand, analytic evaluation is still

possible by an alternative method; for completeness, the latter method is discussed in some detail, too.

Since the actual computations are rather lengthy and tedious, they are collected in Appendix C. The final expressions obtained are fairly compact; they have been used to arrive at the numerical results discussed in Chapter 6.

In the discretized integral relations (5.4.1) and (5.4.2), and hence, in the final square system of linear, algebraic equations, the contributions from the known source terms p^{ext} and/or v_i^{ext} (cf. (4.3.13) and (4.3.21)) are still to be considered.

First of all, the parts in these domain integrals that are associated with gravity are reduced to surface integrals over the boundary surface ∂D of each homogeneous (sub)domain D. For this purpose, we take into account that the Green's functions G^q and Γ_i^q are interrelated through (cf. (4.5.19) and (4.5.20))

$$\Gamma_i^q(\underline{x}',\underline{x}) = K_{ij}\partial_j G^q(\underline{x}',\underline{x}), \tag{5.4.8}$$

and, similarly, the Green's functions Γ_i^f and G_{ij}^f through (cf. (4.5.26) and (4.5.27)).

$$G_{ij}^f(\underline{x}',\underline{x}) = K_{jp}\partial_p \Gamma_i^f(\underline{x}',\underline{x}) + K_{ji}\delta(\underline{x} - \underline{x}'). \tag{5.4.9}$$

Furthermore, since ρ has a constant value throughout D, it follows with the aid of Gauss' theorem, and in (4.3.21) also with the aid of the integral property of the three-dimensional delta function, that p^{ext} and v_i^{ext} can be written as (cf. (4.3.13))

$$p^{ext}(\underline{x}') = \rho g_i K_{ij} \int_{\underline{x}\in\partial D} \nu_j(\underline{x}) G^q(\underline{x}',\underline{x}) dA$$

$$+ \int_{\underline{x}\in D} [G^q(\underline{x}',\underline{x})q(\underline{x}) + \Gamma_i^q(\underline{x}',\underline{x})f_i(\underline{x})]dV, \tag{5.4.10}$$

and (cf. (4.3.21) and (4.3.8))

$$v_i^{ext}(\underline{x}') = \chi_D(\underline{x}')\rho g_j K_{ji} + \rho g_j K_{jp} \int_{\underline{x}\in\partial D} \nu_p(\underline{x})\Gamma_i^f(\underline{x}',\underline{x})dA$$

$$+ \int_{\underline{x}\in D} [\Gamma_i^f(\underline{x}',\underline{x})q(\underline{x}) + G_{ij}^f(\underline{x}',\underline{x})f_j(\underline{x})]dV, \qquad (5.4.11)$$

respectively. After applying to the surface integrals on the right-hand sides of (5.4.10) and (5.4.11) the discretization scheme outlined in the present chapter, it readily follows that they are to be replaced by (cf. (5.1.1), (5.3.1) and (5.3.2))

$$\rho g_i K_{ij} \int_{\underline{x}\in\partial D} \nu_j(\underline{x})G^q(\underline{x}',\underline{x})dA \approx \rho g_i K_{ij} \sum_{N=1}^{NT} \nu_j(N)IG^q(N,\underline{x}'), \qquad (5.4.12)$$

and

$$\rho g_j K_{jp} \int_{\underline{x}\in\partial D} \nu_p(\underline{x})\Gamma_i^f(\underline{x}',\underline{x})dA \approx \rho g_j K_{jp} \sum_{N=1}^{NT} \nu_p(N)I\Gamma_i^f(N,\underline{x}'), \qquad (5.4.13)$$

where $IG^q(N,\underline{x}')$ and $I\Gamma_i^f(N,\underline{x}')$ are given in (5.4.3) and (5.4.5), respectively, with $\phi(N,I,\underline{x})$ replaced by unity, and, accordingly, the ordering of the vertices has been omitted.

Finally, once the distributions of the injection and force sources acting in D have been specified, we can evaluate their contributions to p^{ext} and v_i^{ext} (cf. (5.4.10) and (5.4.11)). In general, the relevant domain integrals have to be computed with the aid of numerical integration rules. To this end, we subdivide the part(s) of D in which q and f_i differ from zero into a number of tetrahedra and approximate in each tetrahedron q and f_i by a constant value. Hence, in the domain integrals over each tetrahedron q and f_i can be put in front of the relevant integrals and we are left with the integrations of the Green's functions G^q, Γ_i^q, Γ_i^f and G_{ij}^f over the tetrahedra. Obviously, with the aid of (5.4.8), (5.4.9), and the relation (cf. (4.5.20) and (4.5.27))

$$\Gamma_i^f(\underline{x}',\underline{x}) = \Gamma_i^q(\underline{x}',\underline{x}), \tag{5.4.14}$$

in which we have taken into account the symmetry of K_{ij}, the integrals over the tetrahedra containing the Green's functions Γ_i^q, Γ_i^f and G_{ij}^f can with the further application of Gauss' theorem be replaced by surface integrals over the triangular faces of the tetrahedra. The analytic evaluation of the latter surface integrals proceeds along similar lines as the ones outlined in the beginning of this subsection. With this, the analytic evaluation of the domain integrals containing Γ_i^q, Γ_i^f and G_{ij}^f has been settled, and hence, only the domain integration over the tetrahedra of G^q remains to be considered. To this end, we first observe that (cf. (4.5.19))

$$G^q(\underline{x}',\underline{x}) = (1/2)[\det(R_{ij})]^{1/2} K_{ij}\partial_i\partial_j[R_{mn}(x_m' - x_m)(x_n' - x_n)]^{1/2}, \tag{5.4.15}$$

when $\underline{x}\neq\underline{x}'$, which is verified by carrying out the differentiations. Now, upon integrating (5.4.15) over each tetrahedron and using Gauss' theorem in the resulting integrals on the right-hand side, the relevant domain integrals are replaced by surface integrals over the faces of the tetrahedra. The integrands of the latter are of the form $\nu_i K_{ij}\partial_j[R_{mn}(x_m'-x_m)(x_n'-x_n)]^{1/2}$, where ν_i denotes the outwardly directed, constant, unit normal vector on each face. These integrals, too, can be evaluated analytically upon employing the procedures outlined in the first part of the present subsection.

Through these procedures, piecewise constant values of q and f_i lead to contributions to p^{ext} and v_i^{ext} in (5.4.10) and (5.4.11) that can be expressed in terms of elementary analytic functions.

As already remarked in Subsection 3.2.1, most flow configurations met in practice deal with injection (abstraction) sources only, and hence, $f_i=0$ throughout the domain of interest. In regional (large-scale) groundwater flow problems these (injection) sources are commonly represented as point sources (see, e.g., Liggett and Liu, 1983, p. 4).

Taking into account the integral property of three-dimensional delta function, this implies that their contributions to p^{ext} in (5.4.10) and to v_i^{ext} in (5.4.11) reduce to simple multiplications of the source strength of the relevant point source by the corresponding Green's function, in which now the distance from the location of the relevant sources to the point of observation occurs.

5.5. THE INCORPORATION OF THE COMPATIBILITY RELATION

In this section a method is presented to incorporate the compatibility relation (3.4.7) in the numerical procedure.

The compatibility relation (3.4.7) expresses that the out-(in-) flux across the closed boundary surface ∂D of the bounded flow domain D of interest must be equal to the rate at which the sources inject (abstract) a certain net volume into (out of) D. In general, it is conjectured that the discretized version of (3.4.7) will not be satisfied by the solutions of the discretized systems of boundary integral equations. The degree of this violation is related to the ratio of the part(s) of the boundary surface ∂D on which the normal component of the velocity is unknown and the part(s) on ∂D on which it has a known prescribed value. We shall now discuss a method to incorporate the discretized form of the compatibility relation in any of the square systems of linear, algebraic equations by which the boundary integral equations have been replaced.

First of all, we apply the triangulation scheme of Section 5.1 to (3.4.7) and insert in the resulting left-hand side the field representation (5.3.2). In this, by taking into account that in each planar triangle $S_T(N)$ the expansion function $\phi(N,I,\underline{x})$ is nothing but the barycentric coordinate $\lambda(I)$ on $S_T(N)$, each integral over $S_T(N)$ is easily evaluated and leads to a net outward flux $q^S(N)$ on $S_T(N)$

$$q^S(N) = (1/3)A(N) \sum_{I=1}^{3} \nu_i(N,I)v_i(N,I), \qquad (5.5.1)$$

in which A(N) is the scalar area of $S_T(N)$ and $\nu_i(N,I)v_i(N,I)$ is the value of the normal component of the velocity at the I-th vertex of $S_T(N)$. Taking into account that ∂D is subdivided into NT planar triangles, the discretized version of (3.4.7) can be written as

$$(1/3)\sum_{N=1}^{NT} A(N)\sum_{I=1}^{3} v_i(N,I)v_i(N,I) = Q, \qquad (5.5.2)$$

where Q denotes the value that results after the integration over the domain D of the external injection (abstraction) sources acting in D. Now, from Section 5.3 it is known that the 3·NT expansion coefficients for the normal component of the velocity that (5.5.2) would suggest at first sight, correspond to NG global (vertex and nodal) expansion coefficients with $(NT+4)/2 < NG \leq 3 \cdot NT$. Some of their values are known, viz., the variables that correspond to points on ∂D on which the normal component of the velocity has a given prescribed value (cf. Table 4.1), while the values of the remaining ones, viz., the ones that correspond to points on ∂D on which the pressure has a known value (cf. Table 4.1) are, of course, unknown. Now, the first step to incorporate (5.5.2) into the system of linear, algebraic equations (5.4.7) is to rearrange (5.5.2) such that on its left-hand side all unknown global expansion variables for the normal component of the velocity with their corresponding coefficients (i.e., (1/3)A(N) in (5.5.2)) occur and on the right-hand side, in addition to Q, the known ones with their corresponding coefficients. Next, the structure of the vector of unknowns that occurs in this system will be matched to the one in (5.4.7). The latter vector of unknowns, i.e., b_i with $i \in \{1,\ldots,NG\}$, does not only contain the unknown global (vertex and nodal) expansion variables for the normal component of the velocity, but also the unknown global (vertex and nodal) expansion variables for the pressure. However, in (5.5.2) we can easily replace the vector of unknown global expansion variables for the normal component of the velocity by the vector $\{b_i;\ i \in \{1,\ldots,NG\}\}$ of (5.4.7) provided that we take the coefficients multiplying the unknown global pressure expansion variables occurring in $\{b_i;\ i \in \{1,\ldots,NG\}\}$ equal to zero. In this way, (5.5.2) is replaced by

$$\sum_{i=1}^{NG} d_i b_i = h, \qquad (5.5.3)$$

in which the coefficients d_i that correspond to (unknown) pressure variables are put equal to zero. The known scalar quantity h on the right-hand side of (5.5.3) contains, apart from Q, all known values of the global expansion variables for the normal component of the velocity and their multiplying coefficients. The structure of the discretized version of the compatibility relation as given in (5.5.3) now matches the one of (5.4.7). To satisfy (5.4.7) and (5.5.3) simultaneously, we now minimize the following squared error:

$$\text{ERROR} = \sum_{i=1}^{NG} \left[\sum_{j=1}^{NG} a_{i,j}b_j - c_i\right]^2 + \xi\left[\sum_{j=1}^{NG} d_j b_j - h\right]^2, \qquad (5.5.4)$$

in which ξ is a positive parameter. The minimum of ERROR is attained when $\{b_m;\ m\in\{1,\ldots,NG\}\}$ satisfies the system of linear, algebraic equations

$$\sum_{j=1}^{NG} \left[\sum_{i=1}^{NG} a_{i,m}a_{i,j} + \xi d_j d_m\right]b_j = \sum_{i=1}^{NG} a_{i,m}c_i + \xi d_m h, \qquad (5.5.5)$$

for all $m\in\{1,\ldots,NG\}$. By varying the parameter ξ in (5.5.5), one influences the relative importance of taking into account the (discretized) compatibility relation in this system. For $\xi=0$, the square system (5.5.5) has the same form as the original one in (5.4.7), be it that it is multiplied on both sides by the transpose of the matrix of coefficients.

The only remaining question is the choice of a suitable value for the parameter ξ. This value must be established by trial and error.

CHAPTER 6

NUMERICAL RESULTS FOR TEST FLOWS

In the present chapter some numerical experiments are carried out in order to test the performance of the boundary-integral-equation method for analyzing steady groundwater flow problems as it has been developed in the previous chapters. The test flow taken for this purpose is a uniform source-free one; it is considered in a cube as the computational domain of interest. The cube is filled with a homogeneous medium, either isotropic or anisotropic (but reciprocal); both cases are considered. Then the flow velocity is an, arbitrarily oriented, vector of constant magnitude, and the accompanying pressure varies linearly with position. The boundary surface of the cube is discretized into triangles; examples of this are shown in Figure 6.1 in Section 6.1. The cube-shaped domain D under consideration is defined by

$$D = \{\underline{x} \in R^3;\ 0<x_1<1, 0<x_2<1, 0<x_3<1\}. \tag{6.0.1}$$

The closed boundary surface of D is denoted by ∂D. The unit vector along the normal to ∂D, pointing away from D, is denoted by $\underline{\nu}$. ∂D is the union of two sets, ∂D_1 and ∂D_2, respectively. On ∂D_1 the pressure will be prescribed and on ∂D_2 the normal component of the flow velocity (cf. Table 4.1). Throughout the computational domain under consideration the vectorial acceleration of free fall is taken to be $\underline{g}=-g\underline{i}_3$ (see Figure 6.1 in Section 6.1), where g denotes the (constant) scalar acceleration of free fall.

In Section 6.1 we analyze the boundary integral equations that are obtained upon using the source-type integral relation for the pressure field. In discretizing these integral equations the flow field quantities are, on each triangle, as is customary done in the literature (see, e.g., Jawson and Symm, 1977, p. 233), approximated by constants. The values of the latter are attributed to the field values at the barycenters of the relevant triangles. Subsequently, collocation is applied at the barycenters of all triangles involved. The errors in the results obtained in this way are typically related to the geometrical discretization of the faces of the cube. Numerical experiments are carried out to investigate the effects of incorporating the compatibility relation for the velocity in the discretized system of boundary integral equations in the manner discussed in Section 5.5.

In Section 6.2, the numerical experiments of Section 6.1 are repeated, but now with the piecewise linear interpolation scheme discussed in Section 5.3, in combination with the collocation method of Section 5.4. Since the piecewise linear expansion functions comply exactly with the structure of the test flow field, the results obtained are expected to be exact in the number of digits that is used to represent the numbers in the computer code. This expectation is confirmed. Also, the performance of the system of boundary integral equations resulting from the integral relation for the velocity field is tested, and the performance of mixtures of the two systems. In discretizing these systems, we only employ the piecewise linear field representations of Section 5.3, together with the collocation method of Section 5.4. Since, in all these cases, the field representations employed match the structures of the test flows exactly, all solutions turn out to be, as expected, exact within the computational accuracy employed. This confirmation is regarded as an important test on the correctness of the computer code developed.

Conclusions about the above numerical experiments are drawn in Section 6.3.

The algorithms have been implemented in the Fortran 77 language. All computations have been performed on an IBM PC/AT (operating at 6 MHz) with floating point processor, while the Ryan-McFarland Fortran 77 V 2.00 compiler has been used.

6.1. NUMERICAL RESULTS; PIECEWISE CONSTANT INTERPOLATION

In the present section we investigate some of the numerical features of the boundary-integral-equation method, when it is applied in its simplest version, i.e., when the integral relation for the pressure and the piecewise constant approximation for the flow field quantities are used.

Inspection of the expressions for the Green's functions pertaining to a homogeneous and reciprocal medium of infinite extent reveals that the ones pertaining to a point injection source, i.e., G^q defined by (4.5.19) and Γ_i^q defined by (4.5.20), have the simplest structure. Since the latter ones apply to the integral relation for the pressure field, we investigate the system of boundary integral equations that follows from it first. In its most general form the relevant system is given by (4.4.2) - (4.4.4), to which (4.5.19) and (4.5.20) now apply. In a first numerical study the system is applied to a homogeneous and isotropic medium inside the cube-shaped computational domain D, defined by (6.0.1). In D we consider the following mathematical test flow:

$$\underline{v} = 3^{-1/2}(\underline{i}_1 + \underline{i}_2 + \underline{i}_3) \tag{6.1.1}$$

and

$$p = -3^{-1/2}R(x_1 + x_2 + x_3) - \rho g(x_3 - 1) + 3^{1/2}R, \tag{6.1.2}$$

i.e., a uniform flow with constant diagonal flow velocity from $\underline{x}=\underline{0}$ to $\underline{x}=(\underline{i}_1+\underline{i}_2+\underline{i}_3)$ and with a linearly varying pressure. Note that at $\underline{x}=(\underline{i}_1+\underline{i}_2+\underline{i}_3)$, we have taken $p=0$; at $\underline{x}=\underline{0}$ we then have $p=\rho g+3^{1/2}R$. Clearly, (6.1.1) - (6.1.2) satisfy the basic groundwater flow equations (3.3.5) and (3.3.6) with $q=0$, $\underline{f}=\underline{0}$, $R_{ij}=R\delta_{ij}$ and $\underline{g}=-g\underline{i}_3$.

Now, (4.4.2) - (4.4.3) serve as the system of boundary integral equations. As a consequence of the assumed isotropy of the homogenous medium, R_{ij} occurring in the expressions (4.5.19) and (4.5.20) for the Green's functions G^q and Γ_i^q, respectively, is to be replaced by $R\delta_{ij}$ (cf. (B.1.1) and (B.1.2)). Since ∂D in (4.4.2) - (4.4.3) is the boundary surface of the unit cube, it is clear that ∂D can be represented in an exact manner by the planar triangles of Chapter 5 (cf. (5.1.1)). Each face of the cube is, in an identical manner, subdivided into NT/6 triangles, where NT=24 (see Figure 6.1a), NT=48 (see Figure 6.1b), NT=96 (see Figure 6.1c) and NT=144 (see Figure 6.1d), respectively. As regards the discretization patterns that are used, it is obvious that the one depicted in Figure 6.1a is the almost simplest one we can employ. Clearly, the one shown in Figure 6.1b is just a straightforward extension of the one in Figure 6.1a. With regard to the patterns of Figures 6.1c and 6.1d it is observed that the one shown in Figure 6.1d is similar to the one in Figure 6.1c, except for a finer discretization around the corners of the cube. The latter two have been chosen to analyze the effects of such a partially finer discretization.

On each triangle, both the known and the unknown field distributions of the pressure and the normal component of the flow velocity are approximated by a constant, whose value is attributed to the field value at the barycenter of the relevant triangle. Subsequently, NT out of the resulting 2×NT known and unknown field values are taken as the global expansion coefficients, and collocation is applied at the barycenters of all triangles. The resulting system of linear, algebraic equations contains in its coefficients the surface integrals IG^q and $I\Gamma^q$ as defined by (5.4.3) and (5.4.4), respectively, in which, as a consequence of the piecewise constant interpolation, the linear interpolation function ϕ (cf. (5.3.3)) is replaced by unity. For these surface integrals the analytic expressions derived in Appendix C (cf. Section C.1) are used. Finally, each system of linear, algebraic equations is solved by a direct procedure, viz., either a Gaussian elimination or a Gauss-Jordan elimination.

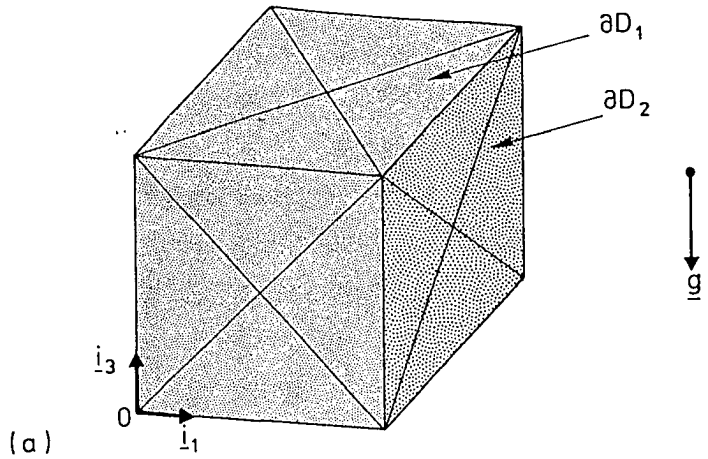
∂D1
∂D2
g
i3
0
i1
(a)

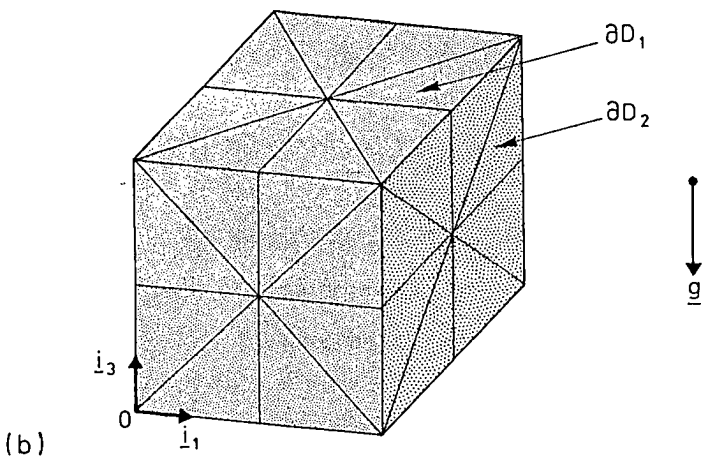
∂D1
∂D2
g
i3
0
i1
(b)

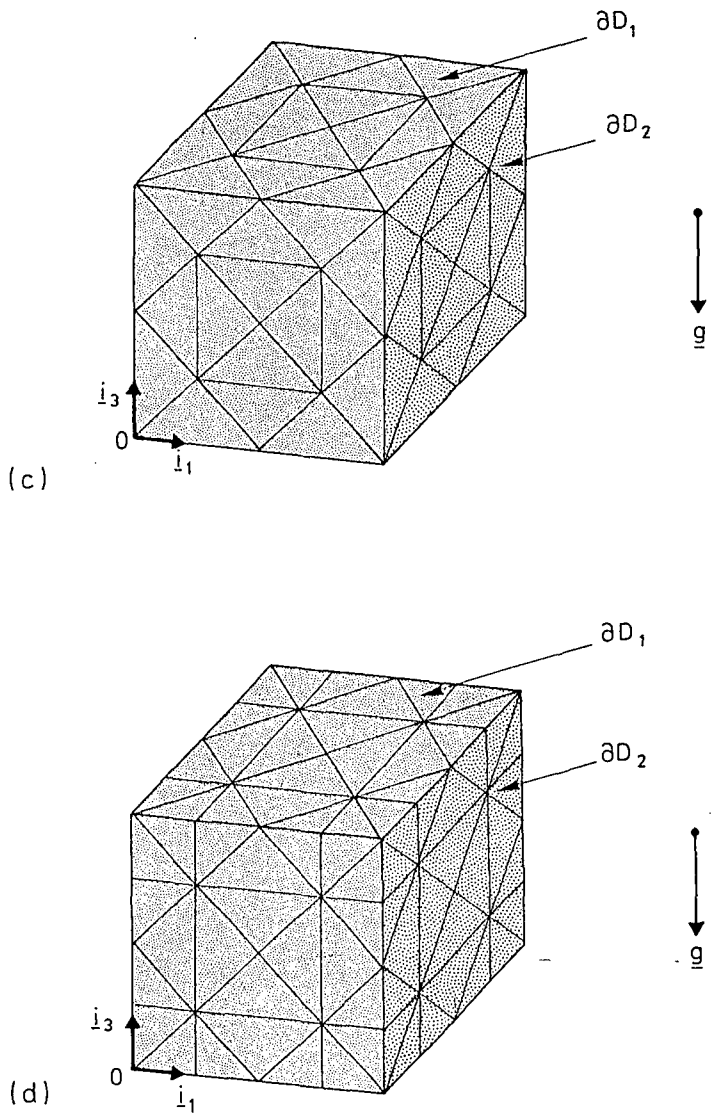

Fig 6.1. The unit cube D as the computational domain of interest. The boundary surface ∂D of D is the union of ∂D_1 and ∂D_2. On ∂D_1, p is prescribed and on ∂D_2, $v_i v_i$. ∂D is represented by: (a) NT=24 triangles, (b) NT=48 triangles, (c) NT=96 triangles, and (d) NT=144 triangles.

The system (4.4.2) - (4.4.3), discretized in the indicated manner, has been tested for the test flow (6.1.1) - (6.1.2), with ρ=1, R=1 and g=-1, for the following three cases:

$$\text{(i)}\quad \partial D_1 = \{\underline{x}\in R^3;\ x_1=0, 0<x_2<1, 0<x_3<1\} \quad \text{and}$$
$$\partial D_2 = \partial D \setminus \partial D_1, \tag{6.1.3}$$

$$\text{(ii)}\quad \partial D_1 = \{\underline{x}\in R^3;\ x_1=0, 0<x_2<1, 0<x_3<1\} \cup \{\underline{x}\in R^3;\ 0<x_1<1, x_2=1, 0<x_3<1\} \cup \{\underline{x}\in R^3;\ 0<x_1<1, 0<x_2<1, x_3=1\} \quad \text{and}$$
$$\partial D_2 = \partial D \setminus \partial D_1, \tag{6.1.4}$$

and

$$\text{(iii)}\quad \partial D_2 = \{\underline{x}\in R^3;\ x_1=1, 0<x_2<1, 0<x_3<1\} \quad \text{and}$$
$$\partial D_1 = \partial D \setminus \partial D_2, \tag{6.1.5}$$

where on ∂D_1 the field distribution of the pressure is prescribed and the one of the normal component of the flow velocity is unknown, while on ∂D_2 the field distribution of the pressure is unknown and the one of the normal component of the flow velocity is prescribed. The different boundary conditions (6.1.3), (6.1.4) and (6.1.5) are schematically visualized in Figures 6.2a, 6.1b and 6.1c, respectively.

In order to quantify the error of a particular solution of the boundary value problems two error criteria are used, viz., a local one and a global root-mean-square one. Let p_{ex} denote the exact field value of the pressure at the barycenter of a particular triangle on ∂D and let p_{comp} be the computed value at that point. Then the local error ERR(p) in

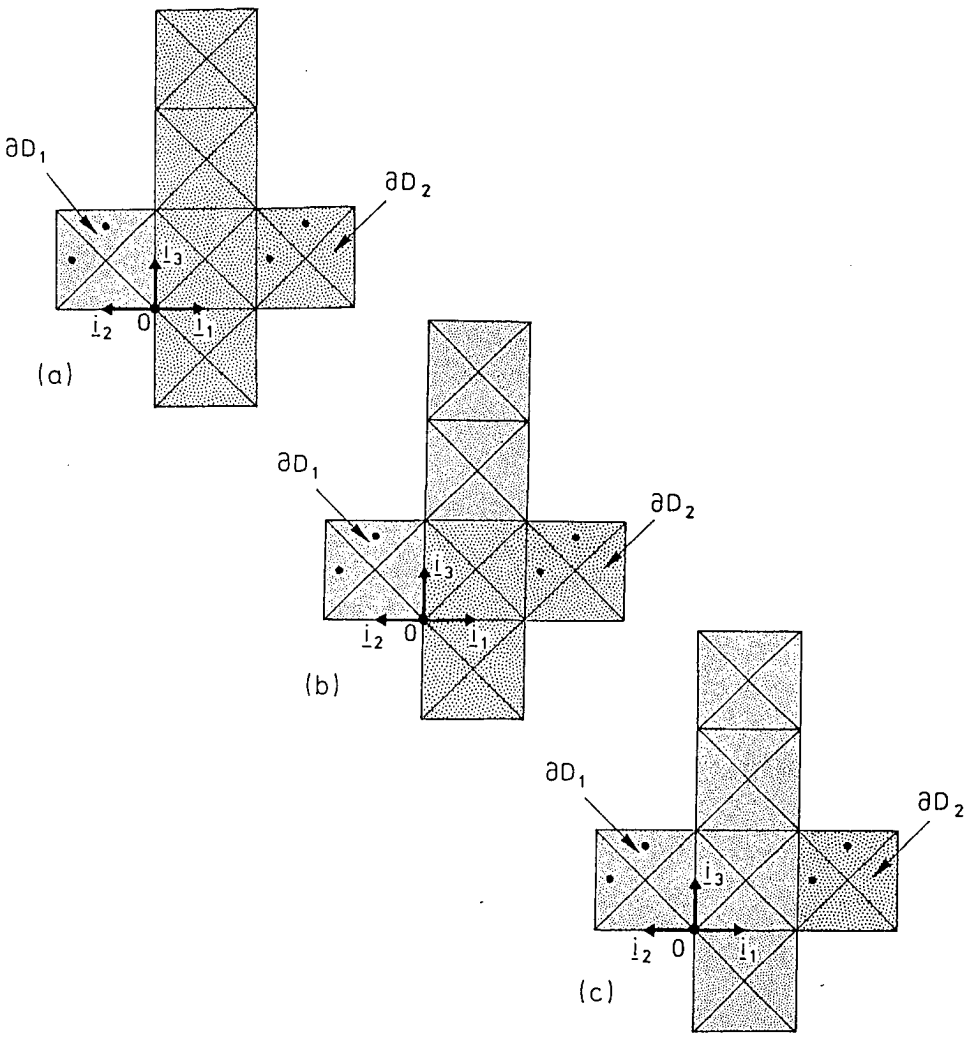

Fig 6.2. Schematic visualization of the different boundary conditions that have been chosen to apply to the boundary surface ∂D: (a) the boundary condition (6.1.3), (b) the boundary condition (6.1.4), and (c) the boundary condition (6.1.5). ∂D has been discretized into 24 triangles (cf. Figure 6.1a). The dots indicate the barycenters of the triangles at which the local errors in p and $\nu_i v_i$ have been computed (cf. Tables 6.2a, 6.2b, and 6.2c, for NT=24).

the pressure at the relevant point is taken to be

$$ERR(p) = |p_{comp} - p_{ex}|/\max(|p_{ex,bary}|), \tag{6.1.6}$$

where $\max(|p_{ex,bary}|)$ denotes the maximum of the absolute values of p_{ex} at the barycenters of the triangles spanning ∂D. Similarly, the local error $ERR(\nu_i v_i)$ in the normal component of the flow velocity at the barycenter of a particular triangle on ∂D is defined by

$$ERR(\nu_i v_i) = |\nu_i v_{i,comp} - \nu_i v_{i,ex}|, \tag{6.1.7}$$

where $\nu_i v_{i,comp}$ is the computed value of the normal flow velocity and $\nu_i v_{i,ex}$ is its exact value, and where it has been taken into account that for our test flow $\max(|\underline{v}_{ex}|)=1$ (cf. (6.1.1)). Further, the global root-mean-square error RMSE(p) in the computed pressure is defined by

$$RMSE(p) = [\int_{\partial D_2} |p_{comp} - p_{ex}|^2 dA / \int_{\partial D_2} |p_{ex}|^2 dA]^{1/2}, \tag{6.1.8}$$

and, similarly, the global root-mean-square error $RMSE(\nu_i v_i)$ in the computed normal flow velocity is taken to be

$$RMSE(\nu_i v_i) = [\int_{\partial D_1} |\nu_i v_{i,comp} - \nu_i v_{i,ex}|^2 dA / \int_{\partial D_1} |\nu_i v_{i,ex}|^2 dA]^{1/2}. \tag{6.1.9}$$

A summary of the global root-mean-square errors obtained for the three cases (6.1.3) - (6.1.5) with NT=24, NT=48, NT=96 and NT=144, respectively, is presented in Table 6.1. Typical values of the local errors in p and $\nu_i v_i$ at the barycenters of some triangles spanning ∂D are listed in Tables 6.2a, 6.2b and 6.2c. A first inspection of Table 6.1 shows that, as we would expect, both the value of RMSE(p) and $RMSE(\nu_i v_i)$ decrease as the number of triangles employed increases. A further inspection learns that the results obtained for the pressure are more

accurate than the ones obtained for the normal component of the velocity. Perhaps this has to do with the fact that p is solved from an integral equation of the second kind, while $v_i v_i$ is solved from an integral

Table 6.1. Global root-mean-square errors in p and $v_i v_i$.

test case	NT=24 RMSE(p)	NT=48 RMSE(p)	NT=96 RMSE(p)	NT=144 RMSE(p)
(i)	0.0512	0.0336	0.0201	0.0172
(ii)	0.0328	0.0229	0.0120	0.0103
(iii)	0.0143	0.0110	0.0056	0.0055

test case	RMSE($v_i v_i$)	RMSE($v_i v_i$)	RMSE($v_i v_i$)	RMSE($v_i v_i$)
(i)	0.3103	0.2153	0.1386	0.1209
(ii)	0.2903	0.2120	0.1541	0.1448
(iii)	0.2521	0.1972	0.1527	0.1501

equation of the first kind (cf. Section 4.4). As a consequence, the part of the system of linear, algebraic equations that corresponds to the unknown pressures might be somewhat better conditioned than the part that corresponds to the unknown normal flow velocities. Finally, Table 6.1 illustrates that for all discretizations that have been used, the value of RMSE(p) decreases if we consider in succession the test cases (i), (ii) and (iii). This behavior can be understood upon recalling that in each of the discretization patterns used, the number of points

Table 6.2a. Test case (i); local errors in p and $\nu_i v_i$ at the barycenters of some triangles spanning ∂D.

ERR(p) at	NT=24	NT=48	NT=96	NT=144
(1,1/6,1/2)	0.0196			
(1,1/2,5/6)	0.0524			
(1,1/3,5/6)		0.0234		
(1,2/3,5/6)		0.0381		
(1,1/6,1/2)			0.0076	0.0065
(1,1/3,1/2)			0.0074	0.0062
(1,1/2,5/6)			0.0169	0.0139
(1,1/2,2/3)			0.0123	0.0102

ERR($\nu_i v_i$) at	NT=24	NT=48	NT=96	NT=144
(0,5/6,1/2)	0.0871			
(0,1/2,5/6)	0.2379			
(0,2/3,5/6)		0.1400		
(0,1/3,5/6)		0.1064		
(0,5/6,1/2)			0.0182	0.0154
(0,2/3,1/2)			0.0368	0.0340
(0,1/2,5/6)			0.0391	0.0373
(0,1/2,2/3)			0.0487	0.0456

Table 6.2b. Test case (ii); local errors in p and $v_i v_i$ at the barycenters of some triangles spanning ∂D.

ERR(p) at	NT=24	NT=48	NT=96	NT=144
(1,1/6,1/2)	0.0163			
(1,1/2,5/6)	0.0030			
(1,1/3,5/6)		0.0026		
(1,2/3,5/6)		0.0015		
(1,1/6,1/2)			0.0040	0.0032
(1,1/3,1/2)			0.0042	0.0036
(1,1/2,5/6)			0.0015	0.0013
(1,1/2,2/3)			0.0024	0.0020
ERR($v_i v_i$) at	**NT=24**	**NT=48**	**NT=96**	**NT=144**
(0,5/6,1/2)	0.0943			
(0,1/2,5/6)	0.0877			
(0,2/3,5/6)		0.0570		
(0,1/3,5/6)		0.1120		
(0,5/6,1/2)			0.0505	0.0470
(0,2/3,1/2)			0.0129	0.0085
(0,1/2,5/6)			0.0767	0.0664
(0,1/2,2/3)			0.0123	0.0063

Table 6.2c. Test case (iii); local errors in p and $v_i v_i$ at the barycenters of some triangles spanning ∂D.

ERR(p) at	NT=24	NT=48	NT=96	NT=144
(1,1/6,1/2)	0.0070			
(1,1/2,5/6)	0.0069			
(1,1/3,5/6)		0.0063		
(1,2/3,5/6)		0.0033		
(1,1/6,1/2)			0.0030	0.0028
(1,1/3,1/2)			0.0016	0.0014
(1,1/2,5/6)			0.0001	0.0001
(1,1/2,2/3)			0.0005	0.0004
ERR($v_i v_i$) at	**NT=24**	**NT=48**	**NT=96**	**NT=144**
(0,5/6,1/2)	0.0747			
(0,1/2,5/6)	0.0750			
(0,2/3,5/6)		0.0510		
(0,1/3,5/6)		0.1022		
(0,5/6,1/2)			0.0442	0.0408
(0,2/3,1/2)			0.0018	0.0042
(0,1/2,5/6)			0.0713	0.0614
(0,1/2,2/3)			0.0006	0.0049

(barycenters) at which the pressure is calculated decreases in this succession (cf. Figure 6.2). A similar behavior was expected to hold for the values for RMSE($v_i v_i$). However, only when ∂D is discretized into a relatively large number of triangles (NT=144) such a behavior, although less pronounced, manifests itself. When ∂D is discretized into less elements, the values of RMSE($v_i v_i$) are, as compared to the corresponding variations in the values of RMSE(p), rather constant. The results shown in the Tables 6.2a, 6.2b and 6.2c again indicate that the results for p are more accurate than the ones for $v_i v_i$, i.e., the local errors follow in this respect the same pattern as the global errors. Inspection of these tables, in particular the columns for NT=96 and NT=144, further learns that a finer discretization around the corners of the cube (cf. Figures 6.1c and 6.1d) leads to smaller local errors in the pressure and in the normal flow velocity at points (barycenters) located around the center of each face of the cube, i.e., farther away from the corners. We also observe that, except for the results obtained when ∂D was discretized in only 24 or 48 triangles, ERR(p) decreases if p needs computation in fewer points on ∂D (cf. Figures 6.2a, 6.2b and 6.2c). Finally, the numerical data in Table 6.2 illustrate that for the method under consideration local errors in the computed pressure of less than one per cent and in the normal flow velocity of only a few per cents are arrived at, upon using only a relatively small number of triangles ($NT \geq 96$).

The computation time to calculate the pressure and the normal flow velocity at the barycenters of 24 triangles spanning the boundary surface ∂D of the unit cube D (cf. Figure 6.1a) was approximately 35 s. This computation time includes the time needed to solve the system of linear, algebraic equations not only with the aid of a Gaussian elimination, but (in order to verify the results from the latter) with the aid of a Gauss-Jordan elimination as well. Using successively 48, 96 and 144 triangles to solve each boundary value problem, both elimination procedures being

Table 6.3a. Global root-mean-square errors obtained with the aid of (5.5.5) for some typical values of the parameter ξ; ∂D has been subdivided into 24 triangles.

value	(i)		(ii)		(iii)	
of ξ	RMSE(p)	RMSE($v_i v_i$)	RMSE(p)	RMSE($v_i v_i$)	RMSE(p)	RMSE($v_i v_i$)
0	0.05121	0.31031	0.03279	0.29033	0.01428	0.25213
0.001	0.05078	0.31036	0.03260	0.29009	0.01419	0.25207
0.020	0.04388	0.32982	0.02882	0.28801	0.01225	0.25178
0.040	0.04163	0.39031	0.02463	0.29205	0.00997	0.25391
0.110	0.09520	0.87784	0.01577	0.38732	0.00069	0.29556
0.180	0.23003	1.84530	0.04763	0.68214	0.01888	0.44087

Table 6.3b. Global root-mean-square errors obtained with the aid of (5.5.5) for some typical values of the parameter ξ; ∂D has been subdivided into 48 triangles.

value	(i)		(ii)		(iii)	
of ξ	RMSE(p)	RMSE($v_i v_i$)	RMSE(p)	RMSE($v_i v_i$)	RMSE(p)	RMSE($v_i v_i$)
0	0.03662	0.21534	0.02287	0.21189	0.01104	0.19717
0.001	0.03638	0.21536	0.02278	0.21178	0.01099	0.19715
0.020	0.03247	0.22233	0.02091	0.21041	0.01013	0.19699
0.050	0.02930	0.25922	0.01788	0.21203	0.00870	0.19810
0.160	0.06372	0.58967	0.01043	0.27267	0.00341	0.22313
0.240	0.11832	0.97839	0.02073	0.38343	0.00663	0.27281

employed, the computation times were approximately 2.5 m., 10 m., and 25 m., respectively. Clearly, doubling the number of triangles employed, induces a multiplication by a factor of four of the computation time consumed.

In Table 6.3a the results of taking into account the compatibility relation for the velocity via the method of Section 5.5 (cf. (5.5.5)) for some typical values of the parameter ξ are shown for the case that ∂D has been discretized into 24 triangles. Table 6.3b contains the results of the latter numerical experiment with ∂D discretized into 48 triangles. First of all, the results shown in Tables 6.3a and 6.3b clearly demonstrate the strong influence of the parameter ξ on the values of RMSE(p) and RMSE($\nu_i v_i$). Inspection of these tables further shows that in all test cases considered and for both discretizations employed the global errors in the computed pressure can considerably be reduced by the implementation of the compatibility relation for the velocity field in the discretized system of integral equations. The results for the normal flow velocity, however, can hardly be improved. For the values of ξ that correspond to the improved results for the pressure, an increase in errors in the computed normal velocity is obtained, i.e., the values of ξ for which the improved results for $\nu_i v_i$ are obtained do not match the values of ξ for which the (most) improved results for p are arrived at. To conclude, since the improved results for p and $\nu_i v_i$ can only be obtained after a tedious trial and error procedure, the use of the incorporation of the compatibility relation for the velocity field with the method discussed in Section 5.5 is, especially for large systems of linear, algebraic equations, debatable.

A next choice to test the numerical features of the boundary-integral-equation method, is to apply the above numerical experiments to the system of integral equations that follows from the integral relation for the velocity field. For the flow configuration at hand the relevant system is given by (4.4.6) - (4.4.7), where the Green's

functions Γ_i^f and G_{ij}^f are defined by (4.5.27) and (4.5.26), respectively, in which R_{ij} is to be replaced by $R\delta_{ij}$ (cf. (B.2.1) and (B.2.2)). In order to make a fair comparison between the two systems, the system (4.4.6) - (4.4.7) is to be treated in the same manner as the previous one, i.e., the flow field quantities are to be represented again by constants on each triangle. However, as we have seen in Appendix B, Section B.2, the integral relation for the velocity field and, hence, the relevant integral equations are arrived at on the assumption that the pressure is continuously differentiable in the neighborhood of a point of observation on ∂D. Now, upon approximating on each triangle the pressure (as well as the normal component of the velocity) by a constant, jumps in the approximated field values occur across the common edges of two adjacent triangles which upon taking the derivative lead to delta functions along the edges. Hence, if the system (4.4.6) - (4.4.7) is implemented in this manner and subsequently solved, the results obtained will, in general, show large errors. This is confirmed by the following numerical experiments. First of all, we have tested the corresponding integral representation (4.4.5) at several observation points located in the interior of the unit cube D, filled by the homogeneous and isotropic medium used before. The flow field quantities from (6.1.1) - (6.1.2) were sampled at the barycenters of the triangulated boundary surface and subsequently used as the piecewise constant representations at this surface in the integral representation (4.4.5). At all observation points considered the computed values of the flow velocity field were (completely) incorrect and no appreciable improvements were obtained when using 96 or 144 triangles instead of 24. Secondly, similar numerical experiments have been carried out to test (4.4.5) for the point of observation located at the barycenters of the triangles spanning ∂D. Again, totally incorrect values for the velocity field were obtained, irrespective of whether we used 24, 96 or 144 triangles to represent ∂D. From these experiments we conclude that implementation of the actual system (4.4.6) - (4.4.7) when using a piecewise constant interpolation scheme, is just a waste of time. With the integral representation for the

velocity and, hence, from the resulting boundary integral equations, reliable results can therefore only be obtained if at least linear interpolation between the vertices is employed to represent the relevant flow field quantities on each triangle. The results of the corresponding scheme will be discussed in Section 6.2.

6.2. NUMERICAL RESULTS; PIECEWISE LINEAR INTERPOLATION

In this section, we investigate some of the numerical features of the boundary-integral-equation method in case the piecewise linear interpolation scheme of Section 5.3, in combination with the collocation method of Section 5.4, is employed. Not only the system of boundary integral equations resulting from the integral relation for the pressure field is considered, but also the one following from the integral relation for the velocity field, and mixtures of the two integral relations. The integral equations are applied to test flows in both isotropic and anisotropic (but reciprocal) media.

Throughout this section the source-free unit cube D, defined by (6.0.1) (cf. Figure 6.1), will serve again as the computational domain of interest. If D is filled by a homogeneous and isotropic medium, the uniform flow defined by (6.1.1) - (6.1.2) is again taken as the mathematical test flow. If D is filled by a homogeneous and anisotropic, but reciprocal, medium the following mathematical test flow is employed:

$$\underline{v} = 3^{-1/2}(\underline{i}_1 + \underline{i}_2 + \underline{i}_3) \tag{6.2.1}$$

and

$$p = - 3^{-1/2}(x_i R_{i1} + x_i R_{i2} + x_i R_{i3}) - \rho g(x_3 - 1) + 3^{-1/2}\sum_{i=1}^{3}\sum_{j=1}^{3} R_{ij}, \tag{6.2.2}$$

where (R_{ij}) is a symmetrical and positive definite tensor of rank two. Clearly, (6.2.1) and (6.2.2) constitute a uniform flow with a constant diagonal flow velocity from $\underline{x}=\underline{0}$ to $\underline{x}=(\underline{i}_1+\underline{i}_2+\underline{i}_3)$ and with a linearly varying pressure. Note that at $\underline{x}=(\underline{i}_1+\underline{i}_2+\underline{i}_3)$, we have taken $p=0$; at $\underline{x}=\underline{0}$ we

then have $p=\rho g+3^{-1/2}\sum_{i=1}^{3}\sum_{j=1}^{3}R_{ij}$. Obviously, (6.2.1) - (6.2.2) satisfy the basic groundwater flow equations (3.3.5) and (3.3.6) with $q=0$, $\underline{f}=\underline{0}$ and $\underline{g}=-g\underline{i}_3$.

In discretizing any of the boundary integral equations, the resulting system of linear, algebraic equations will, both for the isotropic and the anisotropic case, contain in its coefficients the surface integrals IG^q and $I\Gamma_i^q$, as defined by (5.4.3) and (5.4.4), respectively, and/or $I\Gamma_i^f$ and IG_i^f, as defined by (5.4.5) and (5.4.6), respectively. For these integrals the analytic expressions derived in Appendix C are used. In view of the fact that the relevant expressions are rather lengthy, it is clear that in implementing them errors in the software can easily occur. Hence, before we actually tested any of the systems of boundary integral equations for the mathematical test flows (6.1.1) - (6.1.1) or (6.2.1) - (6.2.2), we have followed a procedure similar to the one outlined at the end of Section 6.1, i.e., we have first extensively tested the integral representations for the pressure and the velocity fields. Both representations were applied to the unit cube D and were tested for observation points located in the interior of D as well as for points located on the boundary surface ∂D of D. As regards the latter points two categories were distinguished (cf. Figure 6.1), viz. (a) nodes in the interior of a face of the cube, and (b) non-nodal points in the interior of some triangle on ∂D. The non-nodal points in a triangle S_T have, to retain symmetry, been specified through the three relations

$$\underline{x}_{ob}(1) = (1 - 2\delta)\underline{x}_1 + \delta\underline{x}_2 + \delta\underline{x}_3 \qquad \text{for } 0<\delta<1, \tag{6.2.3a}$$

$$\underline{x}_{ob}(2) = \delta\underline{x}_1 + (1 - 2\delta)\underline{x}_2 + \delta\underline{x}_3 \qquad \text{for } 0<\delta<1, \tag{6.2.3b}$$

and

$$\underline{x}_{ob}(3) = \delta\underline{x}_1 + \delta\underline{x}_2 + (1 - 2\delta)\underline{x}_3 \qquad \text{for } 0<\delta<1, \tag{6.2.3c}$$

where $\underline{x}_{ob}(1)$, $\underline{x}_{ob}(2)$ and $\underline{x}_{ob}(3)$ denote the three (non-nodal) observation points in S_T, while $\underline{x}_1$, $\underline{x}_2$ and $\underline{x}_3$ are the position vectors of the vertices of S_T. For δ, values varying from $\delta=10^{-1}$ to $\delta=10^{-4}$ have been chosen, causing the observation points to move close to one of the vertices of the triangle under consideration. In the testing of the integral representations (4.4.1) and (4.4.5) for the pressure field and the velocity field, respectively, the flow field data needed on the triangulated boundary surface ∂D, i.e., the values of p and $\nu_i v_i$ at the vertices of the triangles spanning ∂D, were, in the isotropic case, obtained from (6.1.1) - (6.1.2) with $\rho=1$, $R=1$ and $g=-1$. Similarly, in the anisotropic case, the data needed on the discretized boundary surface ∂D were obtained from (6.2.1) - (6.2.2) with $\rho=1$, $g=-1$, while for (R_{ij}) we have taken

$$(R_{ij}) = \begin{bmatrix} 1 & -(3^{1/2})/2 & 0 \\ -(3^{1/2})/2 & 2 & 0 \\ 0 & 0 & 3 \end{bmatrix}, \tag{6.2.4a}$$

$$(R_{ij}) = \begin{bmatrix} 2 & 1 & 1 \\ 1 & 2 & 1 \\ 1 & 1 & 2 \end{bmatrix}, \tag{6.2.4b}$$

and

$$(R_{ij}) = \begin{bmatrix} 4 & 1 & 2 \\ 1 & 5 & 3 \\ 2 & 3 & 6 \end{bmatrix}, \tag{6.2.4c}$$

respectively; these tensors are symmetric and positive definite. The tests on the integral representations have been performed for ∂D discretized into 24, 96, 144 triangles (cf. Figures 6.1a, 6.1c and 6.1d, respectively). Since the local piecewise linear field representations comply exactly with the structure of the isotropic and anisotropic test flows under consideration, the computed values of the pressure and the flow velocity must be exact, within the computational accuracy employed, at all observation points at hand. Typical values of the absolute errors

in the computed values of p and v_i at observation points located in the interior of D and at the nodes in the interior of a face of the cube are of the order of 10^{-11} when 24 triangles span ∂D and of the order of 10^{-9} when 144 triangles span ∂D (cf. Figures 6.1a and 6.1d). The occurring loss in accuracy is ascribed to the accumulation of round-off errors in the arithmetic operations carried out on the numbers used in the computer code. Further, typical values of the absolute errors in the computed values of p and v_i at non-nodal points in the interior of some triangle on ∂D are, ∂D being subdivided into 24 triangles (cf. Figure 6.1a), of the order of 10^{-11} for $\delta=10^{-1}$ and of the order of 10^{-8} for $\delta=10^{-4}$. The latter loss in precision can be understood by taking into account that the values for the expressions for the surface integrals IG^q and $I\Gamma_i^q$, and/or $I\Gamma_i^f$ and IG_i^f will become less accurate if the distance between the point of observation and a vertex of a triangle becomes very small (which happens, e.g., for $\delta=10^{-4}$).

In addition to the above tests the integral representation for the pressure field has also been tested for two other categories of observation points on ∂D, viz. nodes on the edges of D and nodes at its corners. These tests have been carried out for the unit cube D filled by a homogeneous and isotropic medium with the test flow (6.1.1) - (6.1.2) with $\rho=1$, $R=1$ and $g=-1$, as well as for D filled by a homogeneous and anisotropic (but reciprocal) medium with the test flow (6.2.1) - (6.2.2) with $\rho=1$, $g=-1$ and (R_{ij}) given by (6.2.4a), (6.2.4b), (6.2.4c), respectively. Now, from Appendix B, Section B.1.2, we have learned that when the point of observation $\underline{x}'$ is located on the boundary surface ∂D of a homogeneous and isotropic medium D, the integral representation for the pressure field at $\underline{x}'$, as given by (B.1.16), holds on the assumption that around $\underline{x}'$ ∂D is locally flat. To prove this we have followed the procedure of excluding from D a semi-ball with $\underline{x}'$ as center, and subsequently letting the radius of this semi-ball go to zero. If the point of observation $\underline{x}'$ coincides with a node on an edge of the homogeneous and isotropic unit cube D, we can repeat this procedure by now excluding from D, symmetrically around $\underline{x}'$, a quarter of a ball, and

again letting its radius tend to zero. We then arrive at the integral representation for p as given by (B.1.16), but with the factor of 1/2 replaced by 1/4. Furthermore, when the observation point is located at a corner of the homogeneous and isotropic unit cube D, one eighth of the above ball is excluded from D. The procedure of letting the radius of the ball go to zero leads again to the integral representation for p as given in (B.1.16), but with the factor of 1/2 replaced by 1/8. The factors of 1/2, 1/4, and 1/8 are nothing but the fractions of the total solid angle at which the cube-shaped domain D is seen from the corresponding observation points. The occurrence of the factors of 1/4 and 1/8, as well as the factor of 1/2 previously, were confirmed numerically.

The testing of the integral representation for the pressure field at edges and corners of the cube D has for the test flows considered before also been carried out in case D was filled by a homogeneous and anisotropic, but reciprocal, medium. In this respect it is observed that the value of the solid angle needed at the point of observation on edges or in corners are, for the isotropic case, obtained by taking for the boundary surface of the domain excluded around the singularity (point of observation) a sphere. (Note that in the actual evaluation of the solid angle the shape of the surface over which the relevant surface integral is calculated is immaterial.) For the anisotropic case it proves to be easiest to take as the surface used to calculate the "affine" solid angle the boundary surface of a tetrahedral/polyhedral domain excluding the singularity. For this, we put the analytic results of Appendix C, Section C.2, judiciously together and obtain the analytic expressions for the "affine" solid angles needed for observation points located on edges or in corners of the cube D. Using this procedure, the integral representation for the pressure field has been tested at the same points of observation and for the same discretizations that have been considered in the isotropic case. Since in all cases considered the local piecewise linear interpolation scheme again matches the structure of the test flows in D, exact results, within the computational accuracy employed, were obtained. These additional numerical experiments are a test on the

correctness of the implementation of the analytic expressions derived in Appendix C for the integrals IG^q and $I\Gamma_i^q$, both for the anisotropic case.

After the integral representations (4.4.1) and (4.4.5) had been tested in the manners indicated above, we have implemented the systems of boundary integral equations resulting from (4.4.1), (4.4.5), as well as their combinations (cf. Section 4.4). They have been applied to the isotropic test flow used before. In their discretization we have, together with the piecewise linear field representations of Section 5.3, employed the method of collocation discussed in Section 5.4. In the computer code developed, all nodal points on ∂D at which collocation was to be applied were, for reasons of simplicity in implementing the codes, treated as multiple nodes (cf. Section 5.4). Also, instead of applying collocation at the vertices of the triangles, collocation was applied in the immediate vicinity of the vertices for which, to retain symmetry, the collocation points (6.2.3a) - (6.2.3c) were chosen. A code that automatically distinguishes between simple and multiple nodes is under development. The systems were tested for the given boundary values according to (6.1.3), (6.1.4) and (6.1.5), respectively. The boundary surface ∂D was subdivided into 24 triangles. The computation time for each test case was approximately 20 m. As was to be expected, all results were exact within the computational accuracy employed. Using 24 triangles to represent ∂D and taking $\delta=10^{-1}$ to locate the collocation points in the vicinity of the vertices of the triangles, the absolute errors in the computed values of the pressure and the normal velocity at the collocation points are of the order of 10^{-10}.

The above numerical experiments are to be considered as essential tests on the correctness of the computer code developed. The outcome of the tests gives confidence to apply the code to actual steady groundwater flow problems met in practice. For this, a larger computer system than the IBM PC/AT must be employed.

6.3. CONCLUSIONS

The numerical experiments discussed in this chapter are a first investigation into the performance of the boundary-integral-equation method as it has been developed in the previous chapters.

In Section 6.1 we have investigated some of the numerical features of the boundary-integral-equation method when it was applied in its simplest version, i.e., when a piecewise constant approximation for the flow field quantities is used. The resulting systems of boundary integral equations have been applied to a cube as the computational domain of interest. The cube was filled by a homogeneous and isotropic medium. In this cube a uniform source-free flow served as the mathematical test flow. Three different mixtures of Dirichlet and Neumann conditions were applied to the boundary surface of the cube.

As regards the integral equations resulting form the representation for the pressure field the errors in the computed pressure and the normal component of the flow velocity are typically related to the geometrical discretization of the boundary surface of the cube. The results obtained for the pressure were, for each discretization used and for each of the boundary conditions considered, more accurate than the ones obtained for the normal flow velocity. The numerical experiments also learned that, for a fixed number of triangles used in the subdivision of the faces of the cube, the errors in the computed pressure decrease if the numbers of points at which this quantity remains to be calculated decreases. Only for a relatively fine discretization of the faces of the cube a similar behavior, although less pronounced, was found to hold for the errors in the computed normal flow velocities. We further observed that a finer partial discretization around edges entails a decrease in the errors of the computed pressure and normal flow velocity at locations that were not part of this finer discretization. Furthermore, implementation of the

compatibility relation for the velocity in the discretized system of integral equations shows that, doing this, more accurate results can indeed be obtained. The improved results are, however, only arrived at after a tedious trial and error procedure; therefore, its use in practice, especially when large systems of linear, algebraic equations are needed, is debatable.

As regards the integral equations resulting from the integral representation for the velocity field large errors in the computed pressure and normal velocity occurred, irrespective of whether we used finer discretizations on the boundary surface of the cube or not. In view of the higher singularities in the kernels of the relevant integral representation (equations), with which a piecewise constant approximation is not compatible, this can be understood. From the system of boundary integral equations resulting from the integral relation for the velocity field reliable results can therefore only be obtained if at least linear local expansion of the flow field quantities is employed.

In Section 6.2 we have investigated some of the numerical features of the boundary integral equations in case the piecewise linear interpolation scheme of Section 5.3, together with the collocation method of Section 5.4, were employed. To this end, we have first extensively tested, in a systematic manner, both the integral representation for the pressure field and the one for the velocity field. Again the unit cube was taken as the computational domain of interest; it was filled by a homogeneous isotropic or anisotropic medium. Uniform source-free flows served as the mathematical test flows. The two integral representations and their corresponding integral equations have been tested for points of observation located in the interior of the cube as well as for observation points located at the interior nodes of the triangulated faces of the cube and at interior points in the triangles spanning the boundary surface of the cube. Since the local piecewise linear interpolations for the flow field quantities on the discretized faces of the cube match the structure of the isotropic and anisotropic test flows

exactly, the results obtained were all exact within the computational accuracy employed.

In all the numerical experiments considered sofar, field evaluation has been carried out at points that were located on a flat part of the boundary. In order to investigate what happens when an observation point is located on an edge or in a corner we have, both analytically and numerically, investigated the integral representation for the pressure field at such points of observation. It is noted that this investigation is only meaningful if the quantity that is to be considered is a continuous one. For both the isotropic and the anisotropic case agreement was reached within the computational accuracy employed.

The outcome of all tests show the correctness of the computer code developed; this gives the confidence that the boundary integral equations developed in this thesis can successfully be employed to solve actual three-dimensional steady groundwater flow problems.

APPENDIX A

THE AVERAGING THEOREM

In this appendix, a theorem is derived that relates the fluid phase average of the spatial derivative of an arbitrary fluid quantity ψ (ψ may be a scalar or a Cartesian component of a vector or tensor of arbitrary rank), to the spatial derivative of the fluid phase average of ψ and an additional term.

Consider the representative elementary domain D_ε as it has been introduced in Section 3.1, where D_ε^f denotes the subdomain of D_ε that contains the fluid phase and D_ε^s the subdomain of D_ε where the solid material is present. The closed boundary surfaces of D_ε, D_ε^f, and D_ε^s are denoted by ∂D_ε, ∂D_ε^f, and ∂D_ε^s, respectively. The intersections of ∂D_ε and ∂D_ε^f and of ∂D_ε and ∂D_ε^s are denoted by S_ε^f and S_ε^s, respectively, while the intersection of ∂D_ε^f and ∂D_ε^s is denoted by Σ_ε (see Figure A.1). The unit vector along the normal to ∂D_ε^f is directed away from D_ε^f and is denoted by ν_i. Finally, V_ε, V_ε^f, and V_ε^s, denote the volumes of D_ε, D_ε^f, and D_ε^s, respectively.

Let the fluid phase average of ψ, designated as $\langle\psi\rangle$, be defined by (cf. (3.1.9))

$$\langle\psi\rangle(\underline{x},t) = V_\varepsilon^{-1} \int_{\underline{x}' \in D_\varepsilon^f(\underline{x})} \psi(\underline{x}',t)dV. \tag{A.1}$$

Now, upon taking the spatial derivative of $\langle\psi\rangle$ and employing the definition of derivative, it follows that (see Figure A.2)

$$h_i \partial_i \langle\psi\rangle(\underline{x},t) = V_\varepsilon^{-1}\left[\int_{\underline{x}' \in D_\varepsilon^f(\underline{x}+\underline{h})} \psi(\underline{x}',t)dV - \int_{\underline{x}' \in D_\varepsilon^f(\underline{x})} \psi(\underline{x}',t)dV\right], \tag{A.2}$$

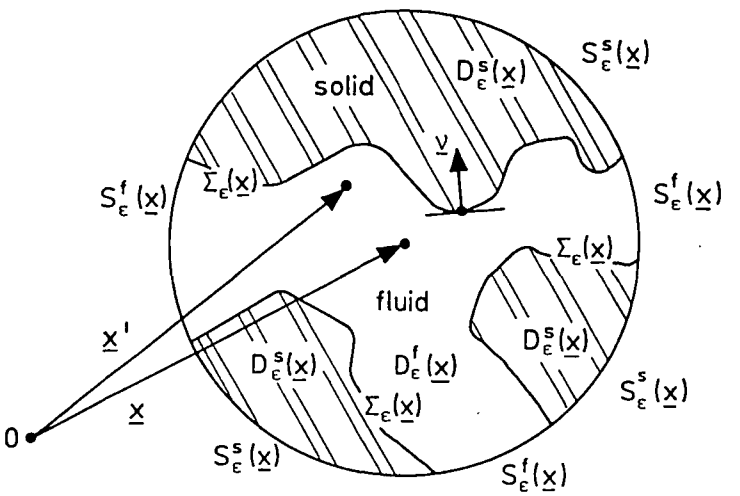

Fig. A.1. Bounded averaging domain (schematically) $D_\varepsilon = D_\varepsilon^f \cup D_\varepsilon^s$ interior to the closed boundary surface $\partial D_\varepsilon = S_\varepsilon^f \cup S_\varepsilon^s$ The closed boundary surfaces of D_ε^f and D_ε^s are denoted by $\partial D_\varepsilon^f = S_\varepsilon^f \cup \Sigma_\varepsilon$ and $\partial D_\varepsilon^s = S_\varepsilon^s \cup \Sigma_\varepsilon$, respectively, where Σ_ε represents the fluid-solid interface(s) in D_ε. The solid material present in D_ε^s is assumed to be rigid and immovable.

where $D_\varepsilon^f(\underline{x}+\underline{h})$ results from the translation of $D_\varepsilon(\underline{x})$, and hence $D_\varepsilon^f(\underline{x})$, over the small vectorial distance $\underline{h}$ (see Figure A.2). Inspection of the right-hand side of (A.2) reveals that the elementary volumes that remain after the subtraction of the volumes of $D_\varepsilon^f(\underline{x}+\underline{h})$ and $D_\varepsilon^f(\underline{x})$ can, as h_i tends to zero, be written as $\nu_i h_i dA$, where dA is an elementary area of S_ε^f

(see Figure A.2). Hence, the right-hand side of (A.2) leads, in limit $h_i \to 0$, to

$$V_\varepsilon^{-1}\left[\int_{\underline{x}' \in D_\varepsilon^f(\underline{x}+\underline{h})} \psi(\underline{x}',t)dV - \int_{\underline{x}' \in D_\varepsilon^f(\underline{x})} \psi(\underline{x}',t)dV\right]$$

$$\approx V_\varepsilon^{-1} \int_{\underline{x}' \in S_\varepsilon^f(\underline{x})} h_i \nu_i(\underline{x}')\psi(\underline{x}',t)dA. \qquad (A.3)$$

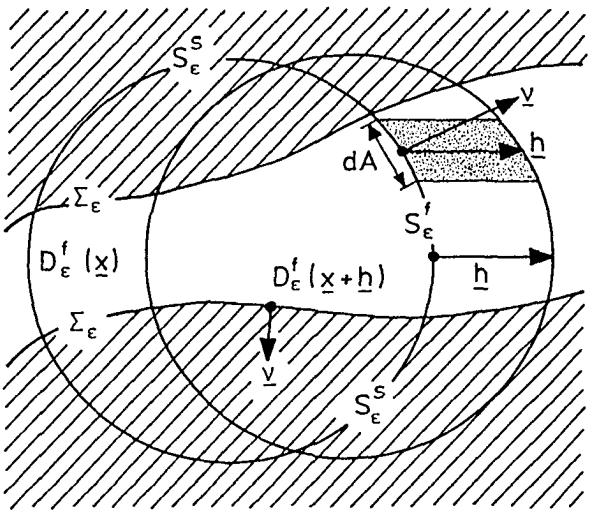

Fig. A.2. $D_\varepsilon^f(\underline{x}+\underline{h})$ results upon translating D_ε over a small vectorial distance $\underline{h}$.

Now,

$$\int_{\underline{x}' \in S_\varepsilon^f(\underline{x})} h_i \nu_i \psi \, dA = \int_{\underline{x}' \in \partial D_\varepsilon^f(\underline{x})} h_i \nu_i \psi \, dA - \int_{\underline{x}' \in \Sigma_\varepsilon(\underline{x})} h_i \nu_i \psi \, dA. \quad (A.3)$$

Upon applying Gauss' theorem to the first integral on the right-hand side, i.e., using

$$\int_{\underline{x}' \in \partial D_\varepsilon^f(\underline{x})} h_i \nu_i \psi \, dA = \int_{\underline{x}' \in D_\varepsilon^f(\underline{x})} h_i \partial_i' \psi \, dA, \tag{A.4}$$

where ∂_i' denotes partial differentiation with respect to x_i', and collecting the results, it follows that

$$h_i \partial_i \langle \psi \rangle (\underline{x},t) = h_i \langle \partial_i' \psi \rangle (\underline{x},t) - \int_{\underline{x}' \in \Sigma_\varepsilon(\underline{x})} h_i \nu_i(\underline{x}') \psi(\underline{x}',t) dA. \tag{A.5}$$

Equation (A.5) holds for any h_i. As a consequence, we have

$$\partial_i \langle \psi \rangle (\underline{x},t) = \langle \partial_i' \psi \rangle (\underline{x},t) - \int_{\underline{x}' \in \Sigma_\varepsilon(\underline{x})} \nu_i(\underline{x}') \psi(\underline{x}',t) dA. \tag{A.6}$$

Equation (A.6) is referred to as the averaging theorem and is used in Chapter 3.

APPENDIX B

DETAILED DERIVATION OF THE SOURCE-TYPE INTEGRAL RELATIONS PERTAINING TO A HOMOGENEOUS AND RECIPROCAL MEDIUM

In present appendix the derivation of the source-type integral relations for the pressure field and the velocity field pertaining to a bounded domain occupied by a homogeneous and reciprocal medium is discussed in more detail.

The Green's solutions of Section 4.5 for the flow field in homogeneous and reciprocal media of infinite extent all are regular throughout the three-dimensional space R^3 except at a single point, the source point, where they are singular. As a consequence of this property, the Green's solutions cannot be directly used in the global form of the reciprocity theorem given in the main text in (4.1.7), if the source point is situated either in the interior of the domain of application of the reciprocity theorem, or on its boundary.

The purpose of the present appendix is to discuss the derivations of the source-type integral relations for the pressure and velocity fields for these cases with the aid of a detailed limiting procedure. In Section B.1 this analysis is carried out for the source-type integral relation for the pressure field when the relevant homogeneous medium is isotropic. In Section B.2 the analysis is carried out for the source-type integral relation for the velocity field pertaining to such a medium. The extension of the analysis to the case of a homogeneous and anisotropic, but reciprocal, medium is discussed in Section B.3.

B.1. SOURCE-TYPE INTEGRAL RELATION FOR THE PRESSURE FIELD (ISOTROPIC CASE)

In this section we derive the source-type integral relation for the pressure field pertaining to a bounded domain D occupied by a homogeneous and isotropic medium.

As a starting point, we recapitulate the injection-source (scalar and vector) Green's functions for a homogeneous and isotropic medium of infinite extent, i.e., (cf. (4.5.19), (4.5.20), (4.5.16), (4.5.17) and (4.1.9))

$$G^q = (R/4\pi)|\underline{x} - \underline{x}'|^{-1} \tag{B.1.1}$$

and

$$\Gamma_i^q = (4\pi)^{-1}\partial_i|\underline{x} - \underline{x}'|^{-1}, \tag{B.1.2}$$

where R is the constant scalar resistivity of the medium under consideration. From (B.1.1) and (B.1.2) it is apparent that G^q and Γ_i^q both are singular at the source point $\underline{x}=\underline{x}'$. In Subsections B.1.1, B.1.2 and B.1.3, the derivation of the integral relation for the pressure field is discussed in case this source point is located in the interior of D, on its boundary surface ∂D, or outside $D \cup \partial D$, i.e., in D', respectively.

B.1.1. PRESSURE FIELD; THE CASE $\underline{x}' \in D$

In this subsection we consider the case where the source point with position vector $\underline{x}'$ is an interior point of D. To handle this situation the reciprocity theorem (4.1.7) is applied to the domain $D\backslash B_\delta(\underline{x}')$ where

$$B_\delta(\underline{x}') = \{\underline{x}\in R^3;\ 0\leq|\underline{x}-\underline{x}'|<\delta \text{ with } \delta>0\}. \tag{B.1.3}$$

The boundary surface of the ball $B_\delta(\underline{x}')$ is the sphere $\partial B_\delta(\underline{x}')$; the exterior of $B_\delta(\underline{x}')$ is denoted by $B'_\delta(\underline{x}')$. The ball's radius δ is assumed to be so small (eventually we shall consider the limit $\delta\to 0$) that $\partial B_\delta(\underline{x}')$ is completely interior to the boundary surface ∂D of D (see Figure B.1).

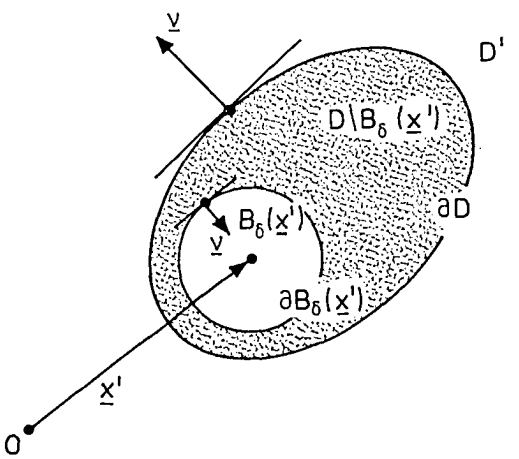

Fig. B.1. The ball $B_\delta(\underline{x}')$ around $\underline{x}=\underline{x}'$ with boundary surface $\partial B_\delta(\underline{x}')$ and radius δ is excluded from the domain to which the reciprocity theorem (4.1.7) applies.

In applying the reciprocity theorem to the domain $D\backslash B_\delta(\underline{x}')$, State A is identified with the actual flow state. The auxiliary flow State B is identified with the Green's flow state generated by a point-injection source at $\underline{x}=\underline{x}'$ in an unbounded, homogeneous and isotropic medium with the same constitutive properties as the ones in the actual flow state. The Green's functions G^q and Γ_i^q defined by (B.1.1) and (B.1.2), respectively, apply to the latter auxiliary state. Since the point source generating these fields is located outside the domain of application, we have (cf. (4.1.7), (4.3.2) - (4.3.7), and (4.3.11))

$$\int_{\underline{x}\in\partial B_\delta(\underline{x}')} (G^q v_i + \Gamma_i^q p)\nu_i \, dA = \int_{\underline{x}\in D\backslash B_\delta(\underline{x}')} [G^q q + \Gamma_i^q(\rho g_i + f_i)]dV - \int_{\underline{x}\in\partial D} (G^q v_i + \Gamma_i^q p)\nu_i \, dA. \qquad (B.1.4)$$

We first examine the surface integral over $\partial B_\delta(\underline{x}')$ in some more detail. On $\partial B_\delta(\underline{x}')$ we have (see Figure B.1)

$$\nu_i = -(x_i - x_i')/|\underline{x} - \underline{x}'| \qquad \text{when } \underline{x}\in\partial B_\delta(\underline{x}'), \qquad (B.1.5)$$

and hence (cf. (B.1.2))

$$\nu_i \Gamma_i^q = (4\pi)^{-1}|\underline{x} - \underline{x}'|^{-2} = (4\pi\delta^2)^{-1} \qquad \text{when } \underline{x}\in\partial B_\delta(\underline{x}'). \qquad (B.1.6)$$

On the assumption that p is continuous at $\underline{x}=\underline{x}'$, we have (cf. (B.1.4))

$$\int_{\underline{x}\in\partial B_\delta(\underline{x}')} \Gamma_i^q \nu_i p \, dA = (4\pi\delta^2)^{-1}\int_{\underline{x}\in\partial B_\delta(\underline{x}')} p \, dA = p(\underline{x}') + o(1) \text{ as } \delta\to 0. \qquad (B.1.7)$$

On the further assumption that v_i is bounded on $\partial B_\delta(\underline{x}')$ it is easily verified that the remaining integral on the left-hand side of (B.1.4) leads to (cf. (B.1.1))

$$\int_{\underline{x}\in\partial B_\delta(\underline{x}')} G^q v_i \nu_i \, dA = R(4\pi\delta)^{-1} \int_{\underline{x}\in\partial B_\delta(\underline{x}')} v_i \nu_i \, dA = O(\delta) \text{ as } \delta\to 0. \tag{B.1.8}$$

Further, in the limit $\delta\to 0$, the volume integral in (B.1.4) leads to

$$\int_{\underline{x}\in D\setminus B_\delta(\underline{x}')} [G^q q + \Gamma_i^q(\rho g_i + f_i)] dV$$

$$= \int_{\underline{x}\in D} [G^q q + \Gamma_i^q(\rho g_i + f_i)] dV + O(\delta) \text{ as } \delta\to 0, \tag{B.1.9}$$

where the integral on the right-hand side is to be understood as a convergent improper integral. Upon collecting the results (B.1.4) and (B.1.7) - (B.1.9), we have, in the limit $\delta\to 0$,

$$p(\underline{x}') = -\int_{\underline{x}\in\partial D} (G^q v_i + \Gamma_i^q p)\nu_i \, dA + \int_{\underline{x}\in D} [G^q q + \Gamma_i^q(\rho g_i + f_i)] dV \quad \text{when } \underline{x}'\in D, \tag{B.1.10}$$

which complies with (4.3.12) when $\underline{x}'\in D$, in case the latter is applied to a homogeneous and isotropic medium.

B.1.2. PRESSURE FIELD; THE CASE $\underline{x}'\in\partial D$

For the source point located on the boundary surface ∂D of D, we exclude from the domain of application of the reciprocity theorem (4.1.7) the part $D \setminus B_\delta(\underline{x}')$ of the ball $B_\delta(\underline{x}')$ defined by (B.1.3) that intersects D. Now, $\partial B_\delta(\underline{x}')$ is the part of the boundary surface of $B_\delta(\underline{x}')$ that intersects D and Σ_δ denotes the part of ∂D that lies inside $B_\delta(\underline{x}')$ (see

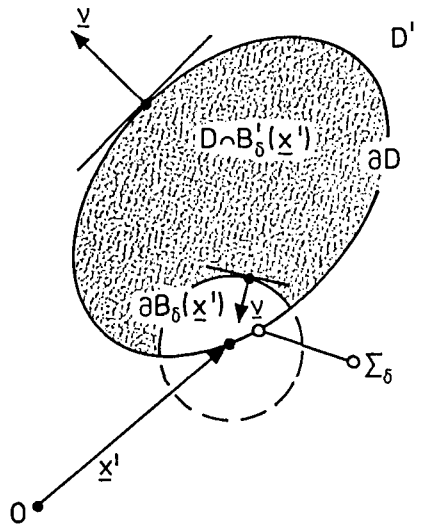

Fig. B.2. The domain $D \setminus B_\delta(\underline{x}')$ is excluded from the domain to which the reciprocity theorem (4.1.7) applies.

Figure B.2). Upon applying now (4.1.7) to $D \setminus B'_\delta(\underline{x}')$ and taking the States A and B as before, we obtain

$$\int_{\underline{x}\in\partial B_\delta(\underline{x}')} (G^q v_i + \Gamma_i^q p)\nu_i dA = \int_{\underline{x}\in D\setminus B'_\delta(\underline{x}')} [G^q q + \Gamma_i^q(\rho g_i + f_i)]dV$$

$$- \int_{\underline{x}\in\partial D\setminus\Sigma_\delta} (G^q v_i + \Gamma_i^q p)\nu_i dA, \qquad \text{(B.1.11)}$$

to which (B.1.1) and (B.1.2) apply and where, from now on, it is assumed that ∂D has a unique tangent plane at $\underline{x}=\underline{x}'$. In the left-hand side of (B.1.11) we have, on the assumption that v_i is bounded on $\partial B_\delta(\underline{x}')$,

$$\int_{\underline{x}\in\partial B_\delta(\underline{x}')} G^q v_i \nu_i \, dA = R(4\pi\delta)^{-1} \int_{\underline{x}\in\partial B_\delta(\underline{x}')} v_i \nu_i \, dA = O(\delta) \text{ as } \delta\to 0. \tag{B.1.12}$$

On the further assumption that p is continuous at $\underline{x}=\underline{x}'$, followed by the use of (B.1.6), we now have

$$\int_{\underline{x}\in\partial B_\delta(\underline{x}')} \Gamma_i^q \nu_i p \, dA = (4\pi\delta^2)^{-1} \int_{\underline{x}\in\partial B_\delta(\underline{x}')} p \, dA = (1/2)p(\underline{x}') + o(1) \text{ as } \delta\to 0. \tag{B.1.13}$$

Similar to (B.1.9), the volume integral in (B.1.11) leads to

$$\int_{\underline{x}\in D\setminus B'_\delta(\underline{x}')} [G^q q + \Gamma_i^q(\rho g_i + f_i)] dV$$

$$= \int_{\underline{x}\in D} [G^q q + \Gamma_i^q(\rho g_i + f_i)] dV + O(\delta) \text{ as } \delta\to 0, \tag{B.1.14}$$

where the resulting integral on the right-hand side is to be understood as a convergent improper integral. Finally, for the surface integral on the right-hand side of (B.1.11) we have in the limit $\delta\to 0$

$$\int_{\underline{x}\in\partial D\setminus\Sigma_\delta} (G^q v_i + \Gamma_i^q p)\nu_i \, dA = \fint_{\underline{x}\in\partial D} (G^q v_i + \Gamma_i^q p)\nu_i \, dA + O(\delta) \text{ as } \delta\to 0, \tag{B.1.15}$$

where $\fint$ denotes that the relevant integral is interpreted as a Cauchy principal value, i.e., the singularity of the integrand is excluded in a symmetrical manner. After this interpretation it can for the case at hand be shown that the integral is an improper convergent one. Collecting the results and taking the limit $\delta\to 0$, (B.1.11) - (B.1.15) lead to

$$(1/2)p(\underline{x}') = -\fint_{\underline{x}\in\partial D} (G^q v_i + \Gamma_i^q p)\nu_i \, dA$$

$$+ \int_{\underline{x}\in D} [G^q q + \Gamma_i^q(\rho g_i + f_i)]dV \qquad \text{when } \underline{x}'\in\partial D. \qquad (B.1.16)$$

This source-type integral relation for the pressure at $x=\underline{x}'$, with $\underline{x}'\in\partial D$, is identical to the one in (4.3.12) when $\underline{x}'\in\partial D$, in case the latter is applied to a homogeneous and isotropic medium.

B.1.3. PRESSURE FIELD; THE CASE $\underline{x}'\in D'$

In the case $\underline{x}'\in D'$, i.e., the source point is located outside D U ∂D, it is obvious that G^q and Γ_i^q are both regular throughout D. Hence, in this case the reciprocity theorem (4.1.7) can be used directly. Taking in (4.1.7) the States A and B as before, it immediately follows that for $\underline{x}'\in$ D', the source-type integral relation for the pressure field in a homogeneous and isotropic medium is arrived at by directly employing (B.1.1) and (B.1.2). The resulting integral relation is identical to the one in (4.3.12) when $\underline{x}'\in D'$, in case the latter is applied to a homogeneous and isotropic medium.

To conclude this section it should be noted that with the introduction of the characteristic domain function $\chi_D(\underline{x}')$, defined by (4.3.9), the results for the pressure field obtained in the Subsections B.1.1, B.1.2 and the present one, can conveniently be combined to the one presented in (4.3.12).

B.2. SOURCE-TYPE INTEGRAL RELATION FOR THE VELOCITY FIELD (ISOTROPIC CASE)

In this section we derive the source-type integral relation for the velocity field pertaining to a bounded domain D occupied by a homogeneous and isotropic medium.

As a starting point, we recapitulate the force-source (vector and tensor) Green's functions pertaining to a homogenous and isotropic medium of infinite extent, i.e., (cf. (4.5.26), (4.5.27), (4.5.16), (4.5.17) and (4.1.9))

$$G^f_{ij} = (4\pi R)^{-1}\partial_i\partial_j|\underline{x} - \underline{x}'|^{-1} + R^{-1}\delta_{ij}\delta(\underline{x} - \underline{x}') \qquad (B.2.1)$$

and

$$\Gamma^f_i = (4\pi)^{-1}\partial_i|\underline{x} - \underline{x}'|^{-1}, \qquad (B.2.2)$$

where R is the constant scalar resistivity of the medium under consideration. From (B.2.1) and (B.2.2) it is apparent that G^f_{ij} and Γ^f_i both are singular at the source point $\underline{x}=\underline{x}'$. In Subsections B.2.1, B.2.2 and B.2.3, the derivation of the integral relation for the velocity field is discussed in case this source point is located in the interior of D, on its boundary surface ∂D, or outside $D \cup \partial D$, i.e., in D', respectively.

B.2.1. VELOCITY FIELD; THE CASE $\underline{x}' \in D$

In this subsection we consider the case where the source point with position vector $\underline{x}'$ is an interior point of D. Similar to the "pressure

case" discussed in Subsection B.1.1, the reciprocity theorem (4.1.7) is applied to the domain $D\backslash B_\delta(\underline{x}')$ where the ball $B_\delta(\underline{x}')$ is defined by (B.1.3) (see Figure B.1). In applying the reciprocity theorem (4.1.7) to the domain $D\backslash B_\delta(\underline{x}')$ we again identify State A with the actual flow state. The flow State B is now identified with the one that is generated by a point-force source at $\underline{x}=\underline{x}'$, in addition to a source distribution that compensates gravity (cf. (4.3.14)). These source distributions apply to an unbounded, homogeneous and isotropic medium with the same constitutive properties as the ones in the actual flow state. The Green's functions G^f_{ij} and Γ^f_i defined by (B.2.1) and (B.2.2), respectively, apply to this auxiliary state. Since the point source generating these fields is located outside the domain of application, we have (cf. (4.1.7), (4.3.2) - (4.3.3), (4.3.14) - (4.3.17), and (4.3.19))

$$\int_{\underline{x}\in\partial B_\delta(\underline{x}')} (\Gamma^f_i v_j + G^f_{ij} p)\nu_j dA = \int_{\underline{x}\in D\backslash B_\delta(\underline{x}')} [\Gamma^f_i q + G^f_{ij}(\rho g_j + f_j)]dV$$

$$- \int_{\underline{x}\in\partial D} (\Gamma^f_i v_j + G^f_{ij} p)\nu_j dA. \qquad (B.2.3)$$

We first examine the surface integral on the left-hand side of (B.2.3) in some more detail. On the assumption that v_i is continuous at $\underline{x}=\underline{x}'$ we have (cf. (B.2.2) and (B.1.5))

$$\int_{\underline{x}\in\partial B_\delta(\underline{x}')} \Gamma^f_i v_j \nu_j dA = (4\pi\delta^2)^{-1} \int_{\underline{x}\in\partial B_\delta(\underline{x}')} \nu_i v_j \nu_j dA$$

$$= (1/3)v_i(\underline{x}') + o(1) \text{ as } \delta\to 0, \qquad (B.2.4)$$

which is easily verified by carrying out the relevant integration with the aid of spherical coordinates around $\underline{x}=\underline{x}'$ as variables of integration. To evaluate the remaining part of the integral on the left-hand side in (B.2.3) we assume that the pressure is continuously differentiable at $\underline{x}=\underline{x}'$ and write

$$p(\underline{x}) = p(\underline{x}') + (x_m - x_m')\partial_m' p(\underline{x}') + o(\delta) \text{ as } \delta \to 0 \text{ for } \underline{x} \in \partial B_\delta(\underline{x}'), \quad (B.2.5)$$

where ∂_m' denotes differentiation with respect to x_m'. Using (B.2.5) and (B.2.1) in the relevant integral, we then have

$$\int_{\underline{x} \in \partial B_\delta(\underline{x}')} G_{ij}^f \nu_j p \, dA$$

$$= (4\pi R)^{-1} \int_{\underline{x} \in \partial B_\delta(\underline{x}')} [p(\underline{x}') + (x_m - x_m')\partial_m' p(\underline{x}')] \nu_j \partial_j \partial_i |\underline{x} - \underline{x}'|^{-1} dA$$

$$+ o(1) \text{ as } \delta \to 0. \quad (B.2.6)$$

Since with aid of Gauss' theorem it follows that (see Figure B.1)

$$\int_{\underline{x} \in \partial B_\delta(\underline{x}')} \nu_i dA = 0, \quad (B.2.7)$$

the first part of the integral on the right-hand side of (B.2.6) leads to

$$\int_{\underline{x} \in \partial B_\delta(\underline{x}')} p(\underline{x}') \nu_j \partial_j \partial_i |\underline{x} - \underline{x}'|^{-1} dA$$

$$= 2p(\underline{x}')\delta^{-3} \int_{\underline{x} \in \partial B_\delta(\underline{x}')} \nu_i dA = 0 \quad \text{for } \delta > 0, \quad (B.2.8)$$

while for the remaining part we obtain

$$\int_{\underline{x} \in \partial B_\delta(\underline{x}')} (x_m - x_m')\partial_m' p(\underline{x}') \nu_j \partial_j \partial_i |\underline{x} - \underline{x}'|^{-1} dA$$

$$= -2\delta^{-2} \int_{\underline{x} \in \partial B_\delta(\underline{x}')} \nu_i \nu_m [\partial_m' p(\underline{x}')] dA = -(8\pi/3)\partial_i' p(\underline{x}'). \quad (B.2.9)$$

This result easily is verified by carrying out the relevant integration with the aid of spherical coordinates around $\underline{x}=\underline{x}'$ as variables of integration. Using (B.2.8) and (B.2.9) in (B.2.6) we have

$$\int_{\underline{x}\in\partial B_\delta(\underline{x}')} G^f_{ij}\nu_j p dA = -(2/3)R^{-1}\partial'_i p(\underline{x}') + o(1) \text{ as } \delta\to 0. \qquad (B.2.10)$$

Next, it readily follows that for the first part of the volume integral in (B.2.3) we have (cf. (B.2.2))

$$\int_{\underline{x}\in D\setminus B_\delta(\underline{x}')} \Gamma^f_i q dV = \int_{\underline{x}\in D} \Gamma^f_i q dV + O(\delta) \quad \text{as } \delta\to 0, \qquad (B.2.11)$$

where the integral on the right-hand side is as a convergent improper integral. As regards the remaining part of the volume integral in (B.2.3) we successively take into account the expression (B.2.1) for G^f_{ij}, use the fact that this expression is regular throughout $D\setminus B_\delta(\underline{x}')$, and rewrite the relevant integral, assuming that f_j is continuously differentiable, as

$$\begin{aligned}
&\int_{\underline{x}\in D\setminus B_\delta(\underline{x}')} G^f_{ij}(\rho g_j + f_j)dV \\
&= (4\pi R)^{-1}\Big(\int_{\underline{x}\in D\setminus B_\delta(\underline{x}')} \partial_j[(\rho g_j + f_j)\partial_i|\underline{x}-\underline{x}'|^{-1}]dV \\
&\quad - \int_{\underline{x}\in D\setminus B_\delta(\underline{x}')} [\partial_j(\rho g_j + f_j)]\partial_i|\underline{x}-\underline{x}'|^{-1}dV\Big). \qquad (B.2.12)
\end{aligned}$$

With the aid of Gauss' theorem the first integral on the right-hand side can be rewritten as (see Figure B.1)

$$\begin{aligned}
&\int_{\underline{x}\in D\setminus B_\delta(\underline{x}')} \partial_j[(\rho g_j + f_j)\partial_i|\underline{x}-\underline{x}'|^{-1}]dV \\
&= \int_{\underline{x}\in\partial D} \nu_j(\rho g_j + f_j)\partial_i|\underline{x}-\underline{x}'|^{-1}dA
\end{aligned}$$

$$+ \int_{\underline{x}\in\partial B_\delta(\underline{x}')} \nu_j(\rho g_j + f_j)\partial_i|\underline{x} - \underline{x}'|^{-1}dA, \qquad (B.2.13)$$

where, similar to (B.2.4), it is easily verified that

$$\int_{\underline{x}\in\partial B_\delta(\underline{x}')} \nu_j(\rho g_j + f_j)\partial_i|\underline{x} - \underline{x}'|^{-1}dA = (4\pi/3)(\rho g_i + f_i(\underline{x}')) + o(1)$$

$$\text{as } \delta\to 0. \qquad (B.2.14)$$

For the remaining volume integral on the right-hand side of (B.2.12) we have

$$\int_{\underline{x}\in D\setminus B_\delta(\underline{x}')} [\partial_j(\rho g_j + f_j)]\partial_i|\underline{x} - \underline{x}'|^{-1}dV$$

$$= \int_{\underline{x}\in D} [\partial_j(\rho g_j + f_j)]\partial_i|\underline{x} - \underline{x}'|^{-1}dV + O(\delta) \text{ as } \delta\to 0, \qquad (B.2.15)$$

where the volume integral on the right-hand side is a convergent improper integral. Hence, upon using (B.2.13) - (B.2.15), together with (B.2.2), in (B.2.12), we have

$$\int_{\underline{x}\in D\setminus B_\delta(\underline{x}')} G^f_{ij}(\rho g_j + f_j)dV$$

$$= (1/3)R^{-1}(\rho g_i + f_i(\underline{x}')) + R^{-1}\Big(\int_{\underline{x}\in\partial D} \Gamma^f_i(\rho g_j + f_j)\nu_j dA$$

$$- \int_{\underline{x}\in D} \Gamma^f_i\partial_j(\rho g_j + f_j)dV\Big) + o(1) \text{ as } \delta\to 0. \qquad (B.2.16)$$

Collecting the results, it follows that, in the limit $\delta\to 0$, (B.2.3) leads to

$$(1/3)v_i(\underline{x}') - (2/3)R^{-1}\partial'_i p(\underline{x}') - (1/3)R^{-1}(\rho g_i + f_i(\underline{x}'))$$

$$= -\int_{\underline{x}\in\partial D}(\Gamma_i^f v_j + G_{ij}^f p)\nu_j dA + R^{-1}\int_{\underline{x}\in\partial D}\Gamma_i^f(\rho g_j + f_j)\nu_j dA$$

$$+\int_{\underline{x}\in D}\Gamma_i^f[q - R^{-1}\partial_j(\rho g_j + f_j)]dV \qquad \text{when } \underline{x}'\in D. \tag{B.2.17}$$

In (B.2.17) we further take into account the equation of motion (3.3.6), in which we replace R_{ij} by $R\delta_{ij}$, $\underline{x}$ by $\underline{x}'$, and ∂_i by ∂_i'. Then we arrive at

$$v_i(\underline{x}') = R^{-1}(\rho g_i + f_i(\underline{x}'))$$

$$-\int_{\underline{x}\in\partial D}(\Gamma_i^f v_j + G_{ij}^f p)\nu_j dA + R^{-1}\int_{\underline{x}\in\partial D}\Gamma_i^f(\rho g_j + f_j)\nu_j dA$$

$$+\int_{\underline{x}\in D}\Gamma_i^f[q - R^{-1}\partial_j(\rho g_j + f_j)]dV \qquad \text{when } \underline{x}'\in D, \tag{B.2.18}$$

which is the source-type integral representations for the velocity field when the source point is an interior point of D. Note that all integrals in (B.2.18) are convergent (improper) integrals.

It remains to be shown that (B.2.18) is identical to the integral representation (4.3.20) when $\underline{x}'\in D$, in case the latter is applied to a homogeneous and isotropic medium. To this end we successively directly employ (B.2.1) and (B.2.2) in (4.3.20), take in (4.3.21) further into account the relation $G_{ij}^f = R^{-1}(\partial_j\Gamma_i^f + \delta_{ij}\delta(\underline{x}-\underline{x}'))$, and use the property of the delta function as shown in (4.3.8). Then we arrive at

$$v_i(\underline{x}') = R^{-1}(\rho g_i + f_i(\underline{x}')) - \int_{\underline{x}\in\partial D}(\Gamma_i^f v_j + G_{ij}^f p)\nu_j dA$$

$$+\int_{\underline{x}\in D}\Gamma_i^f[q + R^{-1}(\rho g_j + f_j)\partial_j\Gamma_i^f]dV \qquad \text{when } \underline{x}'\in D. \tag{B.2.19}$$

Obviously, the second part of the volume integral in (B.2.19) is divergent. The detailed analysis leading to (B.2.18) learns how this part is to be interpreted, viz. as the combination of the second surface

integral on the right-hand side of (B.2.18), together with the second part of the volume integral in (B.2.18).

B.2.2. VELOCITY FIELD; THE CASE $\underline{x}' \in \partial D$

For the source point located on the boundary surface ∂D of D, we exclude from the domain of application of the reciprocity theorem (4.1.7) the common part $D \cap B_\delta(\underline{x}')$ of D and the ball $B_\delta(\underline{x}')$ defined by (B.1.3) (see Figure B.2). Upon applying (4.1.7) to the domain $D \setminus B'_\delta(\underline{x}')$ and taking the States A and B as before, we obtain

$$\int_{\underline{x} \in \partial B_\delta(\underline{x}') \cup (\partial D \setminus \Sigma_\delta)} (\Gamma^f_i v_j + G^f_{ij} p)\nu_j \, dA$$

$$= \int_{\underline{x} \in D \setminus B'_\delta(\underline{x}')} [\Gamma^f_i q + G^f_{ij}(\rho g_j + f_j)] dV, \qquad \text{(B.2.20)}$$

where $\partial B_\delta(\underline{x}')$ is the part of the boundary surface of $B_\delta(\underline{x}')$ that intersects D, and Σ_δ denotes the part of ∂D that lies inside $B_\delta(\underline{x}')$ (see Figure B.2). From now on, it is assumed that ∂D has a unique tangent plane at $\underline{x}=\underline{x}'$. In (B.2.20), G^f_{ij} and Γ^f_i are given by (B.2.1) and (B.2.2), respectively. Since the point source generating these fields is located outside the domain of application, we have

$$G^f_{ij} = R^{-1} \partial_j \Gamma^f_i. \qquad \text{(B.2.21)}$$

With the aid of the identity

$$\varepsilon_{lmn}\varepsilon_{lki} = \delta_{mk}\delta_{ni} - \delta_{mi}\delta_{nk}, \qquad \text{(B.2.22)}$$

it is further easily verified that

$$\nu_j \partial_j \Gamma_i^f = \varepsilon_{ilk}\varepsilon_{lmn}\nu_m \partial_n \Gamma_k^f \qquad \text{when } \underline{x} \neq \underline{x}', \tag{B.2.23}$$

and hence we have

$$p\nu_j \partial_j \Gamma_i^f = \varepsilon_{ilk}\varepsilon_{lmn}\nu_m \partial_n (p\Gamma_k^f) - \varepsilon_{ilk}\varepsilon_{lmn}\nu_m (\partial_n p)\Gamma_k^f \quad \text{when } \underline{x} \neq \underline{x}'. \tag{B.2.24}$$

Now, upon using (B.2.21), together with (B.2.24), in the left-hand side of (B.2.20), we obtain

$$\begin{aligned} &\int_{\underline{x} \in \partial B_\delta(\underline{x}') \cup (\partial D \setminus \Sigma_\delta)} (\Gamma_i^f v_j + G_{ij}^f p)\nu_j \, dA \\ &= R^{-1} \int_{\underline{x} \in \partial B_\delta(\underline{x}') \cup (\partial D \setminus \Sigma_\delta)} \varepsilon_{ilk}\varepsilon_{lmn}\nu_m \partial_n (p\Gamma_k^f) dA \\ &+ \int_{\underline{x} \in \partial B_\delta(\underline{x}') \cup (\partial D \setminus \Sigma_\delta)} (\Gamma_i^f \nu_j v_j - R^{-1}\varepsilon_{ilk}\varepsilon_{lmn}\nu_m (\partial_n p)\Gamma_k^f) dA. \end{aligned} \tag{B.2.25}$$

The first integral on the right-hand side vanishes. This follows by recalling that $\partial B_\delta(\underline{x}') \cup (\partial D \setminus \Sigma_\delta)$ is a closed surface (see Figure B.2), which can always be written as the union of two open surfaces, $[\partial B_\delta(\underline{x}') \cup (\partial D \setminus \Sigma_\delta)]^{(1)}$ and $[\partial B_\delta(\underline{x}') \cup (\partial D \setminus \Sigma_\delta)]^{(2)}$ for example, and applying Stokes' theorem to the integrals over these open surfaces. The resulting line integrals along the closed boundary curve of $[\partial B_\delta(\underline{x}') \cup (\partial D \setminus \Sigma_\delta)]^{(1)}$ and along the closed boundary curve of $[\partial B_\delta(\underline{x}') \cup (\partial D \setminus \Sigma_\delta)]^{(2)}$ cancel in view of their opposite directions of circulation. To handle the remaining surface integral on the right-hand side of (B.2.25) we start by employing the equation of motion (3.3.6), in which we replace R_{ij} by $R\delta_{ij}$, and rewriting v_j as

$$v_j = R^{-1}(-\partial_j p + \rho g_j + f_j). \tag{B.2.26}$$

Further, we take into account that (cf. (B.2.22))

$$\epsilon_{ilk}\epsilon_{lmn}\nu_m(\partial_n p)\Gamma_k^f = (\partial_i p)\nu_k\Gamma_k^f - \nu_i(\partial_k p)\Gamma_k^f. \tag{B.2.27}$$

We then obtain

$$\int_{\underline{x}\in\partial B_\delta(\underline{x}')\cup(\partial D\setminus\Sigma_\delta)} (\Gamma_i^f v_j + G_{ij}^f p)\nu_j dA$$

$$= R^{-1}\int_{\underline{x}\in\partial B_\delta(\underline{x}')\cup(\partial D\setminus\Sigma_\delta)} \Gamma_i^f(\rho g_j + f_j)\nu_j dA$$

$$- R^{-1}\int_{\underline{x}\in\partial B_\delta(\underline{x}')\cup(\partial D\setminus\Sigma_\delta)} [\Gamma_i^f\nu_j(\partial_j p) + (\partial_i p)\nu_k\Gamma_k^f - \nu_i(\partial_k p)\Gamma_k^f]dA. \tag{B.2.28}$$

In this equation we first examine the surface integral over $\partial B_\delta(\underline{x}')$ in the second integral on the right-hand side. For $\underline{x}$ on $\partial B_\delta(\underline{x}')$ we have (cf. (B.1.6) and (B.2.2), and Figure B.2)

$$\Gamma_i^f = (4\pi\delta^2)^{-1}\nu_i \qquad \text{when } \underline{x}\in\partial B_\delta, \tag{B.2.29}$$

and hence

$$\nu_i\Gamma_i^f = (4\pi\delta^2)^{-1} \qquad \text{when } \underline{x}\in\partial B_\delta. \tag{B.2.30}$$

On the assumption that $\partial_i p$ is continuous at $\underline{x}=\underline{x}'$ we then have

$$\int_{\underline{x}\in\partial B_\delta(\underline{x}')} (\partial_i p)\nu_k\Gamma_k^f]dA = (4\pi\delta^2)^{-1}\int_{\underline{x}\in\partial B_\delta(\underline{x}')} (\partial_i p)dA$$

$$= (1/2)\partial_i' p(\underline{x}') + o(1) \text{ as } \delta\to 0, \tag{B.2.31}$$

while with the aid of (B.2.29) it follows that

$$\int_{\underline{x}\in\partial B_\delta(\underline{x}')} [\Gamma_i^f\nu_j(\partial_j p) - \nu_i(\partial_k p)\Gamma_k^f]dA$$

$$= (4\pi\delta^2)^{-1}\int_{\underline{x}\in\partial B_\delta(\underline{x}')} [\nu_i\nu_j(\partial_j p) - \nu_i\nu_k(\partial_k p)]dA = 0 \quad \text{for } \delta>0, \tag{B.2.32}$$

since the integrand vanishes. In the limit $\delta\to 0$, we further have (cf. (B.2.28))

$$\int_{\underline{x}\in\partial D\setminus\Sigma_\delta} [\Gamma_i^f\nu_j(\partial_j p) + (\partial_i p)\nu_k\Gamma_k^f - \nu_i(\partial_k p)\Gamma_k^f]dA$$

$$= \oint_{\underline{x}\in\partial D} [\Gamma_i^f\nu_j(\partial_j p) + (\partial_i p)\nu_k\Gamma_k^f - \nu_i(\partial_k p)\Gamma_k^f]dA \quad \text{as } \delta\to 0, \tag{B.2.33}$$

where $\oint$ denotes that this integral is to be interpreted as a Cauchy principal value, i.e., the singularity of the integrand is excluded in a symmetrical manner. After this interpretation it can for the case at hand be shown that the integral is an improper convergent one. Collecting the results we obtain

$$\int_{\underline{x}\in\partial B_\delta(\underline{x}')\cup(\partial D\setminus\Sigma_\delta)} (\Gamma_i^f v_j + G_{ij}^f p)\nu_j dA$$

$$= R^{-1}\int_{\underline{x}\in\partial B_\delta(\underline{x}')\cup(\partial D\setminus\Sigma_\delta)} \Gamma_i^f(\rho g_j + f_j)\nu_j dA$$

$$- R^{-1}\oint_{\underline{x}\in\partial D} [\Gamma_i^f\nu_j(\partial_j p) + (\partial_i p)\nu_k\Gamma_k^f - \nu_i(\partial_k p)\Gamma_k^f]dA$$

$$- (1/2)R^{-1}\partial_i' p(\underline{x}') + o(1) \text{ as } \delta\to 0. \tag{B.2.34}$$

Subsequently, we investigate the right-hand side of (B.2.20). Here, we have (cf. (B.2.11))

$$\int_{\underline{x}\in D\setminus B_\delta'(\underline{x}')} \Gamma_i^f q dV = \int_{\underline{x}\in D} \Gamma_i^f q dV + O(\delta) \text{ as } \delta\to 0, \tag{B.2.35}$$

where the volume integral on the right-hand side is a convergent improper one. As regards the remaining part we successively take into account (B.2.21), assume that f_j is continuously differentiable, and observe that

$$G^f_{ij}(\rho g_j + f_j) = R^{-1}\{\partial_j[\Gamma^f_i(\rho g_j + f_j)] - \Gamma^f_i\partial_j(\rho g_j + f_j)\}. \qquad (B.2.36)$$

Using this in the volume integral in (B.2.20) we have

$$\int_{\underline{x}\in D\setminus B'_\delta(\underline{x}')} G^f_{ij}(\rho g_j + f_j)\,dV$$

$$= R^{-1}\int_{\underline{x}\in\partial B_\delta(\underline{x}')\cup(\partial D\setminus\Sigma_\delta)} \Gamma^f_i(\rho g_j + f_j)\nu_j\,dA$$

$$- R^{-1}\int_{\underline{x}\in D\setminus B'_\delta(\underline{x}')} \Gamma^f_i\partial_j(\rho g_j + f_j)\,dV, \qquad (B.2.37)$$

where the surface integral results from a direct application of Gauss' theorem. Further, in the limit $\delta\to 0$, we have

$$\int_{\underline{x}\in D\setminus B'_\delta(\underline{x}')} \Gamma^f_i\partial_j(\rho g_j + f_j)\,dV = \int_{\underline{x}\in D} \Gamma^f_i\partial_j(\rho g_j + f_j)\,dV + O(\delta) \text{ as } \delta\to 0, \qquad (B.2.38)$$

where the volume integral on the right-hand side is a convergent improper one. Collecting the results (B.2.34), (B.2.35), (B.2.37) and (B.2.38) in (B.2.20), it follows that, in the limit $\delta\to 0$, we arrive at

$$-(1/2)R^{-1}\partial'_i p(\underline{x}') - R^{-1}\int_{\underline{x}\in\partial D}[\Gamma^f_i\nu_j(\partial_j p) + (\partial_i p)\nu_k\Gamma^f_k - \nu_i(\partial_k p)\Gamma^f_k]dA$$

$$= \int_{\underline{x}\in D}\Gamma^f_i[q - R^{-1}\partial_j(\rho g_j + f_j)]dV \qquad \text{when } \underline{x}'\in\partial D. \qquad (B.2.39)$$

Finally, upon using in (B.2.39) the equation of motion (3.3.6), in which we replace R_{ij} by $R\delta_{ij}$, $\underline{x}$ by $\underline{x}'$, and ∂_i by ∂'_i, we end up with

$$(1/2)v_i(\underline{x}') = (1/2)R^{-1}(\rho g_i + f_i(\underline{x}'))$$
$$+ R^{-1}\int_{\underline{x}\in\partial D}[\Gamma_i^f \nu_j(\partial_j p) + (\partial_i p)\nu_k\Gamma_k^f - \nu_i(\partial_k p)\Gamma_k^f]dA$$
$$+ \int_{\underline{x}\in D}\Gamma_i^f[q - R^{-1}\partial_j(\rho g_j + f_j)]dV \quad \text{when } \underline{x}'\in\partial D, \quad (B.2.40)$$

which is the desired source-type integral relation for the velocity field when the source point is located on the boundary surface of D. Note that in the surface integral we can always replace $(\partial_j p)$, and/or $(\partial_i p)$ and $(\partial_k p)$, by the expression that follows upon using the equation of motion.

The integral relation for the velocity field for $\underline{x}'\in\partial D$ that is obtained upon directly employing (B.2.1) and (B.2.2) in (4.3.20) and using the property of the delta function as shown in (4.3.8), contains divergent integrals. The above detailed derivation shows how these integrals are to be interpreted.

B.2.3. VELOCITY FIELD; THE CASE $\underline{x}'\in D'$

In the case $\underline{x}'\in D'$, i.e., when the source point is located outside D U ∂D, it is obvious that G_{ij}^f and Γ_i^f are both regular throughout D. Hence, in this case the reciprocity theorem (4.1.7) can be used directly. Taking in (4.1.7) the States A and B as before, it immediately follows that for $\underline{x}'\in$ D' the source-type integral relation in a homogeneous and isotropic medium is arrived at by directly employing (B.2.1) and (B.2.2). The resulting integral relation is identical to the one in (4.3.20) when $\underline{x}'\in$ D', in case the latter is applied to a homogeneous and isotropic medium.

B.3. SOURCE-TYPE INTEGRAL RELATIONS FOR THE GROUNDWATER FLOW FIELD IN THE CASE OF A HOMOGENEOUS AND ANISOTROPIC, BUT RECIPROCAL, MEDIUM

For the case of a homogeneous and anisotropic, but reciprocal, medium the technique of excluding the singularity can be most easily carried out by introducing successively the coordinate transformations used in Appendix C (Section C.2), i.e., the ones defined by (C.2.8) and (C.2.9), respectively. In this manner, the relevant analysis is reduced to the one of an isotropic medium in the coordinate system defined by (C.2.11).

APPENDIX C

CALCULATION OF THE SURFACE INTEGRALS OCCURRING IN THE DISCRETIZED BOUNDARY INTEGRAL EQUATIONS

In this appendix we derive analytic expressions for the surface integrals IG^q, $I\Gamma^q$, $I\Gamma_i^f$ and IG_i^f, that are given in (5.4.3) - (5.4.6) and occur in the application of the boundary-integral-equation method. The technique will be discussed for the triangle S_T. The integrals to be evaluated are recapitulated below (cf. (5.4.3) - (5.4.6)):

$$IG^q(I,\underline{x}') = \int_{\underline{x}\in S_T} \phi(I,\underline{x})G^q(\underline{x}',\underline{x})dA, \tag{C.1}$$

$$I\Gamma^q(I,\underline{x}') = \int_{\underline{x}\in S_T} \phi(I,\underline{x})\Gamma_i^q(\underline{x}',\underline{x})\nu_i dA, \tag{C.2}$$

$$I\Gamma_i^f(I,\underline{x}') = \int_{\underline{x}\in S_T} \phi(I,\underline{x})\Gamma_i^f(\underline{x}',\underline{x})dA, \tag{C.3}$$

$$IG_i^f(I,\underline{x}') = \int_{\underline{x}\in S_T} \phi(I,\underline{x})G_{ij}^f(\underline{x}',\underline{x})\nu_j dA, \tag{C.4}$$

where $I\in\{1,2,3\}$, $\phi(I,\underline{x})$ is defined in (5.1.24) and the Green's functions G^q, Γ^q, Γ_i^f and G_{ij}^f are given in (4.5.19), (4.5.20), (4.5.27) and (4.5.26). Note that in (C.2) and (C.4) the unit vector ν_i along the normal to S_T has a constant value for all $\underline{x}\in S_T$. Henceforth, it assumed that in (C.1) - (C.4) the point of observation with position vector $\underline{x}'$ is neither a point of S_T nor of its boundary C_T.

In the analytic evaluation of the integrals in (C.1) - (C.4) it will prove to be advantageous to treat the case where they apply to isotropic media separately from the general case where they apply to anisotropic media; in Section C.1 the isotropic case is discussed and in Section C.2 the anisotropic case.

Although the analysis presented in this appendix is applied to a planar triangle, it applies to an arbitrary, planar, polygonal disk as well.

C.1. ANALYTIC EVALUATION OF THE SURFACE INTEGRALS (ISOTROPIC CASE)

In this section we derive the analytic expressions for the integrals in (C.1) - (C.4) in case they apply to isotropic media. With the aid of (4.5.19), (4.5.20), (4.5.26), (4.5.27), (4.1.9) and (4.5.40) it follows that for an isotropic medium (C.1) - (C.4) are given by

$$IG^{q}(I,\underline{x}') = (R/4\pi) \int_{\underline{x}\in S_T} \phi(I,\underline{x})|\underline{x} - \underline{x}'|^{-1} dA, \tag{C.1.1}$$

$$I\Gamma^{q}(I,\underline{x}') = (4\pi)^{-1} \int_{\underline{x}\in S_T} \phi(I,\underline{x})\nu_i \partial_i |\underline{x} - \underline{x}'|^{-1} dA, \tag{C.1.2}$$

$$I\Gamma_i^{f}(I,\underline{x}') = (4\pi)^{-1} \int_{\underline{x}\in S_T} \phi(I,\underline{x})\partial_i |\underline{x} - \underline{x}'|^{-1} dA, \tag{C.1.3}$$

$$IG_i^{f}(I,\underline{x}') = (4\pi R)^{-1} \int_{\underline{x}\in S_T} \phi(I,\underline{x})\nu_j \partial_j \partial_i |\underline{x} - \underline{x}'|^{-1} dA, \tag{C.1.4}$$

where R is the constant resistivity of the medium under consideration. As we have argued in Subsection 5.4.3, the main tool in the analytic evaluation of the above integrals is Stokes' theorem that enables us to rewrite the integrals over S_T to integrals along its boundary C_T. The details of this procedure are outlined in Subsection C.1.1; in Subsection C.1.2 we show that the resulting line integrals along each edge of the boundary curve C_T of S_T are expressible in terms of elementary analytic functions. In the procedure discussed in Subsection C.1.1, we shall encounter one surface integral that cannot be cast into a form amenable to an application of Stokes' theorem. This integral is, apart from a constant, nothing but the solid angle at which the relevant triangle is observed from the point of observation. Its value is in Subsection C.1.3

determined by applying geometrical considerations, where a purely analytic determination is given as well.

C.1.1. REDUCTION OF THE SURFACE INTEGRALS TO CONTOUR INTEGRALS

In this subsection we reduce each of the surface integrals (C.1.1) - (C.1.4) to one or more line integrals along the boundary curve C_T of S_T plus a surface integral whose evaluation will be discussed in detail in Subsection C.1.3. The first relation that we use in (C.1.1) is

$$\phi(I,x)|\underline{x} - \underline{x}'|^{-1} = - [\partial_i\phi(I,x)]\partial_i|\underline{x} - \underline{x}'| + (1/2)\partial_i\partial_i[\phi(I,x)|\underline{x} - \underline{x}'|], \qquad (C.1.5)$$

where $\phi(I,\underline{x})$ and the constant $\partial_i\phi(I,\underline{x})$ are given in (5.1.24) and (5.1.26), respectively. Equation (C.1.5) is easily verified by carrying out the differentiations at the right-hand side and taking into that $\partial_i\phi(I,\underline{x})$ is a constant. Since $\partial_i\phi(I,\underline{x})$ lies in the plane of S_T, we have

$$\nu_i\partial_i\phi(I,\underline{x}) = 0. \qquad (C.1.6)$$

As a next step towards the replacement of $IG^q(I,\underline{x}')$ by a to contour integral we take into account that

$$\partial_i = \nu_j\nu_j\partial_i = \varepsilon_{lmk}\nu_m\partial_k\varepsilon_{lpi}\nu_p + \nu_i\nu_j\partial_j, \qquad (C.1.7)$$

where ε_{lmk} is the Levi-Civita tensor defined in (5.1.7). In (C.1.7), we have used the fact that $\nu_j\nu_j=1$, and the ε-δ identity

$$\varepsilon_{lmk}\varepsilon_{lpi} = \delta_{mp}\delta_{ki} - \delta_{mi}\delta_{kp}. \qquad (C.1.8)$$

Employing (C.1.7) in (C.1.5), we obtain the expression

$$\phi(I,\underline{x})|\underline{x}-\underline{x}'|^{-1} = -[\partial_i\phi(I,\underline{x})][\varepsilon_{lmk}\nu_m\partial_k\varepsilon_{lpi}\nu_p + \nu_i\nu_j\partial_j]|\underline{x}-\underline{x}'|$$
$$+ (1/2)\varepsilon_{lmk}\nu_m\partial_k\varepsilon_{lpi}\nu_p\partial_i[\phi(I,\underline{x})|\underline{x}-\underline{x}'|]$$
$$+ (1/2)\nu_i\nu_j\partial_j\partial_i[\phi(I,\underline{x})|\underline{x}-\underline{x}'|]. \qquad (C.1.9)$$

With the further aid of (C.1.6) and the relation

$$\nu_i\nu_j\partial_j\partial_i[\phi(I,\underline{x})|\underline{x}-\underline{x}'|] = \phi(I,\underline{x})[1 + \nu_i(x_i - x_i')\nu_j\partial_j]|\underline{x}-\underline{x}|^{-1}, \qquad (C.1.10)$$

it follows from (C.1.9) that

$$\phi(I,\underline{x})|\underline{x}-\underline{x}'|^{-1} = -2[\partial_i\phi(I,\underline{x})]\varepsilon_{lmk}\nu_m\partial_k\varepsilon_{lpi}\nu_p|\underline{x}-\underline{x}'|$$
$$+ \varepsilon_{lmk}\nu_m\partial_k\varepsilon_{lpi}\nu_p\partial_i[\phi(I,\underline{x})|\underline{x}-\underline{x}'|]$$
$$+ \phi(I,\underline{x})\nu_i(x_i - x_i')\nu_j\partial_j|\underline{x}-\underline{x}'|^{-1}. \qquad (C.1.11)$$

Taking into account that $\partial_i\phi(I,\underline{x})$ has a constant value on S_T, the surface integral over S_T of the first term on the right-hand side of (C.1.11) can be reduced to a contour integral along the boundary curve C_T of S_T by applying Stokes' theorem. Also the surface integral over S_T of the second term on the right-hand side of (C.1.11) can be handled in this way. Further, in view of the fact that $\nu_i(x_i-x_i')$, i.e., the (signed) distance from $\underline{x}'$ to the plane S_T, is constant for all $\underline{x}\in S_T$, it is apparent that the surface integral over S_T of the last term on the right-hand side of (C.1.11) equals $4\pi\nu_i(x_i-x_i')\times I\Gamma^q(I,\underline{x}')$ (cf. (C.1.2)). Hence, upon substituting (C.1.11) in (C.1.1) and using Stokes' theorem, we are led to

$$IG^q(I,\underline{x}') = (R/4\pi)\{-2[\partial_i\phi(I,\underline{x})]\int_{\underline{x}\in C_T} \tau_l\varepsilon_{lpi}\nu_p|\underline{x}-\underline{x}'|ds$$

$$+\int_{\underline{x}\in C_T}\tau_l\varepsilon_{lpi}\nu_p\partial_i[\phi(I,\underline{x})|\underline{x}-\underline{x}'|]ds\}$$

$$+R\nu_i(x_i-x_i')I\Gamma^q(I,\underline{x}), \qquad (C.1.12)$$

where τ_l is the unit tangent along C_T in the direction of circulation that forms a right-hand system with ν_l. Since C_T is the union of three straight edges $\{C_T(1),C_T(2),C_T(3)\}$ the unit tangent vector $\tau_l(J)$ will have a constant value along $C_T(J)$. Upon using this property in (C.1.12) and carrying out the differentiation in the integrand of the second line integral, it follows that

$$IG^q(I,\underline{x}') = (R/4\pi)\{-[\partial_i\phi(I,\underline{x})]\sum_{J=1}^{3}\varepsilon_{ilp}\tau_l(J)\nu_pL1(J,\underline{x}')$$

$$+\sum_{J=1}^{3}L2(I,J,\underline{x}')\}+R\nu_i(x_i-x_i')I\Gamma^q(I,\underline{x}), \qquad (C.1.13)$$

in which $L1(J,\underline{x}')$ and $L2(I,J,\underline{x}')$ are defined as

$$L1(J,\underline{x}') = \int_{\underline{x}\in C_T(J)}|\underline{x}-\underline{x}'|ds \qquad (C.1.14)$$

and

$$L2(I,J,\underline{x}') = \int_{\underline{x}\in C_T(J)}\phi(I,\underline{x})\tau_l(J)\varepsilon_{lpi}\nu_p(x_i-x_i')|\underline{x}-\underline{x}'|^{-1}ds, \qquad (C.1.15)$$

respectively. In Subsection C.1.2 these line integrals are evaluated analytically. In (C.1.13) we are left with the evaluation of $I\Gamma^q(I,x')$. Now, from (C.1.2) and (C.1.3) it is clear that

$$I\Gamma^q(I,\underline{x}') = \nu_iI\Gamma_i^f(I,\underline{x}'). \qquad (C.1.16)$$

Therefore, we discuss the evaluation of $I\Gamma_i^f(I,\underline{x}')$, which is needed anyway, first, and use the result in (C.1.16). To this end, we rewrite the integrand of $I\Gamma_i^f(I,\underline{x}')$ as (cf. (C.1.3))

$$\phi(I,\underline{x})\partial_i|\underline{x}-\underline{x}'|^{-1} = \partial_i[\phi(I,\underline{x})|\underline{x}-\underline{x}'|^{-1}] - [\partial_i\phi(I,\underline{x})]|\underline{x}-\underline{x}'|^{-1}, \tag{C.1.17}$$

where in the last term we further employ the relation

$$|\underline{x}-\underline{x}'|^{-1} = \varepsilon_{lmk}\nu_m\partial_k\varepsilon_{lpi}\nu_p\partial_i|\underline{x}-\underline{x}'| + \nu_i(x_i-x_i')\nu_j\partial_j|\underline{x}-\underline{x}'|^{-1}, \tag{C.1.18}$$

that follows from (C.1.11) with $\phi(I,\underline{x})$ replaced by unity. Using (C.1.7) and (C.1.6) in the first *term* on the right-hand side of (C.1.17), it then follows that

$$\begin{aligned}\phi(I,\underline{x})\partial_i|\underline{x}-\underline{x}'|^{-1} &= \varepsilon_{lmk}\nu_m\partial_k\varepsilon_{lpi}\nu_p[\phi(I,\underline{x})|\underline{x}-\underline{x}'|^{-1}]\\ &+ \phi(I,\underline{x})\nu_i\nu_j\partial_j|\underline{x}-\underline{x}'|^{-1}\\ &- [\partial_i\phi(I,\underline{x})][\varepsilon_{lmk}\nu_m\partial_k\varepsilon_{lpj}\nu_p\partial_j|\underline{x}-\underline{x}'|\\ &+ \nu_j(x_j-x_j')\nu_k\partial_k|\underline{x}-\underline{x}'|^{-1}].\end{aligned} \tag{C.1.19}$$

Substituting (C.1.19) in (C.1.3) and using Stokes' theorem, together with the constancy of $\nu_j(x_j-x_j')$ during the integration over S_T, and the fact that the unit tangents along the (straight) edges of S_T are constants, we end up with

$$\begin{aligned}I\Gamma_i^f(I,\underline{x}') &= \nu_i I\Gamma^q(I,\underline{x}) + (4\pi)^{-1}\{\textstyle\sum_{J=1}^{3}\varepsilon_{ilp}\tau_l(J)\nu_p L3(I,J,\underline{x}')\\ &- [\partial_i\phi(I,\underline{x})][\textstyle\sum_{J=1}^{3} L4(J,\underline{x}') - \nu_j(x_j-x_j')\Omega(\underline{x}')]\},\end{aligned} \tag{C.1.20}$$

in which $L3(I,J,\underline{x}')$, $L4(J,\underline{x}')$ and $\Omega(\underline{x}')$ are defined as

$$L3(I,J,\underline{x}') = \int_{\underline{x}\in C_T(J)} \phi(I,\underline{x})|\underline{x} - \underline{x}'|^{-1} ds, \qquad (C.1.21)$$

$$L4(J,\underline{x}') = \int_{\underline{x}\in C_T(J)} \tau_l(J)\varepsilon_{lmk}\nu_m(x_k - x_k')|\underline{x} - \underline{x}'|^{-1} ds, \qquad (C.1.22)$$

and

$$\Omega(\underline{x}') = -\int_{\underline{x}\in S_T} \nu_k \partial_k |\underline{x} - \underline{x}'|^{-1} dA, \qquad (C.1.23)$$

respectively. $\Omega(\underline{x}')$ equals the solid angle subtended by the triangle S_T at the point of observation with position vector $\underline{x}'$ (see, e.g., Spiegel, 1974, p. 124); its value is, both geometrically and analytically, determined in Subsection C.1.3. The analytic evaluation of the line integrals $L3(I,J,\underline{x}')$ and $L4(J,\underline{x}')$ is discussed in the next subsection. It should be noted that upon multiplying (C.1.20) on both sides by ν_i, and using (C.1.6) and the fact that $\nu_i\varepsilon_{ilp}\tau_l(J)\nu_p=0$, the right-hand side reduces to $I\Gamma^q(I,\underline{x}')$.

To evaluate $I\Gamma^q(I,\underline{x}')$, we first extend through (5.1.24) the domain of $\phi(I,\underline{x})$ to the entire R^3 and rewrite $\phi(I,\underline{x})$ as

$$\phi(I,\underline{x}) = \phi(I,\underline{x}') + [\partial_j\phi(I,\underline{x})](x_j - x_j') \qquad (\text{where } \underline{x}'\in R^3), \qquad (C.1.24)$$

and use this to rewrite the integrand of $I\Gamma^q(I,\underline{x}')$ as (cf. (C.1.2))

$$\phi(I,\underline{x})\nu_i\partial_i|\underline{x} - \underline{x}'|^{-1} = \phi(I,\underline{x}')\nu_i\partial_i|\underline{x} - \underline{x}'|^{-1}$$

$$+ \nu_i(x_i - x_i')[\partial_j\phi(I,\underline{x})]\partial_j|\underline{x} - \underline{x}'|^{-1}. \qquad (C.1.25)$$

Further, we have on account of (C.1.7) and (C.1.6)

$$[\partial_j\phi(I,\underline{x})]\partial_j|\underline{x}-\underline{x}'|^{-1} = [\partial_i\phi(I,\underline{x})]\varepsilon_{lmk}\nu_m\partial_k\varepsilon_{lpi}\nu_p|\underline{x}-\underline{x}'|^{-1}. \quad (C.1.26)$$

Using this result in (C.1.25), (C.1.2) can upon applying Stokes' theorem be rewritten as

$$I\Gamma^q(I,\underline{x}') = (4\pi)^{-1}\{\nu_j(x_j - x_j')\sum_{J=1}^{3}[\partial_i\phi(I,\underline{x})]\varepsilon_{ilp}\tau_l(J)\nu_p L5(J,\underline{x}') - \phi(I,\underline{x}')\Omega(\underline{x}')\}, \quad (C.1.27)$$

where for x_j in $\nu_j(x_j-x_j')$ we can take any point in S_T (e.g., a vertex) and where $L5(J,\underline{x}')$ is defined as

$$L5(J,\underline{x}') = \int_{\underline{x}\in C_T(J)} |\underline{x}-\underline{x}'|^{-1}ds. \quad (C.1.28)$$

The evaluation of (C.1.28) is discussed in the next subsection.

Finally, to reduce the surface integral $IG_i^f(I,\underline{x}')$ (cf. (C.1.4)) to line integrals along the boundary curve C_T and an additional surface integral that can be identified with $\Omega(\underline{x}')$, we first consider the relation

$$\phi(I,\underline{x})\nu_j\partial_j\partial_i|\underline{x}-\underline{x}'|^{-1} = \varepsilon_{lmk}\nu_m\partial_k\varepsilon_{lpi}\partial_p[\phi(I,\underline{x}')|\underline{x}-\underline{x}'|^{-1}] + \nu_i\partial_j\partial_j[\phi(I,\underline{x})|\underline{x}-\underline{x}'|^{-1}] - [\partial_i\phi(I,\underline{x})]\nu_j\partial_j|\underline{x}-\underline{x}'|^{-1}, \quad (C.1.29)$$

which is verified by using identity (C.1.8) and taking into account (C.1.6). Recalling that $(4\pi|\underline{x}-\underline{x}'|)^{-1}$ is the Green's function of Poisson's equation and using (C.1.7) and (C.1.6), it is easily verified that the second term on the right-hand side of (C.1.29) can be written as

$$\nu_i\partial_j\partial_j[\phi(I,\underline{x})|\underline{x}-\underline{x}'|^{-1}] = 2\nu_i[\partial_j\phi(I,\underline{x})]\varepsilon_{lmk}\nu_m\partial_k\varepsilon_{lpj}\nu_p|\underline{x}-\underline{x}'|^{-1}$$

when $\underline{x} \neq \underline{x}'$. (C.1.30)

Using (C.1.30) in (C.1.29) and substituting the result in (C.1.4), we arrive after applying Stokes' theorem at

$$IG_i^f(I,\underline{x}') = (4\pi R)^{-1}\{\sum_{J=1}^{3} \varepsilon_{ilp}\tau_l(J)[\partial_p\phi(I,\underline{x})]L5(J,\underline{x}')$$

$$+ 2\nu_i\sum_{J=1}^{3} [\partial_j\phi(I,\underline{x})]\varepsilon_{jlp}\tau_l(J)\nu_p L5(J,\underline{x}')$$

$$- \sum_{J=1}^{3} L6_i(I,J,\underline{x}') + [\partial_i\phi(I,\underline{x})]\Omega(\underline{x}')\}, \qquad (C.1.31)$$

where $L5(J,\underline{x}')$ is given by (C.1.28), $\Omega(\underline{x})$ by (C.1.23) and $L6_i(I,J,\underline{x}')$ is defined as

$$L6_i(I,J,\underline{x}') = \int_{\underline{x}\in C_T(J)} \phi(I,\underline{x})\varepsilon_{ijk}\tau_j(J)(x_k - x_k')|\underline{x} - \underline{x}'|^{-3}ds. \qquad (C.1.32)$$

The evaluation of (C.1.32) is discussed in the next subsection.

C.1.2. EVALUATION OF THE LINE INTEGRALS

In the present subsection we discuss the evaluation of the line integrals $L1(J,\underline{x}')$, $L2(I,J,\underline{x}')$, $L3(I,J,\underline{x}')$, $L4(J,\underline{x}')$, $L5(J,\underline{x}')$ and $L6_i(I,J,\underline{x}')$ that have been introduced in Subsection C.1.1.

Inspection of (C.1.15) and (C.1.22) reveals that $L4(J,\underline{x}')$ results from $L2(I,J,\underline{x}')$ by replacing $\phi(I,\underline{x})$ by the value one. Similarly, inspection of (C.1.21) and (C.1.28) reveals that $L5(J,\underline{x}')$ is obtained from $L3(I,J,\underline{x}')$ by replacing $\phi(I,\underline{x})$ by the value one. Hence, we only have to investigate the evaluation of $L1(J,\underline{x}')$, $L2(I,J,\underline{x}')$, $L3(I,J,\underline{x}')$ and $L6_i(I,J,\underline{x}')$.

For this purpose we consider the straight line segment (edge) $C_T(J)$ with $J\in\{1,2,3\}$; it is indicated in Figure C.1. Along $C_T(J)$ we have

$$\tau_i(J) = a_i(J)/a(J) \qquad \text{with } J\in\{1,2,3\}, \tag{C.1.33}$$

where $a_i(J)$ is the vectorial length and $a(J)$ the scalar length of $C_T(J)$. Taking into account the chosen orientation of $C_T(J)$ (cf. Section 5.1), it

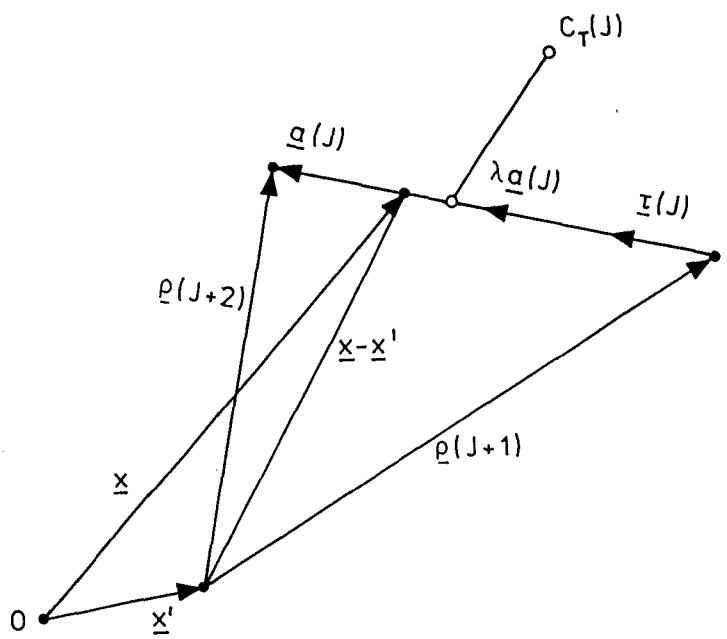

Fig. C.1. Configuration employed in the analytic evaluation of the line integrals.

is apparent that the starting point and the end point of $C_T(J)$ are the vertices P_K and P_I of triangle S_T, respectively, where $\{I,J,K\}=$ cycl$\{1,2,3\}$. In the subsequent analysis we also employ the vectorial distances from the point of observation to the starting point and the end point of $C_T(J)$. These are introduced as (see Figure C.1)

$$\rho_i(J+1) = x_i(J+1) - x_i' \qquad \text{with } J\in\{1,2,3\}, \tag{C.1.34}$$

and

$$\rho_i(J+2) = x_i(J+2) - x_i' \qquad \text{with } J\in\{1,2,3\}, \tag{C.1.35}$$

respectively, where $x_i(J+1)$ is the position vector of the starting point of $C_T(J)$ and $x_i(J+2)$ the position vector of the end point of $C_T(J)$ and hence $a_i(J)=x_i(J+2) - x_i(J+1)$. In (C.1.34) and (C.1.35) the convention applies that $\rho_i(4)=\rho_i(1)$, $x_i(4)=x_i(1)$, $\rho_i(5)=\rho_i(2)$ and $x_i(5)=x_i(2)$. Upon comparing (C.1.34) and (C.1.35) with the notation introduced in Section 5.1 for the vertices of S_T, it is apparent that $x_i(J+1)$ is the position vector of vertex P_K and $x_i(J+2)$ the position vector of vertex P_I of S_T, with $\{I,J,K\}=$cycl$\{1,2,3\}$. Further, the corresponding length $\rho(J)$ of $\rho_i(J)$ is given by

$$\rho(J) = [\rho_i(J)\rho_i(J)]^{1/2} \qquad \text{with } J\in\{1,2,3\}. \tag{C.1.36}$$

Along $C_T(J)$ we now have (see Figure C.1)

$$x_i - x_i' = \rho_i(J+1) + \lambda a_i(J) \qquad \text{with } 0 \leq \lambda \leq 1 \text{ and } J\in\{1,2,3\}, \tag{C.1.37}$$

and

$$ds = a(J)d\lambda \qquad \text{with } J\in\{1,2,3\}. \tag{C.1.38}$$

From (C.1.24) and (C.1.37) we further have

$$\phi(I,\underline{x}) = \phi(I,\underline{x}') + [\partial_i\phi(I,\underline{x})][\rho_i(J+1) + \lambda a_i(J)] \text{ when } \underline{x}\in C_T(J), \text{ with } I\in\{1,2,3\} \text{ and } J\in\{1,2,3\}, \quad (C.1.39)$$

where in view of (5.1.26) and (5.1.12) it is clear that $[\partial_i\phi(I,\underline{x})]a_i(J)$ equals 0, -1, or +1, depending on the actual values of I and J.

With the aid of (C.1.37) - (C.1.39) the integrals $L1(J,\underline{x}')$, $L2(I,J,\underline{x}')$, $L3(I,J,\underline{x}')$ and $L6_i(I,J,\underline{x}')$ can be rewritten as (cf. (C.1.14), (C.1.15), (C.1.21) and (C.1.32))

$$L1(J,\underline{x}') = a(J)\int_{\lambda=0}^{1} D(\lambda)d\lambda, \quad (C.1.40)$$

$$L2(I,J,\underline{x}') = a_i(J)\varepsilon_{ijk}\nu_j\rho_k(J+1)\{[\partial_m\phi(I,\underline{x})]a_m(J)\int_{\lambda=0}^{1}\lambda[D(\lambda)]^{-1}d\lambda,$$

$$+ \{\phi(I,\underline{x}') + [\partial_m\phi(I,\underline{x})]\rho_m(J+1)\}\int_{\lambda=0}^{1}[D(\lambda)]^{-1}d\lambda\}, \quad (C.1.41)$$

$$L3(I,J,\underline{x}') = a(J)\{[\phi(I,\underline{x}') + [\partial_i\phi(I,\underline{x})]\rho_i(J+1)]\int_{\lambda=0}^{1}[D(\lambda)]^{-1}d\lambda$$

$$+ [\partial_i\phi(I,\underline{x})]a_i(J)\int_{\lambda=0}^{1}\lambda[D(\lambda)]^{-1}d\lambda\}, \quad (C.1.42)$$

$$L6_i(I,J,\underline{x}') = \varepsilon_{ijk}a_j(J)\rho_k(J+1)\{[\partial_m\phi(I,\underline{x})]a_m(J)\int_{\lambda=0}^{1}\lambda[D(\lambda)]^{-3}d\lambda$$

$$+ [\phi(I,\underline{x}') + [\partial_m\phi(I,\underline{x})]\rho_m(J+1)]\int_{\lambda=0}^{1}[D(\lambda)]^{-3}d\lambda\}, \quad (C.1.43)$$

where (cf. (4.5.23), (4.5.25), (4.5.56) and (C.1.37))

$$D(\lambda) = [\rho_i(J+1)\rho_i(J+1) + 2\lambda a_i(J)\rho_i(J+1) + \lambda^2 a_i(J)a_i(J)]^{1/2}. \quad (C.1.44)$$

The remaining scalar integrals are elementary (see, e.g., Gradshteyn and Ryzhik, 1980, pp. 81-83); they are given by

$$\int_{\lambda=0}^{1} [D(\lambda)]^{-1} d\lambda = \begin{cases} \Lambda(J,\underline{x}'), \\ \Lambda S(J,\underline{x}') \text{ if } a_i(J)\rho_i(J+1) = -a(J)\rho(J+1) \\ \qquad \text{and } a_i(J)\rho_i(J+2) = -a(J)\rho(J+2), \end{cases} \tag{C.1.45}$$

$$\int_{\lambda=0}^{1} \lambda[D(\lambda)]^{-1} d\lambda = [a(J)]^{-2}[\rho(J+2) - \rho(J+1) - a_i(J)\rho_i(J+1)\int_{\lambda=0}^{1} [D(\lambda)]^{-1} d\lambda], \tag{C.1.46}$$

$$\int_{\lambda=0}^{1} D(\lambda) d\lambda = (1/2)[a(J)]^{-2}\{a_i(J)[\rho_i(J+2)\rho(J+2) - \rho_i(J+1)\rho(J+1)] + \Xi(J,\underline{x}')\int_{\lambda=0}^{1} [D(\lambda)]^{-1} d\lambda\}, \tag{C.1.47}$$

$$\int_{\lambda=0}^{1} [D(\lambda)]^{-3} d\lambda = \begin{cases} T(J,\underline{x}'), \\ TS1(J,\underline{x}') \text{ if } a_i(J)\rho_i(J+1) = a(J)\rho(J+1), \\ TS2(J,\underline{x}') \text{ if } a_i(J)\rho_i(J+1) = -a(J)\rho(J+1), \end{cases} \tag{C.1.48}$$

$$\int_{\lambda=0}^{1} \lambda[D(\lambda)]^{-3} d\lambda = \begin{cases} A(J,\underline{x}'), \\ AS1(J,\underline{x}') \text{ if } a_i(J)\rho_i(J+1) = a(J)\rho(J+1), \\ AS2(J,\underline{x}') \text{ if } a_i(J)\rho_i(J+1) = -a(J)\rho(J+1), \end{cases} \tag{C.1.49}$$

where $\Lambda(J,\underline{x}')$, $\Lambda S(J,\underline{x}')$, $\Xi(J,\underline{x}')$, $T(J,\underline{x}')$, $TS1(J,\underline{x}')$, $TS2(J,\underline{x}')$, $A(J,\underline{x}')$, $AS1(J,\underline{x}')$ and $AS2(J,\underline{x}')$, are defined as

$$\Lambda(J,\underline{x}') = [a(J)]^{-1} \ln\left[\frac{a_i(J)\rho_i(J+2) + a(J)\rho(J+2)}{a_i(J)\rho_i(J+1) + a(J)\rho(J+1)}\right], \tag{C.1.50}$$

$$\Lambda S(J,\underline{x}') = [a(J)]^{-1} \ln\left[-\frac{\rho(J+1)}{\rho(J+2)}\right], \tag{C.1.51}$$

$$\Xi(J,\underline{x}') = [a(J)\rho(J+1)]^2 - [a_i(J)\rho_i(J+1)]^2, \tag{C.1.52}$$

$$T(J,\underline{x}') = [\Xi(J,\underline{x}')]^{-1}\left[\frac{a_i(J)\rho_i(J+2)}{\rho(J+2)} - \frac{a_i(J)\rho_i(J+1)}{\rho(J+1)}\right], \tag{C.1.53}$$

$$TS1(J,\underline{x}') = [2a(J)]^{-1}\{[\rho(J+1)]^{-2} - [\rho(J+2)]^{-2}\}, \tag{C.1.54}$$

$$TS2(J,\underline{x}') = [2a(J)]^{-1}\{[\rho(J+2)]^{-2} - [\rho(J+1)]^{-2}\}, \tag{C.1.55}$$

$$A(J,\underline{x}') = [\Xi(J,\underline{x}')]^{-1}\left[\rho(J+1) - \frac{\rho_i(J+1)\rho_i(J+2)}{\rho(J+2)}\right], \tag{C.1.56}$$

$$AS1(J,\underline{x}') = (1/2)[a(J)]^{-2}\{[\rho(J+1)]^{-1} - [2a(J) + \rho(J+1)][\rho(J+2)]^{-2}\}, \tag{C.1.57}$$

$$AS2(J,\underline{x}') = (1/2)[a(J)]^{-2}\{[\rho(J+1)]^{-1} - [\rho(J+2) - 2a(J)][\rho(J+2)]^{-2}\}. \tag{C.1.58}$$

With the aid of these standard integrals the final expressions for the line integrals are obtained as

$$L1(J,\underline{x}') = [2a(J)]^{-1}\{a_i(J)[\rho_i(J+2)\rho(J+2) - \rho_i(J+1)\rho(J+1)] + \Xi(J,\underline{x}')\Lambda(J,\underline{x}')\}, \tag{C.1.59}$$

$$L2(I,J,\underline{x}') = a_i(J)\epsilon_{ijk}\nu_j\rho_k(J+1)\{[a(J)]^{-2}[\partial_m\phi(I,\underline{x})]a_m(J) \times [\rho(J+2) - \rho(J+1) - a_n(J)\rho_n(J+1)\Lambda(J,\underline{x}')] + [\phi(I,\underline{x}') + [\partial_m\phi(I,\underline{x})]\rho_m(J+1)]\Lambda(J,\underline{x}')\}, \tag{C.1.60}$$

$$L3(I,J,\underline{x}') = a(J)\{[\phi(I,\underline{x}') + [\partial_i\phi(I,\underline{x})]\rho_i(J+1)]\Lambda(J,\underline{x}') + [a(J)]^{-2} \times [\partial_i\phi(I,\underline{x})]a_i(J)[\rho(J+2) - \rho(J+1) - a_j(J)\rho_j(J+1)\Lambda(J,\underline{x}')]\},$$

(C.1.61)

$$L4(J,\underline{x}') = a_i(J)\varepsilon_{ijk}\nu_j\rho_k(J+1)\Lambda(J,\underline{x}'), \tag{C.1.62}$$

$$L5(J,\underline{x}') = a(J)\Lambda(J,\underline{x}'), \tag{C.1.63}$$

and

$$L6_i(I,J,\underline{x}') = \varepsilon_{ijk}a_j(J)\rho_k(J+1)\{[\partial_m\phi(I,\underline{x})]a_m(J)A(J,\underline{x}') + [\phi(I,\underline{x}') + [\partial_m\phi(I,\underline{x})]\rho_m(J+1)]T(J,\underline{x}')\}, \tag{C.1.64}$$

where $\Lambda(J,\underline{x}')$ is to be replaced by $\Lambda S(J,\underline{x}')$ if either $a_i(J)\rho_i(J+1) = -a(J)\rho(J+1)$ or $a_i(J)\rho_i(J+2) = -a(J)\rho(J+2)$, $T(J,\underline{x}')$ by $TS1(J,\underline{x}')$ and $A(J,\underline{x}')$ by $AS1(J,\underline{x}')$ if $a_i(J)\rho_i(J+1) = a(J)\rho(J+1)$, and, finally, $T(J,\underline{x}')$ by $TS2(J,\underline{x}')$ and $A(J,\underline{x}')$ by $AS2(J,\underline{x}')$ if $a_i(J)\rho_i(J+1) = -a(J)\rho(J+1)$. With this, the analytic evaluation of the line integrals has been completed.

C.1.2. EVALUATION OF THE SOLID ANGLE SUBTENDED BY A PLANAR TRIANGLE

In the present subsection we determine from geometrical considerations as well as with the aid of an analytic method different from the one employed in Subsection C.1.1, the value of the surface integral Ω defined by (C.1.23).

As we have seen in Subsection C.1.1, the surface integral Ω occurs as a secondary result in the analytic evaluation of the integrals IG^q, $I\Gamma^q$, $I\Gamma_i^f$ and IG_i^f, and cannot be evaluated with a straightforward utilization of Stokes' theorem. Since, however, $\Omega(\underline{x}')$ represents the solid angle at which the triangle S_T is observed from a point of observation with position vector $\underline{x}'$, its value can be determined with the aid of the

theory of spherical geometry. To this end, it is recalled that the (numerical) value of the solid angle $\Omega(\underline{x}')$ subtended by a planar triangle S_T at a point $\underline{x}'$ equals the area of the spherical triangle that results upon projecting S_T on a sphere with unit radius and center at $\underline{x}'$ (see, e.g., Spiegel, 1974, p. 124). Now, expressions for the area of a spherical triangle can be found in (old) textbooks on spherical trigonometry. In our analysis we have used the following one (see, Todhunter and Leathem, 1901, p. 103):

$$\Omega(\underline{x}') = 2\text{sign}[\nu_i \rho_i(1)] \arccos \left[\frac{1 + \sum_{J=1}^{3} \cos(\alpha(J))}{4\prod_{J=1}^{3} \cos((1/2)\alpha(J))} \right], \qquad (C.1.65)$$

in which $\cos(\alpha(J))$ is defined by

$$\cos(\alpha(J)) = \frac{\rho_i(J+1)\rho_i(J+2)}{\rho(J+1)\rho(J+2)} \qquad \text{with } J \in \{1,2,3\}, \qquad (C.1.66)$$

and where ν_i is the (constant) unit vector along the normal to S_T and $\rho_i(J+1)$ and $\rho(J+1)$ the vectorial and scalar distances from $\underline{x}'$ to the $(J+1)$-th vertex of S_T, respectively (cf. (C.1.34) and (C.1.36)). For a geometrical interpretation of $\alpha(J)$ we refer to Todhunter and Leathem (1901). Another, slightly more compact, expression for $\Omega(\underline{x}')$ resulting from the one given in (C.1.65) is presented by Van Oosterom and Strackee (1983).

As noted in the introduction to this subsection, an expression for $\Omega(\underline{x}')$ in terms of elementary functions can also be obtained in a purely analytic manner. To this end, we first decompose in the integrand of (C.1.23) the vectorial distance between the point of observation $\underline{x}'$ and the point of integration $\underline{x}$ in S_T into a part that is normal to S_T and a part that is parallel to it, i.e.,

$$x_i - x_i' = \zeta \nu_i + y_i \qquad \text{with } \underline{x} \in S_T, \qquad (C.1.67)$$

where ζ is given by

$$\zeta = \nu_i(x_i - x_i') \qquad \text{with } \underline{x} \in S_T, \tag{C.1.68}$$

and has a constant value for all $\underline{x} \in S_T$. Since $\underline{y}$ is a vector in the plane of S_T we can represent this vector with respect to some local, two-dimensional orthogonal Cartesian reference frame in this plane. Let y_α with $\alpha=1,2$ denote the Cartesian coordinates in this reference frame, where for repeated Greek subscripts the summation convention applies to the range $\alpha=1, 2$, and let partial differentiation with respect to y_α be denoted by ∂_α. Then, upon employing (C.1.67) in (C.1.23), taking into account that $\underline{\nu}$ and $\underline{y}$ are mutually perpendicular, and adopting the above notation in the result, we have

$$\Omega(\zeta) = \int_{\underline{y} \in S_T} \zeta(\zeta^2 + y_\alpha y_\alpha)^{-3/2} dA. \tag{C.1.69}$$

When $\zeta = 0$ and $\underline{y} \notin S_T$, $\Omega = 0$; when $\zeta \to 0$ and $\zeta \to 0$, and $\underline{y} \in S_T$, geometrical considerations learn that $\Omega \to 2\pi$ and $\Omega \to -2\pi$, respectively. Henceforth, we assume ζ to be unequal to zero, i.e., $\underline{x}'$ is not lying in the plane of S_T. As a next step in our analysis, we differentiate (C.1.69) on both sides with respect to ζ and apply in the resulting right-hand side the relation

$$(\zeta^2 + y_\alpha y_\alpha)^{-3/2} - 3\zeta^2(\zeta^2 + y_\alpha y_\alpha)^{-5/2} = -\partial_\alpha[y_\alpha(\zeta^2 + y_\beta y_\beta)^{-3/2}]. \tag{C.1.70}$$

This leads to

$$\Omega'(\zeta) = -\int_{\underline{y} \in S_T} \partial_\alpha[y_\alpha(\zeta^2 + y_\beta y_\beta)^{-3/2}] dA, \tag{C.1.71}$$

where $\Omega'(\zeta)$ denotes the derivative of $\Omega(\zeta)$ with respect to ζ. Now, with the aid of the two-dimensional form of Gauss' theorem, the surface

integral over S_T in (C.1.71) can be replaced by a contour integral along its boundary curve C_T. In this, taking into account that C_T is the union of three straight line segments $\{C_T(1),C_T(2),C_T(3)\}$, where the outwardly directed unit vector along the normal to $C_T(J)$, with $J\in\{1,2,3\}$, in the plane of S_T is given by $[a(J)]^{-1}\underline{L}(J)$ (cf. (5.1.10)), and rewriting the result with respect to the original reference frame, we end up with (cf. (C.1.71))

$$\Omega'(\zeta) = -\sum_{J=1}^{3} [a(J)]^{-1}L_i(J)\int_{\underline{y}\in C_T(J)} y_i(\zeta^2 + y_j y_j)^{-3/2}ds. \qquad (C.1.72)$$

To solve $\Omega(\zeta)$, and hence $\Omega(\underline{x}')$, from (C.1.72) it is advantageous to first integrate both sides of it with respect to ζ. In this, the appropriate end point of the interval of integration is obtained upon taking into account that $\Omega(\zeta)$ tends to zero as $\zeta \to \infty$ (cf. (C.1.69). We then have

$$\begin{aligned}\Omega(\zeta) &= \sum_{J=1}^{3} [a(J)]^{-1}L_i(J)\int_{\underline{y}\in C_T(J)} y_i\Big[\int_{\bar{\zeta}=\zeta}^{\infty} (\bar{\zeta}^2 + y_k y_k)^{-3/2}d\bar{\zeta}\Big]ds \\ &= \sum_{J=1}^{3} [a(J)]^{-1}L_i(J)\int_{\underline{y}\in C_T(J)} y_i(y_j y_j)^{-1}[1 - \zeta(\zeta^2 + y_k y_k)^{-1/2}]ds \\ &= \sum_{J=1}^{3} [L7(J,\zeta) - L8(J,\zeta)], \qquad (C.1.73)\end{aligned}$$

where $L7(J,\zeta)$ and $L8(J,\zeta)$ are defined by

$$L7(J,\zeta) = [a(J)]^{-1}L_i(J)\int_{\underline{y}\in C_T(J)} y_i(y_j y_j)^{-1}ds \qquad (C.1.74)$$

and

$$L8(J,\zeta) = \zeta[a(J)]^{-1}L_i(J)\int_{\underline{y}\in C_T(J)} y_i(y_j y_j)^{-1}(\zeta^2 + y_k y_k)^{-1/2}ds. \qquad (C.1.75)$$

To express $L7(J,\zeta)$ and $L8(J,\zeta)$ in terms of elementary analytic functions, we first apply (C.1.37), together with (C.1.67) and (C.1.38), to (C.1.74) and (C.1.75), and take into account that $L_i(J)$ and ν_i, and $L_i(J)$ and $a_i(J)$ are mutually perpendicular (see Fig. 5.1). We then have (cf. (C.1.74))

$$L7(J,\zeta) = L_i(J)\rho_i(J+1)\int_{\lambda=0}^{1} [D1(\lambda,\zeta)]^{-2}d\lambda \qquad (C.1.76)$$

and (cf. (C.1.75))

$$L8(J,\zeta) = \zeta L_i(J)\rho_i(J+1)\int_{\lambda=0}^{1} [D(\lambda)]^{-1}[D1(\lambda,\zeta)]^{-2}d\lambda, \qquad (C.1.77)$$

where $D1(\lambda,\zeta)$ is defined by

$$D1(\lambda,\zeta) = [-\zeta^2 + \rho_i(J+1)\rho_i(J+1) + 2\lambda a_i(J)\rho_i(J+1) + \lambda^2 a_i(J)a_i(J)]^{1/2}, \qquad (C.1.78)$$

and $D(\lambda)$ by (C.1.44). The integral on the right-hand side of (C.1.76) is elementary (see, e.g., Gradshteyn and Ryzhik, 1980, p. 68); it is given by

$$\int_{\lambda=0}^{1} [D1(\lambda,\zeta)]^{-2}d\lambda = |L_i(J)\rho_i(J+1)|^{-1}\arctan(\theta 1(J)), \qquad (C.1.79)$$

where we have used the addition rule for two arctan-functions and $\theta 1(J)$ is defined by

$$\theta 1(J) = \frac{|L_i(J)\rho_i(J+1)|a_j(J)[\rho_j(J+2) - \rho_j(J+1)]}{|L_i(J)\rho_i(J+1)|^2 + a_i(J)\rho_i(J+1)a_j(J)\rho_j(J+2)}. \qquad C.1.80)$$

To evaluate the remaining integral on the right-hand side of (C.1.77), we first reduce it to a more convenient form by applying successively the

following two algebraic substitutions (see, e.g., Gradstheyn and Ryzhik, 1980, pp. 80-81):

$$\lambda = t - a_i(J)\rho_i(J+1)/[a_j(J)a_j(J)], \tag{C.1.81}$$

and

$$t\left[t^2 + \frac{\rho_i(J+1)\rho_i(J+1)a_j(J)a_j(J) - [a_i(J)\rho_i(J+1]^2}{a_k(J)a_k(J)a_l(J)a_l(J)}\right]^{-1/2} = w. \tag{C.1.82}$$

Then, after a tedious but straightforward analysis we end up with

$$\int_{\lambda=0}^{1} [D(\lambda)]^{-1}[D1(\lambda,\zeta)]^{-2}d\lambda = \{|\zeta||L_i(J)\rho_i(J+1)|\}^{-1}\arctan\{\theta 2(J)\}, \tag{C.1.83}$$

where we used the addition rule for two arctan-functions and $\theta 2(J)$ is defined by

$$\theta 2(J) = \frac{\zeta|L_i(J)\rho_i(J+1)|[a_j(J)\rho_j(J+2)\rho(J+1) - a_j(J)\rho_j(J+1)\rho(J+2)]}{\zeta^2 a_i(J)\rho_i(J+1)a_j(J)\rho_j(J+2) + \rho(J+1)\rho(J+2)|L_i(J)\rho_i(J+1)|^2}. \tag{C.1.84}$$

Using (C.1.79) in (C.1.76) and (C.1.83) in (C.1.77), it readily follows that $\Omega(\zeta)$ is given by

$$\Omega(\zeta) = \sum_{J=1}^{3} \text{sign}\{L_i(J)\rho_i(J+1)\}\arctan\{\theta 1(J)\}$$

$$- \text{sign}(\zeta)\sum_{J=1}^{3} \text{sign}\{L_i(J)\rho_i(J+1)\}\arctan\{\theta 2(J)\}. \tag{C.1.85}$$

Equation (C.1.85) constitutes, upon taking into account (C.1.68), the analytic expression for $\Omega(\underline{x}')$.

Haitjema (1987) also presented, by a different method, a completely analytic manner to arrive at an expression for the solid angle subtended by a planar disk.

Obviously, the analytic method discussed in the present subsection is not limited in applying it to the evaluation of $\Omega(\underline{x}')$; in fact, it can be directly employed for the evaluation of (C.1.1) - (C.1.4) as well. This procedure has been followed by Van der Weiden and De Hoop (1988).

In the numerical experiments discussed in Chapter 6 both the geometrical expression for $\Omega(\underline{x}')$ and the one resulting from the purely analytic evaluation have been employed. Naturally, no differences in the numerical values of $\Omega(\underline{x}')$ resulting from either (C.1.65) or (C.1.85) occurred.

C.2. ANALYTIC EVALUATION OF THE SURFACE INTEGRALS (ANISOTROPIC CASE)

In present section we derive the analytic expressions for the integrals (C.1) - (C.4) in case they apply to anisotropic media

With the aid of (4.5.19), (4.5.20), (4.5.26) and (4.5.27) it follows that for an anisotropic medium (C.1) - (C.4) are given by

$$IG^q(I,\underline{x}') = (4\pi)^{-1}\Delta^{1/2} \int_{\underline{x}\in S_T} \phi(I,\underline{x})[D(\underline{x},\underline{x}')]^{-1} dA, \tag{C.2.1}$$

$$I\Gamma^q(I,\underline{x}') = (4\pi)^{-1}\Delta^{1/2} \int_{\underline{x}\in S_T} \phi(I,\underline{x})\nu_i K_{ij}\partial_j[D(\underline{x},\underline{x}')]^{-1} dA, \tag{C.2.2}$$

$$I\Gamma_i^f(I,\underline{x}') = (4\pi)^{-1}\Delta^{1/2} \int_{\underline{x}\in S_T} \phi(I,\underline{x})K_{ji}\partial_j[D(\underline{x},\underline{x}')]^{-1} dA, \tag{C.2.3}$$

$$IG_i^f(I,\underline{x}') = (4\pi R)^{-1}\Delta^{1/2} \int_{\underline{x}\in S_T} \phi(I,\underline{x})\nu_j K_{jp}K_{qi}\partial_p\partial_q[D(\underline{x},\underline{x}')]^{-1} dA, \tag{C.2.4}$$

where Δ and $D(\underline{x},\underline{x}')$ are defined as (cf. (4.5.9) and (4.5.16))

$$\Delta = \det(R_{ij}), \tag{C.2.5}$$

$$D(\underline{x},\underline{x}') = [R_{ij}(x_i - x_i')(x_j - x_j')]^{1/2}, \tag{C.2.6}$$

and K_{ij} is the symmetric and positive definite inverse of the constant resistivity R_{ij} $(=R_{ji})$ of the medium under consideration.

To evaluate (C.2.1) - (C.2.4) analytically, we first subject the integrals to a coordinate transformation similar to the one used in

Section 4.5. Then, in the new coordinate system, the integrals will acquire an "isotropic" form and we can employ the techniques of Section C.1. After the relevant expressions in the new coordinate system have been obtained, they are transformed back to the original coordinate system. The details of the transformation procedure applied to (C.2.1) - (C.2.4) are discussed in Subsection C.2.1, while in Subsection C.2.2 we discuss the evaluation of those line integrals that have not already been treated in Section C.1.

C.2.1. TRANSFORMATION OF THE "ANISOTROPIC" SURFACE INTEGRALS TO AN "ISOTROPIC" FORM

In this subsection the surface integrals (C.2.1) - (C.2.4) are subjected to a coordinate transformation such that they will acquire their "isotropic" form. In the new coordinate system we evaluate the transformed surface integrals with aid of the techniques outlined in Subsection C.1.1. In this procedure some not yet encountered line integrals will show up. Their analytic evaluation is discussed in detail in Subsection C.2.2.

In (C.2.1) we first apply (C.1.24). This yields

$$\int_{\underline{x}\in S_T} \phi(I,\underline{x})[D(\underline{x},\underline{x}')]^{-1} dA = \phi(I,\underline{x}') \int_{\underline{x}\in S_T} [D(\underline{x},\underline{x}')]^{-1} dA + [\partial_i \phi(I,\underline{x})] \int_{\underline{x}\in S_T} (x_i - x_i')[D(\underline{x},\underline{x}')]^{-1} dA. \quad (C.2.7)$$

Now, in the integrals on the right-hand side of (C.2.7) we employ the following orthogonal transformation

$$x_p = \beta_{pq} y_q, \quad (C.2.8)$$

where the columns of the matrix (β_{pq}) are the normalized right eigenvectors of (R_{ij}) corresponding to the q-th eigenvalue $s^{(q)}$ of (R_{ij}) (cf. (4.5.3)). This orthogonal transformation is followed by the introduction of the the variables z_q through

$$z_q = [s^{(q)}]^{1/2} y_q, \tag{C.2.9}$$

and, hence, we have

$$x_p = \beta_{pq} [s^{(q)}]^{-1/2} z_q, \tag{C.2.10}$$

and inversely

$$z_p = [s^{(q)}]^{1/2} \beta_{pq}^{-1} x_q. \tag{C.2.11}$$

Taking into account that

$$\beta_{ip} R_{ij} \beta_{jq} = s^{(p)} \delta_{pq}, \tag{C.2.12}$$

it is clear that $D(\underline{x},\underline{x}')$ transforms into $D(\underline{z},\underline{z}')$ given by (cf. (C.2.6))

$$D(\underline{z},\underline{z}') = |\underline{z} - \underline{z}'|, \tag{C.2.13}$$

while the integrals on the right-hand side of (C.2.7) transform into

$$\int_{\underline{x} \in S_T} [D(\underline{x},\underline{x}')]^{-1} dA = (A/A^*) \int_{\underline{z} \in S_T^*} |\underline{z} - \underline{z}'|^{-1} dA \tag{C.2.14}$$

and

$$\int_{\underline{x} \in S_T} (x_i - x_i') [D(\underline{x},\underline{x}')]^{-1} dA$$

$$= (A/A^*)\beta_{ip}(s^{(p)})^{-1/2}\int_{\underline{z}\in S_T^*} \partial_{z_p}|\underline{z} - \underline{z}'|\,dA, \qquad (C.2.15)$$

where S_T^*, with scalar area A^*, denotes the transformed planar triangle S_T in the $\{z_1,z_2,z_3\}$ coordinate system, ∂_{z_p} denotes differentiation with respect to z_p, and where we have taken into account that the elementary areas on the two sides of both (C.2.14) and (C.2.15) are proportional to the total areas of the triangles in the two different coordinate systems. The position vectors of the vertices of S_T^* in the $\{z_1,z_2,z_3\}$ coordinate system follow from (C.2.11) , while the scalar area A^* of S_T^*, expressed in terms of geometrical quantities in the original $\{x_1,x_2,x_3\}$ coordinate system, is given by (cf. (5.1.9), (5.1.5), (C.2.11), (C.1.8) and (5.1.3))

$$A^* = [A_i^*A_i^*]^{1/2} = \{(1/2)\varepsilon_{ijk}[z_j(I) - z_j(K)][z_k(J) - z_k(I)]$$

$$\times (1/2)\varepsilon_{imn}[z_m(I) - z_m(K)][z_n(J) - z_n(I)]\}^{1/2}$$

$$= (1/2)\{[x_i(I) - x_i(K)]R_{ip}[x_p(I) - x_p(K)]$$

$$\times [x_j(J) - x_j(I)]R_{jq}[x_q(J) - x_q(I)]$$

$$- ([x_i(I) - x_i(K)]R_{ip}[x_p(J) - x_p(I)])^2\}^{1/2}$$

$$= (1/2)\{a_i(J)R_{ip}a_p(J)a_j(K)R_{jq}a_q(K)$$

$$- [a_i(J)R_{ip}a_p(K)]^2\}^{1/2} \text{ with } \{I,J,K\}=\text{cycl}\{1,2,3\}. \qquad (C.2.16)$$

Now, to evaluate the surface integrals on the right-hand sides of (C.2.14) and (C.2.15), we rewrite their integrands to such forms that Stokes' theorem in the $\{z_1,z_2,z_3\}$ coordinate system can be used. To this end, we employ in (C.2.14) a relation similar to the one given in (C.1.11) in which $\phi(I,\underline{x})$ is replaced by unity and the differentiations

are carried out with respect to z_i. Then after utilization of Stokes' theorem, it is easily verified that (C.2.14) leads to

$$\int_{\underline{x}\in S_T} [D(\underline{x},\underline{x}')]^{-1} dA = (A/A^*)\{\int_{\underline{z}\in C_T^*} \tau_l^* \varepsilon_{lpi} \nu_p^* \partial_{z_i} |\underline{z} - \underline{z}'| ds$$

$$+ \nu_i^*(z_i - z_i') \int_{\underline{z}\in S_T^*} \nu_j^* \partial_{z_j} |\underline{z} - \underline{z}'|^{-1} dA\}, \quad (C.2.17)$$

where τ_l^* is the unit tangent vector along the boundary curve C_T^* of S_T^* in the direction of circulation that forms a right-handed system with ν_i^*, the constant unit vector along the normal to S_T^* given by (cf. (5.1.8) and (C.2.16))

$$\nu_i^* = A_i^*/A^*. \quad (C.2.18)$$

In (C.2.17), similar to the isotropic case, we have taken into account that $\nu_i^*(z_i - z_i')$ has a constant value for all $\underline{z}\in S_T^*$. The surface integral on the right-hand side of (C.2.17) equals minus the solid angle $\Omega^*(\underline{z}')$ at which the triangle S_T^* is observed from the point of observation $\underline{z}'$, i.e. (cf. (C.1.23)),

$$\Omega^*(\underline{z}') = -\int_{\underline{z}\in S_T^*} \nu_j^* \partial_{z_j} |\underline{z} - \underline{z}'|^{-1} dA. \quad (C.2.19)$$

For its value we can use the expressions presented in Subsection C.1.3 (cf. (C.1.65) and (C.1.85)). Obviously, the geometrical quantities occurring in these expressions now refer to the $\{z_1,z_2,z_3\}$ coordinate system. With the aid of the inverse transformation (C.2.11) they can be expressed again in terms of the geometrical quantities pertaining to the original $\{x_1,x_2,x_3\}$ coordinate system (cf. (C.2.16)). In the numerical experiments discussed in Chapter 6 we have followed this procedure to handle the "anisotropic solid angle".

Returning to (C.2.15), we successively employ in its right-hand side (C.1.7), where the differentiations are now carried out with respect to z_i, use Stokes' theorem, and are led to

$$\int_{\underline{x}\in S_T} (x_i - x_i')[D(\underline{x},\underline{x}')]^{-1} dA$$

$$= (A/A^*)\beta_{ip}(s^{(p)})^{-1/2}\{\int_{\underline{z}\in C_T^*} \tau_l^* \epsilon_{lmp} \nu_m^* |\underline{z} - \underline{z}'| ds,$$

$$+ \nu_p^* \nu_q^* (z_q - z_q') \int_{\underline{z}\in S_T^*} |\underline{z} - \underline{z}'|^{-1} dA\}. \qquad (C.2.20)$$

Using (C.2.14) and (C.2.17) in the surface integral on the right-hand side of (C.2.20), and using the resulting expression for (C.2.20), together with (C.2.17) and (C.2.19), in (C.2.7), and substituting this in (C.2.1), it follows that $IG^q(I,\underline{x}')$ can be written as

$$IG^q(I,\underline{x}') = (4\pi)^{-1}\Delta^{1/2}(A/A^*)\{\phi(I,\underline{x}')[\int_{\underline{z}\in C_T^*} \tau_l^* \epsilon_{lpi} \nu_p^* \partial_{z_i} |\underline{z} - \underline{z}'| ds$$

$$- \nu_i^*(z_i - z_i')\Omega^*(\underline{z}')] + [\partial_i \phi(I,\underline{x})]\beta_{ip}(s^{(p)})^{-1/2}$$

$$\times [\int_{\underline{z}\in C_T^*} \tau_l^* \epsilon_{lmp} \nu_m^* |\underline{z} - \underline{z}'| ds$$

$$+ \nu_p^* \nu_q^* (z_q - z_q')\{\int_{\underline{z}\in C_T^*} \tau_l^* \epsilon_{lmn} \nu_m^* \partial_{z_n} |\underline{z} - \underline{z}'| ds$$

$$- \nu_m^*(z_m - z_m')\Omega^*(\underline{z}')\}]\}. \qquad (C.2.21)$$

Taking into account that C_T^* is the union of the edges $\{C_T^*(1), C_T^*(2), C_T^*(3)\}$ where each edge is a straight line segment, it is apparent that along each $C_T^*(J)$ with $J\in\{1,2,3\}$, the corresponding unit tangent vector $\tau_l^*(J)$

has a constant value. Using these properties of C_T^* in (C.2.21), it readily follows that (C.2.21) can be expressed as

$$IG^q(I,\underline{x}') = (4\pi)^{-1}\Delta^{1/2}(A/A^*)\{[\phi(I,\underline{x}') +$$

$$+ [\partial_i\phi(I,\underline{x})]\beta_{ip}(s^{(p)})^{-1/2}\nu_p^*\nu_q^*(z_q - z_q')]\sum_{J=1}^{3} AL2(J,\underline{z}')$$

$$+ [\partial_i\phi(I,\underline{x})]\beta_{ip}(s^{(p)})^{-1/2}[\sum_{J=1}^{3}\epsilon_{plm}\tau_l^*(J)\nu_m^* AL1(J,\underline{z}')$$

$$- \nu_p^*[\nu_q^*(z_q - z_q')]^2\Omega^*(\underline{z}')] - \phi(I,\underline{x}')\nu_i^*(z_i - z_i')\Omega^*(\underline{z}')\}, \tag{C.2.22}$$

in which AL1(J,$\underline{z}'$) and AL2(J,$\underline{z}'$) are defined by

$$AL1(J,\underline{z}') = \int_{\underline{z}\in C_T^*(J)} |\underline{z} - \underline{z}'|\,ds \tag{C.2.23}$$

and

$$AL2(J,\underline{z}') = \int_{\underline{z}\in C_T^*(J)} \tau_l^*\epsilon_{lpi}\nu_p^*(z_i - z_i')|\underline{z} - \underline{z}'|^{-1}ds. \tag{C.2.24}$$

Upon comparing the structure of the line integral AL1(J,$\underline{z}'$) with the one of L1(J,$\underline{x}'$) in (C.1.14), it is apparent that the results of the analytic evaluation of L1(J,$\underline{x}'$), as discussed in Subsection C.1.2, can straightforwardly be used in the evaluation of AL1(J,$\underline{z}'$). In this, we only have to transform the results obtained in the $\{z_1,z_2,z_3\}$ coordinate system back to the original $\{x_1,x_2,x_3\}$ coordinate system. Similarly, in the analytic evaluation of AL2(J,$\underline{z}'$) we use the results obtained in the evaluation of L2(I,J,$\underline{x}'$) (cf. (C.1.15)) in which we replace $\phi(I,\underline{x}')$ by unity. Again, the inverse transformation is applied to the results obtained in the transformed coordinate system. To complete the evaluation of $IG^q(I,\underline{x}')$, we also apply the inverse transformation to the quantities ν_p^*, $\tau_l^*(J)$, $(z_q - z_q')$ and their combinations. Since the evaluation of AL1

and AL2, and the application of the inverse transformation (C.2.11) contain no new ingredients and are straightforward procedures, they are not worked out in detail.

Similar to the isotropic case, inspection of (C.2.2) and (C.2.3) reveals that (note that $K_{ij}=K_{ji}$)

$$I\Gamma^q(I,\underline{x}') = \nu_i I\Gamma^f_i(I,\underline{x}'). \tag{C.2.25}$$

Hence, we first discuss the evaluation of (C.2.3) and apply (C.2.25) in the resulting expression to arrive at the expression for $I\Gamma^q(I,\underline{x}')$. To this end, we first use (C.1.24) in the integral on the right-hand side of (C.2.3) and observe that

$$\int_{\underline{x}\in S_T} \phi(I,\underline{x})K_{ji}\partial_j[D(\underline{x},\underline{x}')]^{-1}dA = -\phi(I,\underline{x}')\int_{\underline{x}\in S_T}(x_i - x_i')[D(\underline{x},\underline{x}')]^{-3}dA$$

$$- [\partial_j\phi(I,\underline{x})]\int_{\underline{x}\in S_T}(x_j - x_j')(x_i - x_i')[D(\underline{x},\underline{x}')]^{-3}dA. \tag{C.2.26}$$

Now, upon applying the transformation (C.2.10) to the surface integrals on the right-hand side of (C.2.24) and taking (C.2.12) into account, it is easily verified that we have

$$-\int_{\underline{x}\in S_T}(x_i - x_i')[D(\underline{x},\underline{x}')]^{-3}dA$$

$$= (A/A^*)\beta_{ip}(s^{(p)})^{-1/2}\int_{\underline{z}\in S_T^*}\partial_{z_p}|\underline{z} - \underline{z}'|^{-1}dA \tag{C.2.27}$$

and

$$-\int_{\underline{x}\in S_T}(x_j - x_j')(x_i - x_i')[D(\underline{x},\underline{x}')]^{-3}dA$$

$$= (A/A^*)\beta_{jp}(s^{(p)})^{-1/2}\beta_{iq}(s^{(q)})^{-1/2}\{\int_{\underline{z}\in S_T^*} \partial_{z_q}[(z_p - z'_p)|\underline{z} - \underline{z}'|^{-1}]dA$$

$$- \delta_{pq}\int_{\underline{z}\in S_T^*} |\underline{z} - \underline{z}'|^{-1}dA\}. \qquad (C.2.28)$$

Upon using in the right-hand side of (C.2.27) a relation similar to the one in (C.1.19) in which we replace $\phi(I,\underline{x}')$ by unity and carrying out the differentiations with respect to z_i, the surface integral over S_T^* can, with the further utilization of Stokes' theorem, be replaced by a contour integral along C_T^* and an additional surface integral that can be identified with $\Omega^*(\underline{z}')$. We have (cf. (C.2.25), C.1.19) and (C.2.19))

$$- \int_{\underline{x}\in S_T} (x_i - x'_i)[D(\underline{x},\underline{x}')]^{-3}dA$$

$$= (A/A^*)\beta_{ip}(s^{(p)})^{-1/2}\{\int_{\underline{z}\in C_T^*} \tau_l^*\varepsilon_{lmp}\nu_m^*|\underline{z} - \underline{z}'|^{-1}ds - \nu_p^*\Omega^*(\underline{z}')\}. \qquad (C.2.29)$$

To evaluate the first surface integral on the right-hand side of (C.2.28) we first rewrite its integrand as

$$\partial_{z_q}[(z_p - z'_p)|\underline{z} - \underline{z}'|^{-1}] = \varepsilon_{lmk}\nu_m^*\partial_{z_k}\varepsilon_{lnq}\nu_n^*(z_p - z'_p)|\underline{z} - \underline{z}'|^{-1}$$

$$+ \nu_p^*\nu_q^*|\underline{z} - \underline{z}'|^{-1}$$

$$+ \nu_q^*\nu_j^*(z_j - z'_j)[\varepsilon_{lmk}\nu_m^*\partial_{z_k}\varepsilon_{lnp}\nu_n^*|\underline{z} - \underline{z}'|^{-1}$$

$$+ \nu_p^*\nu_l^*\partial_{z_l}|\underline{z} - \underline{z}'|^{-1}], \qquad (C.2.30)$$

which can be verified with the aid of the identity (C.1.8) and by carrying out the relevant differentiations. Then, with the aid of Stokes'

theorem, the fact that $\nu_j^*(z_j - z_j')$ has a constant value for all $\underline{z} \in S_T^*$, and the further aid of (C.2.14), (C.2.17) and (C.2.19), the relevant integral yields

$$\int_{\underline{z}\in S_T^*} \partial_{z_q}[(z_p - z_p')|\underline{z} - \underline{z}'|^{-1}]dA$$

$$= \int_{\underline{z}\in C_T^*} \tau_l^* \varepsilon_{lnq} \nu_n^*(z_p - z_p')|\underline{z} - \underline{z}'|^{-1} ds + \nu_p^* \nu_q^*[- \nu_m^*(z_m - z_m')\Omega^*(\underline{z}')$$

$$+ \int_{\underline{z}\in C_T^*} \tau_l^* \varepsilon_{lmn} \nu_m^*(z_n - z_n')|\underline{z} - \underline{z}'|^{-1} ds] + \nu_q^* \nu_j^*(z_j - z_j')[- \nu_p^* \Omega^*(\underline{z}')$$

$$+ \int_{\underline{z}\in C_T^*} \tau_l^* \varepsilon_{lnp} \nu_n^* |\underline{z} - \underline{z}'|^{-1} ds]. \qquad (C.2.31)$$

With the aid of (C.2.14), (C.2.17) and (C.2.19) it further follows that the remaining surface integral on the right-hand side of (C.2.28) can be written as

$$\int_{\underline{z}\in S_T^*} |\underline{z} - \underline{z}'|^{-1} dA = \int_{\underline{z}\in C_T^*} \tau_l^* \varepsilon_{lmn} \nu_m^*(z_n - z_n')|\underline{z} - \underline{z}'|^{-1} ds$$

$$- \nu_m^*(z_m - z_m')\Omega^*(\underline{z}'). \qquad (C.2.32)$$

Now, taking into account that C_T^* is the union of the edges $\{C_T^*(1), C_T^*(2), C_T^*(3)\}$, where the unit tangent along each edge has a constant value, and collecting the results (C.2.27) - (C.2.32) in (C.2.26), it follows that $I\Gamma_i^f(I,\underline{x}')$ can be written as (cf. (C.2.24))

$$I\Gamma_i^f(I,\underline{x}') = (4\pi)^{-1} \Delta^{1/2} (A/A^*)[\phi(I,\underline{x}')\beta_{ip}(s^{(p)})^{-1/2}$$

$$\times [\textstyle\sum_{J=1}^{3} \varepsilon_{plm} \tau_l^*(J) \nu_m^* AL3(J,\underline{z}') - \nu_p^* \Omega^*(\underline{z}')]$$

$$+ [\partial_j \phi(I,\underline{x})]\beta_{jp}(s^{(p)})^{-1/2} \beta_{iq}(s^{(q)})^{-1/2}[\nu_p^* \nu_q^* \textstyle\sum_{J=1}^{3} AL2(J,\underline{z}')$$

$$- \delta_{pq}\sum_{J=1}^{3} AL2(J,\underline{z}') + \nu_q^*\nu_m^*(z_m - z_m')\sum_{J=1}^{3}\varepsilon_{pln}\tau_l^*(J)\nu_n^* AL3(J,\underline{z}')$$

$$+ \sum_{J=1}^{3}\varepsilon_{qln}\tau_l^*(J)\nu_n^* AL4_p(J,\underline{z}') - 2\nu_p^*\nu_q^*\nu_m^*(z_m - z_m')\Omega^*(\underline{z}')$$

$$+ \delta_{pq}\nu_m^*(z_m - z_m')\Omega^*(\underline{z}')]\}, \qquad (C.2.33)$$

in which $AL3(J,\underline{z}')$ and $AL4_p(J,\underline{z}')$ are defined by

$$AL3(J,\underline{z}') = \int_{\underline{z}\in C_T^*(J)} |\underline{z} - \underline{z}'|^{-1} ds \qquad (C.2.34)$$

and

$$AL4_p(J,\underline{z}') = \int_{\underline{z}\in C_T^*(J)} (z_p - z_p')|\underline{z} - \underline{z}'|^{-1} ds. \qquad (C.2.35)$$

Comparison of the structure of $AL3(J,\underline{z}')$ with the one of $L5(J,\underline{x}')$ in (C.1.28) reveals that we can use the analytic expressions obtained for $L5(J,\underline{x}')$ where the relevant results now apply to the $\{z_1,z_2,z_3\}$ coordinate system and have to be transformed back to the original $\{x_1,x_2,x_3\}$ coordinate system with the aid of (C.2.11). Since this procedure contains no new aspects it is not worked out in detail. The structure of $AL4_p(J,\underline{z}')$, however, is different from the ones of the line integrals that occurred in the isotropic case, and, therefore, its evaluation is discussed in Subsection C.2.2. Finally, to arrive at the expression for $I\Gamma_i^f(I,\underline{x}')$ in (C.2.33) with respect to the original $\{x_1,x_2,x_3\}$ coordinate system, we also apply the inverse transformation (C.2.11) to the quantities ν_p^*, $\tau_l^*(J)$, (z_p-z_p'), and their combinations.

Now, to arrive at the analytic expression for $I\Gamma^q(I,\underline{x}')$ (cf. (C.2.25)), we simply multiply (C.2.33) on both sides by ν_i, i.e., the unit vector along the normal to the (non-transformed) triangle S_T.

Finally, we discuss the analytic evaluation of (C.2.4). To this end, we proceed along lines similar to the ones discussed in the evaluation of

(C.2.1) and (C.2.3), i.e., we successively apply to (C.2.4), (C.1.24), the transformation (C.2.10), and take (C.2.12) into account. We then have

$$
\begin{aligned}
&IG_i^f(I,\underline{x}') \\
&= (4\pi)^{-1}\Delta^{1/2}(A/A^*)\{\phi(I,\underline{x}')[\,-\nu_j K_{ji}\int_{\underline{z}\in S_T^*}|\underline{z}-\underline{z}'|^{-3}dA \\
&+ 3\nu_j\beta_{jq}(s^{(q)})^{-1/2}\beta_{ip}(s^{(p)})^{-1/2}\int_{\underline{z}\in S_T^*}(z_p-z_p')(z_q-z_q')|\underline{z}-\underline{z}'|^{-5}dA] \\
&- [\partial_m\phi(I,\underline{x})][\nu_j K_{ji}\beta_{mp}(s^{(p)})^{-1/2}\int_{\underline{z}\in S_T^*}(z_p-z_p')|\underline{z}-\underline{z}'|^{-3}dA \\
&- 3\nu_j(x_j-x_j')\beta_{mp}(s^{(p)})^{-1/2}\beta_{iq}(s^{(q)})^{-1/2} \\
&\times\int_{\underline{z}\in S_T^*}(z_p-z_p')(z_q-z_q')|\underline{z}-\underline{z}'|^{-5}dA]\}. \qquad (C.2.36)
\end{aligned}
$$

With the aid of (C.2.19) and using the fact that $\nu_i^*(z_i-z_i')$ has a constant value for all $\underline{z}\in S_T^*$, it is clear that the first surface integral on the right-hand side (C.2.36) can be written as

$$
\int_{\underline{z}\in S_T^*}|\underline{z}-\underline{z}'|^{-3}dA = [\nu_m^*(z_m-z_m')]^{-1}\Omega^*(\underline{z}'). \qquad (C.2.37)
$$

Further, from (C.2.27) and (C.2.29), it follows directly that for the third surface integral on the right-hand side of (C.2.34) we have

$$
\int_{\underline{z}\in S_T^*}(z_p-z_p')|\underline{z}-\underline{z}'|^{-3}dA = -\sum_{J=1}^{3}\varepsilon_{pln}\tau_l^*(J)\nu_n^*AL3(J,\underline{z}') + \nu_p^*\Omega^*(\underline{z}'), \qquad (C.2.38)
$$

where AL3(J,$\underline{z}'$) is defined in (C.2.34). Clearly, this leaves only the second and the last surface integral on the right-hand side of (C.2.34) to be evaluated. To this end we first observe the following relation

$$
\begin{aligned}
&3(z_p - z_p')(z_q - z_q')|\underline{z} - \underline{z}'|^{-5} \\
&= \varepsilon_{lmk}\nu_m^*\partial_{z_k}\varepsilon_{lnq}\nu_n^*\partial_{z_p}|\underline{z} - \underline{z}'|^{-1} + \nu_q^*\varepsilon_{lmk}\nu_m^*\partial_{z_k}\varepsilon_{lnp}\partial_{z_n}|\underline{z} - \underline{z}'|^{-1} \\
&\quad + \nu_p^*\nu_q^*\partial_{z_k}\partial_{z_k}|\underline{z} - \underline{z}'|^{-1} + \delta_{pq}|\underline{z} - \underline{z}'|^{-3}, \qquad \text{(C.2.39)}
\end{aligned}
$$

which can be easily verified with the aid of the identity (C.1.8) and upon carrying out the relevant differentiations. Now, upon integrating (C.2.39) on both sides over the triangle S_T^* and using Stokes' theorem in the first and second resulting surface integral on the right-hand side, we have

$$
\begin{aligned}
&3\int_{\underline{z}\in S_T^*}(z_p - z_p')(z_q - z_q')|\underline{z} - \underline{z}'|^{-5}dA \\
&= -\int_{\underline{z}\in C_T^*}\tau_l^*\varepsilon_{lnq}\nu_n^*(z_p - z_p')|\underline{z} - \underline{z}'|^{-3}ds \\
&\quad - \nu_q^*\int_{\underline{z}\in C_T^*}\tau_l^*\varepsilon_{lnp}(z_n - z_n')|\underline{z} - \underline{z}'|^{-3}ds \\
&\quad + \nu_p^*\nu_q^*\int_{\underline{z}\in S_T^*}\partial_{z_k}\partial_{z_k}|\underline{z} - \underline{z}'|^{-1}dA + \delta_{pq}\int_{\underline{z}\in S_T^*}|\underline{z} - \underline{z}'|^{-3}dA. \qquad \text{(C.2.40)}
\end{aligned}
$$

Now, taking into account that C_T^* is the union of the edges $\{C_T^*(1), C_T^*(2), C_T^*(3)\}$, and using the fact that $\underline{z}\neq\underline{z}'$, it is with the further aid of (C.2.37) easily verified that (C.2.40) can be written as

$$
3\int_{\underline{z}\in S_T^*}(z_p - z_p')(z_q - z_q')|\underline{z} - \underline{z}'|^{-5}dA
$$

$$= - \sum_{J=1}^{3} \varepsilon_{qln}\tau_l^*(J)\nu_n^* AL5_p(J,\underline{z}') - \nu_q^* \sum_{J=1}^{3} AL6_p(J,\underline{z}')$$

$$+ \delta_{pq}[\nu_n(z_n - z_n')]^{-1}\Omega^*(\underline{z}'), \qquad (C.2.41)$$

where $AL5_p(J,\underline{z}')$ and $AL6_p(J,\underline{z}')$ are defined by

$$AL5_p(J,\underline{z}') = \int_{\underline{z}\in C_T^*(J)} (z_p - z_p')|\underline{z} - \underline{z}'|^{-3}ds \qquad (C.2.42)$$

and

$$AL6_p(J,\underline{z}') = \int_{\underline{z}\in C_T^*(J)} \varepsilon_{pln}\tau_l^*(J)(z_n - z_n')|\underline{z} - \underline{z}'|^{-3}ds. \qquad (C.2.43)$$

respectively. Upon comparing the structure of $AL6_p(J,\underline{z}')$ with the one of $L6_p(I,J,\underline{x}')$ in (C.1.32), it is clear that if in (C.1.32) $\phi(I,\underline{x})$ is replaced by unity, their structures are the same. Hence, in the analytic evaluation of $AL6_p(J,\underline{z}')$ we can employ the results obtained for $L6_p(I,J,\underline{x}')$, where in the resulting expressions we use the inverse transformation (C.2.11) in order to obtain them in terms of geometrical quantities referring to the original $\{x_1,x_2,x_3\}$ coordinate system. Since the structure of $AL5_p(J,\underline{z}')$ differs from ones we have seen sofar, this integral is evaluated analytically in the next subsection. Finally, upon using (C.2.37), (C.2.38), (C.2.39) and (C.2.41) in (C.2.36), it follows that $IG_i^f(I,\underline{x}')$ can be expressed as

$$IG_i^f(I,\underline{x}') = (4\pi)^{-1}\Delta^{1/2}(A/A^*)\{\phi(I,\underline{x}')[- \nu_j K_{ji}[\nu_k^*(z_k - z_k')]^{-1}\Omega^*(\underline{z}')$$

$$- \nu_j\beta_{jq}(s^{(q)})^{-1/2}\beta_{ip}(s^{(p)})^{-1/2}(\sum_{J=1}^{3} \varepsilon_{qln}\tau_l^*(J)\nu_n^* AL5_p(J,\underline{z}')$$

$$+ \nu_q^* \sum_{J=1}^{3} AL6_p(J,\underline{z}') - \delta_{pq}[\nu_n^*(z_n - z_n')]^{-1}\Omega^*(\underline{z}'))]$$

$$+ [\partial_m\phi(I,\underline{x})][\nu_j K_{ji}\beta_{mp}(s^{(p)})^{-1/2}$$

$$\times \left(\sum_{J=1}^{3} \varepsilon_{pln}\tau_l^*(J)\nu_n^* AL3(J,\underline{z}') - \nu_p^*\Omega^*(\underline{z}')\right)$$

$$- \nu_j(x_j - x_j')\beta_{mp}\left(s^{(p)}\right)^{-1/2}\beta_{iq}\left(s^{(p)}\right)^{-1/2}$$

$$\times \left(\sum_{J=1}^{3}\varepsilon_{qln}\tau_l^*(J)\nu_n^* AL5_p(J,\underline{z}') + \nu_q^*\sum_{J=1}^{3} AL6_p(J,\underline{z}')\right.$$

$$\left. - \delta_{pq}[\nu_n^*(z_n - z_n')]^{-1}\Omega^*(\underline{z}')\right)\Big]\Big\}. \qquad (C.2.44)$$

To obtain the expression for $IG_i^f(I,\underline{x}')$ in terms of quantities referring to the original $\{x_1,x_2,x_3\}$ coordinate system we apply again (C.2.11) to the quantities $\tau_l^*(J)$, ν_n^*, $(z_i - z_i')$ and their combinations. With this and the further expressions for Ω^*, AL3, $AL5_p$ and $AL6_p$ in terms of elementary functions in the $\{x_1,x_2,x_3\}$ coordinate system, the evaluation of (C.1.4) has been completed.

C.2.2. EVALUATION OF THE LINE INTEGRALS

In the present subsection the line integrals $AL4_p(J,\underline{x}')$ and $AL5_p(I,J,\underline{x}')$, defined by (C.2.35) and (C.2.42), respectively, are evaluated analytically since their structures do not directly comply with the ones discussed in Subsection C.1.2. They are expressed in terms of elementary analytic functions pertaining to the original $\{x_1,x_2,x_3\}$ coordinate system.

In (C.2.35) and (C.2.42) we consider in the $\{z_1,z_2,z_3\}$ coordinate system the straight line segment (edge) $C_T^*(J)$ with $J\in\{1,2,3\}$. Similar to the isotropic case we introduce in this coordinate system the vectorial distance from the point of observation with position vector z_i' to the starting point of $C_T^*(J)$ with position vector $z_i(J+1)$ as (cf. (C.1.34))

$$\rho_i^*(J+1) = z_i(J+1) - z_i' \qquad \text{with } J\in\{1,2,3\}, \qquad (C.2.45)$$

and from the z_i' to the end point of $C_T^*(J)$ with position vector $z_i(J+2)$ as (cf. (C.1.35))

$$\rho_i^*(J+2) = z_i(J+2) - z_i' \qquad \text{with } J\in\{1,2,3\}. \tag{C.2.46}$$

In (C.2.45) and (C.2.46) the convention applies that $\rho_i^*(4)=\rho_i^*(1)$, $z_i(4)=z_i(1)$, $\rho_i^*(5)=\rho_i^*(2)$ and $z_i(5)=z_i(2)$. The corresponding length $\rho^*(J)$ of $\rho_i^*(J)$ is given by

$$\rho^*(J) = [\rho_i^*(J)\rho_i^*(J)]^{1/2} \qquad \text{with } J\in\{1,2,3\}. \tag{C.2.47}$$

Along $C_T^*(J)$ we have (cf. Figure C.1)

$$z_i - z_i' = \rho_i^*(J+1) + \lambda a_i^*(J) \qquad \text{with } 0 \leq \lambda \leq 1 \text{ and } J\in\{1,2,3\}, \tag{C.2.48}$$

and

$$ds(\underline{z}) = a^*(J)d\lambda \qquad \text{with } J\in\{1,2,3\}. \tag{C.2.49}$$

where $a_i^*(J)$ is the vectorial length of $C_T^*(J)$ and $a^*(J)$ its scalar length. With the aid of (C.2.45) - (C.2.49) the integrals $AL4_p(J,\underline{z}')$ and $AL5_p(J,\underline{z}')$ yield (cf. (C.2.35))

$$AL4_p(J,\underline{z}') = a^*(J)[\rho_p^*(J+1)\int_{\lambda=0}^{1}[D^*(\lambda)]^{-1}d\lambda + a_p^*(J)\int_{\lambda=0}^{1}\lambda[D^*(\lambda)]^{-1}d\lambda], \tag{C.2.50}$$

and (cf. (C.2.42))

$$AL5_p(J,\underline{z}') = a^*(J)[\rho_p^*(J+1)\int_{\lambda=0}^{1}[D^*(\lambda)]^{-3}d\lambda + a_p^*(J)\int_{\lambda=0}^{1}\lambda[D^*(\lambda)]^{-3}d\lambda], \tag{C.2.51}$$

where (cf. (C.1.44))

$$D^*(\lambda) = [\rho_i^*(J+1)\rho_i^*(J+1) + 2\lambda a_i^*(J)\rho_i^*(J+1) + \lambda^2 a_i^*(J)a_i^*(J)]^{1/2}. \quad (C.2.52)$$

The integrals on the right-hand sides of (C.2.50) and (C.2.51) are elementary and have the same structure as the ones in (C.1.45), (C.1.46), (C.1.48) and (C.1.49). For completeness, the expressions for (C.2.50) and (C.2.52) are given explicitly in terms of the quantities referring to the original coordinate system. Taking into account the results of Subsection C.1.2 and utilizing the inverse transformation (C.2.11), it can be verified that the integrals on the right-hand sides of (C.2.50) and (C.2.51) are expressible as

$$\int_{\lambda=0}^{1} [D^*(\lambda)]^{-1} d\lambda = \begin{cases} A\Lambda(J,\underline{x}'), \\ A\Lambda S(J,\underline{x}') \text{ if } a_i(J)R_{ij}\rho_j(J+1) = -Aa(J)A\rho(J+1) \\ \qquad \text{and } a_i(J)R_{ij}\rho_j(J+2) = -Aa(J)A\rho(J+2), \end{cases} \quad (C.2.53)$$

$$\int_{\lambda=0}^{1} \lambda[D^*(\lambda)]^{-1} d\lambda = [Aa(J)]^{-2}[A\rho(J+2) - A\rho(J+1) - a_i(J)R_{ij}\rho_j(J+1)\int_{\lambda=0}^{1} [D^*(\lambda)]^{-1} d\lambda], \quad (C.2.54)$$

$$\int_{\lambda=0}^{1} [D^*(\lambda)]^{-3} d\lambda = \begin{cases} AT(J,\underline{x}'), \\ ATS1(J,\underline{x}') \text{ if } a_i(J)R_{ij}\rho_j(J+1) = Aa(J)A\rho(J+1), \\ ATS2(J,\underline{x}') \text{ if } a_i(J)R_{ij}\rho_j(J+1) = -Aa(J)A\rho(J+1), \end{cases} \quad (C.2.55)$$

$$\int_{\lambda=0}^{1} \lambda[D^*(\lambda)]^{-3} d\lambda = \begin{cases} AA(J,\underline{x}'), \\ AAS1(J,\underline{x}') \text{ if } a_i(J)R_{ij}\rho_j(J+1) = Aa(J)A\rho(J+1), \\ AAS2(J,\underline{x}') \text{ if } a_i(J)R_{ij}\rho_j(J+1) = -Aa(J)A\rho(J+1) \end{cases} \quad (C.2.56)$$

where $A\Lambda(J,\underline{x}')$, $A\Lambda S(J,\underline{x}')$, $AT(J,\underline{x}')$, $ATS1(J,\underline{x}')$, $ATS2(J,\underline{x}')$, $AA(J,\underline{x}')$, $AAS1(J,\underline{x}')$, $AAS2(J,\underline{x}')$, $Aa(J)$ and $A\rho(J)$ are defined by

$$AA(J,\underline{x}') = [Aa(J)]^{-1} \ln\left[\frac{a_i(J)R_{ij}\rho_j(J+2) + Aa(J)A\rho(J+2)}{a_i(J)R_{ij}\rho_j(J+1) + Aa(J)A\rho(J+1)}\right], \quad (C.2.57)$$

$$AAS(J,\underline{x}') = [Aa(J)]^{-1} \ln\left[\frac{A\rho(J+1)}{A\rho(J+2)}\right], \quad (C.2.58)$$

$$AT(J,\underline{x}') = [A\Xi(J,\underline{x}')]^{-1}\left[\frac{a_i(J)R_{ij}\rho_j(J+2)}{A\rho(J+2)} - \frac{a_i(J)R_{ij}\rho_j(J+1)}{A\rho(J+1)}\right], \quad (C.2.59)$$

$$ATS1(J,\underline{x}') = [2Aa(J)]^{-1}\{[A\rho(J+1)]^{-2} - [A\rho(J+2)]^{-2}\}, \quad (C.2.60)$$

$$ATS2(J,\underline{x}') = [2Aa(J)]^{-1}\{[A\rho(J+2)]^{-2} - [A\rho(J+1)]^{-2}\}, \quad (C.2.61)$$

$$AA(J,\underline{x}') = [A\Xi(J,\underline{x}')]^{-1}\left[A\rho(J+1) - \frac{\rho_i(J+1)R_{ij}\rho_j(J+2)}{A\rho(J+2)}\right], \quad (C.2.62)$$

$$AAS1(J,\underline{x}') = (1/2)[Aa(J)]^{-2}\{[A\rho(J+1)]^{-1} - [2Aa(J) + A\rho(J+1)][A\rho(J+2)]^{-2}\}, \quad (C.2.63)$$

$$AAS2(J,\underline{x}') = (1/2)[Aa(J)]^{-2}\{[A\rho(J+1)]^{-1} - [A\rho(J+2) - 2Aa(J)][A\rho(J+2)]^{-2}\}, \quad (C.2.64)$$

$$Aa(J) = [a_i(J)R_{ij}a_j(J)]^{1/2}, \quad (C.2.65)$$

and

$$A\rho(J) = [\rho_i(J)R_{ij}\rho_j(J)]^{1/2}, \quad (C.2.66)$$

and where $A\Xi(J,\underline{x}')$ is defined by

$$A\Xi(J,\underline{x}') = [Aa(J)A\rho(J+1)]^2 - [a_i(J)R_{ij}\rho_j(J+1)]^2, \quad (C.2.67)$$

With the aid of these standard integrals the final expressions for the line integrals $AL4_p(J,\underline{x}')$ and $AL5_p(J,\underline{x}')$ are obtained as (cf. (C.2.11), (C.1.34) and (C.1.35))

$$AL4_p(J,\underline{z}') = Aa(J)\left[s^{(p)}\right]^{1/2}\beta_{pq}^{-1}\{\rho_q(J+1)AA(J,\underline{x}') + a_q(J)[Aa(J)]^{-2} \times [A\rho(J+2) - A\rho(J+1) - a_m(J)R_{mn}\rho_n(J+1)AA(J,\underline{x}')]\} \tag{C.2.68}$$

and

$$AL5_p(J,\underline{z}') = Aa(J)\left[s^{(p)}\right]^{1/2}\beta_{pq}^{-1}[\rho_q(J+1)T(J,\underline{x}') + a_q(J)AA(J,\underline{x}')], \tag{C.2.69}$$

respectively, where $AA(J,\underline{x}')$ is to be replaced by $AAS(J,\underline{x}')$ if either $a_i(J)R_{ij}\rho_j(J+1) = -Aa(J)A\rho(J+1)$ or $a_i(J)R_{ij}\rho_j(J+2) = -Aa(J)A\rho(J+2)$, $AT(J,\underline{x}')$ by $ATS1(J,\underline{x}')$ and $AA(J,\underline{x}')$ by $AAS1(J,\underline{x}')$ if $a_i(J)R_{ij}\rho_j(J+1) = Aa(J)A\rho(J+1)$, and, finally, $AT(J,\underline{x}')$ by $ATS2(J,\underline{x}')$ and $AA(J,\underline{x}')$ by $AAS2(J,\underline{x}')$ if $a_i(J)R_{ij}\rho_j(J+1) = -Aa(J)A\rho(J+1)$. With this, the analytic evaluation of the line integrals $AL4_p(J,\underline{x}')$ and $AL5_p(J,\underline{x}')$ has been completed.

REFERENCES

Aris, R. (1962), Vectors, Tensors, and the Basic Equations of Fluid Mechanics, Prentice-Hall, Englewood Cliffs, NJ.

Auriault, J.L., L. Borne, and R. Chambon (1985), "Dynamics of saturated porous media, checking of the generalized law of Darcy", J. Acoust. Soc. Am., vol. 77, no. 5, pp. 1641-1650.

Aziz, K. and A. Settari (1983), Petroleum Reservoir Simulation, Applied Science Publishers Ltd., London.

Bachmat, Y. and J. Bear (1987), On the Concept and Size of a Representative Elementary Volume (REV). In: J. Bear and M.Y. Corapcioglu (Eds.), Advances in Transport Phenomena in Porous Media, NATO/ASI series, Martinus Nijhoff Publishers, Dordrecht.

Barr, R.C., T.C. Pilkington, J.P. Boineau, and M.S. Spach (1966), "Determining Surface Potentials from Current Dipoles, with Application to Electrocardiography", IEEE Trans. on Bio-Medical Engineering, vol. BME-13, no. 2, pp. 88-92.

Batchelor, G.K. (1983), An Introduction to Fluid Mechanics, Cambridge University Press, Cambridge.

Baveye, P. and G. Sposito (1984), "The Operational Significance of the Continuum Hypothesis in the Theory of Water Movement Trough Soils and Aquifers", Water Resour. Res., vol. 20, no. 5, pp. 521-530.

Bear, J. (1972), Dynamics of Fluids in Porous Media, Elsevier, New York.

Bear, J. and Y. Bachmat (1983), "On the equivalence of areal and volumetric averages transport phenomena in porous media", Adv. Water Res., vol. 6, pp. 53-62.

Bird, R.B., W.E. Stewart and E.N. Lightfoot (1960), Transport Phenomena, John Wiley & Sons Inc., New York.

Birtles, A.B., B.J. Mayo and A.W. Bennett (1973), "Computer technique for solving 3-dimensional electron-optics and capacitance problems", Proc. IEE, vol. 120, no. 2, pp. 213-220.

Bowen, R.M. (1976), Theory of Mixtures. In: A.C. Eringen (Ed.), Continuum Physics, vol. III, Academic Press, New York.

Bowen, R.M. (1984), Porous Media Model Formulations by the Theory of Mixtures. In: J. Bear and M.Y. Corapcioglu (Eds.), Fundamentals of Transport Phenomena in Porous Media, NATO/ASI series, Martinus Nijhoff Publishers, Dordrecht.

Brenner, H. (1963), "The Stokes resistance of an arbitrary particle", Chem. Eng. Sci., vol. 18, pp. 1-25.

Brinkman, H.C. (1947), "A calculation of the viscous force exerted by a flowing fluid on a dense swarm of particles", Appl. Sci. Res., vol. A1, pp. 27-34.

Burridge, R. and J.B. Keller (1981), "Poroelasticity equations derived from microstructure", J. Acoust. Soc. Am., vol. 70, no. 4, pp. 1140-1146.

Coleman, B.D. and W. Noll (1963), "The Thermodynamics of Elastic Materials with Heat Conduction and Viscosity", Arch. Rational Mech. Anal., vol. 13, pp. 167-178.

Cruse, T.A. (1969), "Numerical solutions in three dimensional elastostatics", Int. J. Solids Structures, vol. 5, pp. 1259-1274.

Cruse, T.A. (Ed.) (1988), Advanced Boundary Element Methods, IUTAM Symposium San Antonio, Texas, 1987, Springer-Verlag, Berlin.

de la Cruz, V. and T.J.T. Spanos (1983), "Mobilization of Oil Ganglia", Am. Inst. Chem. Eng. J., vol. 29, no. 5, pp. 854-858.

de la Cruz, V. and T.J.T. Spanos (1985), "Seismic wave propagation in a porous medium", Geophysics, vol. 50, no. 10, pp. 1556-1565.

Darcy, H. (1856), Les Fontaines Publiques de la Ville de Dijon, Victor Dalmont, Paris.

Dybbs, A. and S. Schweitzer (1973), "Conservation Equations for Nonisothermal Flow in Porous Media", J. Hydrology, vol. 20, pp. 171-180.

Eringen, A.C. (1967), Mechanics of Continua, John Wiley & Sons Inc., New York.

Gray, W.G. and K. O'Neill (1976), "On the General Equations for Flow in Porous Media and Their Reduction to Darcy's Law", Water Resour. Res., vol. 12, no. 2, pp. 148-154.

Gray, W.G. and P.C.Y. Lee (1977), "On the theorems for local volume averaging of multiphase systems", Int. J. Multiphase Flow, vol. 3, pp. 333-340.

van der Grinten, J.G.M. (1987), An Experimental Study of Shock-Induced Wave Propagation in Dry, Water-Saturated, and Partially Saturated Porous Media, Ph.D.-Thesis, Eindhoven University of Technology, Eindhoven, the Netherlands, 111 pp.

Haitjema, H.M. (1987), "Evaluating solid angles using contour integrals", Appl. Math. Modelling, vol. 11, pp. 69-71.

Harrington, R.F. (1968), Field computation by moment methods, The Macmillan Company, New York.

Hassanizadeh, M. and W.G. Gray (1979a), "General conservation equations for multi-phase systems: 1. Averaging procedure", Adv. Water Res., vol. 2, pp. 131-144.

Hassanizadeh, M. and W.G. Gray (1979b), "General conservation equations for multi-phase systems: 2. Mass, momentum, energy, and entropy equation", Adv. Water Res., vol. 2, pp. 191-203.

Hassanizadeh, M. and W.G. Gray (1980), "General conservation equations for multi-phase systems: 3. Constitutive theory for porous media flow", Adv. Water Res., vol. 3, 1980, pp. 25-40.

van Herk, A. (1980), Three-dimensional analysis of magnetic fields in recording head configurations, Ph.D.-Thesis, Delft University of Technology, Delft, the Netherlands, 205 pp.

Herman, G.C. (1981a), "Scattering of transient acoustic waves by an inhomogeneous obstacle", J. Acoust. Soc. Am., vol. 69, pp. 909-915.

Herman, G.C. (1981b), Scattering of transient acoustic waves in fluids and solids, Ph.D.-Thesis, Delft University of Technology, Delft, the Netherlands, 183 pp.

Herman, G.C. (1982), "Scattering of transient elastic waves by an inhomogeneous obstacle: Contrast in volume density of mass", J. Acoust. Soc. Am., vol. 71, pp. 264-272.

de Hoop, A.T. (1977), General considerations on the integral-equation formulation of diffraction problems. In: Modern Topics in Electromagnetics and Antennas, Stevenage (England), PPL Conference Publication 13, Peter Peregrinus Ltd., London, Chapter 6, pp. 6.1-6.59.

de Hoop, A.T. (1982), The Vector Integral-Equation Method for Computing Three-Dimensional Magnetic Fields. In: Integral Equations and Operator Theory, vol. 5, Birkhauser-Verlag, Basel, pp. 459-474.

Jawson, M.A. and G.T. Symm (1977), Integral Equation Methods in Potential Theory and Elastostatics, Academic Press, London.

de Jong, G. (1981), "Vector Integral Representations in Gravimetry", Bull. Geod., vol. 55, pp. 59-72.

Kantorovich, L.V. and V.I. Krylov (1964), Approximate Methods of Higher Analysis, P. Noordhoff, Groningen, the Netherlands.

Keller, J.B. (1980), Darcy's law for flow in porous media and the two-space method. In: R.L. Sternberg, A.J. Kalinowski, and J.S. Papadakis (Eds.), Nonlinear Partial Differential Equations in Engineering and Applied Science, Marcel Dekker Inc., New York.

Kellogg, O.D. (1954), Foundations of Potential Theory, Dover Publications, Inc., New York.

Landau, L.D. and E.M. Lifshitz (1966), Fluid Mechanics, Pergamon Press, Oxford.

Lehner, F.K. (1979), "A Derivation of the Field Equations for Slow Viscous Flow through a Porous Medium", Ind. Eng. Chem. Fundam., vol. 18, no. 1, pp. 41-45.

Liggett, J.A. and P.L-F. Liu (1983), The Boundary Integral Equation Method for Porous Media Flow, George Allen & Unwin, London.

Lindholm, D.A. (1980), "Notes on Boundary Integral Equations for Three-Dimensional Magnetostatics", IEEE Trans. on Magnetics, vol. MAG-16, no. 6, pp. 1409-1413.

Malvern, L.E. (1969), Introduction to the Mechanics of a Continuous Medium, Prentice-Hall, Englewood Cliffs, NJ.

McConnell, A.J. (1957), Applications of Tensor Analysis, Dover Publications, Inc., New York.

Morse, P.M. and H. Feshbach (1953), Methods of Theoretical Physics, McGraw-Hill Book Company, New York.

Muskat, M. (1946), The Flow of Homogeneous Fluids Through Porous Media, McGraw-Hill Book Company, New York (1937); 2nd printing by Edwards Brothers, Ann Arbor, MI.

Naber, G.L. (1980), Topological methods in Euclidean spaces, Cambridge University Press, Cambridge.

van Oosterom, A. and J. Strackee (1983), "The Solid Angle of a Plane Triangle", IEEE Trans. on Bio-Medical Engineering, vol. BME-30, no. 2, pp. 125-126.

Pinder, G.F. and W.G. Gray (1977), Finite element simulation in surface and subsurface hydrology, Academic Press, New York.

Polubarinova-Kochina, P.Ya. (1962), Theory of Ground Water Movement, Princeton University Press, Princeton, NJ.

Rao, S.M., A.W. Glisson, D.R. Wilton and B.S. Vidula (1979), "A Simple Numerical Solution Procedure for Statics Problems Involving Arbitrary-Shaped surfaces", IEEE Trans. Ant. Prop., vol. AP-27, no. 5, pp. 604-608.

Remson, I., C.A. Appel and R.A. Webster (1965), "Ground-Water Models Solved by Digital Computer", J. Hydraul. Div. Amer. Soc. Civil Eng., vol. 91, no. HY 3, pp. 133-147.

Rizzo, F.J. and D.J. Shippy (1977), "An advanced boundary integral equation method for three-dimensional thermoelasticity", Int. J. Num. Meth. Engng., vol. 11, pp. 1753-1768.

Scheidegger, A.E. (1963), The Physics of Flow through Porous Media, Oxford University Press, London.

Slattery, J.C. (1967), "General Balance Equation for a Phase Interface", Ind. Eng. Chem. Fundam., vol. 6, no. 1, pp. 108-115.

Slattery, J.C. (1967), "Flow of Viscoelastic Fluids Through Porous Media", Am. Inst. Chem. Eng. J., vol. 13, no. 6, pp. 1066-1071.

Slattery, J.C. (1969), "Single-Phase Flow through Porous Media", Am. Inst. Chem. Eng. J., vol. 15, no. 6, pp. 866-872.

Spiegel, M.R. (1974), Theory and Problems of Vector Analysis and an introduction to Tensor Analysis, McGraw-Hill Book Company, New York.

Tan, T.H. (1975a), "Scattering of elastic waves by elastically transparent obstacles (integral-equation method)", Appl. Sci. Res., vol. 31, pp. 29-51.

Tan, T.H. (1975b), Diffraction theory for time-harmonic elastic waves, Ph.D.-Thesis, Delft University of Technology, Delft, the Netherlands, 182 pp.

Thurston, R.N. (1964), Wave Propagation in Fluids and Normal Solids. In: W.P. Mason (Ed.), Physical Acoustics, vol. I, part A, Academic Press, New York.

Todhunter, I. and J.G. Leathem (1901), Spherical Trigonometry, Macmillan and Co., London.

Tritton, D.J. (1977), Physical Fluid Dynamics, Van Nostrand Reinhold Company, New York.

Truesdell, C. and R.A. Toupin (1960), The Classical Field Theories. In: S. Flugge (Ed.), Principles of Classical Mechanics and Field Theory, Encyclopedia of Physics", vol. III/1, Springer-Verlag, Berlin.

de Vries, S. and A.T. de Hoop, "A linearized theory of acoustic waves in a fluid-saturated porous solid", to be submitted in 1988 to the Journal of the Acoustical Society of America.

Waldvogel, J. (1979), "The Newtonian Potential of Homogeneous Polyhedra", J. Appl. Math. Phys. (ZAMP), vol. 30, pp. 388-398.

van der Weiden, R.M. and A.T. de Hoop (1988), The Boundary-Integral-Equation Method for Computing the Three-Dimensional Flow of Groundwater. In: Th.A. Cruse (Ed.), Advanced Boundary Element Methods, IUTAM Symposium San Antonio, Texas, 1987, Springer-Verlag, Berlin, pp. 451-458.

Whitaker, S. (1967), "Diffusion and Dispersion in porous media", Am. Inst. Chem. Eng. J., vol. 13, no. 3, pp. 420-427.

Whitaker, S. (1969), "Advances in the theory of fluid motion in porous media", Ind. Chem. Eng. J., vol. 61, no. 12, pp. 14-28.

Wilton, D.R., S.M. Rao, A.W. Glisson, D.H. Schaubert, O.M. Al-Bundak and C.M. Butler (1984), "Potential Integrals for Uniform and Linear Source Distributions on Polygonal and Polyhedral Domains", IEEE Trans. Ant. Prop., vol. AP-32, no. 3, pp. 276-281.

SAMENVATTING

In dit proefschrift wordt onderzoek verricht aan het berekenen van driedimensionale stationaire grondwaterstromingsproblemen met behulp van de randintegraalvergelijkingsmethode.

Grondwater speelt een belangrijke rol in veel problemen die met het ingrijpen van de mens op zijn omgeving verband houden. Als voorbeeld wordt genoemd het ontwerpen en realiseren van allerlei civieltechnische constructies zoals dijken, dammen, wegen, funderingen en dergelijke, waarbij de grond als constructie-element wordt gebruikt. Ook bij het beheer van ondergrondse waterreservoirs ten dienste van de drinkwatervoorziening en/of voor agrarische doeleinden is kennis omtrent de stroming van het grondwater onontbeerlijk.

In het algemeen is het doel van ieder onderzoek aan de stroming van grondwater het verkrijgen van inzicht in het gemiddelde, zogenaamde macroscopische, gedrag van die stroming in een bepaald gedeelte van de ondergrond. Oplossingen voor dit soort problemen zijn in het algemeen gebaseerd op het beginsel van het behoud van massa en op generalisaties van een experimenteel opgestelde bewegingsvergelijking: de wet van Darcy. Alhoewel met deze wet vele praktische grondwaterstromingsproblemen kunnen worden opgelost, bestaat de behoefte aan een meer theoretische ondergrond ervoor. In het eerste gedeelte van dit proefschrift is daartoe onderzocht op welke wijze de macroscopische bewegingsvergelijking voor de stroming van grondwater kan worden afgeleid uit de fundamentele wetten van de vloeistofmechanica, wanneer deze wetten worden toegepast op het poreuze medium dat als model voor de met water verzadigde ondergrond dient. De overweging die hierin wordt gevolgd is, dat de macroscopische vergelijkingen worden verkregen door het ruimtelijk middelen van de

basisvergelijkingen op de schaal van de afmetingen van de poriën, de zogenaamde microscopische schaal. Dit middelen vindt plaats over een zogenaamd representatief elementair middelingsgebied. De macroscopische basisvergelijkingen die op deze wijze worden verkregen - een macroscopische continuiteitsvergelijking en een generaliseerde vorm van de wet van Darcy - worden vervolgens aangevuld met (macroscopische) randvoorwaarden en tenslotte gebruikt om stationaire grondwaterstromings-problemen te formuleren als (mathematische) randwaardeproblemen.

Als methode van oplossing van deze randwaardeproblemen is gekozen voor het gebruik van randintegraalvergelijkingen. De randintegraal-vergelijkingen volgen uit geschikte integraalvoorstellingen voor de fundamentele stromingsgrootheden, te weten de macroscopische druk en de macroscopische stromingssnelheid; zij drukken deze grootheden uit in gerelateerde grootheden op het randoppervlak van de van belang zijnde stromingsconfiguratie. Op hun beurt worden de integraalvoorstellingen verkregen uit een reciprociteitsrelatie. Deze reciprociteitsrelatie wordt uit de basisvergelijkingen afgeleid en legt op een bepaalde wijze een verband tussen de grootheden optredende in twee mogelijke, doch onderling verschillende, grondwaterstromingstoestanden. De ene stromingstoestand wordt geïdentificeerd met de werkelijke stromingstoestand van het grondwater, terwijl voor de andere toestand geschikte "hulptoestanden" worden gekozen. Voor deze laatste worden zogenaamde Greense toestanden gekozen, die achtereenvolgens behoren bij een injectiepuntbron en een mechanische puntkracht. Dit proces leidt tot de gewenste integraalvoorstellingen. Alle bevatten zij singuliere kernfuncties van het Greense type. Zodra deze laatste bekend zijn, worden de verschillende randintegraalvergelijkingsformuleringen verkregen door in de integraalvoorstellingen het waarnemingspunt op het randoppervlak van de stromingsconfiguratie te kiezen. Aangezien in het algemeen alleen voor onbegrensde, homogene en reciproke media de Greense kernfuncties expliciet kunnen worden bepaald, worden de randintegraalvergelijkingen in praktische toepassingen alleen gebruikt voor stuksgewijs homogene en anisotrope, doch reciproke, media.

Vervolgens worden de randintegraalvergelijkingen numeriek opgelost. Hiertoe is een eenvoudige en efficiënte methode ontwikkeld. De ontwikkelde methode is getest op een aantal eenvoudige isotrope en anisotrope, doch reciproke, stromingsconfiguraties. Opgemerkt wordt, dat de ingewikkeldheid van in de praktijk te behandelen configuraties slechts wordt beperkt door de geheugencapaciteit en de snelheid van de beschikbare rekenmachine.

Hieronder volgt een wat meer gedetailleerde samenvatting van de verschillende hoofdstukken.

In Hoofdstuk 2 wordt een overzicht gegeven van de basisvergelijkingen voor de isotherme stroming van viskeuze vloeistoffen. Bij beschouwing van de stroming van grondwater als de stroming van water door een poreus medium beschrijven deze vergelijkingen de stroming op de schaal van de afmetingen van de porien (de microscopische schaal). Er wordt aangetoond, dat voor veel praktische situaties de samendrukbaarheid van de vloeistof met voldoende nauwkeurigheid kan worden verwaarloosd en dat de niet-stationaire en niet-lineaire bewegingsvergelijking eveneens met voldoende nauwkeurigheid door een stationaire en lineaire vergelijking kan worden benaderd.

Met de vereenvoudigde microscopische basisvergelijkingen uit Hoofdstuk 2 als uitgangspunt worden in Hoofdstuk 3 de macroscopische basisvergelijkingen voor de stationaire stroming van grondwater afgeleid. Hiertoe wordt middeling over het representative elementaire middelingsgebied uitgevoerd. De uitdrukkingen die na dit "volume-middelen" worden verkregen, hebben alle een goed gedefinieerde fysische betekenis en kunnen op een eenvoudige wijze worden gerelateerd aan de macroscopische stromingsgrootheden die in de praktijk van belang zijn.

In Hoofdstuk 4 worden de integraalvoorstellingen voor de druk en de stromingssnelheid van het grondwater afgeleid. Er wordt een overzicht gegeven van de verschillende randintegraalvergelijkingsformuleringen die uit deze integraalvoorstellingen volgen. Tevens worden de Greense

functies voor een onbegrensd homogeen en anisotroop, doch reciprook, medium bepaald.

In Hoofdstuk 5 wordt een numerieke methode besproken waarmee de verkregen randintegraalvergelijkingen kunnen worden opgelost. Deze methode berust op het benaderen van het betreffende randoppervlak door een eindig aantal vlakke driehoekige elementen. Vervolgens worden op ieder element de druk en de normale component van de stromingssnelheid ontwikkeld in polynomen van de graad één. Hierna wordt op de gediscretiseerde randintegraalvergelijkingen de collocatiemethode ("point matching") toegepast. Een en ander resulteert in een (eindig) stelsel lineaire, algebraïsche vergelijkingen, dat via een directe methode wordt opgelost. In de discretisatieprocedure worden alle oppervlakte-integralen over de vlakke driehoekige elementen analytisch bepaald.

Om de ontwikkelde programmatuur te testen, worden in Hoofdstuk 6 een aantal numerieke experimenten uitgevoerd. Eenvoudige teststromingen in met homogene, isotrope en anisotrope, doch reciproke, media gevulde rechthoekige blokken worden behandeld. Voor die teststromingen waarvan de druk en de stromingssnelheid exact door polynomen van ten hoogste de graad één kunnen worden weergegeven, blijken de resultaten exact te zijn in het aantal cijfers dat bij de representatie van de getallen in het rekenmachineprogramma is gebruikt. Voor algemenere configuraties hangt de nauwkeurigheid af van de gebruikte verdeling van het randoppervlak in vlakke driehoekige elementen.

Het ontwikkelde programma kan dienen als bestanddeel bij het analyseren van niet-stationaire grondwaterstromingsproblemen (bijvoorbeeld het bepalen van het bewegende grensvlak tussen zoet en zout grondwater, als gevolg van het toevoegen of onttrekken van water).

Alle ontwikkelde programmatuur is geschreven in Fortran 77 en geïmplementeerd op een IBM PC/AT.

LEVENSBERICHT

De samensteller van dit proefschrift werd op 8 mei 1958 te Amsterdam geboren. Na het behalen van het einddiploma Gymnasium β aan het Willem de Zwijger Lyceum te Bussum ging hij in 1977 naar Delft om aan de Technische Hogeschool elektrotechniek te studeren. Zijn afstuudeerwerk verrichtte hij onder leiding van Prof.Dr.Ir. H. Blok en Dr. A.G. Tijhuis; het handelde over de verstrooiing van elektromagnetische golven aan een cirkelcylindrisch object. In 1983 werd hem het diploma van elektrotechnisch ingenieur uitgereikt.

Sinds 1 december 1983 is hij als onderzoekmedewerker in dienst van de Nederlandse organisatie voor wetenschappelijk onderzoek (N.W.O.), voorheen de Nederlandse organisatie voor zuiver-wetenschappelijk onderzoek (Z.W.O.), en gestationeerd bij de vakgroep Gezondheidstechniek en Waterbeheersing van de faculteit der Civiele Techniek van de Technische Universiteit Delft. Daar heeft hij gedurende de afgelopen jaren - onder leiding van Prof.Dr.Ir. A.T. de Hoop van de faculteit der Elektrotechniek (vakgroep Elektromagnetisme) en de faculteit der Technische Wiskunde en Informatica (vakgroep Toegepaste Analyse) en Prof.Dr.Ir. J.C. van Dam van de faculteit der Civiele Techniek (vakgroep Gezondheidstechniek en Waterbeheersing) - gewerkt aan een door de Stichting voor de Technische Wetenschappen (S.T.W.) gesubsidieerd onderzoekproject op het gebied van het modelleren van stationaire grondwaterstromings- problemen met behulp van de randintegraalvergelijkingsmethode. Deze onderzoekingen hebben geleid tot het samenstellen van dit proefschrift.